University of Bielefeld
Department of Cell Biology

Blood plasma-mediated effects on regenerative features of a novel adult human cardiac stem cell population

Cumulative Dissertation
Submitted for the fulfilment of the requirements
for the doctoral degree of natural science
Doctor rerum naturalis (Dr. rer. nat.)

By Anna Höving
2021

Supervised by

Prof. Dr. Christian Kaltschmidt

Following publications originated within the scope of this PhD Thesis:
(* included in the dissertation)

Original research articles:

1.) *

"Blood Serum stimulates p38-mediated proliferation and changes in global gene expression of adult human cardiac stem cells" **Höving A**, Schmidt K, Merten M, Hamidi J, Rott AK, Faust I, Greiner J , Gummert J, Kaltschmidt B, Kaltschmidt C *, Knabbe C * (2020) Cells 9(6):1472

2.) *

"Transcriptome analysis reveals high similarities between adult human cardiac stem cells and neural crest-derived stem cells" **Höving A**, Sielemann K, Greiner J, Kaltschmidt B, Knabbe C*, Kaltschmidt C*. (2020) Biology 9(12):435

3.) *

"Human blood serum induces p38-MAPK-dependent migration dynamics of adult human cardiac stem cells – Single cell analysis via a microfluidic-based cultivation platform" **Höving A** *, Schmitz J *, Schmidt K, Greiner J, Knabbe C, Kaltschmidt B, Grünberger A, Kaltschmidt C. *under review* (Biology)

4.) *

"Identification of a Novel High Yielding Source of Multipotent Adult Human Neural Crest-Derived Stem Cells" Schürmann M, Brotzmann V, Bütow M, Greiner J, **Höving A**, Kaltschmidt C, Kaltschmidt B, Sudhoff H (2018) Stem Cell Reviews and Reports 14(2): 277–285

5.)

„Nanopore Sequencing reveals global Transcriptome Signatures of mitochondrial and ribosomal Gene Expressions in various human Cancer Stem-like Cell Populations" Witte K *, Hertel O *, Windmöller B, Helweg L, **Höving A**, Knabbe C, Busche T, Greiner J, Kalinowski J, Noll T, Mertzlufft F, Beshay M, Pfitzenmaier J, Kaltschmidt B, Kaltschmidt C, Banz-Jansen C *, Simon M * (2021) Cancers 13(5):1136

Reviews:

1.) *

"Between fate choice and self-renewal - Heterogeneity of adult neural crest-derived stem cells" **Höving A***, Windmöller B*, Knabbe C, Kaltschmidt B, Kaltschmidt C, Greiner J. *accepted for publication* (Frontiers in Cell and Developmental Biology)

Table of Contents

1. Abbreviations

ACTB	β-actin
AD	Alzheimer's disease
AdMSC	Adipose-derived mesenchymal stem cell
ADSC	Adipose-derived stem cell
AKT	Protein kinase B
ALS	Amyotrophic lateral sclerosis
AMPA	α-amino-3-hydroxy-5-methyl-4-isoxazolepropionic acid
ASC	Adult stem cell
bFGF	Basic fibroblast growth factor
CA1	Cornu Ammonis 1
CA3	Cornu Ammonis 3
CCL11	C-C motif chemokine 11
CD105	Cluster of differentiation 105
CD31	Custer of differentiation 31
CD34	Cluster of differentiation 34
CDC	Cardiosphere-derived cell
cKit	Stem cell factor receptor kinase
CSC	Cardiac stem cell
CVD	Cardiovascular disease
Cx43	Connexin 43
CXCR4	CXC chemokine receptor 4
DNA	Deoxyribonucleic acid
DG	Dentate gyrus
EC	Erythrocyte concentrate
ESC	Embryonic stem cell
FFP	Fresh frozen plasma
GDF11	Growth differentiation factor 11
GDF8	Growth differentiation factor 8
GFP	Green flourescent protein
GJA1	Gap junction alpha-1 protein
GO	Gene Ontology
hCSC	Human cardiac stem cell
HF	Heart failure
HSA	Human serum albumin
HSC	Hematopoietic stem cell
HUVEC	Human umbilical vein endothelial cells
IHD	Ischemic heart disease
IL24	Interleukin 24
iPSC	Induced pluripotent stem cells
Isl1	Insulin gene enhancer protein 1
ITSC	Inferior turbinate stem cell
KA	Kainic acid, 2-carboxy-4-isopropenyl-pyrrolidin-3-ylacetic acid
KEGG	Kyoto Encyclopedia of Genes

Klf4	Kruppel-like factor 4
KMT2D	Histone-lysine N-methyltransferase 2D
LAA	Left atrial appendage
MAPK	Mitogen-activated protein kinase
MaSc	Mammalian suspension cells
MCP1	Monocyte chemotactic protein 1
MI	Myocardial infarct
miRNA	Micro ribonucleic acid
MMP9	Matrix metalloproteinase 9
MSC	Mesenchymal stem cells
MTSC	Middle turbinate stem cell
NCSC	Neural crest-derived stem cell
NF-κB	Nuclear factor κB
NSC	Neural stem cell
Oct4	Octamer-binding transcription factor 4
p38-MAPK	P38 mitogen-activated protein kinase
p75 NTR	P75 neurotrophin receptor
PAX	Paired box
PCA	Principal component analysis
PD	Parkinson's disease
PI3K	Phosphoinositide 3-kinase
RET	Ret proto-oncogene
RNA-Seq	Ribonucleic acid sequencing
RNS	Reactive nitrogen species
ROS	Reactive oxygen species
SA-β-Gal	Senescence-associated-beta-galactosidase
Sca1	Stem cell antigen-1
SDF-1	Stromal-derived factor-1
siRNA	Small interfering ribonucleic acid
Sox2	Sex determining region Y-box 2
β-Gal	Beta-galactosidase
SVZ	Subventricular zone
TGF-β1	Transforming growth factor beta 1
TIMP2	Tissue inhibitor of metalloproteinases 2
VGlut	Vesicular glutamate transporter

2. List of Figures

3. Abstract

During lifetime, the human organism is exposed to a progressive decline in organ function and regeneration considered as the ageing process. Several age-associated diseases such as cardiovascular- and neurodegenerative diseases or cancer are described along with their cellular pathologies. Although tissue regeneration substantially relies on the functionality of endogenous adult stem cell populations found in various organs including the heart, a complex interaction with systemic factors carried by the blood is evident. Thus, young blood or blood products are increasingly recognized as potential therapeutic agents to target age-associated malignancies. In this regard, prominent studies in the murine model gained attention by rejuvenating old mice with blood or blood products from young mice. However, the transition of these promising results to the human system remains challenging. Here, adequate cellular models need to be established to study the effects of human blood plasma on the regeneration of human tissues and particularly the heart.

Facing this challenge, this thesis describes the age-specific effects of human blood plasma and blood serum on a human cardiac stem cell (hCSC)-based model for heart regeneration in terms of proliferation, migration, senescence, and global gene expression. Here, the identification of a novel multipotent hCSC population from the heart auricle of patients undergoing routine cardiac surgery enabled the establishment of a cellular model to study human cardiac regeneration. These cells can easily be isolated and expanded in culture and express common markers for cardiac stem cell populations. Moreover, hCSCs showed neural crest-specific stem cell markers and high transcriptional similarities with a known neural crest-derived stem cell population. Their differentiation capacities into mesodermal as well as neuro-ectodermal derivates further suggest a potential relation to the neural crest. Treatment of hCSCs with human plasma and serum greatly induced their proliferation with no significant differences regarding age and sex of the plasma donors. In contrast, age-dependent effects were detectable in the serum-mediated protection against senescence with serum from old (> 60 years) female donors showing the highest rate of protection compared to male or young female donors. Further, the migrative capacities of hCSCs in terms of migration distance and velocity were significantly increased after serum treatment. A global transcriptomic analysis of serum-treated hCSCs revealed an age-dependent increase of differential gene expression in hCSCs treated with young sera

compared to untreated cells and the upregulation of genes associated to the p38 mitogen-activated protein kinase (p38-MAPK)-pathway. Pharmacological inhibition of p38-MAPK significantly reduced the beneficial effects of human blood serum in terms of decreased proliferation and migration as well as increased senescence. Next to its beneficial effects on the successfully established cellular model system for cardiac ageing and regeneration, human serum was applied to *ex vivo* cultured mouse hippocampal slices as an experimental model for neurodegenerative diseases. Here, human blood plasma as well as human serum albumin (HSA) as the most abundant plasma protein revealed significant neuroprotective effects against kainic acid (KA)-mediated neuronal cell death compared to untreated hippocampal slice cultures.

In summary, the here presented results show the identification of a novel hCSC population and its developmental relation to the neural crest as well as its successful application as a screening system for human blood plasma-mediated regenerative responses. On functional level, p38-MAPK was identified as crucial mediator of the blood-plasma-based induction of hCSC-proliferation and -migration as well as protection of hCSCs against senescence. Future studies will carefully investigate the regulatory mechanisms upstream and downstream of p38-MAPK signaling in serum-treated hCSCs and might enable the identification of the responsible plasma components. Finally, this work provides valuable insights into the beneficial effects of human blood plasma on the regenerative function of adult human cardiac stem cells and builds a basis for the potential clinical use of human blood plasma as well as cardiac stem cells in regenerative medicine.

4. Zusammenfassung

Der menschliche Organismus ist während seiner Lebenszeit einem kontinuierlichen Alterungsprozess mit einem Abbau von Organfunktionen ausgesetzt. Zahlreiche Krankheiten wie etwa kardiovaskuläre oder neurodegenerative Erkrankungen sowie ihre zelluläre Pathologie wurden bisher mit dem Alterungsprozess assoziiert. Obwohl die Regeneration von Gewebe zu einem großen Teil auf der Funktionalität endogener adulter Stammzellpopulationen beruht, welche unter anderem im Herzen gefunden wurden, ist eine komplexe Interaktion mit systemischen, über das Blut transportierten Faktoren unbestreitbar. In diesem Zusammenhang haben prominente Studien im murinen Modellsystem für Aufmerksamkeit gesorgt, indem alte Mäuse und ihre Organe durch die Gabe von Blut oder Blutprodukten junger Mäuse verjüngt wurden. Eine Übertragung dieser vielversprechenden Ergebnisse vom murinen auf das humane System bleibt jedoch weiterhin eine Herausforderung und es bedarf der Entwicklung adäquater Modellsysteme, um die Effekte von humanem Blutplasma auf regenerative Prozesse in humanen Zellen und Geweben, insbesondere dem Herzen, zu studieren.

Im Kontext dieser Fragestellungen beschreibt die vorliegende Arbeit die Etablierung eines auf humanen kardialen Stammzellen (human cardiac stem cells, hCSC) basierenden Modellsystems für Herzregeneration sowie die altersspezifischen Effekte von Blutplasma und Blutserum auf hCSCs bezüglich Proliferation, Migration, Seneszenz und Genexpression. Hierbei ermöglichte die Identifizierung einer neuen multipotenten hCSC Population aus dem Herzohrgewebe kardiochirurgischer Patienten die Entwicklung eines zellulären Modellsystems zur Untersuchung kardialer Regeneration. Diese Stammzellen können sehr effizient isoliert und *in vitro* expandiert werden und exprimieren übliche Marker kardialer Stammzellpopulationen. Zudem wurde gezeigt, dass hCSCs zusätzlich neuralleistenspezifische Marker exprimieren und ihr globales Genexpressionsprofil dem bekannter Neuralleistenstammzellpopulationen ähnelte. In diesem Zusammenhang weist die Differenzierungskapazität von hCSCs in Zellen sowohl mesodermaler als auch neuro-ektodermaler Herkunft auf einen potenziellen entwicklungsbiologischen Ursprung in der Neuralleiste hin.

Die Behandlung mit humanem Blutplasma und Serum induzierte die Proliferation von hCSCs deutlich, wobei keine signifikanten Unterschiede zwischen den unterschiedlichen

Altersgruppen und Geschlechtern der Plasmaspender detektierbar waren. Im Gegensatz hierzu waren altersabhängige Effekte in dem Schutz vor Seneszenz durch humanes Serum sichtbar, wobei Serum alter (> 60 Jahre) Spenderinnen verglichen mit männlichen Spendern oder jungen Spenderinnen (< 20 Jahre) den besten Schutz vor Seneszenz vermittelte. Des Weiteren konnte beobachtet werden, dass sowohl die Migrationsdistanz als auch die Migrationsgeschwindigkeit von hCSCs nach der Behandlung mit Serum signifikant erhöht waren. Die Analyse des Transkriptoms von serumbehandelten hCSCs im Vergleich zu unbehandelten Zellen ließ einen Anstieg in der differentiellen Genexpression von hCSCs welche mit den Seren junger männlicher Spender behandelt wurden erkennen. Hier wurde zudem eine Überexpression bestimmter Gene in Verbindung mit dem p38 *mitogen-activated protein kinase* (p38-MAPK) -Signalweg gezeigt. Die pharmakologische Inhibition von p38-MAPK in serumbehandelten hCSCs blockierte die vorteilhaften Effekte von Blutserum und führte in weiteren *in vitro* Untersuchungen zu einer signifikant reduzierten Proliferation und Migration sowie zu einem Anstieg der zellulären Seneszenz.

Neben der erfolgreichen Etablierung von hCSCs als Modellsystem für kardiales Altern und kardiale Regeneration wurden in dieser Arbeit die Effekte von Blutplasma auf murine hippokampale Schnittkulturen als Modelsystem für neurodegenerative Krankheiten untersucht. Hier zeigten sowohl humanes Blutplasma als auch das abundanteste Plasmaprotein Albumin (*human serum albumin*, HSA) deutliche protektive Effekte gegen neuronalen Zelltod durch Kainsäure (*kainic acid*, KA).

Zusammenfassend beinhalten die hier präsentierten Ergebnisse sowohl die Identifizierung einer neuen Population kardialer Stammzellen als auch die erfolgreiche Anwendung dieser hCSCs als Untersuchungssystem für blutplasmainduzierte regenerative Prozesse. Auf funktioneller Ebene wurde p38-MAPK als wichtiger Signalweg innerhalb der serum-vermittelten Proliferation und Migration und des Schutzes vor Seneszenz beschrieben. Basierend auf der vorliegenden Arbeit können zukünftige weitere Forschungen die vorgeschaltete und nachgeschaltete Regulation des p38-MAPK-Signalwegs in serumbehandelten hCSCs untersuchen und so möglicherweise die hier aktiven Plasmakomponenten identifizieren. Abschließend liefert diese Arbeit einen wertvollen Beitrag zur Aufklärung plasma-induzierter Effekte auf die Funktion kardialer Stammzellen und damit eine vielversprechende Basis für zukünftige potenzielle Anwendungen von sowohl Blutplasma als auch kardialen Stammzellen in der regenerativen Medizin.

5. Introduction

5.1. The ageing human body

5.1.1. Ageing as a risk factor for multiple diseases

Ageing is a process, which can be defined as time-dependent functional decline of tissues and organisms. To date, multiple age-associated malignancies are described such as cardiovascular- or neurodegenerative diseases and cancer. As one example, the incidence of cervical cancer worldwide increased from two cases per 100,000 women and year at age 20 to 38 cases at age 54 (Arbyn et al. 2020). In the years 2000 – 2010, the age-specific incidences of all cancer types in both sexes had a maximum level in the group of ages 80 – 84 years (Thakkar et al. 2014). The group of 75+ years was also projected to be the group with the highest incidence rates of all cancer types in 2035 (Smittenaar et al. 2016). Age was further considered to be one of the major risk factors for Parkinson's disease (PD) (Balestrino and Schapira 2020) with a prevalence of 1903 cases in the group of age 80+ (Pringsheim et al. 2014). Moreover, it was shown that incidence rates for dementia in people older than 60 years double every 10 years (Prince et al. 2013). Moreover, in 2020, 83 % of patients with Alzheimer's disease (AD) were 75 years or older (Alzheimer's-Association 2020). An evaluation demonstrated, the prevalence of cardiovascular diseases (CVD) in the UK to be highest in the group of 75+ years old people with 31 % – 34 % while in the group of 16 – 44 years, the prevalence was only 2 % (Bhatnagar et al. 2016). In the Netherlands, a study showed that the prevalence of CVD gradually increased from the age of 50 along with the amount of different manifestations of CVD (van der Ende et al. 2017). Although age as a direct causality of these pathologies has not yet been proven, it clearly remains as the highest risk factor (Niccoli and Partridge 2012, Franceschi et al. 2018). In general, a time-dependent accumulation of cellular damage could be observed in all ageing tissues (Kirkwood 2005, Vijg and Campisi 2008, Gems and Partridge 2013). However, the cell biological and molecular mechanisms behind these processes are far from being completely understood.

5.1.2. Cellular hallmarks of ageing

In 2013, López-Otín and colleagues determined the ageing phenotype by categorizing nine hallmarks of ageing (López-Otín et al. 2013). One hallmark of cellular ageing is the stable arrest of the cell cycle, called senescence, which results in decreased proliferative capacities (Hayflick and Moorhead 1961). During ageing, cells increasingly undergo senescence with morphological and metabolic changes (Collado et al. 2007, Kuilman et al. 2010). Senescent cells are characterized by the high abundance of the enzyme beta-galactosidase (β-Gal), detectable at conditions of pH 6 while the normal activity of lysosomal β-Gal is only detectable at pH 4 (Kurz et al. 2000). In 1995, Dimri and colleagues detected increasing accumulation of β-Gal activity at pH 6 in the dermis and epidermis of human skin samples from donors of different ages (Dimri et al. 1995). Since β-Gal at pH 6 could only be detected in senescent cells and not in immortalized cell populations or proliferating cells, Dimri termed this phenomenon senescence-associated β-Gal (SA-β-Gal) (Dimri et al. 1995, Debacq-Chainiaux et al. 2009). In the following years, more studies validated this age-associated activation of SA-β-Gal, establishing SA-β-Gal as a prominent biomarker of cellular senescence. For instance, chondrocytes from articular cartilage of osteoarthritis patients exhibited significantly elevated levels of SA-β-Gal activity when compared to healthy tissue (Price et al. 2002). Further, in atherosclerosis patients, vascular smooth muscle cells in atherosclerotic plaques showed increased SA-β-Gal activity compared to normal vessels from the same patients (Matthews et al. 2006). Increased activity of SA-β-Gal in human liver tissue was also associated with progressive hepatitis C and hepatocellular carcinomas but also with advanced age of healthy people(Paradis et al. 2001). *In vitro* experiments with serially passaged human umbilical vein endothelial cells (HUVEC) and rabbit aortic smooth muscle cells likewise demonstrated high levels of SA-β-Gal activity in late passage cultures compared to early passages (van der Loo et al. 1998).

Next to senescence, stem cell exhaustion is a further hallmark of ageing and can be observed in various tissues with age-associated decline in their regenerative potential. As one example, hematopoietic stem cells (HSCs) of old mice possessed less proliferative potential than HSCs of young mice, leading to diminished hematopoiesis and thus decreased production of immune cells (Rossi et al. 2007, Shaw et al. 2010). This decline in proliferation was reported to be accompanied by overexpression of p16^{INK4a}, a marker of cellular senescence (Janzen et al. 2006). Decreased functional capacities of neuronal

progenitors in the ageing mouse forebrain were accompanied with reduced proliferation of progenitor cells in the subventricular zone and neurogenesis in the olfactory bulb and potentially caused by increased expression of p16^{INK4a} (Molofsky et al. 2006). Although bone fracture healing was shown to be not decreased in healthy elderly patients (Wollstein et al. 2020), the risk for osteoporosis-associated fractures increased with age (Compston et al. 2019). Moreover, osteoporosis was partially caused by inhibited differentiation of mesenchymal stem cells (MSCs) and progenitor cells into osteoblasts (Feng and McDonald 2011). In other studies, satellite cells of the skeletal muscle showed decreased proliferative capacities upon injury which was a consequence of diminished Delta/Notch-signaling (Carlson et al. 2008, Conboy and Rando 2012). Moreover, with increasing age, satellite cells were reported to lose their ability to switch from a quiescent state to an activated state following p16^{INK4a} overexpression (Sousa-Victor et al. 2014). Finally, as the leading cause of death worldwide (Nowbar et al. 2019), cardiovascular diseases were shown to be accompanied by a reduced regenerative potential of quiescent cardiac stem cells and decreased cardiomyocyte-proliferation (Laflamme and Murry 2011, Aguilar-Sanchez et al. 2018). In 2007, Sharpless and DePinho introduced a 'stem-cell hypothesis' for age-associated conditions postulating that anti-cancer mechanisms such as telomere shortening lead to aged stem cells with reduced regenerative function and consequently to an overall ageing of the body (Sharpless and DePinho 2007). This hypothesis points out that stem cell-based regeneration relies on a fragile equilibrium between proliferation and/or differentiation on the one side and protection from cancer on the other side. Thus, targeting single genes or pathways in order to oppose the ageing process harbors great risks for unwanted side-effects.

5.1.3. The potential of young blood and blood plasma for treating for systemic ageing

In the last years ageing research has become a growing field and multiple scientific attempts were proposed to target the ageing process and thus to increase health span. Since ageing can be considered as a systemic process with dynamically changing factors, a potential treatment should address multiple pathways and their regulation. Blood and its liquid part blood plasma act as transport organ, connecting all tissues of the body by carrying nutrients and metabolites as well as signaling molecules. Blood plasma consists to

90 % of water, 8 % of proteins, 0.9 % of salts and 1.1 % of organic substances. Proteins found in plasma mainly comprise albumins, globulins and coagulation proteins but also cytokines and hormones (Krebs 1950, Anderson and Anderson 2002, Elghblawi 2018, Mathew et al. 2020). These interactive and omnipresent characteristics of the blood underline its importance in systemic ageing and degeneration. Ageing research gained momentum with the first heterochronic parabiosis experiments resulted in remarkably systemic responses of old mice to blood of young mice (Conboy et al. 2005). Heterochronic parabiosis is a surgical technique where two animals (mice) are manipulated to share the same circulatory system, leading to systemic administration of young blood and blood borne factors to an old animal and *vice versa*. In 2005, Conboy and colleagues performed heterochronic parabiosis experiments in mice and detected significantly enhanced regeneration of muscle tissue after injury in old animals that shared a blood circulation with young partners (Conboy et al. 2005). Next to increased regenerative capacities of old muscle tissue, this study further revealed increased proliferation of hepatocytes in aged mice undergoing heterochronic parabiosis compared to isochronic parabionts (Conboy et al. 2005). The Wyss-Coray group detected beneficial effects of young blood on the aging hippocampus of old parabionts on molecular, structural and cognitive level (Villeda et al. 2014). A rejuvenating effect of young blood on pancreas tissue of aged mice could be shown in heterochronic parabiosis experiments measuring increased proliferation of β-cells (Salpeter et al. 2013). However, critics repeatedly referred to the artificial characteristics of the experimental system parabiosis, since next to blood borne factors which are shared in both animals also physiological differences between old and young mice could influence the experimental outcome. For instance, young mice have a significantly lower blood pressure (Loffredo et al. 2013). Further, the old heterochronic parabiont benefits from the younger organs like lungs, liver and kidney in terms of more efficient removal of metabolites and improved blood oxygenation (Conboy et al. 2015). Proceeding from the promising results in heterochronic parabiosis experiments with mice, further studies focused the question to which extend these data could be reproduced in the human system. In this regard, Castellano and coworkers applied human umbilical cord blood plasma to aged mice and detected enhanced synaptic plasticity, leading to improved cognitive function. Moreover, comparisons of human umbilical cord plasma with plasma of young and old adult people via protein microarrays revealed the tissue inhibitor of

metalloproteinases 2 (TIMP2) to be enriched in umbilical cord plasma. Additional depletion experiments suggested a direct connection of TIMP2 abundance with the beneficial effects of cord plasma (Castellano et al. 2017). Recently, the first clinical trials were conducted investigating the effects of blood or plasma from young administered to old participants. Edgren and colleagues performed a retrospective cohort study using data from the Scandinavian Donations and Transfusions database assessing a potential association between donor age and sex and the recipient's survival rate of red blood cell transfusions. Here, data of 968 264 patients did not show a connection between donor age and sex and the survival rates of the recipients (Edgren et al. 2017). Further, the Wyss-Coray group performed a phase I clinical study, testing safety, tolerability, and feasibility of fresh frozen plasma (FFP) from young donors (age 18 - 30) infused to 18 patients with Alzheimer's disease (Sha et al. 2019). This study aimed to translate the promising results in mice to the human system and showed the general safety and general feasibility of the procedure. Moreover, a clinical study with the blood plasma-derived product GRF6019, a plasma fraction of about 400 proteins, is already finished but peer-reviewed results are only available regarding safety and tolerability (Hannestad et al. 2020) while detailed readout of the respective manifestations of AD within these patients has not yet been published. Although the idea of young blood as a source of diverse beneficial factors that ameliorate the phenotypic manifestations of ageing is tempting, a recent review by Hofmann reminded that a transition of these promising results from the murine to the human system was so far not successful (Hofmann 2018).

5.1.4. Blood-borne anti-ageing and pro-ageing factors

In the following years, studies dealing with the 'rejuvenating agent' young blood focused on specific factors such as cytokines, chemokines or micro ribonucleic acids (miRNAs). Proteomic analyses of old and young blood and plasma have revealed a range of factors that increase or decline with age. Chiao and colleagues have identified matrix metalloproteinase 9 (MMP9) and monocyte chemotactic protein 1 (MCP1) as plasma proteins showing elevated levels in aged mice. Moreover, this increase in MMP9 and MCP1 protein-levels in plasma correlated with a cardiac ageing phenotype. The authors therefore concluded that MMP9 and MCP1 could serve as new biomarkers for cardiac ageing (Chiao et al. 2011). A later study showed likewise elevated MCP1 plasma levels in aged and

progeroid mice compared to young individuals. This effect was slightly but not significantly increased in male mice, indicating sex-specific differences of the ageing process. Interestingly, MCP1 plasma levels were also higher in frail patients with aortic stenosis compared to non-frail patients (Yousefzadeh et al. 2018). Another factor which is potentially contributing to the ageing phenotype is the chemokine Eotaxin 1, or C-C motif chemokine 11 (CCL11), which was identified in parabiosis experiments with mice. Here, increasing plasma levels of Eotaxin 1 correlated with decreased neurogenesis and impaired learning and memory in old mice (Villeda et al. 2011). Moreover, Eotaxin 1 was also measured in fresh frozen plasma as well as erythrocyte concentrate (EC) of human transfusion donors with increasing levels in aged donors (Hoefer et al. 2017). In different heterochronic parabiosis studies, Loffredo and coworkers measured plasma levels of the growth differentiation factor 11 (GDF11) which declined with age (Loffredo et al. 2013). Using heterochronic parabiosis, the symptoms of age-related cardiac hypertrophy could be reversed in old mice. This effect was also achieved by only intraperitoneal injection of GDF11, leading to the description of GDF11 as a circulating rejuvenating factor (Loffredo et al. 2013). Contrary results were published in 2015 by Egerman and colleagues who detected increased levels of GDF11 in sera of old rats and humans which inhibited skeletal muscle regeneration in rats. The authors discussed these contradicting results to the Loffredo-study with non-specificity of the used GDF11 antibodies shown by cross reactivity with myostatin (GDF8) (Egerman et al. 2015). Later, the Loffredo-group responded with additional results showing that both, GDF11 and GDF8 decline with age in mice, rats, horses, and sheep and claimed that the increased signal detected by Egerman and colleagues was caused by cross-reactivity of the GDF11 antibody with immunoglobulin, a highly abundant protein in blood which is known to increase with age (Poggioli et al. 2016). These partially contradicting data underline the high interest in potential active components of 'rejuvenating' blood and blood products while the discussion has not yet come to a consensus. Moreover, to understand potential anti-ageing effects of young human blood and plasma on a cellular and molecular level, suitable human cellular model systems are necessary. Here, particularly adult human stem cell populations are increasingly noticed as promising cellular model systems.

5.2. Stem cells

5.2.1. From totipotent to pluripotent stem cells

The highly diverse variety of specialized cell types in the adult organism is derived from the same totipotent stem cell, the zygote. The main characteristics of a stem cell are its ability for self-renewal by symmetric cell divisions and the differentiation into specialized cell types by asymmetric or symmetric cell divisions. Symmetric cell divisions result in the formation of two daughter cells that keep the stem cell-state of the parental stem cell or two differentiating daughter cells while asymmetric cell divisions produce one stem cell and one differentiating cell (He et al. 2009). During embryogenesis and consecutive cell divisions, the so-called developmental potential of the stem cells decreases from totipotency to pluripotency and later multipotency while the determination of each cell to a specific tissue or function increases (Rajagopal and Stanger 2016). In this context, the totipotent zygote is able to give rise to all cell types of the developing organism as well as extraembryonic tissue (e.g. placenta) while pluripotent cells are able to differentiate into cell types of the three germ layers ectoderm, mesoderm and endoderm as well as germ cells. Pluripotent stem cells can only be found in the inner cell mass of the blastocyst during the early stages of embryogenesis as embryonic stem cells (ESCs) (Evans and Kaufman 1981, Martin 1981, Thomson et al. 1998). Since 2006, it is possible to reprogram terminally differentiated cells to a pluripotent state *in vitro* (Takahashi and Yamanaka 2006). Here, the induction of the four pluripotency-associated transcription factors cMyc, Kruppel-like factor 4 (Klf4), octamer-binding transcription factor 4 (Oct4) and sex determining region Y-box 2 (Sox2) generated induced pluripotent stem cells (iPSCs). These iPSCs exhibited all hallmarks of embryonic stem cells like differentiation capacity into cell types of all three germ layers as well as germ cells and contributed to a developing embryo (Takahashi and Yamanaka 2006, Takahashi et al. 2007). However, later studies have shown that iPSCs remained an epigenetic memory of their cell type of origin (Kim et al. 2010, Vaskova et al. 2013) and showed overall high mutation rates (Gore et al. 2011). In further attempts of iPSC-transplantation in mice in order to regenerate injured tissues it was revealed that the induced pluripotency was associated with low genetic stability and thus lead to the formation of tumors in the recipient organisms (Arnhold et al. 2004, Amariglio et al. 2009). These properties of iPSCs hampered their transfer to clinical applications. Compared to

pluripotent stem cells, the term multipotency defines a closer restriction of stem cells to differentiate into derivates of one or two germ layers, particularly into cell types of the tissue of origin (Toma et al. 2001).

5.2.2. Adult stem cells

In the adult human organism, populations of multipotent human stem cells (ASCs) are located in various tissues and organs with prominent examples like mesenchymal stem cells and hematopoietic stem cells in the bone marrow (Becker et al. 1963, Pittenger et al. 1999), neural stem cells (NSCs) in the hippocampus and the subventricular zone (SVZ) of the brain (Johansson et al. 1999) and mesenchymal stem cells in the adipose tissue (Adipose-derived stem cells, ADSCs) (Zuk et al. 2002). ASC populations are key players in endogenous repair mechanisms and are therefore discussed as highly promising tools for regenerative medicine (Conrad and Huss 2005, Gurusamy et al. 2018, Prentice 2019). Here, the biggest advantages of ASCs in comparison with pluripotent stem cells like ESCs or iPSCs are their genetic stability and a decreased potential for tumor formation. Further, ASCs enable the possibility of autologous transplantations without immunosuppression of the recipient. Moreover, ethical issues that need to be considered when working with ESCs are avoided (Mezey et al. 2003, Meza-Zepeda et al. 2008), since ASCs can be taken from adult patients after informed consent. However, the greatest restriction of ASCs in clinical applications lies within their limited differentiation potential and thus decreased regenerative capacity when compared with pluripotent stem cells. Nevertheless, ASCs are subject of highly successful treatments in clinical use (Ghodsizad et al. 2013, Steinberg et al. 2016).

5.2.3. The neural crest and neural crest-derived stem cells

Among the ASCs, a subpopulation of cells exhibits an extraordinary broad potential for differentiation into distinct cell types. These cells are derived from the neural crest, a transient structure of the vertebrate embryo and thus termed neural crest-derived stem cells (NCSCs) (His 1868, Jiang et al. 2002, d'Aquino et al. 2011). During embryogenesis, stem cells migrate out from the neural crest into various parts of the developing body where they give rise to different organs and tissues or remain as quiescent stem cells in an undifferentiated state. The various populations of NCSCs can be discriminated according to their region of origin. For example NCSCs from the cranial neural crest could be found in

diverse tissues of the head and neck region like the skin and hair follicles (Toma et al. 2001, Hunt et al. 2008), the periodontal ligament (Techawattanawisal et al. 2007), dental pulp (Waddington et al. 2009) and palatum (Widera et al. 2009, Zeuner et al. 2018), as well as the olfactory epithelium or the respiratory epithelium of the nose (Viktorov et al. 2007, Barraud et al. 2010, Hauser et al. 2012). Derivates of the cardiac neural crest are important in the formation of the cardiac outflow tract (Sieber-Blum 2004) and undifferentiated NCSCs could be found in the ventricles and atrial appendages of the adult mammalian heart (El-Helou et al. 2005, Tomita et al. 2005, El-Helou et al. 2008, Höving et al. 2020b). Other tissues shown to harbor NCSC-populations included the bone marrow (Nagoshi et al. 2011), sciatic nerve (Morrison et al. 1999), dorsal root ganglia (Li et al. 2007) and the carotid body (Pearse et al. 1973, Pardal et al. 2007).

5.2.4. Examples of neural crest-derived stem cell populations

As two examples of niches of adult neural crest-derived stem cells, the inferior turbinate as well as the middle turbinate of the human nose were shown to harbor multipotent stem cell populations which could be easily isolated from the respiratory epithelium of surgical waste during routine surgery. Inferior turbinate stem cells (ITSCs) were first characterized in 2012 as a neural crest-derived stem cell population expressing a wide range of stem cell- and NCSC-markers (Hauser et al. 2012). Further, *in vitro* differentiation assays demonstrated an extraordinary broad differentiation capacity into cell types with neuro-ectodermal as well as mesodermal phenotype. ITSCs efficiently differentiated into functional glutamatergic neurons expressing the neuronal marker β-III-Tubulin at a rate of 70 % (Müller et al. 2015). A differentiation of ITSCs into oligodendrocytes was demonstrated by Ruiz and coworkers following the inhibition of the nuclear factor (NF)-κB subunit c-Rel (Ruiz-Perera et al. 2020). *In vivo,* ITSC-derived dopaminergic neurons efficiently integrated into the rat brain improving the functional outcome of Parkinson's disease symptoms (Müller et al. 2015). Moreover, ITSCs responded to biochemical stimuli or the presence of specific nanopores on substrate surface with differentiation into the osteogenic lineage (Greiner et al. 2019). In addition, ITSCs were introduced as model system for rhinosinusitis, the common cold, to study pharmacological treatments (Müller et al. 2016). Likewise to ITSCs, NCSCs located in the middle turbinate (middle turbinate stem cells, MTSCs) expressed the NCSC-markers Nestin, S100 and p75 neurotrophin

receptor (p75NTR) and exhibited a differentiation capacity into the ectodermal as well as mesodermal lineage (Schürmann et al. 2018). Moreover, high amounts of tissue material could easily be removed during routine nasal biopsies without severely affecting the respiration and olfactory sensing (Scheithauer 2010, Dayal et al. 2016). Here, total turbinectomies of the inferior turbinate may be associated to empty nose syndrome in rare cases (Scheithauer 2010) and the air conditioning capacity of the nasal cavity may be significantly impaired compared to total middle turbinectomy (Dayal et al. 2016). These outcomes presented the middle turbinate and MTSCs as promising NCSC source for potential clinical applications.

5.3. Cardiac stem cells as cellular model systems for age-associated degeneration of the heart

5.3.1. Heart regeneration

Despite the existence of resident cardiac stem cell populations, the regenerative capacities of the aging human heart are limited and cardiovascular diseases are the leading cause of death worldwide (Bhatnagar et al. 2016, Nowbar et al. 2019, WHO 2021). In ischemic heart disease (IHD) as the most common cardiovascular disease, plaques within the coronary arteries can lead to myocardial infarcts (MI) with a blockage of oxygen and nutrient supply for the myocardial tissue. The resulting irreversible loss of cardiomyocytes as the contracting entities of the heart structure is substituted by scar tissue with fibroblasts, leading to decreased cardiac function (Reinecke et al. 2008). This repair process is mediated by intra- and intercellular signaling and its effectiveness determines the further progression into heart failure (HF) (Molenaar et al. 2021). Although mortality directly after MI decreased by 28 % in the last years, the 5-year-incidence of heart failure following MI increased by 25 %, underlining the poor regenerative capacities of cardiac tissue especially in elderly patients (Velagaleti et al. 2008, Ezekowitz et al. 2009). During fetal development, proliferating cardiomyocytes could be detected in the growing heart (Laflamme and Murry 2011). However, the proliferative capacities of cells in the adult human heart were described to be generally low with a yearly turnover of 0.5 % – 1 % (Bergmann et al. 2009, Bergmann et al. 2015).

5.3.2. Adult cardiac stem cell populations

Although the adult heart was long time considered as a terminally differentiated organ with low regenerative potential, rare populations of adult stem cells have been found in the murine heart (Beltrami et al. 2003, Koninckx et al. 2013) and later also in the human heart (Bearzi et al. 2007). These cardiac stem cell populations were found to be multipotent, giving rise to cardiac endothelium and myocardium, although the *in vivo* contribution to regenerative processes is still under debate (Breckwoldt et al. 2016, He et al. 2020). Initially, most cardiac stem cell (CSC) populations were identified based on their expression of the stem cell factor receptor kinase cKit (Beltrami et al. 2003, Urbanek et al. 2006, Bearzi et al. 2007, Tallini et al. 2009, Zaruba et al. 2010). However, cKit expression was also identified in non-cardiac cells like interstitial Cajal cells and HSCs (Escribano et al. 1998, Morita et al. 2003, Rusu et al. 2014, Ilie et al. 2015), making its suitability as unique marker for cardiac stem cells unlikely (Sultana et al. 2015). In later studies, the pool of genes and proteins defining CSCs has been extended to a range of other stem cell markers. The transcription factor Insulin gene enhancer protein 1 (Isl1) has been detected in mouse embryonic stem cells that were able to differentiate into cardiomyocytes, smooth muscle cells and endothelial cells (Cai et al. 2003, Moretti et al. 2006). Stem cell antigen-1 (Sca1)[+] cells were found in the murine heart that may contributed to endogenous repair mechanisms (Matsuura et al. 2004) and further expressed the endothelial cell marker cluster of differentiation 31 (CD31) (Oh et al. 2003). Populations of human cardiac stem cells and cardiac progenitor cells were described to express Sca1 and cluster of differentiation 105 (CD105), while the expression of cKit was only scarce (Smits et al. 2009). Other human cardiac stem cell populations were isolated based on their ability to form spheres (cardiosphere-derived cells, CDC) (Barile et al. 2013) or by the expression of aldehyde dehydrogenase (Koninckx et al. 2013). However, the developmental origin of these adult human cardiac stem cell populations was not investigated so far.

5.3.3. Isolation of a novel population of NC-derived human cardiac stem cell population

To establish a cellular model system for cardiac regeneration, this thesis presents the identification of an adult NC-derived cardiac stem cell population in the human heart (human cardiac stem cells, hCSCs). The human heart auricle (left atrial appendage, LAA)

(Figure 1 A) was obtained from aged patients undergoing cardiac surgery. The routinely amputation of the LAA during surgery aims to minimize the risk for the formation of blood clots which could lead to stroke (Endo et al. 2017). Here, a large amount of tissue (Figure 1 B) could be used for the subsequent isolation of cells via explant culture (Figure 1 C).
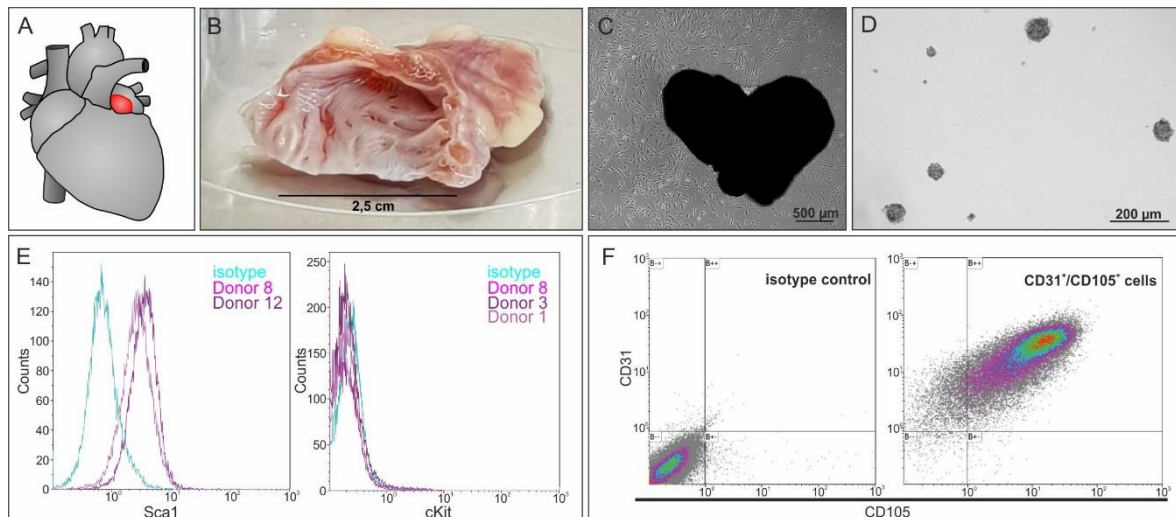

Figure 1: Successful Isolation of CD105⁺/CD31⁺/Sca1⁺ cells from the human heart auricle. A) The human heart auricle (left atrial appendage, LAA) is routinely removed during cardiac surgery. B) Large amounts of tissue are available after LAA amputation. C) After eight days of culture, cells migrate out of the tissue clumps. D) Clonally grown cells spontaneously form spheres. E) Isolated cells express the cardiac stem cell marker Sca1 but not cKit. F) Isolated cells are double positive for the previous described markers of adult human cardiac stem cells CD105 and CD31. Modified from (Höving et al. 2020a)

These cells showed the ability for self-renewal by forming secondary spheres out of clonally grown populations with a clonal efficiency of 22.7 % (Figure 1 D), an important hallmark of stem cells (He et al. 2009). To further characterize the marker profile of the isolated cell population, flow cytometry revealed a purity of 87 % to 95.6 % of Sca1⁺ cells and 92.5 % of cells double positive for CD105 and CD31 (Höving et al. 2020a, Höving et al. 2020b) (Figure 1 E, F). The marker Sca1, CD105 and CD31 were likewise described for human cardiac stem cell populations in previous studies (Smits et al. 2009).

Further, the description of hCSCs was extended from known CSC markers to marker proteins that are known to be expressed in other adult stem cell populations. Next to the CSC markers Sca1, CD31 and CD105, hCSCs expressed common markers of NCSCs, like Slug, Nestin, S100 and p75NTR (Figure 2), suggesting a developmental relation to the NC. Since the developmental origin of adult human stem cells cannot be investigated by lineage tracing studies, the sites of malformations and other defects resulting from mutations in NC-associated genes can give valuable insights in this matter.
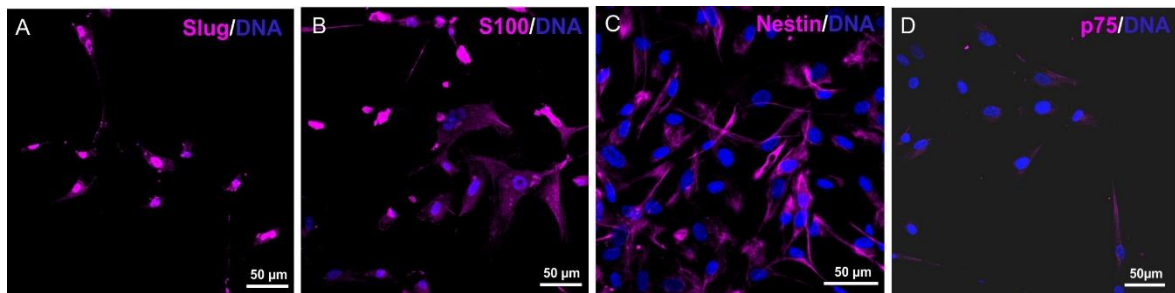
Figure 2: hCSCs express typical markers for NCSCs. A) In vitro cultured hCSCs express the NCSC marker protein Slug. B) In vitro cultured hCSCs express the NCSC marker protein S100. C) In vitro cultured hCSCs express the NCSC marker protein Nestin. D) In vitro cultured hCSCs express the NCSC marker protein p75. Modified from (Höving et al. 2020b)

5.3.4. The neural crest and neural crest-derived stem cells in cardiac development

NCSCs positive for Nestin, an intermediar filament associated with proper self-renewal of stem cells (Park et al. 2010, Kaltschmidt et al. 2012), were already described to be present in the murine heart (El-Helou et al. 2005, Tomita et al. 2005). In particular, the group of El-Helou and coworkers detected a Nestin$^+$ stem cell population in the rat heart, while Tomita and colleagues transferred these findings to the mouse heart and could show that Nestin$^+$ NCSCs were capable to differentiate into cardiomyocytes *in vivo* (Tomita et al. 2005, El-Helou et al. 2008). During embryonic development, cells from the cardiac neural crest contribute to the second heart field, which later develops the cardiac outflow tract and the right ventricle (Morikawa and Cserjesi 2008, Keyte and Hutson 2012). Here, cardiac neural crest cells were described to contribute to the myocardium by myocardialization (Poelmann et al. 1998, Gittenberger-de Groot et al. 2005). In further developmental steps, cardiac neural crest cells were expected to disappear from myocardial tissues undergoing apoptosis. However, in the hearts of adult mice and zebrafish, populations of neural crest-derived stem cells were recently described (El-Helou et al. 2008, Hatzistergos et al. 2015, Leinonen et al. 2016, Meus et al. 2017, Tang et al. 2019). However, in the various stem cell populations isolated from the adult human heart, no potential relation to the neural crest was investigated so far. Notably, a high number of neural crest-related genes was found to be expressed in hCSCs and mutations in these genes were shown to result in craniofacial malformations as well as cardiac defects (Höving et al. 2020b). Malignancies resulting from mutations in NC-associated genes can give valuable insights into human NC-development and its role in organ formation. The Baraitser-Winter syndrome was suggested to be caused by a mutation in the β-actin gene (ACTB), presented by defects in the development of the brain and the structure of the eye but also leading to hearing loss and cardiac

malformations (Cuvertino et al. 2017). Meanwhile, mutations in the gene for Gap junction alpha-1 protein or connexin 43 (GJA1, Cx43) lead to occludential dysplasia shown as digital and craniofacial malformations next to cardiac abnormalities (Paznekas et al. 2003, Debeer et al. 2005). Mutations in the NOTCH1 gene caused not only the Alagille syndrome but also the autosomal dominant form of Adams-Oliver syndrome with partial absence of skull bones and congenital heart defects in 23 % of the patients (Southgate et al. 2015, Masek and Andersson 2017). Hirschsprung's disease is a neurological disorder in the hindgut with 5 % of the patients exhibiting congenital heart diseases and is shown to be caused by a mutation of the ret proto-oncogene (RET) (Robertson et al. 1997, Tuo et al. 2014). Twist was described as a popular marker for neural crest-derived stem cells and mutations in the TWIST-gene caused Saethre-Chotzen syndrome with craniofacial malformations and congenital heart malformations (Kress et al. 2006, Pelc and Mikulewicz 2018). Another consequence of improper neural crest development could be Kabuki syndrome with craniofacial dymorphism, mild-to-moderate intellectual disability and congenital heart defects in 70 % of the patients following mutation of the Histone-lysine N-methyltransferase 2D (KMT2D) gene (Digilio et al. 2017, Adam et al. 2019, Shpargel et al. 2020). Moreover, congenital heart diseases which were described to have direct links to mis-regulated cardiac neural crest development are CHARGE syndrome (Pauli et al. 2017), DiGeorge syndrome (Wurdak et al. 2005) and Alagille syndrome (McDaniell et al. 2006, Humphreys et al. 2012). While adult cardiac stem cells with neural crest origin were already described in animal models such as the murine or the zebrafish system, the existence of NC-derived human cardiac stem cells has not been shown so far (El-Helou et al. 2008, Hatzistergos et al. 2015, Tang et al. 2019). However, a broad range of other human NCSC populations was extensively described in recent years (Viktorov et al. 2007, Hauser et al. 2012, Schürmann et al. 2018), confirming that NCSC populations also exist in the adult human system in many niches. In addition, the wide range of different human cardiac malignancies linked to improper neural crest development suggests the presence of NC-derived human cardiac stem cells in the adult organism.

5.3.5. Identification of NCSC-hallmarks in hCSCs

Regarding their NCSC-like marker profile, hCSCs were subjected to a range of differentiation assays to investigate a putative NC-specific differentiation potential. The

capability of differentiation into mesodermal as well as ectodermal derivates is one hallmark of NCSCs. By application of a defined protocol for myocardial differentiation of CD105$^+$/CD31$^+$/Sca1$^+$ adult cardiac stem cells (Smits et al. 2009) (Figure 3 A), hCSCs successfully differentiated into αActinin$^+$ cardiomyocytes while no expression of αActinin was visible in the undifferentiated cells (Figure 3 B,C) (Höving et al. 2020a). Moreover, coculture experiments of green fluorescent protein (GFP)-marked hCSCs and primary neonatal mouse cardiomyocytes were performed to assess the presence of beating hCSC-derived cardiomyocytes (Figure 3 A). After 11 days of coculture, the first GFP$^+$ beating hCSC-derived cardiomyocytes were observable, confirming successful differentiation of hCSCs into the cardiomyogenic lineage (Figure 3 D) (Höving et al. 2020b). These results further demonstrated that hCSCs were able to integrate into a cardiomyogenic environment *in vitro* and to give rise to functional beating cardiomyocytes like *bona fide* cardiac stem cells. With regard to the literature, assessing the cardiomyogenic potential of adult human (cardiac) stem cells is a complex task (Messina et al. 2004, Bearzi et al. 2007, Oldershaw et al. 2019). Until today, research in stem cell-based cardiac regeneration is mostly focused on pluripotent stem cells, mainly iPSCs, since these have been shown to differentiate much more robustly into functional cardiomyocytes *in vitro* (Zwi-Dantsis et al. 2013, Duelen and Sampaolesi 2017, Lin et al. 2017, Friedman et al. 2018, Kempf and Zweigerdt 2018).
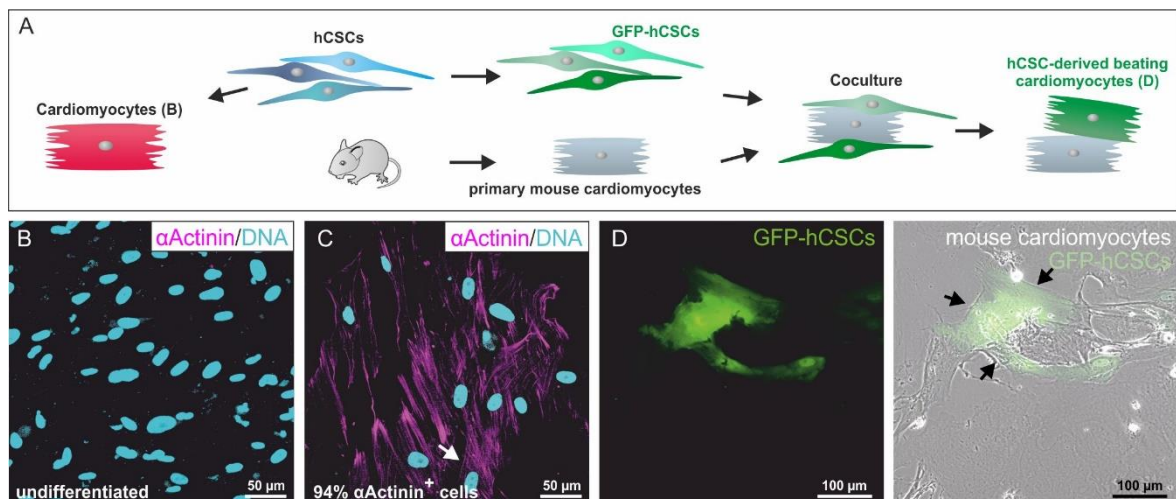
Figure 3: Successful differentiation of hCSCs into functional beating cardiomyocytes. A) Two different strategies were applied to differentiate hCSCs into mature cardiomyocytes. B) Undifferentiated hCSCs did not express the cardiomyocyte-protein αActinin. C) Application of biochemical cues led to the differentiation of hCSCs into αActinin+ cells with a high efficiency of 94 % positive cells. However, spontaneous beating could not be detected. D) Coculture of lentiviral transduced GFP+ hCSCs with primary neonatal mouse cardiomyocytes induced hCSC differentiation into functional beating cardiomyocytes. Beating cells are indicated by arrowheads. Modified from (Höving et al. 2020a, Höving et al. 2020b)

In addition, the ability of hCSCs to undergo differentiation into ectodermal derivates like neurons was tested by the application of a defined medium for glutamatergic neuronal

differentiation of adult human stem cells (Müller et al. 2015). Notably, immunocytochemistry revealed 1% Neurofilament[+]/β-III-Tubulin[+] and 2% Synaptophysin[+]/vesicular glutamate transporter (VGlut)[+] neuron-shaped cells (Figure 4 A) (Höving et al. 2020b). The capability to give rise to cardiomyocytes as well as to neuron-like cells demonstrated an extended differentiation potential of hCSCs into mesodermal and ectodermal cell types. Moreover, hCSCs likewise differentiated into the adipogenic lineage, indicated by positive Oil Red O staining as well as into the osteogenic lineage, depicted by Alizarin Red-stained calcium deposits (Figure 4 B, C), with both differentiations serving as additional examples of mesodermal differentiation. However, a direct comparison with ITSCs, another NCSC population, also showed differences in the differentiation potential of both stem cell populations. ITSCs exhibited a remarkably high ability to differentiate into the neuronal lineage of 70 % (Müller et al. 2015, Ruiz-Perera et al. 2018, Ruiz-Perera et al. 2020), which was significantly higher than in hCSCs. These data suggested that niche-specific differences between distinct NCSC populations existed that could not be explained by a comparison of only cell surface maker expression. In this context, Iancu and coworkers proposed that the sole description of cell surface markers could not be sufficient to distinguish cardiac and non-cardiac cell populations but that it preferably needs an extended marker profile with a combination of cell surface markers and global gene expression (Iancu et al. 2015).
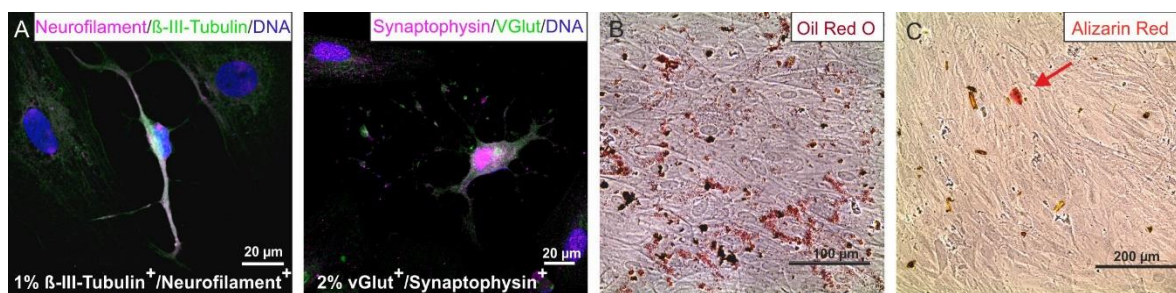
Figure 4: hCSCs differentiate into neuroectodermal and mesodermal phenotypes. A) Upon application of a defined medium, hCSCs differentiated into neuron-like cells with an efficiency of 1 % β-III-Tubulin+/Neurofilament+ cells and 2 % vGlut+/Synaptophysin+ cells. B) hCSCs are capable of adipogenic differentiation indicated by Oil Red O staining. C) hCSCs undergo osteogenic differentiation. Calcium deposits are stained by Alizarin Red (arrowhead). Modified from (Höving et al. 2020b)

5.3.6. Direct comparison of the global gene expression profiles of hCSCs and ITSCs

To further investigate the context between hCSC differentiation capacity and a possible niche-specific expression profile, RNA sequencing (RNA-Seq) of hCSCs and ITSCs from four distinct donors each was performed. RNA-Seq provides quantitative expression data from

thousands of genes within one sample and is thus a powerful tool to compare the expression profiles of biomarkers and their principal signaling pathways within distinct (stem) cell populations. Next to transcriptomic differences between stem cell populations from different sources, RNA-Seq also allows to detect shared gene expression and pathways and with this a more detailed classification of distinct populations (Gunnarsson et al. 2016). A bioinformatic comparison of RNA-Seq data of hCSCs and ITSCs revealed 4367 genes to be significantly differentially expressed between hCSCs and ITSCs (p < 0.05) (Figure 5 A). To reduce this data dimensionality, gene ontology (GO)-term enrichment was performed and revealed that the most significantly enriched GO-terms were clearly linked to the tissues of origin, namely the olfactory epithelium and the heart (Höving et al. 2020b). In detail, the terms 'blood vessel development' ($p \approx 1.9 \times 10^{-7}$), 'blood vessel morphogenesis' ($p \approx 3 \times 10^{-6}$) or 'heart development' ($p \approx 1.5 \times 10^{-5}$) were highly enriched in hCSCs and described an expression profile necessary for cardiovascular development (Figure 5 B). In contrast, the terms 'detection of chemical stimulus involved in sensory perception' ($p \approx 1.5 \times 10^{-4}$), 'sensory perception of chemical stimulus' ($p \approx 1.7 \times 10^{-3}$) and 'detection of chemical stimulus involved in sensory perception of smell/taste' ($p \approx 4.9 \times 10^{-3}$ and $p \approx 5.1 \times 10^{-3}$) were enriched among the genes upregulated in ITSCs (Figure 5 C) (Höving et al. 2020b).
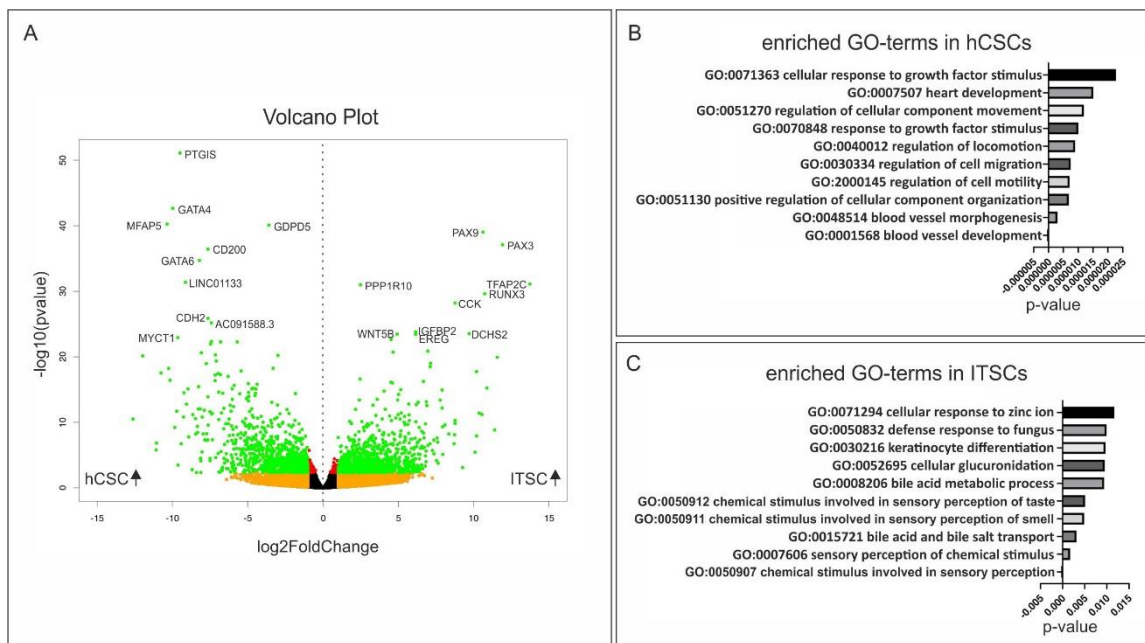
Figure 5: Comparison of the global gene expression profiles of hCSCs and ITSCs. A) Volcano plot depicts 4367 genes to be significantly differentially expressed (p < 0.05) between hCSCs and ITSCs (green points). B) Top 10 most significantly enriched GO-terms of genes upregulated in hCSCs compared to ITSCs. C) Top 10 most significantly enriched GO-terms of genes upregulated in ITSCs compared to hCSCs. Modified from (Höving et al. 2020b)

In other studies comparing different stem cell populations based on RNA-Seq data, Taskiran and colleagues compared human dermal fibroblasts and bone marrow-derived MSCs identifying diverse homeobox genes to be differentially expressed (Taskiran and Karaosmanoglu 2019). Homeobox genes and paired box (PAX) genes act as regulators of morphogenesis and cell differentiation (Mark et al. 1997). Similarly, within this analysis, the genes PAX9 and PAX3 were found to be among the highly upregulated genes in ITSCs compared to hCSCs (Figure 5 A). PAX3 has been associated to proper cranial neural crest development, a subpopulation of neural crest cells particularly giving rise to cells of the head and neck region like bone and cartilage or pigment cells (Tremblay et al. 1995, Bhatt et al. 2013, Boudjadi et al. 2018). Meanwhile, PAX9 was shown to be important in the initiation of tooth development (Bonczek et al. 2017, Wong et al. 2018). In a study of Jansen and colleagues, MSC populations from different sources were compared using microarray technology, showing that the global transcriptome reflects the functional status of these populations. The authors therefore concluded that assessing the transcriptomic profile of a stem cell population is a suitable tool to describe its identity (Jansen et al. 2010). In summary, a side-by-side comparison of hCSCs and ITSCs depicted similarities in terms of NCSC marker expression while RNA-Seq and differentiation assays also showed differences reflecting the particular niches and tissues of origin (Höving et al. 2020b). Considering the here described differences and similarities between hCSCs and ITSCs, a transcriptome-based comparison of hCSCs and ITSCs to other known adult human stem cell populations was performed.

5.3.7. Comparison of hCSCs and ITSCs with known adult human stem cell populations

Transcriptome data of adipose-derived mesenchymal stem cells (AdMSCs) (NCBI GEO-accession number GSE142831), cardiosphere-derived cells (Harvey et al. 2017) and cluster of differentiation 34 (CD34)[+] hematopoietic stem cells (Sinnakannu et al. 2020) were accessed to conduct a comparison of distinct adult human stem cells populations. A principal component analysis (PCA) revealed all cell populations to form single clusters with HSCs being the most separated cluster (Figure 6 A). Moreover, a hierarchical clustered heatmap showing the 200 genes with the highest variance among samples clearly depicted

HSCs as a population with high differential gene expression compared to hCSCs, ITSCs, CDCs and AdMSCs (Figure 6 B).
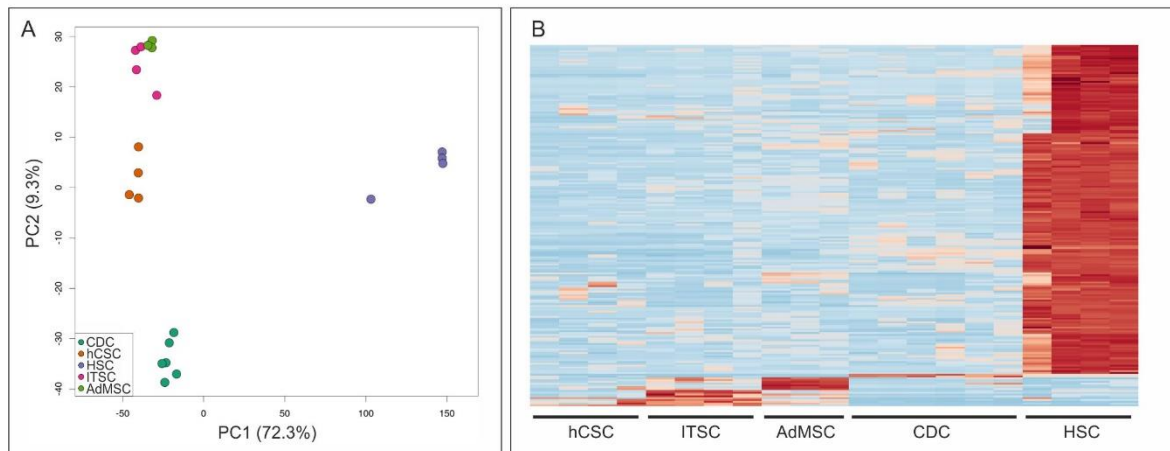

Figure 6: Global gene expression profiling reveals similarities between hCSCs, ITSCs, AdMSCs and CDCs and differences to HSCs. A) Principal component analysis shows distinct clusters of the single stem cell populations with smaller differences between AdMSCs (green), ITSCs (pink), hCSCs (orange) and CSCs (turquoise) and greater differences to HSCs (purple). B) Hierarchical clustered heatmap of the 200 genes with the highest variance among all samples CDC: cardiosphere-derived cells, hCSC: human cardiac stem cells, HSC: hematopoietic stem cells, ITSC: Inferior turbinate stem cells, AdMSC: Adipose-derived Mesenchymal stem cells. Modified from (Höving et al. 2020b)

Interestingly, the transcriptomic profiles of AdMSCs and HSCs seemed to be highly different although both cell populations originally arise from the mesoderm. These results may hint to a shared transcriptomic regulation of adherent cell populations from different niches while HSCs as non-adherent population represent a more distinct type of adult human stem cells. This theory was underlined by the high amount of 16,129 differentially expressed genes between hCSCs and ITSCs compared to HSCs (Figure 7 A), while only 4,367 genes were differentially expressed between hCSCs and ITSCs (Figure 5 A). Accordingly, a functional enrichment analysis of differentially expressed genes between HSCs compared to hCSCs and ITSCs showed an overexpression of adherent stem cell-associated terms in hCSCs and ITSCs. The most significantly upregulated Kyoto Encyclopedia of Genes (KEGG)-pathways in hCSCs and ITSCs when compared to HSCs were 'Focal adhesion' ($q \approx 3.5 \times 10^{-7}$) and 'ECM-receptor interaction' ($q \approx 7.4 \times 10^{-6}$) (Figure 7 B), describing the adherent character of hCSCs and ITSCs as a prominent hallmark in both populations. The corresponding GO-terms comprised stem cell- and tissue repair-associated terms like 'tissue morphogenesis' ($q \approx 1 \times 10^{-19}$), 'vasculature development' ($q \approx 2.1 \times 10^{-19}$), 'blood vessel development' ($q \approx 2 \times 10^{-18}$) and 'embryonic morphogenesis' ($q \approx 4.5 \times 10^{-16}$) (Figure 7 C), while in HSCs the GO-terms 'Immune response-regulating cell surface receptor signaling pathway' ($q \approx 9.1 \times 10^{-5}$), 'immune effector process' ($q \approx 1.5 \times 10^{-4}$) and 'regulation of immune response' ($q \approx 1.8 \times 10^{-4}$) were significantly upregulated (Figure 7 D). The

differential gene expression between hCSCs and ITSCs compared to HSCs thus may reflected their diverging developmental potentials. Regarding the hematopoietic fate of HSCs, these results clearly underlined their immune response-related character. Likewise, previous studies showed an upregulated signaling in immune-regulatory pathways in HSCs (Terskikh et al. 2003, Solaimani Kartalaei et al. 2015, Li et al. 2018).
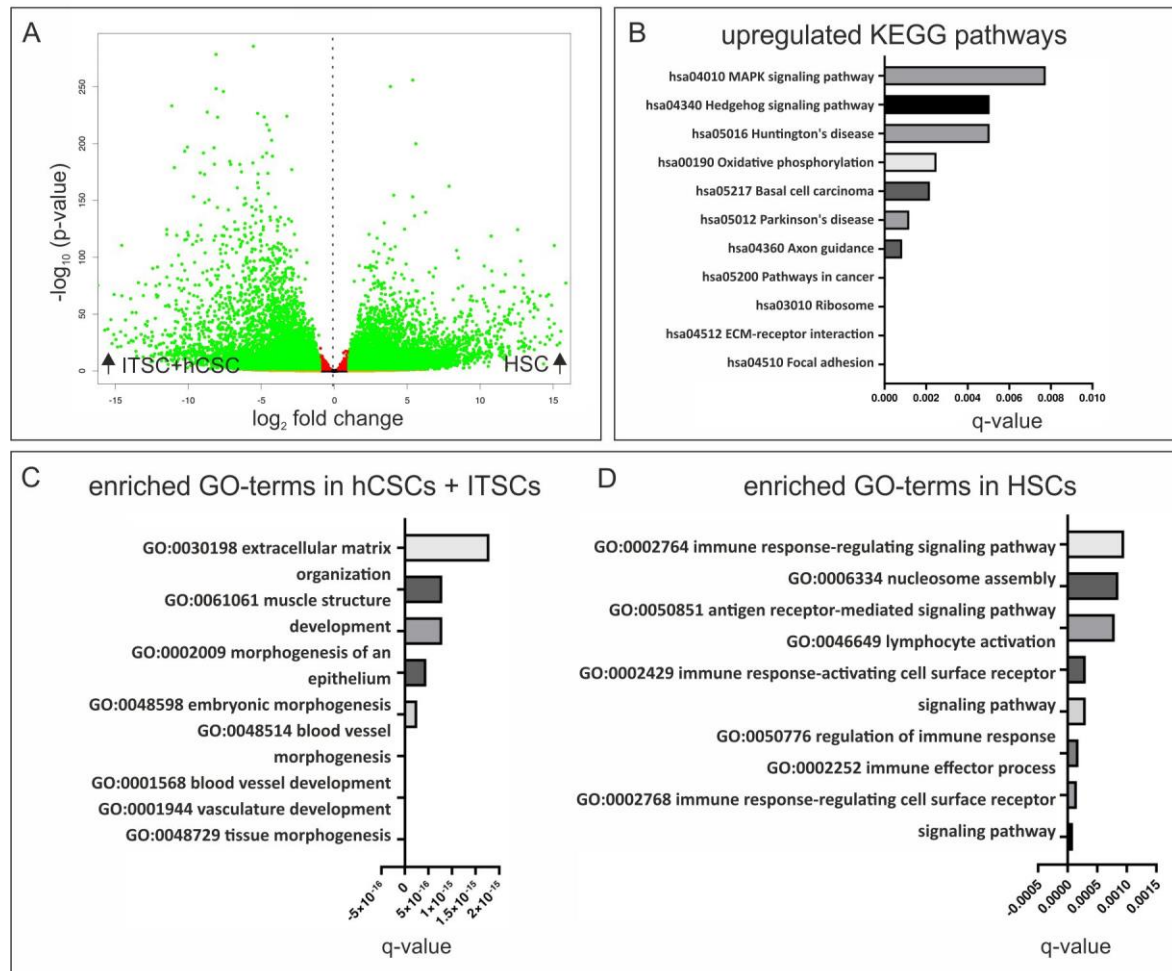
Figure 7: Differential gene expression between hCSCs and ITSCs compared to HSCs. A) Volcano plot depicts 16129 genes to be significantly differentially expressed (p < 0.05) between hCSCs and ITSCs compared to HSCs (green points). B) Top 10 most significantly enriched KEGG pathways of genes upregulated in ITSCs and HCSCs compared to HSCs. C) Top 10 most significantly enriched GO-terms of genes upregulated in ITSCs and hCSCs compared to HSCs. D) Top 10 most significantly enriched GO-terms of genes upregulated in HSCs compared to ITSCs and hCSCs. Modified from (Höving et al. 2020b)

5.3.8. Cardiac stem cell-based approaches for the treatment of a damaged heart

Cardiac stem cells are expected to contribute to endogenous repair mechanisms. However, the overall regenerative capacities of the adult human heart and especially the ageing heart are poor (Breckwoldt et al. 2016). Moreover, direct transplantations of stem cells to a failing heart showed only low success in terms of integration of the stem cells to the recipient's cardiac tissue and thereby regeneration of heart functionality. This limitation

was at least partially caused by a washout due to constant contraction of the cardiac muscle with high pressure and the overall hostile environment of the scar tissue (Zhang et al. 2001, Dow et al. 2005, Qiao et al. 2009). In this regard, the idea of targeting the endogenous regenerative capacities of the human heart as well as cardiomyocyte proliferation is subject of numerous studies aiming to avoid a stem cell transplantation into cardiac tissue (Breckwoldt et al. 2016). In this matter, populations of adult cardiac stem cells could be the ideal model system to study diverse components that potentially influence regenerative activities. Blood serum of young individuals has already shown to increase regeneration of aged and injured tissues in the murine system (Scudellari 2015). Here, the discussion about the active component of young blood serum has not yet come to a consensus, partially caused by discrepancies in the proteomic methods used so far. Further, a translation of these promising results to the human system remains challenging (Hofmann 2018). Therefore, different approaches are necessary to identify potential pathways by these means ultimately also the potentially responsible blood born factors, which are up- or downregulated during the human ageing process and in the respective model systems.

5.4. Treatment with human blood plasma and serum impacts hCSC proliferation, senescence and migration

5.4.1. Induction of hCSC-proliferation by human blood plasma and serum

Since the viability and activity of a cell population can directly be measured by its proliferation rate and the amount of senescent cells (Hayflick and Moorhead 1961), the analysis of human blood plasma and blood serum-mediated effects on hCSC-proliferation and senescence could serve to understand its functionality in regenerative processes (Figure 8 A). Here, exposure of hCSCs to human blood plasma led to the formation of a semi-solid 3D matrix consisting of polymerized fibrin, which was likewise described in plasma-treated ITSCs (Greiner et al. 2011). Blood plasma-treatment significantly increased the proliferation rate of hCSCs 2-fold to 3-fold (Figure 8 B, C).
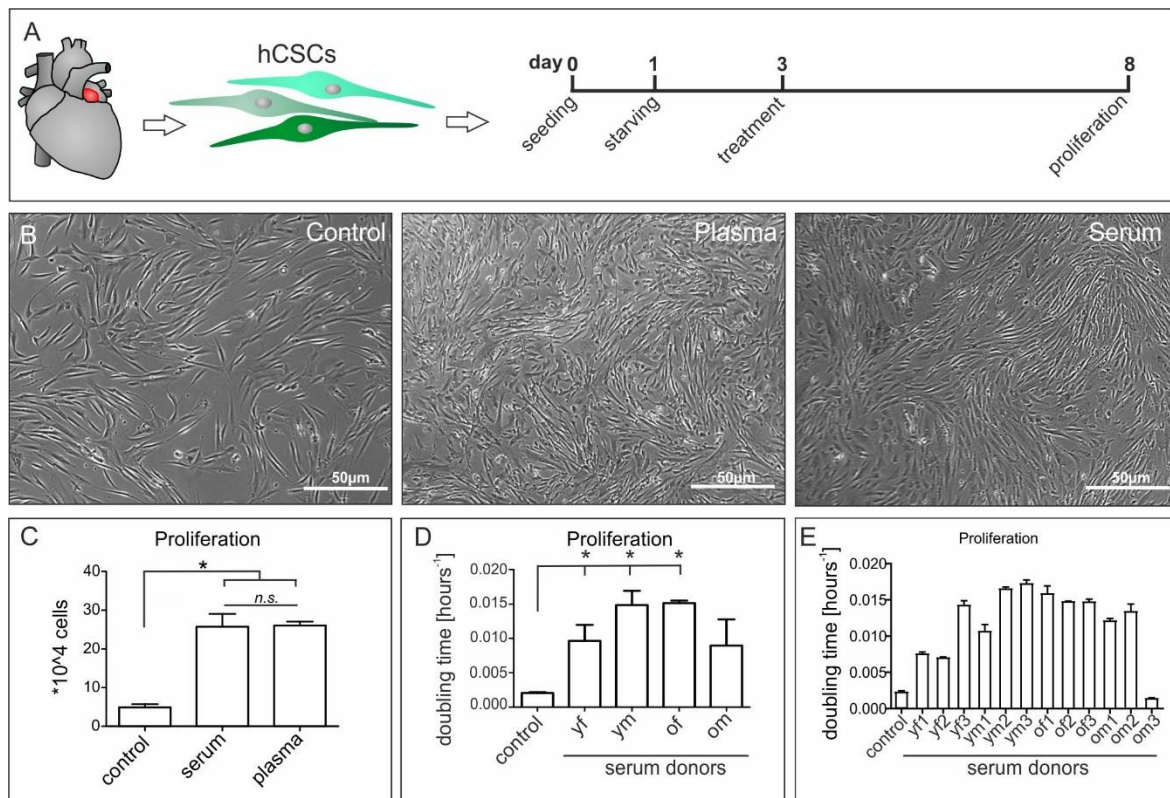
Figure 8: Human blood plasma and blood serum enhance hCSC proliferation. A) After seeding and attachment of the cells to the culture surface, a starvation period was applied to withdraw FCS from the cells. In the treatment period, human serum or human plasma were applied for additional five days before the proliferative response of the cells was examined. B) The application of both, serum and plasma lead to an increase in cell proliferation. C) While serum and plasma both significantly increased hCSC proliferation compared to untreated cells, no difference was detectable between both treatments. D) Blood serum from young female, young male and old female significantly increases the proliferation of hCSCs. E) The induction of hCSC proliferation between the single plasma donors is highly heterogenous. yf: young female, ym: young male, of: old female, om: old male. (Mann-Whitney two-tailed, * p < 0.05 was considered significant, not significant (n.s.) p > 0.05) Modified from (Höving et al. 2020a)

However, the stiffness of the matrix complicated an adequate exchange of the medium. Therefore, blood serum as the liquid part of human blood was applied, resulting in equal proliferation rates of hCSCs compared to hCSCs cultured in plasma (Figure 8 B, C). With no significant difference between the proliferation enhancing effects of human plasma and serum, the number of putative active components of human plasma could successfully be delimited to the serum-borne components. Aiming to transfer the previously described age-dependent beneficial effects of young blood plasma and serum from the murine system to primary human stem cells, human serum was classified according to the donor's sex and age in young (18 - 20 years) and old (> 60 years) samples and applied to hCSCs. Here, again a strongly increased proliferation was detectable, independent of the donors age and sex (Figure 8 D). Moreover, the degree of blood serum-induced proliferation was highly heterogeneous among the distinct plasma donors (Figure 8 E), underlining the necessity of a careful comparison of individual plasma samples. These results were in line

with previous studies demonstrating the efficient promotion of cell proliferation by human serum, plasma and platelet-rich plasma, although age-dependent effects have not been shown so far (Shetty et al. 2007, Berchtold et al. 2008, Lipinski et al. 2010, Greiner et al. 2011, Walenda et al. 2011, Witzeneder et al. 2013, Peters et al. 2015, Shen et al. 2015, Haustead et al. 2016, Stegeman and Weake 2017, Pandey et al. 2019). However, in this regard the proliferation of human cardiac stem cells was not yet investigated.

5.4.2. Human blood serum protects hCSCs against senescence

In addition to proliferation, senescence is another hallmark of a stem cells viability and therefore their regenerative capacity. Notably, treatment of hCSCs with human blood serum significantly decreased the percentage of senescent cells (Figure 9 A, B). Measurements of SA-β-Gal activity in serum-treated hCSCs compared to untreated cells revealed high protective capacities of human serum against cellular senescence in hCSCs in all donor groups (Figure 9 C). Interestingly, in terms of senescence, a significantly lower protection of blood serum from old female donors was detectable compared to male and young female plasma donors (Figure 9 C). Likewise, Lu and coworkers have shown an age-dependent effect of young blood plasma in rodents with significant reversion of senescence in aged hepatic tissue (Liu et al. 2018). This moderate age-dependent difference in senescence of serum-treated hCSCs, which was not observable in terms of proliferation shows the high complexity of the cellular ageing process and the necessity to use multiple assays for assessing the effects of human serum on adult stem cell populations and its underlying regulatory mechanisms.
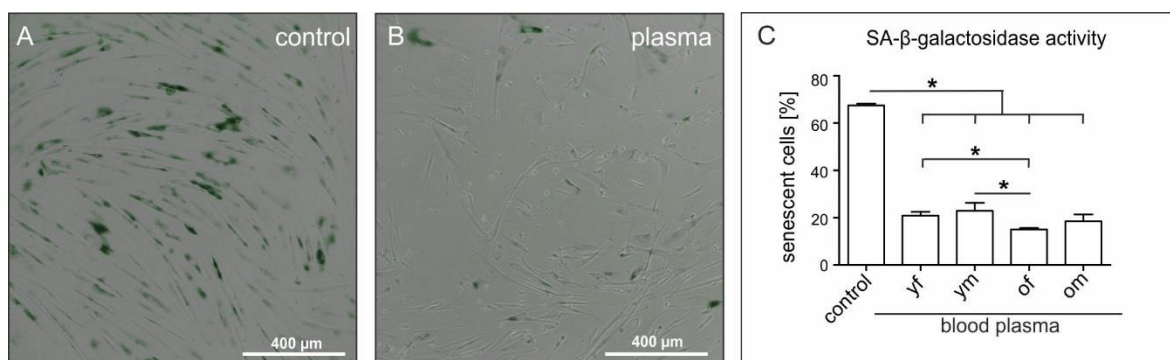
*Figure 9: Blood serum protects hCSCs against senescence. A) hCSCs in serum-free medium show a high amount of senescent cells indicated by activity of SA-β-Gal (blue staining). B) Application of human serum decreased the amount of senescent hCSCs. C) Blood serum from young female, young male, old female and old male donors significantly protect hCSCs from senescence. The protective effects of serum from old female donors is significantly higher compared to young female and young male donors. yf: young female, ym: young male, of: old female, om: old male. (Mann-Whitney two-tailed, * p < 0.05 was considered significant) Modified from (Höving et al. 2020a)*

5.4.3. Human blood serum induces hCSC-migration behavior

Next to proliferation, the ability of a stem cell to migrate to the side of injury is crucial for the regenerative capacities of a tissue and the whole organism. Recent studies suggested an association between age and a stem cells capability to migrate. (Sliogeryte and Gavara 2019, Danielyan et al. 2020). In recent years, various stimuli have been identified that induce or inhibit migratory behavior in diverse cell populations. Next to mechanical factors such as sheer stress or matrix stiffness (Raab et al. 2012, Yuan et al. 2012, Saxena et al. 2018), a range of chemokines, cytokines and growth factors is involved in the regulation of stem cell migration behavior. The response of MSCs to the stromal-derived factor-1 (SDF-1) via the CXC chemokine receptor 4 (CXCR4) seems to be dose-dependent and both induce or inhibit MSC migration (Liu et al. 2011). In a rat model, MSCs overexpressing CXCR4 showed a significantly increased engraftment into infarcted myocardium (Cheng et al. 2008). Treatment of murine cardiac stem cells with the basic fibroblast growth factor (bFGF) increased the migratory behavior *in vitro* and *in vivo*, possibly by activating the Phosphoinositide 3-kinase/Protein kinase B (PI3K/Akt) pathway (Ling et al. 2018). Further, rat MSCs responded to transforming growth factor beta 1 (TGF-β1) treatment with increased CXCR4-dependent migration (Zhang et al. 2016). Recently, Dubon and colleagues showed that p38 mitogen-activated protein kinase (p38-MAPK) mediated the migrative response of murine MSC-like ST2-cells to TGF- β1 (Dubon et al. 2018). P38-MAPK was also shown to be crucial for human umbilical cord blood-derived MSC migration (Ryu et al. 2010). Interestingly, SDF-1, bFGF and TGF-β1 are all transported by blood serum and can be measured in human serum samples (Wakefield et al. 1995, Dobrzycka et al. 2013, Marques et al. 2017), indicating a systemic influence on stem cell migration.
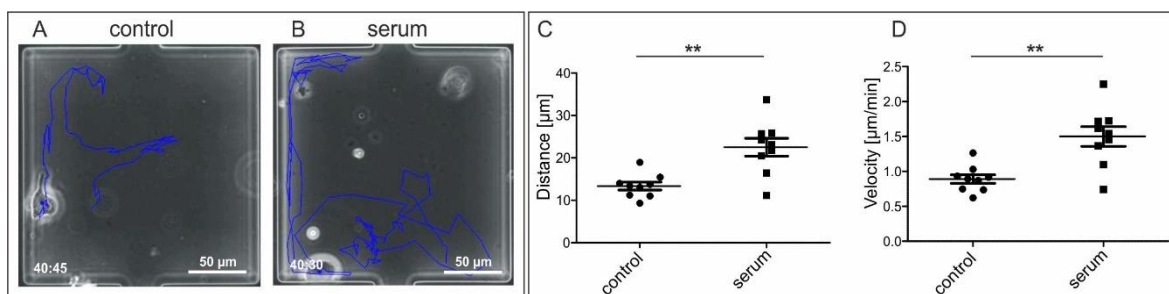
Figure 10: human serum induces hCSC migration. A) hCSCs cultured in serum-free medium remained viable and showed modest cell migration, indicated by the blue track. B) Application of human serum increased migration of hCSCs. C) The distance of hCSC migration significantly increased after the application of blood serum. D) The velocity of hCSC migration significantly increased after application of blood serum. Modified from (Höving, Schmitz et al. under review)

To investigate the effects of serum on the migrative capabilities of hCSCs, a microfluidic-based migration assay was performed. Therefore, the mammalian suspension cells (MaSC) platform, a recently developed microfluidic-based culture system (Schmitz et al. 2020), was used to directly track the migration paths of cultured hCSCs on single cell level. Notably, a direct comparison of hCSC-migration activity in medium supplemented with human blood serum and serum-free medium revealed a strong increase in hCSC migration after serum treatment (Figure 10 A, B). The quantitative evaluation of the resulting data revealed a significantly enhanced migration distance of serum-treated hCSCs compared to untreated cells (Figure 10 C). Likewise, migration velocity of hCSCs was significantly elevated in human serum compared to serum-free medium (Figure 10 D). In accordance to these data, also human articular chondrocytes and MSCs showed increased migration as response to 5 %, 10 % and 20 % serum, although these studies focused on the effect of fetal bovine serum as cell culture additive (Mishima and Lotz 2008). Contrasting results were observed by Kondo and colleagues in human fetal skin fibroblasts and fetal lung fibroblasts which showed diminished migration upon culture in human blood serum (Kondo et al. 1989, Kondo et al. 2000). These studies suggest the effects of human serum on cell migration to be highly dependent on the target cell type, underlining the importance of an investigation in cardiac stem cells.

5.4.4. Identification of genes and pathways affect by serum-treatment of hCSCs using global gene expression analysis

To analyze the underlying molecular networks in the response of hCSCs to human serum, RNA-Seq of hCSCs treated with three different sera of young males, three different sera from old male donors and an untreated control was performed (Höving et al. 2020a). Here, a high differential gene expression was observable between hCSCs treated with young serum compared to untreated cells with 1366 genes being upregulated and 1708 genes being downregulated (Figure 11 A). In contrast, application of old serum only induced the upregulation of 20 genes while 79 genes were downregulated compared to the untreated control (Figure 11 B). These data demonstrate the high impact of young serum on the global gene expression of hCSCs, potentially influencing intracellular signaling for regenerative responses. Likewise, a general decline in gene expression is observable in several ageing tissues (Berchtold et al. 2008, Lipinski et al. 2010, Peters et al. 2015, Haustead et al. 2016,

Stegeman and Weake 2017). For instance, human brain ageing lead to decreased expression of genes associated with autophagy (Lipinski et al. 2010). Moreover, differential gene expression of genes associated with proliferation and migration were shown to be present in aged skin samples (Haustead et al. 2016). However, in contrast to the observable differences in global gene expression between hCSCs treated with old and young serum, significant differences in hCSC proliferation were not detected, suggesting that human serum activated senescence- and proliferation-associated pathways independent of the donor's age.
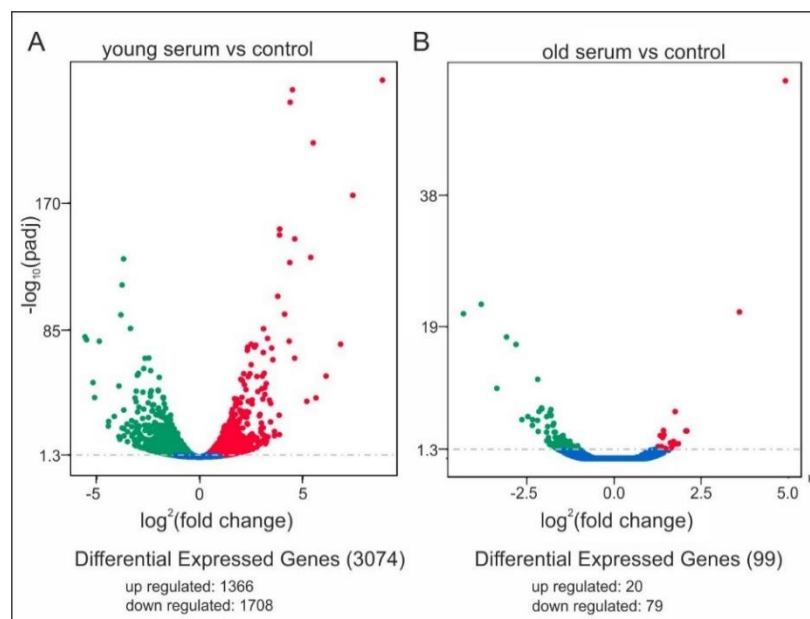
Figure 11: Differential gene expression of hCSCs treated with serum from old or from young donors compared to untreated cells. A) Application of serum from young donors induced the upregulation of 1366 genes (red points) compared to untreated cells while 1708 genes were downregulated (green points). B) Application of serum from old donors induced the upregulation of 20 genes (red points) compared to untreated cells while 79 genes were downregulated (green points). Modified from (Höving et al. 2020a)

Interestingly, the gene expression of the previous discussed pro-ageing chemokine MCP1 was significantly reduced in hCSCs exposed to young serum compared to untreated cells but not in cells treated with old serum. Likewise, MCP1 levels in white adipose tissue of old mice were reduced after heterochronic parabiosis and also in *in vitro* cultured cells upon exposure to young serum (Ghosh et al. 2019). Though, other age-associated factors like Eotaxin and GDF11 were not differentially expressed (Höving et al. 2020a). However, the proinflammatory cytokine interleukin 24 (IL24) was significantly upregulated with a log2fold change of +8.8 in cells treated with young serum compared to untreated cells (Höving et al. 2020a). To further analyze the high number of genes which were shown to

be differentially expressed in serum-treated hCSCs, additional summarizing methods are required.

5.4.5. Identification of p38-MAPK as a mediator of serum-induced proliferation, migration and protection against senescence in hCSCs

Global gene expression data of hCSCs treated with sera from old and young donors were analyzed by generating a heatmap (Figure 12). This allowed the identification of distinct clusters of genes, which were either up- or downregulated in the respective treatment groups, showing clear differences between treatments with old and young sera along the whole transcriptome.
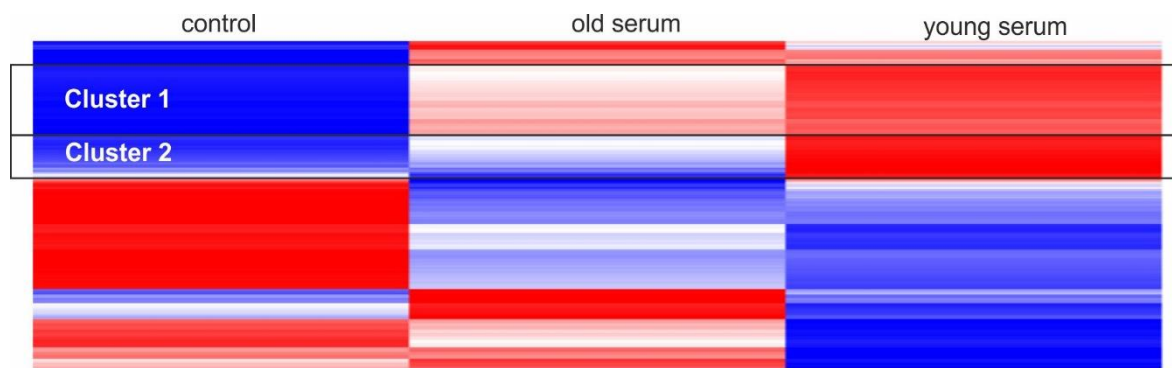
Figure 12: Heatmap of differentially expressed genes in hCSCs treated with serum from old donors and young donors. Two clusters are marked for further analyses. Cluster 1 depicts genes downregulated in untreated cells, modestly upregulated in hCSC treated with serum from old donors and highly upregulated with serum from young donors. Modified from (Höving et al. 2020a)

To further reduce the data dimensionality, GO-term enrichment and KEGG-pathway analysis of a cluster of genes highly upregulated in hCSCs treated with young serum and modestly upregulated after treatment with old serum compared to untreated cells were performed (Figure 12Figure 12, Cluster 1) (Figure 13). Here, the 'p38-MAPK-pathway' (P05918) was the most enriched GO-term, followed by 'oxidative stress response' (P00046) (Figure 13 A). The KEGG pathway analysis within this cluster revealed the pathway 'glutathione metabolism' (hsa00480) to be upregulated (Figure 13 B). These results suggest an antioxidative effect of blood serum on hCSCs. Oxidative stress triggered by intracellular reactive oxygen species (ROS) is one of the major drivers of cellular ageing and senescence (López-Otín et al. 2013).
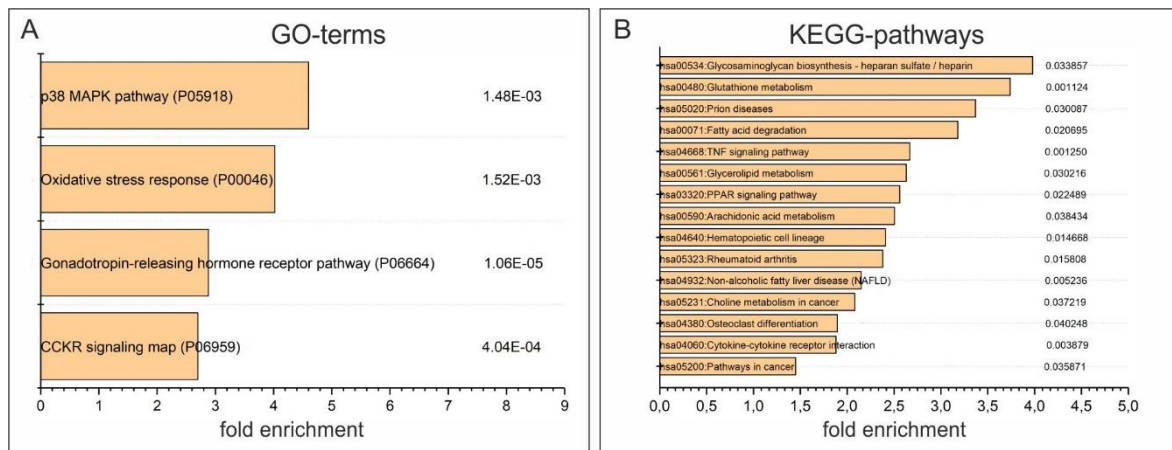
Figure 13: GO-term enrichment and KEGG-pathway analysis of genes in Cluster 1. A) Significantly enriched GO-terms from Cluster 1 (see Figure 12). B) Significantly enriched KEGG-pathways from Cluster 1 (see Figure 12). Modified from (Höving et al. 2020a)

In the cluster of genes upregulated in hCSCs treated with young serum but not differentially expressed in cells cultured in serum from old donors (Figure 12, Cluster 2), the GO-terms 'purine metabolism' (P02769) and 'pentose phosphate pathway' (P02762) were among the most significantly enriched terms (Figure 14 A). These terms are associated with deoxyribonucleic acid (DNA)- and protein-synthesis and crucial for the proliferation of a cell, in accordance with the enhanced serum-mediated proliferation of hCSCs *in vitro*. Moreover, within this cluster the GO-term 'p38-MAPK-pathway' (P05918) was again significantly enriched with 5.5-fold enrichment as well as the KEGG-pathway 'MAPK-signaling pathway' (hsa04010) (Figure 14 B).
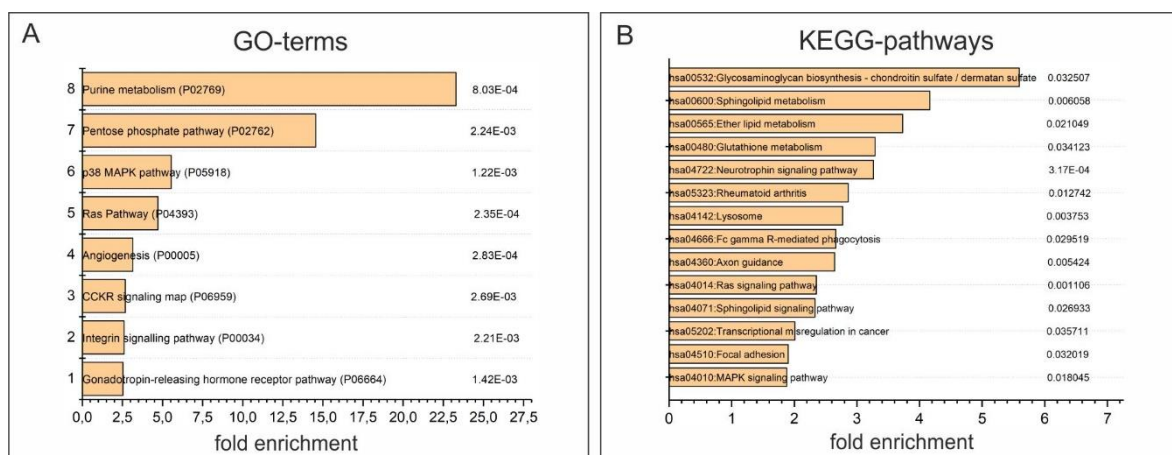
Figure 14: GO-term enrichment and KEGG-pathway analysis of genes in Cluster 2. A) Significantly enriched GO-terms from Cluster 2 (see Figure 12). B) Significantly enriched KEGG-pathways from Cluster 2 (see Figure 12). Modified from (Höving et al. 2020a)

In summary, the enrichment of GO-terms and KEGG-pathways associated to p38-MAPK-signaling along with DNA- and protein-synthesis GO-terms in hCSCs treated with young serum strongly suggested a crucial role of p38-MAPK in the serum-induced proliferation of hCSCs. To gain more functional data in this issue, p38-MAPK-inhibitors were applied to

hCSCs treated with human serum. Here, p38-MAPK inhibition strongly reduced the beneficial effects of human blood serum on hCSCs. The proliferation after simultaneous application of the p38-MAPK-inhibitors and serum was significantly decreased compared to hCSCs cultured in serum only (Figure 15 A). Likewise, the activity of SA-β-Gal was significantly increased in cells treated with serum and p38-MAPK-inhibitor compared to serum or plasma only (Figure 15 B), showing a greatly diminished protection from senescence by human blood serum or plasma. Moreover, the serum-mediated increase in hCSC-migration was reversed after inhibition of p38-MAPK. The quantitative evaluation of the covered tracks documented a significant effect of the p38-MAPK-inhibitor on serum-induced hCSC-migration with significantly decreased distance in cells treated with human serum and p38-MAPK-inhibitor compared to cells cultured in 10 % serum only (Figure 15 C). Next to migration distance, also the velocity of migrating cells was significantly reduced by p38-MAPK-inhibition compared to the migration speed of serum-treated hCSCs (Figure 15 D), strongly suggesting a participation of p38-MAPK-signalling in the human blood serum-mediated migration of hCSCs.
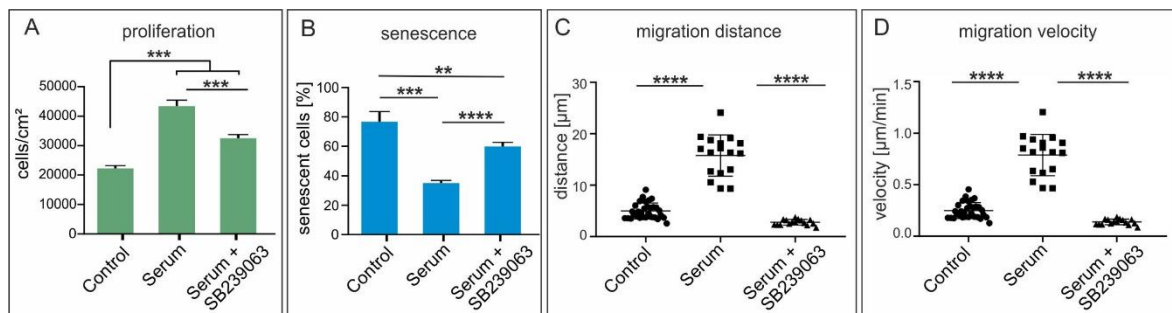
Figure 15: Inhibition of p38-MAPK partially reverses the beneficial effects of human serum on hCSCs. A) Inhibition of p38-MAPK in serum-treated hCSCs with the inhibitor SB239063 significantly reduced proliferation in comparison with serum treatment only. B) Inhibition of p38-MAPK in serum-treated hCSCs with the inhibitor SB239063 significantly increased senescence in comparison with serum treatment only. C) The distance of cell migration significantly increased after application of blood serum. This effect was completely inhibited by the additional application of SB239063. D) The velocity of cell migration significantly increased after application of blood serum. This effect was completely inhibited by the additional application of SB239063. (Mann-Whitney two-tailed, * p < 0.05; ** p < 0.005; *** p < 0.0005; **** p < 0.0001 was considered significant) Modified from (Höving et al. 2020a), (Höving, Schmitz et al. under review)

These data recapitulate the results of the global gene expression analysis, showing a regulatory role of p38-MAPK-signaling in the proliferation, senescence and migration of hCSCs in response to human blood plasma and blood serum. The participation of p38-MAPK-signaling in the regulation of cell proliferation and senescence is well described in several studies. However, dependent on the cell-type, it seemed to have inhibitory as well as enhancing effects (Saika et al. 2004, Zarubin and Han 2005, Chen et al. 2009). Upregulated MAPK-signaling was observed in proliferating aged human skin samples

(Haustead et al. 2016). Interestingly, the upregulation of IL24 in hCSCs treated with young blood serum is in line with a previous report by Tian and colleagues with IL24 as inducer of p38-MAPK activation (Tian et al. 2014). However, the regulation of cell proliferation is a highly complex mechanism in which other relevant pathways could interact with p38-MAPK-signaling in response to human blood serum. In this context, proliferation of hepatic stem cells was described to be co-regulated by p38-MAPK and NF-κB (Yao et al. 2004). In human breast cancer cells, increased proliferation and migration induced by p38-MAPK upregulation were also partially co-regulated by NF-κB and could be reversed by the application of the inhibitor SB203580 or small interfering RNAs (siRNAs) (Chen et al. 2009, Huth et al. 2017). Moreover, p38-MAPK was active in TGF-β1-treated murine MSC-like ST2-cells, resulting in increased migration (Dubon et al. 2018). Also, HUVEC-migration as response to SDF-1 stimulation has been associated with p38-MAPK (Ryu et al. 2010). Further, other groups reported p38-MAPK-dependent migration of mouse neural stem cells (Hamanoue et al. 2016). Moreover, a connection between human serum treatment and p38-MAPK activation resulting in increased migration was also demonstrated in human keratinocytes (Henry et al. 2003). These data strongly indicate a crucial role of p38-MAPK in cell proliferation, senescence and migration while the addressed cell type or tissue should be considered carefully. Moreover, the here demonstrated connection between p38-MAPK signaling and human serum-induced hCSC-migration along with increased proliferation and decreased senescence might enable new therapeutic approaches to enhance endogenous regeneration processes in heart failure patients.

5.5. Neuroprotective effects of human blood plasma and plasma components

5.5.1. Age-associated neurodegenerative diseases and oxidative stress

In contrast to the heart as a terminally differentiated organ upon birth, the mammalian brain constantly develops throughout life (Otsuki and Brand 2020). Nevertheless, the ageing process has a high impact on neuronal regeneration and functionality and is considered as the major risk factor for neurodegenerative diseases like Alzheimer's disease, Parkinson's disease, amyotrophic lateral sclerosis (ALS) and vascular dementia (Checkoway et al. 2011). A major driver of brain ageing and especially neurodegenerative diseases is

oxidative stress resulting from the accumulation of reactive oxygen species (ROS) and reactive nitrogen species (RNS) (Baierle et al. 2015). ROS, like superoxide radicals ($O_2^{\bullet-}$), hydrogen peroxide (H_2O_2), hydroxyl radicals ($\bullet OH$) or singlet oxygen ($^1O_2$), are a by-product of the oxygen metabolism but they are also involved in intracellular signaling in healthy cells as second messengers and participate in several processes like protein phosphorylation, immunity and differentiation (Burton and Jauniaux 2011, Bardaweel et al. 2018). However, with increasing age, ROS accumulates and the antioxidant capacities of a cell or a tissue are overwhelmed leading to damage of membranes and the DNA repair system (Kim et al. 2015). Therefore, oxidative stress is closely associated to ageing and age-related diseases (Liguori et al. 2018). In neurodegenerative diseases such as Alzheimer's disease, Parkinson's disease or cerebral ischemia, ROS can be generated through excess release of excitatory neurotransmitters such as glutamate. Here, the excitation leads to neuronal damage with excess calcium influx and subsequently to the generation of ROS and RNS (Doble 1999, Jellinger and Stadelmann 2000). Kainic acid (KA) (2-carboxy-4-isopropenyl-pyrrolidin-3-ylacetic acid) is a nondegradable structural analog to glutamate and therefore acts as a neurotoxic drug which binds to the α-amino-3-hydroxy-5-methyl-4-isoxazolepropionic acid (AMPA) and KA receptors in the brain (Wang et al. 2005). The neurotoxicity of KA is considered to be with 30-fold higher than glutamate (Bleakman and Lodge 1998), leading to an increase of intracellular ROS followed by neuronal death (Sun et al. 1992, Cheng and Sun 1994, Candelario-Jalil et al. 2001). Systemic administration of KA to rats led to cell death of AMPA and KA receptor-equipped pyramidal neurons in the Cornu Ammonis 1 and Cornu Ammonis 3 (CA1, CA3) regions of the hippocampus, while granule cells of the dentate gyrus (DG) were resistant (Grooms et al. 2000). Moreover, excitatory stress and the resulting intracellular ROS are considered as important drivers of neurological ageing (Michaelis 1998, Albers and Beal 2000), leading to KA-induced hippocampal damage in rodents as prominent model for human ageing and neurodegenerative disorders (Michaelis 1998, Weiss and Sensi 2000, Milatovic et al. 2002). Regarding the treatment of neurodegenerative diseases, impressive results were obtained by the application of young blood plasma or blood serum to aging mice (Wyss-Coray 2016). For instance, Villeda and coworkers detected increased cognitive capacities and improved synaptic plasticity in the hippocampus of aged mice undergoing heterochronic parabiosis (Villeda et al. 2014). Likewise, Castellano and colleagues improved cognitive function in

aged mice by applying human umbilical cord plasma (Castellano et al. 2017). In this matter, more research regarding the underlying molecular mechanisms of hippocampal rejuvenation is necessary.

5.5.2. Mouse hippocampal slice cultures as model system for neurodegenerative diseases

Mouse organotypic brain slices are *ex vivo* cultured tissue compartments of specific regions of the brain. Culturing hippocampal slices in an air-liquid-interface has been shown to maintain synaptic and chemical signaling, supporting the functional analysis of the nervous tissue (Gähwiler 1988, Fridmacher et al. 2003, De Simoni and Yu 2006). Interestingly, Galimberti and colleagues were able to culture viable slices for up to 20 weeks, revealing the neuronal maturation and ageing process to be conducted even *ex vivo* (Galimberti et al. 2006). Neuronal death in brain slices can be visualized by the measurement of propidium iodide (PI) fluorescence which is taken up only by cells with irreversibly damaged membranes or dead cells (Crowley et al. 2016). Thus, hippocampal brain slices are particularly suitable to study the effects of specific compounds such as blood plasma on nervous tissue.

5.5.3. Human blood plasma has neuroprotective effects on hippocampal slice cultures

In the present thesis, the application of human plasma led to significant protection against the neurotoxic effects of KA in CA1, CA3 and DG (Figure 16 A). In detail, the application of KA significantly increased cell death in CA1, CA3 and DG compared to untreated slices as control (Figure 16 B). Further, the application of blood plasma resulted in a slight increase of cell death, which was not significant compared to the untreated control. Importantly, simultaneous treatment with plasma and KA revealed a decrease in neuronal cell death compared to KA alone, which was significant in CA3 and the DG region but not in the CA1 region (Figure 16 B). The slightly increased cell death in hippocampi treated with blood plasma on the one hand and the significant neuroprotective effects of plasma on the other hand indicate multiple plasma components to be active on both processes. A reduction of the diverse components possibly could reduce the neurotoxic effect and enhance the neuroprotective effect.
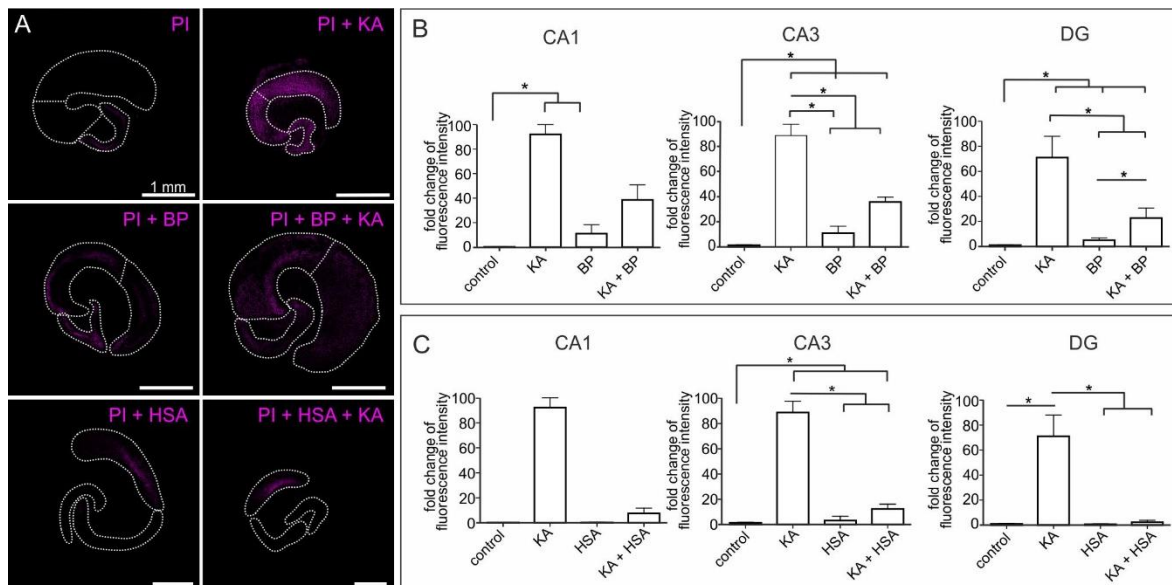
*Figure 16: Human blood plasma and human serum albumin possess neuroprotective effects on ex vivo cultured mouse hippocampal brain slices. A) PI signal in mouse hippocampal slices depicts treatment-dependent neuronal death in the CA1, CA3 and DG regions. Representative images of hippocampi treated KA, BP, BP+KA, HSA and HSA+KA are depicted. B) Human blood plasma has significant neuroprotective properties in the CA1, CA3 and DG regions (Mann-Whitney Test, *p < 0.05 was considered significant). C) Human serum albumin has significant neuroprotective properties in the CA1, CA3 and DG regions (Mann-Whitney Test, *p < 0.05 was considered significant).*

5.5.4. Human serum albumin has neuroprotective effects on hippocampal slice cultures

Human serum albumin (HSA) as the most abundant protein in blood plasma possesses antioxidant capacities (Roche et al. 2008). Moreover, the antioxidant activity of blood plasma was shown to mediate neuroprotection in ischemia and neurological impairments in stroke (Leinonen et al. 2000). The application of HSA to KA-treated hippocampal slices resulted in similar neuroprotective effects like blood plasma in CA1, CA3 and DG (Figure 16 C). Here, the treatment with KA alone again highly induced neuronal cell death in the CA1, CA3 and DG regions. Further, HSA treatment did not lead to additional cell death in the CA1 and DG regions compared to untreated hippocampi. Likewise, the treatment with HSA inhibited the neurotoxic effect of KA significantly in the CA3 and DG regions (Figure 16 C). These results indicate a central role of HSA in the neuroprotective effect of human blood plasma on mouse hippocampal slice cultures. Further experiments might deal with the method of action in the plasma- and HSA-mediated neuroprotection, which might rely on the already known antioxidative capacities of plasma and HSA. In a rage of studies, HSA and other plasma products have already been described as neuroprotective agents, which was mainly regarding the restauration of hemodynamic properties after severe blood loss (Imam et al. 2015, Halaweish et al. 2016). However, *in vitro* assays further revealed direct

neuroprotective activities of Albumin and blood plasma. For instance, the antioxidant activity of bovine serum albumin was linked to reduced DNA damage and apoptosis in rat cortical neurons *in vitro* (Baltanas et al. 2009). Importantly, HSA presents sulfhydryl groups (thiols) which act as scavengers of ROS and RNS such as superoxide hydroxyl and peroxynitrite radicals (Evans 2002). Hence, the antioxidant effects of HSA on the different hippocampal cell types need to be investigated carefully in order to enlighten a potential effect on age-associated neuronal degeneration. In this regard, organotypic slice cultures were introduced as appropriate screening system for the effects of blood plasma and plasma components on neuronal tissues.

6. Summary and Outlook

Within this thesis, human blood serum was analyzed as potential treatment agent for age-associated degeneration using a novel neural crest-derived human cardiac stem cell population from the human heart. Applied to hCSCs as cellular model, human blood serum induced regenerative responses by increasing proliferation, migration and gene expression and decreasing senescence. The results of this work enable the future use of hCSCs as a screening system to identify specific plasma components responsible for increased proliferation and migration or protection from senescence in prospective research (Figure 17). In this regard, the regulatory mechanisms upstream and downstream of p38-MAPK signaling in serum-treated hCSCs should be carefully investigated.
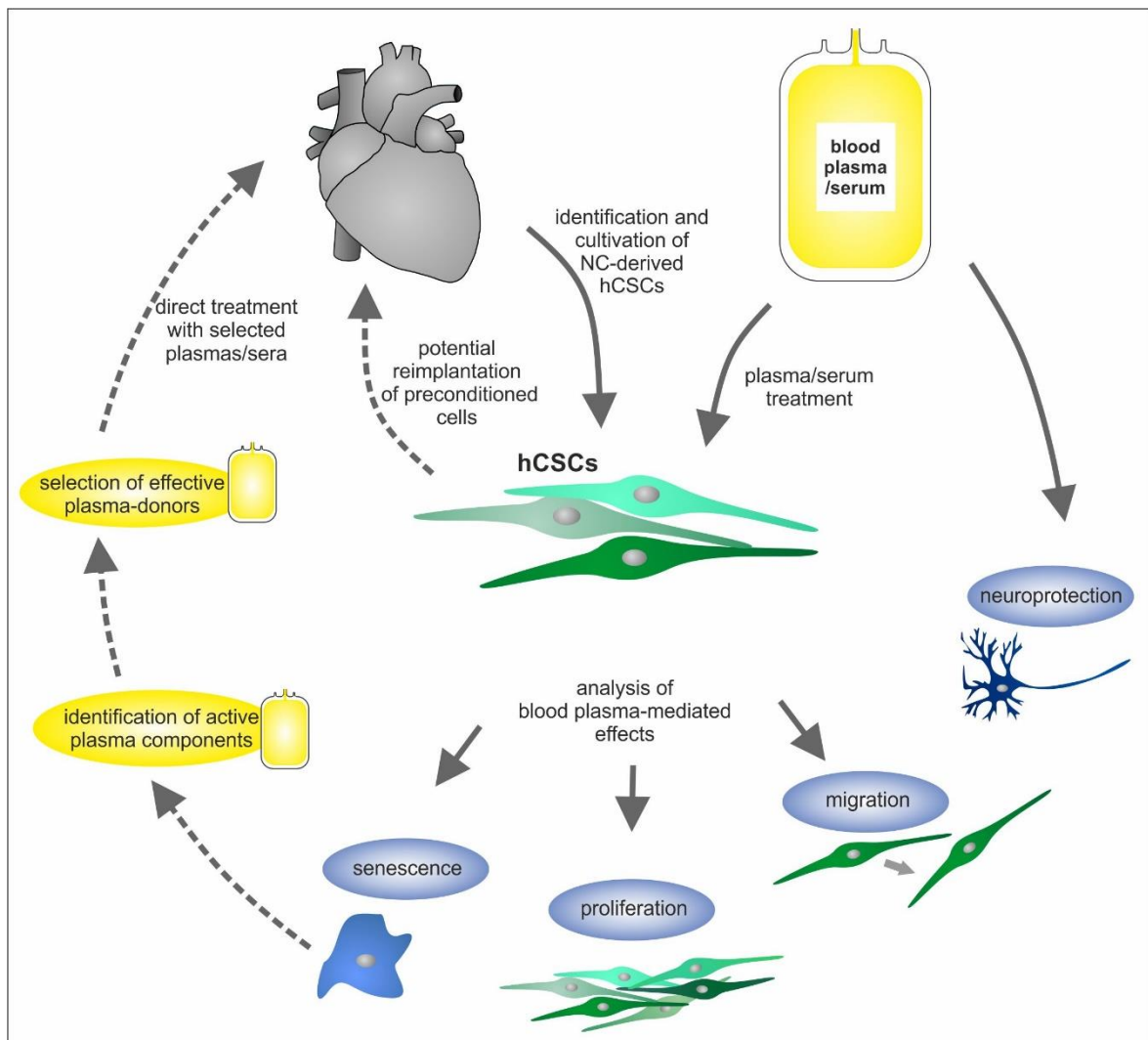
Figure 17: Outlook - Potential applications of human cardiac stem cells as cell-based regenerative treatment of a failing heart or as model to study blood plasma-mediated effects.

In addition, the use of hCSCs as screening system probably enables the testing of human blood serum from various donors regarding specific regenerative hCSC-responses for selecting extraordinary effective plasma samples (Figure 17). The potential transfusion of these selected plasmas or sera to patients undergoing cardiac surgery might support the rehabilitation of the patient. From a cell biological point of view, this thesis describes for the first time a potential developmental relation of hCSCs to the neural crest. The identification and successful *in vitro* expansion of hCSCs may also facilitate potential stem cell-based treatments of a failing human heart. Here, next to the potential direct implantation of hCSCs into the patient, another treatment strategy might be the pretreatment of hCSCs with blood plasma or blood serum from selected donors to trigger regenerative responses ahead of the reimplantation into the patient. In this regard, more investigations regarding the cardiogenic differentiation of hCSCs, for example into endothelial cells, will be needed. Moreover, the potential method of administration needs to be carefully developed in further studies. In summary, the results of this work demonstrate the beneficial effects of human blood plasma on NC-derived adult human cardiac stem cells in terms of proliferation, migration, and protection against senescence, emphasizing the potential clinical use of human blood plasma as therapeutic agent.

7. References

Adam, M. P., Banka, S., Bjornsson, H. T., Bodamer, O., Chudley, A. E., Harris, J., Kawame, H., Lanpher, B. C., Lindsley, A. W., Merla, G., Miyake, N., Okamoto, N., Stumpel, C. T., Niikawa, N. and Kabuki Syndrome Medical Advisory, B. (2019). "*Kabuki syndrome: international consensus diagnostic criteria*." J Med Genet **56**(2): 89-95.

Aguilar-Sanchez, C., Michael, M. and Pennings, S. (2018). "*Cardiac Stem Cells in the Postnatal Heart: Lessons from Development*." Stem Cells Int **2018**: 1247857.

Albers, D. S. and Beal, M. F. (2000). "*Mitochondrial dysfunction and oxidative stress in aging and neurodegenerative disease*." J Neural Transm Suppl **59**: 133-154.

Alzheimer's-Association (2020). "*2020 Alzheimer's disease facts and figures*." Alzheimers Dement.

Amariglio, N., Hirshberg, A., Scheithauer, B. W., Cohen, Y., Loewenthal, R., Trakhtenbrot, L., Paz, N., Koren-Michowitz, M., Waldman, D., Leider-Trejo, L., Toren, A., Constantini, S. and Rechavi, G. (2009). "*Donor-derived brain tumor following neural stem cell transplantation in an ataxia telangiectasia patient*." PLoS Med **6**(2): e1000029.

Anderson, N. L. and Anderson, N. G. (2002). "*The human plasma proteome: history, character, and diagnostic prospects*." Mol Cell Proteomics **1**(11): 845-867.

Arbyn, M., Weiderpass, E., Bruni, L., de Sanjose, S., Saraiya, M., Ferlay, J. and Bray, F. (2020). "*Estimates of incidence and mortality of cervical cancer in 2018: a worldwide analysis*." Lancet Glob Health **8**(2): e191-e203.

Arnhold, S., Klein, H., Semkova, I., Addicks, K. and Schraermeyer, U. (2004). "*Neurally selected embryonic stem cells induce tumor formation after long-term survival following engraftment into the subretinal space*." Invest Ophthalmol Vis Sci **45**(12): 4251-4255.

Baierle, M., Nascimento, S. N., Moro, A. M., Brucker, N., Freitas, F., Gauer, B., Durgante, J., Bordignon, S., Zibetti, M., Trentini, C. M., Duarte, M. M., Grune, T., Breusing, N. and Garcia, S. C. (2015). "*Relationship between inflammation and oxidative stress and cognitive decline in the institutionalized elderly*." Oxid Med Cell Longev **2015**: 804198.

Balestrino, R. and Schapira, A. H. V. (2020). "*Parkinson disease*." Eur J Neurol **27**(1): 27-42.

Baltanas, F. C., Weruaga, E., Valero, J., Recio, J. S. and Alonso, J. R. (2009). "*Albumin attenuates DNA damage in primary-cultured neurons*." Neurosci Lett **450**(1): 23-26.

Bardaweel, S. K., Gul, M., Alzweiri, M., Ishaqat, A., HA, A. L. and Bashatwah, R. M. (2018). "*Reactive Oxygen Species: the Dual Role in Physiological and Pathological Conditions of the Human Body*." Eurasian J Med **50**(3): 193-201.

Barile, L., Gherghiceanu, M., Popescu, L. M., Moccetti, T. and Vassalli, G. (2013). "*Human cardiospheres as a source of multipotent stem and progenitor cells*." Stem Cells Int **2013**: 916837.

Barraud, P., Seferiadis, A. A., Tyson, L. D., Zwart, M. F., Szabo-Rogers, H. L., Ruhrberg, C., Liu, K. J. and Baker, C. V. (2010). "*Neural crest origin of olfactory ensheathing glia*." Proc Natl Acad Sci U S A **107**(49): 21040-21045.

Bearzi, C., Rota, M., Hosoda, T., Tillmanns, J., Nascimbene, A., De Angelis, A., Yasuzawa-Amano, S., Trofimova, I., Siggins, R. W., Lecapitaine, N., Cascapera, S., Beltrami, A.

P., D'Alessandro, D. A., Zias, E., Quaini, F., Urbanek, K., Michler, R. E., Bolli, R., Kajstura, J., Leri, A. and Anversa, P. (2007). "*Human cardiac stem cells*." Proc Natl Acad Sci U S A **104**(35): 14068-14073.

Becker, A. J., Mc, C. E. and Till, J. E. (1963). "*Cytological demonstration of the clonal nature of spleen colonies derived from transplanted mouse marrow cells*." Nature **197**: 452-454.

Beltrami, A. P., Barlucchi, L., Torella, D., Baker, M., Limana, F., Chimenti, S., Kasahara, H., Rota, M., Musso, E., Urbanek, K., Leri, A., Kajstura, J., Nadal-Ginard, B. and Anversa, P. (2003). "*Adult cardiac stem cells are multipotent and support myocardial regeneration*." Cell **114**(6): 763-776.

Berchtold, N. C., Cribbs, D. H., Coleman, P. D., Rogers, J., Head, E., Kim, R., Beach, T., Miller, C., Troncoso, J., Trojanowski, J. Q., Zielke, H. R. and Cotman, C. W. (2008). "*Gene expression changes in the course of normal brain aging are sexually dimorphic*." Proc Natl Acad Sci U S A **105**(40): 15605-15610.

Bergmann, O., Bhardwaj, R. D., Bernard, S., Zdunek, S., Barnabe-Heider, F., Walsh, S., Zupicich, J., Alkass, K., Buchholz, B. A., Druid, H., Jovinge, S. and Frisen, J. (2009). "*Evidence for cardiomyocyte renewal in humans*." Science **324**(5923): 98-102.

Bergmann, O., Zdunek, S., Felker, A., Salehpour, M., Alkass, K., Bernard, S., Sjostrom, S. L., Szewczykowska, M., Jackowska, T., Dos Remedios, C., Malm, T., Andra, M., Jashari, R., Nyengaard, J. R., Possnert, G., Jovinge, S., Druid, H. and Frisen, J. (2015). "*Dynamics of Cell Generation and Turnover in the Human Heart*." Cell **161**(7): 1566-1575.

Bhatnagar, P., Wickramasinghe, K., Wilkins, E. and Townsend, N. (2016). "*Trends in the epidemiology of cardiovascular disease in the UK*." Heart **102**(24): 1945-1952.

Bhatt, S., Diaz, R. and Trainor, P. A. (2013). "*Signals and switches in Mammalian neural crest cell differentiation*." Cold Spring Harb Perspect Biol **5**(2).

Bleakman, D. and Lodge, D. (1998). "*Neuropharmacology of AMPA and kainate receptors*." Neuropharmacology **37**(10-11): 1187-1204.

Bonczek, O., Balcar, V. J. and Sery, O. (2017). "*PAX9 gene mutations and tooth agenesis: A review*." Clin Genet **92**(5): 467-476.

Boudjadi, S., Chatterjee, B., Sun, W., Vemu, P. and Barr, F. G. (2018). "*The expression and function of PAX3 in development and disease*." Gene **666**: 145-157.

Breckwoldt, K., Weinberger, F. and Eschenhagen, T. (2016). "*Heart regeneration*." Biochim Biophys Acta **1863**(7 Pt B): 1749-1759.

Burton, G. J. and Jauniaux, E. (2011). "*Oxidative stress*." Best Pract Res Clin Obstet Gynaecol **25**(3): 287-299.

Cai, C. L., Liang, X., Shi, Y., Chu, P. H., Pfaff, S. L., Chen, J. and Evans, S. (2003). "*Isl1 identifies a cardiac progenitor population that proliferates prior to differentiation and contributes a majority of cells to the heart*." Dev Cell **5**(6): 877-889.

Candelario-Jalil, E., Al-Dalain, S. M., Castillo, R., Martinez, G. and Fernandez, O. S. (2001). "*Selective vulnerability to kainate-induced oxidative damage in different rat brain regions*." J Appl Toxicol **21**(5): 403-407.

Carlson, M. E., Hsu, M. and Conboy, I. M. (2008). "*Imbalance between pSmad3 and Notch induces CDK inhibitors in old muscle stem cells*." Nature **454**(7203): 528-532.

Castellano, J. M., Mosher, K. I., Abbey, R. J., McBride, A. A., James, M. L., Berdnik, D., Shen, J. C., Zou, B., Xie, X. S., Tingle, M., Hinkson, I. V., Angst, M. S. and Wyss-Coray, T. (2017). "*Human umbilical cord plasma proteins revitalize hippocampal function in aged mice*." Nature **544**(7651): 488-492.

Checkoway, H., Lundin, J. I. and Kelada, S. N. (2011). "*Neurodegenerative diseases*." IARC Sci Publ(163): 407-419.

Chen, L., Mayer, J. A., Krisko, T. I., Speers, C. W., Wang, T., Hilsenbeck, S. G. and Brown, P. H. (2009). "*Inhibition of the p38 kinase suppresses the proliferation of human ER-negative breast cancer cells*." Cancer Res **69**(23): 8853-8861.

Cheng, Y. and Sun, A. Y. (1994). "*Oxidative mechanisms involved in kainate-induced cytotoxicity in cortical neurons*." Neurochem Res **19**(12): 1557-1564.

Cheng, Z., Ou, L., Zhou, X., Li, F., Jia, X., Zhang, Y., Liu, X., Li, Y., Ward, C. A., Melo, L. G. and Kong, D. (2008). "*Targeted migration of mesenchymal stem cells modified with CXCR4 gene to infarcted myocardium improves cardiac performance*." Mol Ther **16**(3): 571-579.

Chiao, Y. A., Dai, Q., Zhang, J., Lin, J., Lopez, E. F., Ahuja, S. S., Chou, Y. M., Lindsey, M. L. and Jin, Y. F. (2011). "*Multi-analyte profiling reveals matrix metalloproteinase-9 and monocyte chemotactic protein-1 as plasma biomarkers of cardiac aging*." Circ Cardiovasc Genet **4**(4): 455-462.

Collado, M., Blasco, M. A. and Serrano, M. (2007). "*Cellular senescence in cancer and aging*." Cell **130**(2): 223-233.

Compston, J. E., McClung, M. R. and Leslie, W. D. (2019). "*Osteoporosis*." Lancet **393**(10169): 364-376.

Conboy, I. M., Conboy, M. J. and Rebo, J. (2015). "*Systemic Problems: A perspective on stem cell aging and rejuvenation*." Aging (Albany NY) **7**(10): 754-765.

Conboy, I. M., Conboy, M. J., Wagers, A. J., Girma, E. R., Weissman, I. L. and Rando, T. A. (2005). "*Rejuvenation of aged progenitor cells by exposure to a young systemic environment*." Nature **433**(7027): 760-764.

Conboy, I. M. and Rando, T. A. (2012). "*Heterochronic parabiosis for the study of the effects of aging on stem cells and their niches*." Cell Cycle **11**(12): 2260-2267.

Conrad, C. and Huss, R. (2005). "*Adult stem cell lines in regenerative medicine and reconstructive surgery*." J Surg Res **124**(2): 201-208.

Crowley, L. C., Scott, A. P., Marfell, B. J., Boughaba, J. A., Chojnowski, G. and Waterhouse, N. J. (2016). "*Measuring Cell Death by Propidium Iodide Uptake and Flow Cytometry*." Cold Spring Harb Protoc **2016**(7).

Cuvertino, S., Stuart, H. M., Chandler, K. E., Roberts, N. A., Armstrong, R., Bernardini, L., Bhaskar, S., Callewaert, B., Clayton-Smith, J., Davalillo, C. H., Deshpande, C., Devriendt, K., Digilio, M. C., Dixit, A., Edwards, M., Friedman, J. M., Gonzalez-Meneses, A., Joss, S., Kerr, B., Lampe, A. K., Langlois, S., Lennon, R., Loget, P., Ma, D. Y. T., McGowan, R., Des Medt, M., O'Sullivan, J., Odent, S., Parker, M. J., Pebrel-Richard, C., Petit, F., Stark, Z., Stockler-Ipsiroglu, S., Tinschert, S., Vasudevan, P., Villa, O., White, S. M., Zahir, F. R., Study, D. D. D., Woolf, A. S. and Banka, S. (2017). "*ACTB Loss-of-Function Mutations Result in a Pleiotropic Developmental Disorder*." Am J Hum Genet **101**(6): 1021-1033.

d'Aquino, R., Tirino, V., Desiderio, V., Studer, M., De Angelis, G. C., Laino, L., De Rosa, A., Di Nucci, D., Martino, S., Paino, F., Sampaolesi, M. and Papaccio, G. (2011). "*Human neural crest-derived postnatal cells exhibit remarkable embryonic attributes either in vitro or in vivo*." Eur Cell Mater **21**: 304-316.

Danielyan, L., Schwab, M., Siegel, G., Brawek, B., Garaschuk, O., Asavapanumas, N., Buadze, M., Lourhmati, A., Wendel, H. P., Avci-Adali, M., Krueger, M. A., Calaminus, C., Naumann, U., Winter, S., Schaeffeler, E., Spogis, A., Beer-Hammer, S., Neher, J. J., Spohn, G., Kretschmer, A., Kramer-Albers, E. M., Barth, K., Lee, H. J.,

Kim, S. U., Frey, W. H., 2nd, Claussen, C. D., Hermann, D. M., Doeppner, T. R., Seifried, E., Gleiter, C. H., Northoff, H. and Schafer, R. (2020). "*Cell motility and migration as determinants of stem cell efficacy*." EBioMedicine **60**: 102989.

Dayal, A., Rhee, J. S. and Garcia, G. J. (2016). "*Impact of Middle versus Inferior Total Turbinectomy on Nasal Aerodynamics*." Otolaryngol Head Neck Surg **155**(3): 518-525.

De Simoni, A. and Yu, L. M. (2006). "*Preparation of organotypic hippocampal slice cultures: interface method*." Nat Protoc **1**(3): 1439-1445.

Debacq-Chainiaux, F., Erusalimsky, J. D., Campisi, J. and Toussaint, O. (2009). "*Protocols to detect senescence-associated beta-galactosidase (SA-betagal) activity, a biomarker of senescent cells in culture and in vivo*." Nat Protoc **4**(12): 1798-1806.

Debeer, P., Van Esch, H., Huysmans, C., Pijkels, E., De Smet, L., Van de Ven, W., Devriendt, K. and Fryns, J. P. (2005). "*Novel GJA1 mutations in patients with oculo-dento-digital dysplasia (ODDD)*." Eur J Med Genet **48**(4): 377-387.

Digilio, M. C., Gnazzo, M., Lepri, F., Dentici, M. L., Pisaneschi, E., Baban, A., Passarelli, C., Capolino, R., Angioni, A., Novelli, A., Marino, B. and Dallapiccola, B. (2017). "*Congenital heart defects in molecularly proven Kabuki syndrome patients*." Am J Med Genet A **173**(11): 2912-2922.

Dimri, G. P., Lee, X., Basile, G., Acosta, M., Scott, G., Roskelley, C., Medrano, E. E., Linskens, M., Rubelj, I., Pereira-Smith, O. and et al. (1995). "*A biomarker that identifies senescent human cells in culture and in aging skin in vivo*." Proc Natl Acad Sci U S A **92**(20): 9363-9367.

Doble, A. (1999). "*The role of excitotoxicity in neurodegenerative disease: implications for therapy*." Pharmacol Ther **81**(3): 163-221.

Dobrzycka, B., Mackowiak-Matejczyk, B., Kinalski, M. and Terlikowski, S. J. (2013). "*Pretreatment serum levels of bFGF and VEGF and its clinical significance in endometrial carcinoma*." Gynecol Oncol **128**(3): 454-460.

Dow, J., Simkhovich, B. Z., Kedes, L. and Kloner, R. A. (2005). "*Washout of transplanted cells from the heart: a potential new hurdle for cell transplantation therapy*." Cardiovasc Res **67**(2): 301-307.

Dubon, M. J., Yu, J., Choi, S. and Park, K. S. (2018). "*Transforming growth factor beta induces bone marrow mesenchymal stem cell migration via noncanonical signals and N-cadherin*." J Cell Physiol **233**(1): 201-213.

Duelen, R. and Sampaolesi, M. (2017). "*Stem Cell Technology in Cardiac Regeneration: A Pluripotent Stem Cell Promise*." EBioMedicine **16**: 30-40.

Edgren, G., Ullum, H., Rostgaard, K., Erikstrup, C., Sartipy, U., Holzmann, M. J., Nyren, O. and Hjalgrim, H. (2017). "*Association of Donor Age and Sex With Survival of Patients Receiving Transfusions*." JAMA Intern Med **177**(6): 854-860.

Egerman, M. A., Cadena, S. M., Gilbert, J. A., Meyer, A., Nelson, H. N., Swalley, S. E., Mallozzi, C., Jacobi, C., Jennings, L. L., Clay, I., Laurent, G., Ma, S., Brachat, S., Lach-Trifilieff, E., Shavlakadze, T., Trendelenburg, A. U., Brack, A. S. and Glass, D. J. (2015). "*GDF11 Increases with Age and Inhibits Skeletal Muscle Regeneration*." Cell Metab **22**(1): 164-174.

El-Helou, V., Beguin, P. C., Assimakopoulos, J., Clement, R., Gosselin, H., Brugada, R., Aumont, A., Biernaskie, J., Villeneuve, L., Leung, T. K., Fernandes, K. J. and Calderone, A. (2008). "*The rat heart contains a neural stem cell population; role in sympathetic sprouting and angiogenesis*." J Mol Cell Cardiol **45**(5): 694-702.

El-Helou, V., Dupuis, J., Proulx, C., Drapeau, J., Clement, R., Gosselin, H., Villeneuve, L., Manganas, L. and Calderone, A. (2005). "*Resident nestin+ neural-like cells and fibers are detected in normal and damaged rat myocardium*." Hypertension **46**(5): 1219-1225.

Elghblawi, E. (2018). "*Platelet-rich plasma, the ultimate secret for youthful skin elixir and hair growth triggering*." J Cosmet Dermatol **17**(3): 423-430.

Endo, D., Kato, T. S., Iwamura, T., Oishi, A., Yokoyama, Y., Kuwaki, K., Inaba, H. and Amano, A. (2017). "*The impact of surgical left atrial appendage amputation/ligation on stroke prevention in patients undergoing off-pump coronary artery bypass grafting*." Heart Vessels **32**(6): 726-734.

Escribano, L., Ocqueteau, M., Almeida, J., Orfao, A. and San Miguel, J. F. (1998). "*Expression of the c-kit (CD117) molecule in normal and malignant hematopoiesis*." Leuk Lymphoma **30**(5-6): 459-466.

Evans, M. J. and Kaufman, M. H. (1981). "*Establishment in culture of pluripotential cells from mouse embryos*." Nature **292**(5819): 154-156.

Evans, T. W. (2002). "*Review article: albumin as a drug--biological effects of albumin unrelated to oncotic pressure*." Aliment Pharmacol Ther **16 Suppl 5**: 6-11.

Ezekowitz, J. A., Kaul, P., Bakal, J. A., Armstrong, P. W., Welsh, R. C. and McAlister, F. A. (2009). "*Declining in-hospital mortality and increasing heart failure incidence in elderly patients with first myocardial infarction*." J Am Coll Cardiol **53**(1): 13-20.

Feng, X. and McDonald, J. M. (2011). "*Disorders of bone remodeling*." Annu Rev Pathol **6**: 121-145.

Franceschi, C., Garagnani, P., Morsiani, C., Conte, M., Santoro, A., Grignolio, A., Monti, D., Capri, M. and Salvioli, S. (2018). "*The Continuum of Aging and Age-Related Diseases: Common Mechanisms but Different Rates*." Front Med (Lausanne) **5**: 61.

Fridmacher, V., Kaltschmidt, B., Goudeau, B., Ndiaye, D., Rossi, F. M., Pfeiffer, J., Kaltschmidt, C., Israël, A. and Mémet, S. (2003). "*Forebrain-Specific Neuronal Inhibition of Nuclear Factor-κB Activity Leads to Loss of Neuroprotection*." The Journal of Neuroscience **23**(28): 9403-9408.

Friedman, C. E., Nguyen, Q., Lukowski, S. W., Helfer, A., Chiu, H. S., Miklas, J., Levy, S., Suo, S., Han, J. J., Osteil, P., Peng, G., Jing, N., Baillie, G. J., Senabouth, A., Christ, A. N., Bruxner, T. J., Murry, C. E., Wong, E. S., Ding, J., Wang, Y., Hudson, J., Ruohola-Baker, H., Bar-Joseph, Z., Tam, P. P. L., Powell, J. E. and Palpant, N. J. (2018). "*Single-Cell Transcriptomic Analysis of Cardiac Differentiation from Human PSCs Reveals HOPX-Dependent Cardiomyocyte Maturation*." Cell Stem Cell **23**(4): 586-598 e588.

Gähwiler, B. H. (1988). "*Organotypic cultures of neural tissue*." Trends Neurosci **11**(11): 484-489.

Galimberti, I., Gogolla, N., Alberi, S., Santos, A. F., Muller, D. and Caroni, P. (2006). "*Long-term rearrangements of hippocampal mossy fiber terminal connectivity in the adult regulated by experience*." Neuron **50**(5): 749-763.

Gems, D. and Partridge, L. (2013). "*Genetics of longevity in model organisms: debates and paradigm shifts*." Annu Rev Physiol **75**: 621-644.

Ghodsizad, A., Ruhparwar, A., Bordel, V., Mirsaidighazi, E., Klein, H. M., Koerner, M. M., Karck, M. and El-Banayosy, A. (2013). "*Clinical application of adult stem cells for therapy for cardiac disease*." Cardiovasc Ther **31**(6): 323-334.

Ghosh, A. K., O'Brien, M., Mau, T., Qi, N. and Yung, R. (2019). "*Adipose Tissue Senescence and Inflammation in Aging is Reversed by the Young Milieu*." J Gerontol A Biol Sci Med Sci **74**(11): 1709-1715.

Gittenberger-de Groot, A. C., Bartelings, M. M., Deruiter, M. C. and Poelmann, R. E. (2005). "*Basics of cardiac development for the understanding of congenital heart malformations*." Pediatr Res **57**(2): 169-176.

Gore, A., Li, Z., Fung, H. L., Young, J. E., Agarwal, S., Antosiewicz-Bourget, J., Canto, I., Giorgetti, A., Israel, M. A., Kiskinis, E., Lee, J. H., Loh, Y. H., Manos, P. D., Montserrat, N., Panopoulos, A. D., Ruiz, S., Wilbert, M. L., Yu, J., Kirkness, E. F., Izpisua Belmonte, J. C., Rossi, D. J., Thomson, J. A., Eggan, K., Daley, G. Q., Goldstein, L. S. and Zhang, K. (2011). "*Somatic coding mutations in human induced pluripotent stem cells*." Nature **471**(7336): 63-67.

Greiner, J. F., Gottschalk, M., Fokin, N., Buker, B., Kaltschmidt, B. P., Dreyer, A., Vordemvenne, T., Kaltschmidt, C., Hutten, A. and Kaltschmidt, B. (2019). "*Natural and synthetic nanopores directing osteogenic differentiation of human stem cells*." Nanomedicine **17**: 319-328.

Greiner, J. F., Hauser, S., Widera, D., Muller, J., Qunneis, F., Zander, C., Martin, I., Mallah, J., Schuetzmann, D., Prante, C., Schwarze, H., Prohaska, W., Beyer, A., Rott, K., Hutten, A., Golzhauser, A., Sudhoff, H., Kaltschmidt, C. and Kaltschmidt, B. (2011). "*Efficient animal-serum free 3D cultivation method for adult human neural crest-derived stem cell therapeutics*." Eur Cell Mater **22**: 403-419.

Grooms, S. Y., Opitz, T., Bennett, M. V. and Zukin, R. S. (2000). "*Status epilepticus decreases glutamate receptor 2 mRNA and protein expression in hippocampal pyramidal cells before neuronal death*." Proc Natl Acad Sci U S A **97**(7): 3631-3636.

Gunnarsson, A. P., Christensen, R., Li, J. and Jensen, U. B. (2016). "*Global gene expression and comparison between multiple populations in the mouse epidermis*." Stem Cell Res **17**(1): 191-202.

Gurusamy, N., Alsayari, A., Rajasingh, S. and Rajasingh, J. (2018). "*Adult Stem Cells for Regenerative Therapy*." Prog Mol Biol Transl Sci **160**: 1-22.

Halaweish, I., Bambakidis, T., Nikolian, V. C., Georgoff, P., Bruhn, P., Piascik, P., Buckley, L., Srinivasan, A., Liu, B., Li, Y. and Alam, H. B. (2016). "*Early resuscitation with lyophilized plasma provides equal neuroprotection compared with fresh frozen plasma in a large animal survival model of traumatic brain injury and hemorrhagic shock*." J Trauma Acute Care Surg **81**(6): 1080-1087.

Hamanoue, M., Morioka, K., Ohsawa, I., Ohsawa, K., Kobayashi, M., Tsuburaya, K., Akasaka, Y., Mikami, T., Ogata, T. and Takamatsu, K. (2016). "*Cell-permeable p38 MAP kinase promotes migration of adult neural stem/progenitor cells*." Sci Rep **6**: 24279.

Hannestad, J., Koborsi, K., Klutzaritz, V., Chao, W., Ray, R., Paez, A., Jackson, S., Lohr, S., Cummings, J. L., Kay, G., Nikolich, K. and Braithwaite, S. (2020). "*Safety and tolerability of GRF6019 in mild-to-moderate Alzheimer's disease dementia*." Alzheimers Dement (N Y) **6**(1): e12115.

Harvey, E., Zhang, H., Sepulveda, P., Garcia, S. P., Sweeney, D., Choudry, F. A., Castellano, D., Thomas, G. N., Kattach, H., Petersen, R., Blake, D. J., Taggart, D. P., Frontini, M., Watt, S. M. and Martin-Rendon, E. (2017). "*Potency of Human Cardiosphere-Derived Cells from Patients with Ischemic Heart Disease Is Associated with Robust Vascular Supportive Ability*." Stem Cells Transl Med **6**(5): 1399-1411.

Hatzistergos, K. E., Takeuchi, L. M., Saur, D., Seidler, B., Dymecki, S. M., Mai, J. J., White, I. A., Balkan, W., Kanashiro-Takeuchi, R. M., Schally, A. V. and Hare, J. M. (2015). "*cKit+ cardiac progenitors of neural crest origin*." Proc Natl Acad Sci U S A **112**(42): 13051-13056.

Hauser, S., Widera, D., Qunneis, F., Muller, J., Zander, C., Greiner, J., Strauss, C., Luningschror, P., Heimann, P., Schwarze, H., Ebmeyer, J., Sudhoff, H., Arauzo-Bravo, M. J., Greber, B., Zaehres, H., Scholer, H., Kaltschmidt, C. and Kaltschmidt, B. (2012). "*Isolation of novel multipotent neural crest-derived stem cells from adult human inferior turbinate*." Stem Cells Dev **21**(5): 742-756.

Haustead, D. J., Stevenson, A., Saxena, V., Marriage, F., Firth, M., Silla, R., Martin, L., Adcroft, K. F., Rea, S., Day, P. J., Melton, P., Wood, F. M. and Fear, M. W. (2016). "*Transcriptome analysis of human ageing in male skin shows mid-life period of variability and central role of NF-kappaB*." Sci Rep **6**: 26846.

Hayflick, L. and Moorhead, P. S. (1961). "*The serial cultivation of human diploid cell strains*." Exp Cell Res **25**: 585-621.

He, L., Nguyen, N. B., Ardehali, R. and Zhou, B. (2020). "*Heart Regeneration by Endogenous Stem Cells and Cardiomyocyte Proliferation: Controversy, Fallacy, and Progress*." Circulation **142**(3): 275-291.

He, S., Nakada, D. and Morrison, S. J. (2009). "*Mechanisms of stem cell self-renewal*." Annu Rev Cell Dev Biol **25**: 377-406.

Henry, G., Li, W., Garner, W. and Woodley, D. T. (2003). "*Migration of human keratinocytes in plasma and serum and wound re-epithelialisation*." Lancet **361**(9357): 574-576.

His, W. (1868). *Untersuchungen über die erste Anlage des Wirbeltierleibes. Die erste Entwicklung des Hühnchens im Ei*. Leipzig, Vogel.

Hoefer, J., Luger, M., Dal-Pont, C., Culig, Z., Schennach, H. and Jochberger, S. (2017). "*The "Aging Factor" Eotaxin-1 (CCL11) Is Detectable in Transfusion Blood Products and Increases with the Donor's Age*." Front Aging Neurosci **9**: 402.

Hofmann, B. (2018). "*Young Blood Rejuvenates Old Bodies: A Call for Reflection when Moving from Mice to Men*." Transfus Med Hemother **45**(1): 67-71.

Höving, A. L., Schmidt, K. E., Merten, M., Hamidi, J., Rott, A. K., Faust, I., Greiner, J. F. W., Gummert, J., Kaltschmidt, B., Kaltschmidt, C. and Knabbe, C. (2020a). "*Blood Serum Stimulates p38-Mediated Proliferation and Changes in Global Gene Expression of Adult Human Cardiac Stem Cells*." Cells **9**(6).

Höving, A. L., Sielemann, K., Greiner, J. F. W., Kaltschmidt, B., Knabbe, C. and Kaltschmidt, C. (2020b). "*Transcriptome Analysis Reveals High Similarities between Adult Human Cardiac Stem Cells and Neural Crest-Derived Stem Cells*." Biology (Basel) **9**(12).

Humphreys, R., Zheng, W., Prince, L. S., Qu, X., Brown, C., Loomes, K., Huppert, S. S., Baldwin, S. and Goudy, S. (2012). "*Cranial neural crest ablation of Jagged1 recapitulates the craniofacial phenotype of Alagille syndrome patients*." Hum Mol Genet **21**(6): 1374-1383.

Hunt, D. P., Morris, P. N., Sterling, J., Anderson, J. A., Joannides, A., Jahoda, C., Compston, A. and Chandran, S. (2008). "*A highly enriched niche of precursor cells with neuronal and glial potential within the hair follicle dermal papilla of adult skin*." Stem Cells **26**(1): 163-172.

Huth, H. W., Santos, D. M., Gravina, H. D., Resende, J. M., Goes, A. M., de Lima, M. E. and Ropert, C. (2017). "*Upregulation of p38 pathway accelerates proliferation and migration of MDA-MB-231 breast cancer cells*." Oncol Rep **37**(4): 2497-2505.

Iancu, C. B., Iancu, D., Rentea, I., Hostiuc, S., Dermengiu, D. and Rusu, M. C. (2015). "*Molecular signatures of cardiac stem cells*." Rom J Morphol Embryol **56**(4): 1255-1262.

Ilie, C. A., Rusu, M. C., Didilescu, A. C., Motoc, A. G. and Mogoanta, L. (2015). "*Embryonic hematopoietic stem cells and interstitial Cajal cells in the hindgut of late stage human embryos: evidence and hypotheses*." Ann Anat **200**: 24-29.

Imam, A., Jin, G., Sillesen, M., Dekker, S. E., Bambakidis, T., Hwabejire, J. O., Jepsen, C. H., Halaweish, I. and Alam, H. B. (2015). "*Fresh frozen plasma resuscitation provides neuroprotection compared to normal saline in a large animal model of traumatic brain injury and polytrauma*." J Neurotrauma **32**(5): 307-313.

Jansen, B. J., Gilissen, C., Roelofs, H., Schaap-Oziemlak, A., Veltman, J. A., Raymakers, R. A., Jansen, J. H., Kogler, G., Figdor, C. G., Torensma, R. and Adema, G. J. (2010). "*Functional differences between mesenchymal stem cell populations are reflected by their transcriptome*." Stem Cells Dev **19**(4): 481-490.

Janzen, V., Forkert, R., Fleming, H. E., Saito, Y., Waring, M. T., Dombkowski, D. M., Cheng, T., DePinho, R. A., Sharpless, N. E. and Scadden, D. T. (2006). "*Stem-cell ageing modified by the cyclin-dependent kinase inhibitor p16INK4a*." Nature **443**(7110): 421-426.

Jellinger, K. A. and Stadelmann, C. (2000). "*Mechanisms of cell death in neurodegenerative disorders*." J Neural Transm Suppl **59**: 95-114.

Jiang, Y., Jahagirdar, B. N., Reinhardt, R. L., Schwartz, R. E., Keene, C. D., Ortiz-Gonzalez, X. R., Reyes, M., Lenvik, T., Lund, T., Blackstad, M., Du, J., Aldrich, S., Lisberg, A., Low, W. C., Largaespada, D. A. and Verfaillie, C. M. (2002). "*Pluripotency of mesenchymal stem cells derived from adult marrow*." Nature **418**(6893): 41-49.

Johansson, C. B., Momma, S., Clarke, D. L., Risling, M., Lendahl, U. and Frisén, J. (1999). "*Identification of a Neural Stem Cell in the Adult Mammalian Central Nervous System*." Cell **96**(1): 25-34.

Kaltschmidt, B., Kaltschmidt, C. and Widera, D. (2012). "*Adult craniofacial stem cells: sources and relation to the neural crest*." Stem Cell Rev **8**(3): 658-671.

Kempf, H. and Zweigerdt, R. (2018). "*Scalable Cardiac Differentiation of Pluripotent Stem Cells Using Specific Growth Factors and Small Molecules*." Adv Biochem Eng Biotechnol **163**: 39-69.

Keyte, A. and Hutson, M. R. (2012). "*The neural crest in cardiac congenital anomalies*." Differentiation **84**(1): 25-40.

Kim, G. H., Kim, J. E., Rhie, S. J. and Yoon, S. (2015). "*The Role of Oxidative Stress in Neurodegenerative Diseases*." Exp Neurobiol **24**(4): 325-340.

Kim, K., Doi, A., Wen, B., Ng, K., Zhao, R., Cahan, P., Kim, J., Aryee, M. J., Ji, H., Ehrlich, L. I., Yabuuchi, A., Takeuchi, A., Cunniff, K. C., Hongguang, H., McKinney-Freeman, S., Naveiras, O., Yoon, T. J., Irizarry, R. A., Jung, N., Seita, J., Hanna, J., Murakami, P., Jaenisch, R., Weissleder, R., Orkin, S. H., Weissman, I. L., Feinberg, A. P. and Daley, G. Q. (2010). "*Epigenetic memory in induced pluripotent stem cells*." Nature **467**(7313): 285-290.

Kirkwood, T. B. (2005). "*Understanding the odd science of aging*." Cell **120**(4): 437-447.

Kondo, H., Nomaguchi, T. A. and Yonezawa, Y. (1989). "*Effects of serum from human subjects of different ages on migration in vitro of human fibroblasts*." Mech Ageing Dev **47**(1): 25-37.

Kondo, H., Yonezawa, Y. and Ito, H. (2000). "*Inhibitory effects of human serum on human fetal skin fibroblast migration: migration-inhibitory activity and substances in serum, and its age-related changes*." In Vitro Cell Dev Biol Anim **36**(4): 256-261.

Koninckx, R., Daniels, A., Windmolders, S., Mees, U., Macianskiene, R., Mubagwa, K., Steels, P., Jamaer, L., Dubois, J., Robic, B., Hendrikx, M., Rummens, J. L. and Hensen, K. (2013). "*The cardiac atrial appendage stem cell: a new and promising candidate for myocardial repair*." Cardiovasc Res **97**(3): 413-423.

Krebs, H. A. (1950). "*Chemical composition of blood plasma and serum*." Annu Rev Biochem **19**: 409-430.

Kress, W., Schropp, C., Lieb, G., Petersen, B., Busse-Ratzka, M., Kunz, J., Reinhart, E., Schafer, W. D., Sold, J., Hoppe, F., Pahnke, J., Trusen, A., Sorensen, N., Krauss, J. and Collmann, H. (2006). "*Saethre-Chotzen syndrome caused by TWIST 1 gene mutations: functional differentiation from Muenke coronal synostosis syndrome*." Eur J Hum Genet **14**(1): 39-48.

Kuilman, T., Michaloglou, C., Mooi, W. J. and Peeper, D. S. (2010). "*The essence of senescence*." Genes Dev **24**(22): 2463-2479.

Kurz, D. J., Decary, S., Hong, Y. and Erusalimsky, J. D. (2000). "*Senescence-associated (beta)-galactosidase reflects an increase in lysosomal mass during replicative ageing of human endothelial cells*." J Cell Sci **113 (Pt 20)**: 3613-3622.

Laflamme, M. A. and Murry, C. E. (2011). "*Heart regeneration*." Nature **473**(7347): 326-335.

Leinonen, J. S., Ahonen, J. P., Lonnrot, K., Jehkonen, M., Dastidar, P., Molnar, G. and Alho, H. (2000). "*Low plasma antioxidant activity is associated with high lesion volume and neurological impairment in stroke*." Stroke **31**(1): 33-39.

Leinonen, J. V., Korkus-Emanuelov, A., Wolf, Y., Milgrom-Hoffman, M., Lichtstein, D., Hoss, S., Lotan, C., Tzahor, E., Jung, S. and Beeri, R. (2016). "*Macrophage precursor cells from the left atrial appendage of the heart spontaneously reprogram into a C-kit+/CD45- stem cell-like phenotype*." Int J Cardiol **209**: 296-306.

Li, H. Y., Say, E. H. and Zhou, X. F. (2007). "*Isolation and characterization of neural crest progenitors from adult dorsal root ganglia*." Stem Cells **25**(8): 2053-2065.

Li, P., Wu, M., Lin, Q., Wang, S., Chen, T. and Jiang, H. (2018). "*Key genes and integrated modules in hematopoietic differentiation of human embryonic stem cells: a comprehensive bioinformatic analysis*." Stem Cell Res Ther **9**(1): 301.

Liguori, I., Russo, G., Curcio, F., Bulli, G., Aran, L., Della-Morte, D., Gargiulo, G., Testa, G., Cacciatore, F., Bonaduce, D. and Abete, P. (2018). "*Oxidative stress, aging, and diseases*." Clin Interv Aging **13**: 757-772.

Lin, Y., Linask, K. L., Mallon, B., Johnson, K., Klein, M., Beers, J., Xie, W., Du, Y., Liu, C., Lai, Y., Zou, J., Haigney, M., Yang, H., Rao, M. and Chen, G. (2017). "*Heparin Promotes Cardiac Differentiation of Human Pluripotent Stem Cells in Chemically Defined Albumin-Free Medium, Enabling Consistent Manufacture of Cardiomyocytes*." Stem Cells Transl Med **6**(2): 527-538.

Ling, L., Gu, S., Cheng, Y. and Ding, L. (2018). "*bFGF promotes Sca1+ cardiac stem cell migration through activation of the PI3K/Akt pathway*." Mol Med Rep **17**(2): 2349-2356.

Lipinski, M. M., Zheng, B., Lu, T., Yan, Z., Py, B. F., Ng, A., Xavier, R. J., Li, C., Yankner, B. A., Scherzer, C. R. and Yuan, J. (2010). "*Genome-wide analysis reveals mechanisms modulating autophagy in normal brain aging and in Alzheimer's disease*." Proc Natl Acad Sci U S A **107**(32): 14164-14169.

Liu, A., Guo, E., Yang, J., Yang, Y., Liu, S., Jiang, X., Hu, Q., Dirsch, O., Dahmen, U., Zhang, C., Gewirtz, D. A. and Fang, H. (2018). "*Young plasma reverses age-dependent alterations in hepatic function through the restoration of autophagy*." Aging Cell **17**(1).

Liu, X., Duan, B., Cheng, Z., Jia, X., Mao, L., Fu, H., Che, Y., Ou, L., Liu, L. and Kong, D. (2011). "*SDF-1/CXCR4 axis modulates bone marrow mesenchymal stem cell apoptosis, migration and cytokine secretion*." Protein Cell **2**(10): 845-854.

Loffredo, F. S., Steinhauser, M. L., Jay, S. M., Gannon, J., Pancoast, J. R., Yalamanchi, P., Sinha, M., Dall'Osso, C., Khong, D., Shadrach, J. L., Miller, C. M., Singer, B. S., Stewart, A., Psychogios, N., Gerszten, R. E., Hartigan, A. J., Kim, M. J., Serwold, T., Wagers, A. J. and Lee, R. T. (2013). "*Growth differentiation factor 11 is a circulating factor that reverses age-related cardiac hypertrophy*." Cell **153**(4): 828-839.

López-Otín, C., Blasco, M. A., Partridge, L., Serrano, M. and Kroemer, G. (2013). "*The hallmarks of aging*." Cell **153**(6): 1194-1217.

Mark, M., Rijli, F. M. and Chambon, P. (1997). "*Homeobox genes in embryogenesis and pathogenesis*." Pediatr Res **42**(4): 421-429.

Marques, C. S., Soares, M., Santos, A., Correia, J. and Ferreira, F. (2017). "*Serum SDF-1 levels are a reliable diagnostic marker of feline mammary carcinoma, discriminating HER2-overexpressing tumors from other subtypes*." Oncotarget **8**(62): 105775-105789.

Martin, G. R. (1981). "*Isolation of a pluripotent cell line from early mouse embryos cultured in medium conditioned by teratocarcinoma stem cells*." Proc Natl Acad Sci U S A **78**(12): 7634-7638.

Masek, J. and Andersson, E. R. (2017). "*The developmental biology of genetic Notch disorders*." Development **144**(10): 1743-1763.

Mathew, J., Sankar, P. and Varacallo, M. (2020). *Physiology, Blood Plasma*. StatPearls. Treasure Island (FL).

Matsuura, K., Nagai, T., Nishigaki, N., Oyama, T., Nishi, J., Wada, H., Sano, M., Toko, H., Akazawa, H., Sato, T., Nakaya, H., Kasanuki, H. and Komuro, I. (2004). "*Adult cardiac Sca-1-positive cells differentiate into beating cardiomyocytes*." J Biol Chem **279**(12): 11384-11391.

Matthews, C., Gorenne, I., Scott, S., Figg, N., Kirkpatrick, P., Ritchie, A., Goddard, M. and Bennett, M. (2006). "*Vascular smooth muscle cells undergo telomere-based senescence in human atherosclerosis: effects of telomerase and oxidative stress*." Circ Res **99**(2): 156-164.

McDaniell, R., Warthen, D. M., Sanchez-Lara, P. A., Pai, A., Krantz, I. D., Piccoli, D. A. and Spinner, N. B. (2006). "*NOTCH2 mutations cause Alagille syndrome, a heterogeneous disorder of the notch signaling pathway*." Am J Hum Genet **79**(1): 169-173.

Messina, E., De Angelis, L., Frati, G., Morrone, S., Chimenti, S., Fiordaliso, F., Salio, M., Battaglia, M., Latronico, M. V., Coletta, M., Vivarelli, E., Frati, L., Cossu, G. and Giacomello, A. (2004). "*Isolation and expansion of adult cardiac stem cells from human and murine heart*." Circ Res **95**(9): 911-921.

Meus, M. A., Hertig, V., Villeneuve, L., Jasmin, J. F. and Calderone, A. (2017). "*Nestin Expressed by Pre-Existing Cardiomyocytes Recapitulated in Part an Embryonic Phenotype; Suppressive Role of p38 MAPK*." J Cell Physiol **232**(7): 1717-1727.

Meza-Zepeda, L. A., Noer, A., Dahl, J. A., Micci, F., Myklebost, O. and Collas, P. (2008). "*High-resolution analysis of genetic stability of human adipose tissue stem cells cultured to senescence*." J Cell Mol Med **12**(2): 553-563.

Mezey, E., Key, S., Vogelsang, G., Szalayova, I., Lange, G. D. and Crain, B. (2003). "*Transplanted bone marrow generates new neurons in human brains*." Proc Natl Acad Sci U S A **100**(3): 1364-1369.

Michaelis, E. K. (1998). "*Molecular biology of glutamate receptors in the central nervous system and their role in excitotoxicity, oxidative stress and aging*." Prog Neurobiol **54**(4): 369-415.

Milatovic, D., Gupta, R. C. and Dettbarn, W. D. (2002). "*Involvement of nitric oxide in kainic acid-induced excitotoxicity in rat brain*." Brain Res **957**(2): 330-337.

Mishima, Y. and Lotz, M. (2008). "*Chemotaxis of human articular chondrocytes and mesenchymal stem cells*." J Orthop Res **26**(10): 1407-1412.

Molenaar, B., Timmer, L. T., Droog, M., Perini, I., Versteeg, D., Kooijman, L., Monshouwer-Kloots, J., de Ruiter, H., Gladka, M. M. and van Rooij, E. (2021). "*Single-cell transcriptomics following ischemic injury identifies a role for B2M in cardiac repair*." Commun Biol **4**(1): 146.

Molofsky, A. V., Slutsky, S. G., Joseph, N. M., He, S., Pardal, R., Krishnamurthy, J., Sharpless, N. E. and Morrison, S. J. (2006). "*Increasing p16INK4a expression decreases forebrain progenitors and neurogenesis during ageing*." Nature **443**(7110): 448-452.

Moretti, A., Caron, L., Nakano, A., Lam, J. T., Bernshausen, A., Chen, Y., Qyang, Y., Bu, L., Sasaki, M., Martin-Puig, S., Sun, Y., Evans, S. M., Laugwitz, K. L. and Chien, K. R. (2006). "*Multipotent embryonic isl1+ progenitor cells lead to cardiac, smooth muscle, and endothelial cell diversification*." Cell **127**(6): 1151-1165.

Morikawa, Y. and Cserjesi, P. (2008). "*Cardiac neural crest expression of Hand2 regulates outflow and second heart field development*." Circ Res **103**(12): 1422-1429.

Morita, N., Yamamoto, M. and Tanizawa, T. (2003). "*Correlation of c-kit expression and cell cycle regulation by transforming growth factor-beta in CD34+ CD38- human bone marrow cells*." Eur J Haematol **71**(5): 351-358.

Morrison, S. J., White, P. M., Zock, C. and Anderson, D. J. (1999). "*Prospective identification, isolation by flow cytometry, and in vivo self-renewal of multipotent mammalian neural crest stem cells*." Cell **96**(5): 737-749.

Müller, J., Greiner, J. F., Zeuner, M., Brotzmann, V., Schäfermann, J., Wieters, F., Widera, D., Sudhoff, H., Kaltschmidt, B. and Kaltschmidt, C. (2016). "*1,8-Cineole potentiates IRF3-mediated antiviral response in human stem cells and in an ex vivo model of rhinosinusitis*." Clin Sci (Lond) **130**(15): 1339-1352.

Müller, J., Ossig, C., Greiner, J. F., Hauser, S., Fauser, M., Widera, D., Kaltschmidt, C., Storch, A. and Kaltschmidt, B. (2015). "*Intrastriatal transplantation of adult human neural crest-derived stem cells improves functional outcome in parkinsonian rats*." Stem Cells Transl Med **4**(1): 31-43.

Nagoshi, N., Shibata, S., Hamanoue, M., Mabuchi, Y., Matsuzaki, Y., Toyama, Y., Nakamura, M. and Okano, H. (2011). "*Schwann cell plasticity after spinal cord injury shown by neural crest lineage tracing*." Glia **59**(5): 771-784.

Niccoli, T. and Partridge, L. (2012). "*Ageing as a risk factor for disease*." Curr Biol **22**(17): R741-752.

Nowbar, A. N., Gitto, M., Howard, J. P., Francis, D. P. and Al-Lamee, R. (2019). "*Mortality From Ischemic Heart Disease*." Circ Cardiovasc Qual Outcomes **12**(6): e005375.

Oh, H., Bradfute, S. B., Gallardo, T. D., Nakamura, T., Gaussin, V., Mishina, Y., Pocius, J., Michael, L. H., Behringer, R. R., Garry, D. J., Entman, M. L. and Schneider, M. D. (2003). "*Cardiac progenitor cells from adult myocardium: homing, differentiation, and fusion after infarction*." Proc Natl Acad Sci U S A **100**(21): 12313-12318.

Oldershaw, R., Owens, W. A., Sutherland, R., Linney, M., Liddle, R., Magana, L., Lash, G. E., Gill, J. H., Richardson, G. and Meeson, A. (2019). "*Human Cardiac-Mesenchymal Stem Cell-Like Cells, a Novel Cell Population with Therapeutic Potential*." Stem Cells Dev **28**(9): 593-607.

Otsuki, L. and Brand, A. H. (2020). "*Quiescent Neural Stem Cells for Brain Repair and Regeneration: Lessons from Model Systems*." Trends Neurosci **43**(4): 213-226.

Pandey, S., Hickey, D. U., Drum, M., Millis, D. L. and Cekanova, M. (2019). "*Platelet-rich plasma affects the proliferation of canine bone marrow-derived mesenchymal stromal cells in vitro*." BMC Vet Res **15**(1): 269.

Paradis, V., Youssef, N., Dargere, D., Ba, N., Bonvoust, F., Deschatrette, J. and Bedossa, P. (2001). "*Replicative senescence in normal liver, chronic hepatitis C, and hepatocellular carcinomas*." Hum Pathol **32**(3): 327-332.

Pardal, R., Ortega-Saenz, P., Duran, R. and Lopez-Barneo, J. (2007). "*Glia-like stem cells sustain physiologic neurogenesis in the adult mammalian carotid body*." Cell **131**(2): 364-377.

Park, D., Xiang, A. P., Mao, F. F., Zhang, L., Di, C. G., Liu, X. M., Shao, Y., Ma, B. F., Lee, J. H., Ha, K. S., Walton, N. and Lahn, B. T. (2010). "*Nestin is required for the proper self-renewal of neural stem cells*." Stem Cells **28**(12): 2162-2171.

Pauli, S., Bajpai, R. and Borchers, A. (2017). "*CHARGEd with neural crest defects*." Am J Med Genet C Semin Med Genet **175**(4): 478-486.

Paznekas, W. A., Boyadjiev, S. A., Shapiro, R. E., Daniels, O., Wollnik, B., Keegan, C. E., Innis, J. W., Dinulos, M. B., Christian, C., Hannibal, M. C. and Jabs, E. W. (2003). "*Connexin 43 (GJA1) mutations cause the pleiotropic phenotype of oculodentodigital dysplasia*." Am J Hum Genet **72**(2): 408-418.

Pearse, A. G., Polak, J. M., Rost, F. W., Fontaine, J., Le Lievre, C. and Le Douarin, N. (1973). "*Demonstration of the neural crest origin of type I (APUD) cells in the avian carotid body, using a cytochemical marker system*." Histochemie **34**(3): 191-203.

Pelc, A. and Mikulewicz, M. (2018). "*Saethre-Chotzen syndrome: Case report and literature review*." Dent Med Probl **55**(2): 217-225.

Peters, M. J., Joehanes, R., Pilling, L. C., Schurmann, C., Conneely, K. N., Powell, J., Reinmaa, E., Sutphin, G. L., Zhernakova, A., Schramm, K., Wilson, Y. A., Kobes, S., Tukiainen, T., Ramos, Y. F., Goring, H. H., Fornage, M., Liu, Y., Gharib, S. A., Stranger, B. E., De Jager, P. L., Aviv, A., Levy, D., Murabito, J. M., Munson, P. J., Huan, T., Hofman, A., Uitterlinden, A. G., Rivadeneira, F., van Rooij, J., Stolk, L., Broer, L., Verbiest, M. M., Jhamai, M., Arp, P., Metspalu, A., Tserel, L., Milani, L., Samani, N. J., Peterson, P., Kasela, S., Codd, V., Peters, A., Ward-Caviness, C. K., Herder, C., Waldenberger, M., Roden, M., Singmann, P., Zeilinger, S., Illig, T., Homuth, G., Grabe, H. J., Volzke, H., Steil, L., Kocher, T., Murray, A., Melzer, D., Yaghootkar, H., Bandinelli, S., Moses, E. K., Kent, J. W., Curran, J. E., Johnson, M. P., Williams-Blangero, S., Westra, H. J., McRae, A. F., Smith, J. A., Kardia, S. L.,

Hovatta, I., Perola, M., Ripatti, S., Salomaa, V., Henders, A. K., Martin, N. G., Smith, A. K., Mehta, D., Binder, E. B., Nylocks, K. M., Kennedy, E. M., Klengel, T., Ding, J., Suchy-Dicey, A. M., Enquobahrie, D. A., Brody, J., Rotter, J. I., Chen, Y. D., Houwing-Duistermaat, J., Kloppenburg, M., Slagboom, P. E., Helmer, Q., den Hollander, W., Bean, S., Raj, T., Bakhshi, N., Wang, Q. P., Oyston, L. J., Psaty, B. M., Tracy, R. P., Montgomery, G. W., Turner, S. T., Blangero, J., Meulenbelt, I., Ressler, K. J., Yang, J., Franke, L., Kettunen, J., Visscher, P. M., Neely, G. G., Korstanje, R., Hanson, R. L., Prokisch, H., Ferrucci, L., Esko, T., Teumer, A., van Meurs, J. B. and Johnson, A. D. (2015). "*The transcriptional landscape of age in human peripheral blood.*" Nat Commun **6**: 8570.

Pittenger, M. F., Mackay, A. M., Beck, S. C., Jaiswal, R. K., Douglas, R., Mosca, J. D., Moorman, M. A., Simonetti, D. W., Craig, S. and Marshak, D. R. (1999). "*Multilineage potential of adult human mesenchymal stem cells.*" Science **284**(5411): 143-147.

Poelmann, R. E., Mikawa, T. and Gittenberger-de Groot, A. C. (1998). "*Neural crest cells in outflow tract septation of the embryonic chicken heart: differentiation and apoptosis.*" Dev Dyn **212**(3): 373-384.

Poggioli, T., Vujic, A., Yang, P., Macias-Trevino, C., Uygur, A., Loffredo, F. S., Pancoast, J. R., Cho, M., Goldstein, J., Tandias, R. M., Gonzalez, E., Walker, R. G., Thompson, T. B., Wagers, A. J., Fong, Y. W. and Lee, R. T. (2016). "*Circulating Growth Differentiation Factor 11/8 Levels Decline With Age.*" Circ Res **118**(1): 29-37.

Prentice, D. A. (2019). "*Adult Stem Cells.*" Circ Res **124**(6): 837-839.

Price, J. S., Waters, J. G., Darrah, C., Pennington, C., Edwards, D. R., Donell, S. T. and Clark, I. M. (2002). "*The role of chondrocyte senescence in osteoarthritis.*" Aging Cell **1**(1): 57-65.

Prince, M., Bryce, R., Albanese, E., Wimo, A., Ribeiro, W. and Ferri, C. P. (2013). "*The global prevalence of dementia: a systematic review and metaanalysis.*" Alzheimers Dement **9**(1): 63-75 e62.

Pringsheim, T., Jette, N., Frolkis, A. and Steeves, T. D. (2014). "*The prevalence of Parkinson's disease: a systematic review and meta-analysis.*" Mov Disord **29**(13): 1583-1590.

Qiao, H., Surti, S., Choi, S. R., Raju, K., Zhang, H., Ponde, D. E., Kung, H. F., Karp, J. and Zhou, R. (2009). "*Death and proliferation time course of stem cells transplanted in the myocardium.*" Mol Imaging Biol **11**(6): 408-414.

Raab, M., Swift, J., Dingal, P. C., Shah, P., Shin, J. W. and Discher, D. E. (2012). "*Crawling from soft to stiff matrix polarizes the cytoskeleton and phosphoregulates myosin-II heavy chain.*" J Cell Biol **199**(4): 669-683.

Rajagopal, J. and Stanger, B. Z. (2016). "*Plasticity in the Adult: How Should the Waddington Diagram Be Applied to Regenerating Tissues?*" Dev Cell **36**(2): 133-137.

Reinecke, H., Minami, E., Zhu, W. Z. and Laflamme, M. A. (2008). "*Cardiogenic differentiation and transdifferentiation of progenitor cells.*" Circ Res **103**(10): 1058-1071.

Robertson, K., Mason, I. and Hall, S. (1997). "*Hirschsprung's disease: genetic mutations in mice and men.*" Gut **41**(4): 436-441.

Roche, M., Rondeau, P., Singh, N. R., Tarnus, E. and Bourdon, E. (2008). "*The antioxidant properties of serum albumin.*" FEBS Lett **582**(13): 1783-1787.

Rossi, D. J., Bryder, D., Seita, J., Nussenzweig, A., Hoeijmakers, J. and Weissman, I. L. (2007). "*Deficiencies in DNA damage repair limit the function of haematopoietic stem cells with age*." Nature **447**(7145): 725-729.

Ruiz-Perera, L. M., Greiner, J. F. W., Kaltschmidt, C. and Kaltschmidt, B. (2020). "*A Matter of Choice: Inhibition of c-Rel Shifts Neuronal to Oligodendroglial Fate in Human Stem Cells*." Cells **9**(4).

Ruiz-Perera, L. M., Schneider, L., Windmoller, B. A., Muller, J., Greiner, J. F. W., Kaltschmidt, C. and Kaltschmidt, B. (2018). "*NF-kappaB p65 directs sex-specific neuroprotection in human neurons*." Sci Rep **8**(1): 16012.

Rusu, M. C., Duta, I., Didilescu, A. C., Vrapciu, A. D., Hostiuc, S. and Anton, E. (2014). "*Precursor and interstitial Cajal cells in the human embryo liver*." Rom J Morphol Embryol **55**(2): 291-296.

Ryu, C. H., Park, S. A., Kim, S. M., Lim, J. Y., Jeong, C. H., Jun, J. A., Oh, J. H., Park, S. H., Oh, W. I. and Jeun, S. S. (2010). "*Migration of human umbilical cord blood mesenchymal stem cells mediated by stromal cell-derived factor-1/CXCR4 axis via Akt, ERK, and p38 signal transduction pathways*." Biochem Biophys Res Commun **398**(1): 105-110.

Saika, S., Okada, Y., Miyamoto, T., Yamanaka, O., Ohnishi, Y., Ooshima, A., Liu, C. Y., Weng, D. and Kao, W. W. (2004). "*Role of p38 MAP kinase in regulation of cell migration and proliferation in healing corneal epithelium*." Invest Ophthalmol Vis Sci **45**(1): 100-109.

Salpeter, S. J., Khalaileh, A., Weinberg-Corem, N., Ziv, O., Glaser, B. and Dor, Y. (2013). "*Systemic regulation of the age-related decline of pancreatic beta-cell replication*." Diabetes **62**(8): 2843-2848.

Saxena, N., Mogha, P., Dash, S., Majumder, A., Jadhav, S. and Sen, S. (2018). "*Matrix elasticity regulates mesenchymal stem cell chemotaxis*." J Cell Sci **131**(7).

Scheithauer, M. O. (2010). "*Surgery of the turbinates and "empty nose" syndrome*." GMS Curr Top Otorhinolaryngol Head Neck Surg **9**: Doc03.

Schmitz, J., Tauber, S., Westerwalbesloh, C., von Lieres, E., Noll, T. and Grunberger, A. (2020). "*Development and application of a cultivation platform for mammalian suspension cell lines with single-cell resolution*." Biotechnol Bioeng.

Schürmann, M., Brotzmann, V., Butow, M., Greiner, J., Höving, A., Kaltschmidt, C., Kaltschmidt, B. and Sudhoff, H. (2018). "*Identification of a Novel High Yielding Source of Multipotent Adult Human Neural Crest-Derived Stem Cells*." Stem Cell Rev.

Scudellari, M. (2015). "*Ageing research: Blood to blood*." Nature **517**(7535): 426-429.

Sha, S. J., Deutsch, G. K., Tian, L., Richardson, K., Coburn, M., Gaudioso, J. L., Marcal, T., Solomon, E., Boumis, A., Bet, A., Mennes, M., van Oort, E., Beckmann, C. F., Braithwaite, S. P., Jackson, S., Nikolich, K., Stephens, D., Kerchner, G. A. and Wyss-Coray, T. (2019). "*Safety, Tolerability, and Feasibility of Young Plasma Infusion in the Plasma for Alzheimer Symptom Amelioration Study: A Randomized Clinical Trial*." JAMA Neurol **76**(1): 35-40.

Sharpless, N. E. and DePinho, R. A. (2007). "*How stem cells age and why this makes us grow old*." Nat Rev Mol Cell Biol **8**(9): 703-713.

Shaw, A. C., Joshi, S., Greenwood, H., Panda, A. and Lord, J. M. (2010). "*Aging of the innate immune system*." Curr Opin Immunol **22**(4): 507-513.

Shen, J., Gao, Q., Zhang, Y. and He, Y. (2015). "*Autologous plateletrich plasma promotes proliferation and chondrogenic differentiation of adiposederived stem cells*." Mol Med Rep **11**(2): 1298-1303.

Shetty, P., Bharucha, K. and Tanavde, V. (2007). "*Human umbilical cord blood serum can replace fetal bovine serum in the culture of mesenchymal stem cells*." Cell Biol Int **31**(3): 293-298.

Shpargel, K. B., Mangini, C. L., Xie, G., Ge, K. and Magnuson, T. (2020). "*The KMT2D Kabuki syndrome histone methylase controls neural crest cell differentiation and facial morphology*." Development **147**(21).

Sieber-Blum, M. (2004). "*Cardiac neural crest stem cells*." Anat Rec A Discov Mol Cell Evol Biol **276**(1): 34-42.

Sinnakannu, J. R., Lee, K. L., Cheng, S., Li, J., Yu, M., Tan, S. P., Ong, C. C. H., Li, H., Than, H., Anczukow-Camarda, O., Krainer, A. R., Roca, X., Rozen, S. G., Iqbal, J., Yang, H., Chuah, C. and Ong, S. T. (2020). "*SRSF1 mediates cytokine-induced impaired imatinib sensitivity in chronic myeloid leukemia*." Leukemia **34**(7): 1787-1798.

Sliogeryte, K. and Gavara, N. (2019). "*Vimentin Plays a Crucial Role in Fibroblast Ageing by Regulating Biophysical Properties and Cell Migration*." Cells **8**(10).

Smits, A. M., van Vliet, P., Metz, C. H., Korfage, T., Sluijter, J. P., Doevendans, P. A. and Goumans, M. J. (2009). "*Human cardiomyocyte progenitor cells differentiate into functional mature cardiomyocytes: an in vitro model for studying human cardiac physiology and pathophysiology*." Nat Protoc **4**(2): 232-243.

Smittenaar, C. R., Petersen, K. A., Stewart, K. and Moitt, N. (2016). "*Cancer incidence and mortality projections in the UK until 2035*." Br J Cancer **115**(9): 1147-1155.

Solaimani Kartalaei, P., Yamada-Inagawa, T., Vink, C. S., de Pater, E., van der Linden, R., Marks-Bluth, J., van der Sloot, A., van den Hout, M., Yokomizo, T., van Schaick-Solerno, M. L., Delwel, R., Pimanda, J. E., van, I. W. F. and Dzierzak, E. (2015). "*Whole-transcriptome analysis of endothelial to hematopoietic stem cell transition reveals a requirement for Gpr56 in HSC generation*." J Exp Med **212**(1): 93-106.

Sousa-Victor, P., Gutarra, S., Garcia-Prat, L., Rodriguez-Ubreva, J., Ortet, L., Ruiz-Bonilla, V., Jardi, M., Ballestar, E., Gonzalez, S., Serrano, A. L., Perdiguero, E. and Munoz-Canoves, P. (2014). "*Geriatric muscle stem cells switch reversible quiescence into senescence*." Nature **506**(7488): 316-321.

Southgate, L., Sukalo, M., Karountzos, A. S. V., Taylor, E. J., Collinson, C. S., Ruddy, D., Snape, K. M., Dallapiccola, B., Tolmie, J. L., Joss, S., Brancati, F., Digilio, M. C., Graul-Neumann, L. M., Salviati, L., Coerdt, W., Jacquemin, E., Wuyts, W., Zenker, M., Machado, R. D. and Trembath, R. C. (2015). "*Haploinsufficiency of the NOTCH1 Receptor as a Cause of Adams-Oliver Syndrome With Variable Cardiac Anomalies*." Circ Cardiovasc Genet **8**(4): 572-581.

Stegeman, R. and Weake, V. M. (2017). "*Transcriptional Signatures of Aging*." J Mol Biol **429**(16): 2427-2437.

Steinberg, G. K., Kondziolka, D., Wechsler, L. R., Lunsford, L. D., Coburn, M. L., Billigen, J. B., Kim, A. S., Johnson, J. N., Bates, D., King, B., Case, C., McGrogan, M., Yankee, E. W. and Schwartz, N. E. (2016). "*Clinical Outcomes of Transplanted Modified Bone Marrow-Derived Mesenchymal Stem Cells in Stroke: A Phase 1/2a Study*." Stroke **47**(7): 1817-1824.

Sultana, N., Zhang, L., Yan, J., Chen, J., Cai, W., Razzaque, S., Jeong, D., Sheng, W., Bu, L., Xu, M., Huang, G. Y., Hajjar, R. J., Zhou, B., Moon, A. and Cai, C. L. (2015).

"*Resident c-kit(+) cells in the heart are not cardiac stem cells*." Nat Commun **6**: 8701.

Sun, A. Y., Cheng, Y. and Sun, G. Y. (1992). "*Kainic acid-induced excitotoxicity in neurons and glial cells*." Prog Brain Res **94**: 271-280.

Takahashi, K., Tanabe, K., Ohnuki, M., Narita, M., Ichisaka, T., Tomoda, K. and Yamanaka, S. (2007). "*Induction of pluripotent stem cells from adult human fibroblasts by defined factors*." Cell **131**(5): 861-872.

Takahashi, K. and Yamanaka, S. (2006). "*Induction of pluripotent stem cells from mouse embryonic and adult fibroblast cultures by defined factors*." Cell **126**(4): 663-676.

Tallini, Y. N., Greene, K. S., Craven, M., Spealman, A., Breitbach, M., Smith, J., Fisher, P. J., Steffey, M., Hesse, M., Doran, R. M., Woods, A., Singh, B., Yen, A., Fleischmann, B. K. and Kotlikoff, M. I. (2009). "*c-kit expression identifies cardiovascular precursors in the neonatal heart*." Proc Natl Acad Sci U S A **106**(6): 1808-1813.

Tang, W., Martik, M. L., Li, Y. and Bronner, M. E. (2019). "*Cardiac neural crest contributes to cardiomyocytes in amniotes and heart regeneration in zebrafish*." Elife **8**.

Taskiran, E. Z. and Karaosmanoglu, B. (2019). "*Transcriptome analysis reveals differentially expressed genes between human primary bone marrow mesenchymal stem cells and human primary dermal fibroblasts*." Turk J Biol **43**(1): 21-27.

Techawattanawisal, W., Nakahama, K., Komaki, M., Abe, M., Takagi, Y. and Morita, I. (2007). "*Isolation of multipotent stem cells from adult rat periodontal ligament by neurosphere-forming culture system*." Biochem Biophys Res Commun **357**(4): 917-923.

Terskikh, A. V., Miyamoto, T., Chang, C., Diatchenko, L. and Weissman, I. L. (2003). "*Gene expression analysis of purified hematopoietic stem cells and committed progenitors*." Blood **102**(1): 94-101.

Thakkar, J. P., McCarthy, B. J. and Villano, J. L. (2014). "*Age-specific cancer incidence rates increase through the oldest age groups*." Am J Med Sci **348**(1): 65-70.

Thomson, J. A., Itskovitz-Eldor, J., Shapiro, S. S., Waknitz, M. A., Swiergiel, J. J., Marshall, V. S. and Jones, J. M. (1998). "*Embryonic stem cell lines derived from human blastocysts*." Science **282**(5391): 1145-1147.

Tian, H., Zhang, D., Gao, Z., Li, H., Zhang, B., Zhang, Q., Li, L., Cheng, Q., Pei, D. and Zheng, J. (2014). "*MDA-7/IL-24 inhibits Nrf2-mediated antioxidant response through activation of p38 pathway and inhibition of ERK pathway involved in cancer cell apoptosis*." Cancer Gene Ther **21**(10): 416-426.

Toma, J. G., Akhavan, M., Fernandes, K. J., Barnabe-Heider, F., Sadikot, A., Kaplan, D. R. and Miller, F. D. (2001). "*Isolation of multipotent adult stem cells from the dermis of mammalian skin*." Nat Cell Biol **3**(9): 778-784.

Tomita, Y., Matsumura, K., Wakamatsu, Y., Matsuzaki, Y., Shibuya, I., Kawaguchi, H., Ieda, M., Kanakubo, S., Shimazaki, T., Ogawa, S., Osumi, N., Okano, H. and Fukuda, K. (2005). "*Cardiac neural crest cells contribute to the dormant multipotent stem cell in the mammalian heart*." J Cell Biol **170**(7): 1135-1146.

Tremblay, P., Kessel, M. and Gruss, P. (1995). "*A transgenic neuroanatomical marker identifies cranial neural crest deficiencies associated with the Pax3 mutant Splotch*." Dev Biol **171**(2): 317-329.

Tuo, G., Pini Prato, A., Derchi, M., Mosconi, M., Mattioli, G. and Marasini, M. (2014). "*Hirschsprung's Disease and Associated Congenital Heart Defects: A Prospective Observational Study from a Single Institution*." Front Pediatr **2**: 99.

Urbanek, K., Cesselli, D., Rota, M., Nascimbene, A., De Angelis, A., Hosoda, T., Bearzi, C., Boni, A., Bolli, R., Kajstura, J., Anversa, P. and Leri, A. (2006). "*Stem cell niches in the adult mouse heart*." Proc Natl Acad Sci U S A **103**(24): 9226-9231.

van der Ende, M. Y., Hartman, M. H., Hagemeijer, Y., Meems, L. M., de Vries, H. S., Stolk, R. P., de Boer, R. A., Sijtsma, A., van der Meer, P., Rienstra, M. and van der Harst, P. (2017). "*The LifeLines Cohort Study: Prevalence and treatment of cardiovascular disease and risk factors*." Int J Cardiol **228**: 495-500.

van der Loo, B., Fenton, M. J. and Erusalimsky, J. D. (1998). "*Cytochemical detection of a senescence-associated beta-galactosidase in endothelial and smooth muscle cells from human and rabbit blood vessels*." Exp Cell Res **241**(2): 309-315.

Vaskova, E. A., Stekleneva, A. E., Medvedev, S. P. and Zakian, S. M. (2013). "*"Epigenetic memory" phenomenon in induced pluripotent stem cells*." Acta Naturae **5**(4): 15-21.

Velagaleti, R. S., Pencina, M. J., Murabito, J. M., Wang, T. J., Parikh, N. I., D'Agostino, R. B., Levy, D., Kannel, W. B. and Vasan, R. S. (2008). "*Long-term trends in the incidence of heart failure after myocardial infarction*." Circulation **118**(20): 2057-2062.

Vijg, J. and Campisi, J. (2008). "*Puzzles, promises and a cure for ageing*." Nature **454**(7208): 1065-1071.

Viktorov, I. V., Savchenko, E. A. and Chekhonin, V. P. (2007). "*Spontaneous neural differentiation of stem cells in culture of human olfactory epithelium*." Bull Exp Biol Med **144**(4): 596-601.

Villeda, S. A., Luo, J., Mosher, K. I., Zou, B., Britschgi, M., Bieri, G., Stan, T. M., Fainberg, N., Ding, Z., Eggel, A., Lucin, K. M., Czirr, E., Park, J. S., Couillard-Despres, S., Aigner, L., Li, G., Peskind, E. R., Kaye, J. A., Quinn, J. F., Galasko, D. R., Xie, X. S., Rando, T. A. and Wyss-Coray, T. (2011). "*The ageing systemic milieu negatively regulates neurogenesis and cognitive function*." Nature **477**(7362): 90-94.

Villeda, S. A., Plambeck, K. E., Middeldorp, J., Castellano, J. M., Mosher, K. I., Luo, J., Smith, L. K., Bieri, G., Lin, K., Berdnik, D., Wabl, R., Udeochu, J., Wheatley, E. G., Zou, B., Simmons, D. A., Xie, X. S., Longo, F. M. and Wyss-Coray, T. (2014). "*Young blood reverses age-related impairments in cognitive function and synaptic plasticity in mice*." Nat Med **20**(6): 659-663.

Waddington, R. J., Youde, S. J., Lee, C. P. and Sloan, A. J. (2009). "*Isolation of distinct progenitor stem cell populations from dental pulp*." Cells Tissues Organs **189**(1-4): 268-274.

Wakefield, L. M., Letterio, J. J., Chen, T., Danielpour, D., Allison, R. S., Pai, L. H., Denicoff, A. M., Noone, M. H., Cowan, K. H., O'Shaughnessy, J. A. and et al. (1995). "*Transforming growth factor-beta1 circulates in normal human plasma and is unchanged in advanced metastatic breast cancer*." Clin Cancer Res **1**(1): 129-136.

Walenda, T., Bokermann, G., Jost, E., Galm, O., Schellenberg, A., Koch, C. M., Piroth, D. M., Drescher, W., Brummendorf, T. H. and Wagner, W. (2011). "*Serum after autologous transplantation stimulates proliferation and expansion of human hematopoietic progenitor cells*." PLoS One **6**(3): e18012.

Wang, Q., Yu, S., Simonyi, A., Sun, G. Y. and Sun, A. Y. (2005). "*Kainic acid-mediated excitotoxicity as a model for neurodegeneration*." Mol Neurobiol **31**(1-3): 3-16.

Weiss, J. H. and Sensi, S. L. (2000). "*Ca2+-Zn2+ permeable AMPA or kainate receptors: possible key factors in selective neurodegeneration*." Trends Neurosci **23**(8): 365-371.

WHO. (2021). "*Cardiovascular diseases*." Retrieved 09.02.2021, 2021, from https://www.who.int/health-topics/cardiovascular-diseases/#tab=tab_1.

Widera, D., Zander, C., Heidbreder, M., Kasperek, Y., Noll, T., Seitz, O., Saldamli, B., Sudhoff, H., Sader, R., Kaltschmidt, C. and Kaltschmidt, B. (2009). "*Adult palatum as a novel source of neural crest-related stem cells*." Stem Cells **27**(8): 1899-1910.

Witzeneder, K., Lindenmair, A., Gabriel, C., Holler, K., Theiss, D., Redl, H. and Hennerbichler, S. (2013). "*Human-derived alternatives to fetal bovine serum in cell culture*." Transfus Med Hemother **40**(6): 417-423.

Wollstein, R., Trouw, A., Carlson, L., Staff, I., Mastella, D. J. and Ashmead, D. (2020). "*The Effect of Age on Fracture Healing Time in Metacarpal Fractures*." Hand (N Y) **15**(4): 542-546.

Wong, S. W., Han, D., Zhang, H., Liu, Y., Zhang, X., Miao, M. Z., Wang, Y., Zhao, N., Zeng, L., Bai, B., Wang, Y. X., Liu, H., Frazier-Bowers, S. A. and Feng, H. (2018). "*Nine Novel PAX9 Mutations and a Distinct Tooth Agenesis Genotype-Phenotype*." J Dent Res **97**(2): 155-162.

Wurdak, H., Ittner, L. M., Lang, K. S., Leveen, P., Suter, U., Fischer, J. A., Karlsson, S., Born, W. and Sommer, L. (2005). "*Inactivation of TGFbeta signaling in neural crest stem cells leads to multiple defects reminiscent of DiGeorge syndrome*." Genes Dev **19**(5): 530-535.

Wyss-Coray, T. (2016). "*Ageing, neurodegeneration and brain rejuvenation*." Nature **539**(7628): 180-186.

Yao, P., Zhan, Y., Xu, W., Li, C., Yue, P., Xu, C., Hu, D., Qu, C. K. and Yang, X. (2004). "*Hepatocyte growth factor-induced proliferation of hepatic stem-like cells depends on activation of NF-kappaB*." J Hepatol **40**(3): 391-398.

Yousefzadeh, M. J., Schafer, M. J., Noren Hooten, N., Atkinson, E. J., Evans, M. K., Baker, D. J., Quarles, E. K., Robbins, P. D., Ladiges, W. C., LeBrasseur, N. K. and Niedernhofer, L. J. (2018). "*Circulating levels of monocyte chemoattractant protein-1 as a potential measure of biological age in mice and frailty in humans*." Aging Cell **17**(2).

Yuan, L., Sakamoto, N., Song, G. and Sato, M. (2012). "*Migration of human mesenchymal stem cells under low shear stress mediated by mitogen-activated protein kinase signaling*." Stem Cells Dev **21**(13): 2520-2530.

Zaruba, M. M., Soonpaa, M., Reuter, S. and Field, L. J. (2010). "*Cardiomyogenic potential of C-kit(+)-expressing cells derived from neonatal and adult mouse hearts*." Circulation **121**(18): 1992-2000.

Zarubin, T. and Han, J. (2005). "*Activation and signaling of the p38 MAP kinase pathway*." Cell Res **15**(1): 11-18.

Zeuner, M. T., Didenko, N. N., Humphries, D., Stergiadis, S., Morash, T. M., Patel, K., Grimm, W. D. and Widera, D. (2018). "*Isolation and Characterization of Neural Crest-Derived Stem Cells From Adult Ovine Palatal Tissue*." Front Cell Dev Biol **6**: 39.

Zhang, M., Methot, D., Poppa, V., Fujio, Y., Walsh, K. and Murry, C. E. (2001). "*Cardiomyocyte grafting for cardiac repair: graft cell death and anti-death strategies*." J Mol Cell Cardiol **33**(5): 907-921.

Zhang, S. J., Song, X. Y., He, M. and Yu, S. B. (2016). "*Effect of TGF-beta1/SDF-1/CXCR4 signal on BM-MSCs homing in rat heart of ischemia/perfusion injury*." Eur Rev Med Pharmacol Sci **20**(5): 899-905.

Zuk, P. A., Zhu, M., Ashjian, P., De Ugarte, D. A., Huang, J. I., Mizuno, H., Alfonso, Z. C., Fraser, J. K., Benhaim, P. and Hedrick, M. H. (2002). "*Human adipose tissue is a source of multipotent stem cells*." <u>Mol Biol Cell</u> **13**(12): 4279-4295.

Zwi-Dantsis, L., Huber, I., Habib, M., Winterstern, A., Gepstein, A., Arbel, G. and Gepstein, L. (2013). "*Derivation and cardiomyocyte differentiation of induced pluripotent stem cells from heart failure patients*." <u>Eur Heart J</u> **34**(21): 1575-1586.

8. Acknowledgements

This thesis would not have been possible without the support of many people along the way.

First, I would like to thank my supervisors Prof. Dr. Christian Kaltschmidt and Prof. Dr. Cornelius Knabbe for the opportunity to work on a highly relevant project and for their guidance and supervision. I also thank Prof. Dr. Barbara Kaltschmidt for her interest in this project and fruitful discussions. A special thank goes to Dr. Johannes Greiner for his assistance and support in every question and for proofreading this thesis. I further acknowledge the help of Dr. Isabel Faust in the collection of heart auricles and plasma samples.

I also gratefully thank all the current and former members of the Department of Cell Biology for the pleasant working atmosphere. Especially I would like to thank Kazuko Schmidt and Angela Kralemann-Köhler for their excellent teamwork and support in the lab and Beatrice Windmöller for proofreading.

I thank the co-authors of the publications contributing to this thesis: Christian Kaltschmidt, Cornelius Knabbe, Barbara Kaltschmidt, Johannes Greiner, Kazuko Schmidt, Katharina Sielemann, Jassin Hamidi, Ann-Katrin Rott, Madlen Merten, Jan Gummert, Isabel Faust, Matthias Schürmann, Viktoria Brotzmann, Marlena Bütow, Holger Sudhoff, Beatrice Windmöller, Julian Schmitz, Alexander Grünberger, Kaya Witte, Oliver Hertel, Laureen Helweg, Tobias Busche, Jörn Kalinowski, Thomas Noll, Fritz Mertzlufft, Morris Beshay, Jesco Pfitzenmaier, Constanze Banz-Jansen and Matthias Simon.

Especially, I would like to thank my family and friends for their encouragement and support throughout all the time. A very special thank goes to Norman for his infinite patience and tremendous empathy.

9. Declaration

I hereby declare that I am the sole author of the dissertation "**Blood plasma-mediated effects on regenerative features of a novel adult human cardiac stem cell population"** and did not use any material or sources other than the ones I have named. Passages that use wording (or words of that effect), tables or pictures of other sources have always been duly acknowledged with a reference to the original material.

This dissertation or similar versions have not been previously submitted for a degree.

Bielefeld, _____

Anna Lena Höving

10. Publications

Original Research Report

Blood Serum Stimulates p38-Mediated Proliferation and Changes in Global Gene Expression of Adult Human Cardiac Stem Cells

Anna Höving, Kazuko Schmidt, Madlen Merten, Jassin Hamidi, Ann-Katrin Rott, Isabel Faust, Johannes F. W. Greiner, Jan Gummert, Barbara Kaltschmidt, Christian Kaltschmidt*, and Cornelius Knabbe*

Blood Serum Stimulates p38-Mediated Proliferation and Changes in Global Gene Expression of Adult Human Cardiac Stem Cells

Anna L. Höving [1,2,*], **Kazuko E. Schmidt** [1,2], **Madlen Merten** [3], **Jassin Hamidi** [1],
Ann-Katrin Rott [1], **Isabel Faust** [2], **Johannes F. W. Greiner** [1], **Jan Gummert** [4],
Barbara Kaltschmidt [3], **Christian Kaltschmidt** [1,†,*] and **Cornelius Knabbe** [2,†]

[1] Department of Cell Biology, University of Bielefeld, 33615 Bielefeld, Germany;
   kazuko_elena.schmidt1@uni-bielefeld.de (K.E.S.); jhamidi@uni-bielefeld.de (J.H.);
   ann-katrin1207@t-online.de (A.-K.R.); johannes.greiner@uni-bielefeld.de (J.F.W.G.)
[2] Institute for Laboratory- and Transfusion Medicine, Heart and Diabetes Centre NRW, Ruhr University
   Bochum, 32545 Bad Oeynhausen, Germany; ifaust@hdz-nrw.de (I.F.); cknabbe@hdz-nrw.de (C.K.)
[3] AG Molecular Neurobiology, University of Bielefeld, 33615 Bielefeld, Germany;
   Madlen.merten@uni-bielefeld.de (M.M.); Barbara.Kaltschmidt@uni-bielefeld.de (B.K.)
[4] Department of Thoracic and Cardiovascular surgery, Heart and Diabetes Centre NRW, Ruhr-University
   Bochum, 32545 Bad Oeynhausen, Germany; jgummert@hdz-nrw.de
[*] Correspondence: anna.hoeving@uni-bielefeld.de (A.L.H.); c.kaltschmidt@uni-bielefeld.de (C.K.)
[†] These authors contributed equally to this work.

Abstract: During aging, senescent cells accumulate in various tissues accompanied by decreased regenerative capacities of quiescent stem cells, resulting in deteriorated organ function and overall degeneration. In this regard, the adult human heart with a generally low regenerative potential is of extreme interest as a target for rejuvenating strategies with blood borne factors that might be able to activate endogenous stem cell populations. Here, we investigated for the first time the effects of human blood plasma and serum on adult human cardiac stem cells (hCSCs) and showed significantly increased proliferation capacities and metabolism accompanied by a significant decrease of senescent cells, demonstrating a beneficial serum-mediated effect that seemed to be independent of age and sex. However, RNA-seq analysis of serum-treated hCSCs revealed profound effects on gene expression depending on the age and sex of the plasma donor. We further successfully identified key pathways that are affected by serum treatment with p38-MAPK playing a regulatory role in protection from senescence and in the promotion of proliferation in a serum-dependent manner. Inhibition of p38-MAPK resulted in a decline of these serum-mediated beneficial effects on hCSCs in terms of decreased proliferation and accelerated senescence. In summary, we provide new insights in the regulatory networks behind serum-mediated protective effects on adult human cardiac stem cells.

Keywords: blood serum; heart stem cells; p38-MAPK; RNAseq

1. Introduction

Cardiovascular diseases are the major cause of death worldwide and are accompanied by decreased proliferation capacities of resident cardiomyocytes and endothelial cells and a reduced regenerative potential of quiescent cardiac stem cells (CSCs) [1,2]. In addition to cardiovascular diseases, an overall decline in tissue regenerative potential during human ageing is considered a crucial factor for the onset of other age-related diseases such as Alzheimer's disease, diabetes, chronic obstructive pulmonary disease and atherosclerosis [3]. Within the natural ageing process, regenerative capacities of endogenous

stem cell pools decline. This phenomenon is accompanied by the accumulation of senescent cells in various tissues, responsible for deteriorated organ function [4]. Thus, rejuvenating treatment strategies are needed to increase the endogenous regenerative capacities of adult stem cells. Since the loss of regenerative capacities can be detected in nearly all organs of the human body, the question arises of whether this decline is organ-specific. However, with increasing age, patients are often affected by multiple degenerative diseases, which points in the direction that these are maybe triggered by systemic factors. In this regard, several studies have demonstrated a rejuvenating effect of young blood and blood plasma on various adult stem cell populations, while the discussion about the active component of rejuvenating blood plasma or serum and the underlying molecular mechanisms has not yet come to a consensus. As one example, Conboy and colleagues described for the first time the rejuvenation of muscle satellite cells in aged mice that underwent heterochronic parabiosis through reactivation of Notch signaling [5]. Further, in the same experiments the authors also showed enhanced proliferation of hepatocytes, which was due to reduced levels of the chromatin remodeling factor Brm in old heterochronic parabionts [5]. On that topic, emerging evidence on the existence of rejuvenating or pro-aging blood borne factors was provided in the following years, mainly focusing on heterochronic parabiosis experiments. For instance, the Wyss-Coray group investigated the impact of young blood to the aging brain, especially the hippocampus, and demonstrated beneficial effects on the molecular, structural, functional and even cognitive level [6]. Importantly, they were also the first to show that human umbilical cord plasma is able to revitalize hippocampal function in aged mice and hypothesized the protein TIMP2 to be a crucial player in this process [7].

The results of these studies suggest more than one molecular mechanism is activated by young blood serum and responsible for these rejuvenating effects that may act organ or tissue-specifically. However, the translation from mice to the human system seems to be complicated, as publications of convincing results are extremely rare [8]. However, the first clinical trials are currently aiming to treat neurodegenerative diseases with either young plasma transfusions or age-related plasma fractions, so-called chronokines [9]. Next to neurodegeneration, a decline in cardiac function is another significant risk factor during human ageing. Although the adult heart was long ago considered a terminally differentiated organ with low regenerative potential, rare populations of mouse and human cardiac stem cells (CSCs) were found that may contribute to endogenous repair mechanisms [10–12]. Most of these CSCs were defined by the expression of the stem cell factor receptor kinase cKit [10,13–16]. However, a range of other cell surface markers has also been reported. For instance, a population of mouse embryonic Isl1$^+$ stem cells was shown to give rise to cardiomyocytes, endothelial cells and smooth muscle cells [17]; additionally, mouse Sca1$^+$/CD31$^+$/cKit$^-$ cardiac stem cells were described to exhibit regenerative capacities [18]. In the human system, Smits and colleagues described the isolation of a Sca1$^+$/CD105$^+$/CD31$^+$ population that differentiates to cardiomyocytes in vitro [12]. Interestingly, a high cardiomyocyte proliferation has been reported during fetal development, in contrast to decreased proliferation capacity in adult hearts [1,19]. Thus, targeting the proliferation potential of adult stem cells seems to be a crucial step to enhancing endogenous repair mechanisms. It is well known that blood plasma or serum is a powerful additive in cell culture to enhance proliferation [20–23]. Here, most studies focused on the in vitro expansion of human mesenchymal stem cells (MSCs) or hematopoietic stem cells (HSCs) prior to transplantation, highlighting the multiple advantages of human plasma or serum compared with fetal calf serum (FCS) in terms of safety and clinical applicability. However, the effect of human blood plasma on adult human cardiac stem cells and the respective underlying mechanisms still remain unknown.

In the present study, we isolated a Nestin$^+$/S100$^+$ cell population from the human heart auricle that expresses common cardiac progenitor markers such as CD105, CD31 and Sca1. These cells are able to form cardiospheres after clonal growth and differentiate into cardiomyocyte-like cells in vitro. Moreover, we demonstrate that human blood plasma and blood serum significantly increase proliferation and metabolic activity of human cardiac stem cells. Further, we provide RNA-seq data to investigate the global transcriptome of blood-serum-treated human stem cells and thereby analyze the

highly complex regulatory networks that enhance stem cell proliferation. Here, we could successfully identify key pathways that are affected by serum treatment with p38-MAPK and play a regulatory role in protection from senescence and in the promotion of proliferation.

2. Materials and Methods

2.1. Isolation and Cultivation of Adult Human Cardiac Stem Cells from Heart Auricles

Human heart auricles of left atrial appendages were removed from patients undergoing routine heart surgery after informed and written consent according to local and international guidelines (Declaration of Helsinki). Isolation of human cardiac stem cells (hCSCs) and further experimental procedures were ethically approved by the ethics commission of the medical faculty of the Ruhr University Bochum (approval reference number eP-2016-148). After surgical removal, biopsies were cut into small pieces and washed in PBS (Sigma Aldrich, St-Louis, MO, USA). For initial expansion, the tissue clumps were seeded in gelatin B-coated 10 cm Petri dishes (Sarstedt AG and Co., Nürmbrecht, Germany) with human cardiac stem cell medium (hCSC medium) consisting of DMEM/F-12 medium (Sigma Aldrich), basic fibroblast growth factor (bFGF, 5 ng/mL; Peprotech, Hamburg, Germany), epidermal growth factor (EGF, 10 ng/mL; Peprotech) and 10% fetal calf serum (VWR, Radnor, PA, USA). After reaching confluence, tissue clumps were removed and passaging was performed by treatment with trypsin-EDTA (Sigma Aldrich). For further cultivation, cells were again seeded in gelatin B-coated T-25 cell culture flasks (Sarstedt AG and Co.) in hCSC medium. For clonal analysis, cells were seeded in a 96-well plate (Sarstedt AG and Co.) at a density of 1 cell per well. Single cell dilution was verified by microscopy and medium was changed every two to three days. Sphere forming capacity was tested in low-adhesion culture flasks (Greiner Bio-One, Kremsmünster, Austria) with stem cell medium [24]. In the case of this study, cells from a 77-year old female individual were used.

2.2. Immunohistochemistry and Immunocytochemistry

Cryosections of the heart auricle tissue or cultivated cells were fixed for 20 min using 4% paraformaldehyde (PFA), washed and permeabilized in PBS with TritonX-100 (tissue: 0.2%, cells: 0.02%, Applichem, Darmstadt, Germany) and supplemented with 5% goat serum for 30 min. The applied primary antibodies were diluted in PBS as followed: mouse anti-Nestin 1:200 (Millipore, Burlington, MA, USA), rabbit anti-S100B 1:500 (Dako, Glostrup, Denmark), rabbit anti-α-actinin (Cell-Signaling, Danvers, MA, USA), mouse anti Connexin 43 (Millipore). They were applied for 1 h (cells) or for 2 h (sections), both at room temperature (RT). After three washing steps, secondary fluorochrome-conjugated antibodies (Alexa 555 anti-mouse or Alexa 488 anti-rabbit, Invitrogen, Life Technologies GmbH, Carlsbad, CA, USA) were applied for 1 h at RT with a dilution ratio of 1:300. Nuclear staining was realized by incubation with 4,6-diamidin-2-phenylindol (DAPI) (1 µg/mL, Applichem) in PBS for 15 min at RT. Finally, the samples were mounted with Mowiol (self-made). Imaging was performed using a confocal laser scanning microscope (CLSM 780, Carl Zeiss, Oberkochen, Germany) and image processing was executed with ImageJ and CorelDRAW [25] (open source and Corel Corporation).

2.3. Flow Cytometry

Cultivated hCSCs were harvested by centrifugation after treatment with trypsin and subsequently stained with PE-coupled anti-CD105, anti-CD117, anti-Sca1 or anti-CD31 antibody (Miltenyi Biotec, Bergisch Gladbach, Germany) according to manufacturer's guidelines. For isotype controls, hCSCs were stained with PE-coupled IgG1 control antibody or APC-coupled IgG1 control antibody. Analysis was done using Gallios Flow Cytometer (Beckmann Coulter Inc., Brea, CA, USA), while Kaluza Acquisition Software (Beckmann Coulter Inc.) was used for subsequent data acquisition and statistical analysis.

2.4. Cardiac Differentiation of hCSCs

Cardiac differentiation of the isolated cells was induced following the protocol described by Smits and colleagues [12]. Briefly, cells were seeded with a density of 10^5 cells per 6-well in hCSC medium. After 24 h, differentiation was induced with a cardiac differentiation medium consisting of a 1:1-mixture of IMDM (Gibco, Thermo Fisher Scientific, Waltham, MA, USA) and Ham's F12 nutrient mixture with GlutaMAX-I (Gibco), containing 10% horse serum (Dianova, Hamburg, Germany), 1x MEM nonessential amino acids (Bio Whittaker, Lonza, Basel, Switzerland) and 1x insulin-transferrin-selenium (Gibco). Then, 5 μM 5-azacytidine was added in three consecutive days and differentiation medium was refreshed at day 4. Six days after the start of the differentiation, ascorbic acid (Sigma Aldrich) was added every two days and 1 ng/mL transforming growth factor β (TGF-β) (Peprotech, Hamburg, Germany) was added twice weekly. Medium was refreshed every two to three days. After 28 days, the protein expression was analyzed by immunocytochemical staining for α-actinin as described above. As undifferentiated control, cells were cultured in hCSC medium.

2.5. Blood Plasma

Blood plasma samples were collected from routine blood donation service from healthy individual donors. For further comparisons, plasma donors older than 60 years were declared "old," and donors younger than 20 years were declared "young". For the isolation of serum from fresh frozen plasma (FFP), 20% $CaCl_2$ was added in a ratio of 1:50 and incubated at 4 °C overnight. After centrifugation at 1920 RCF for 20 min, blood serum was harvested from the supernatant. In all assays, blood plasma or serum from three different donors was used as biological replicates within the treatment groups.

2.6. p38-MAPK Inhibition

The following p38-MAPK inhibitors were used: BMS-582949 (InvivoChem, Libertyville, IL, USA) and SB239063 (Medchemexpress, Sollentuna, Sweden). BMS-582949 binds to the p38α and induces a less accessible conformation of the activation loop. We further selected SB239063 since it is highly selective (>220-fold selectivity over ERK and JNK1). Inhibitor stock solutions were dissolved in DMSO at a concentration of 10 mM and aliquots were stored at −80 °C. For p38-MAPK inhibition, inhibitors were diluted to 50 μM in the respective assays. DMSO served as control.

2.7. Proliferation Assay

For examination of cell proliferation, a determined cell count was seeded in either 6-well TC-plates (Sarstedt AG and Co.) or TC25 cell culture flasks (Sarstedt AG and Co.). The cells were starved for 48 h in serum-free medium containing DMEM-F12 (Sigma-Aldrich), 200 mM L-glutamine (Sigma-Aldrich), 10 mg/mL penicillin/streptomycin (Sigma-Aldrich), 10 ng/mL EGF (Peprotech) and 5 ng/mL FGF-2 (Peprotech) and then treated with 10% of individual blood serum and p38 inhibitors. Medium, blood serum and p38 inhibitors were renewed every two days. The cells were detached using trypsin (Sigma-Aldrich) and cell count was carried out using a Neubauer chamber.

2.8. Orangu Cell Viability Assay

A cell viability assay using the Orangu Cell Counting Solution (Cell Guidance Systems, Cambridge, UK) was performed with hCSCs in a 96-well TC-Plate (Sarstedt AG and Co.) in hCSC medium. One thousand cells per treatment and a calibration line of 250, 500, 750, 1000, 1500, 2000, 2500 and 3000 cells were seeded. The cells were treated with 10% blood plasma for two days. For evaluation, the cells were incubated with 10 μL Orangu solution for two hours in the dark. Absorbance at 450 nm was measured using a GloMax microplate reader (Promega, Madison, WI, USA).

2.9. Senescence-Associated β-Galactosidase Assay

Activity of Senescence-associated β-Galactosidase was measured according to Debacq-Chainiaux and colleagues [26]. Briefly, cells were washed in PBS (Sigma-Aldrich) and fixed with 4% paraformaldehyde (Sigma-Aldrich) before addition of the staining solution containing 1 mg/mL X-Gal (Carl Roth, Karlsruhe, Germany). Incubation for 18 h at 37°C led to final staining, which could be visualized by phase contrast microscopy.

2.10. RNA Isolation and Sequencing

RNA was isolated from cell pellets using the TRI Reagent Protocol for Suspension Cells (Sigma-Aldrich, Darmstadt, Germany) according to the manufacturer's guidelines. The amount of isolated RNA was determined using a NanoDrop (Thermo Fisher Scientific, Waltham, MA, USA). For storage the samples were kept at −80 °C. Library preparation and sequencing on Illumina Hiseq4000 platform was carried out by Novogene (Beijing, China). After alignment to the reference genome GRCh38 with TopHat v2.0.9, gene expression quantification was performed with HTseq v0.6.1. Raw data are accessible at NCBI Gene Expression Omnibus. Differential gene expression was analyzed using DESeq2 R package (2_1.6.3) and correlation was calculated with the cor.test function. The database DAVID was used for the calculation of overexpressed Gene Ontology (GO)-Terms and pathway analyses [27]. GO terms of differentially expressed genes were determined using the PANTHER classification system [28–30] and analysis of Kyoto Encyclopedia of Genes and Genomes (KEGG) pathway enrichment was performed using KOBAS 3.0 [31,32].

2.11. ELISA

To measure the protein-contents in terms of MCP1, GDF11 and eotaxin of the plasmas used, the following Kits were used according to manufacturer's guidelines: Human MCP-1 (CCL2) mini ABTS ELISA Development Kit (Peprotech), Human Eotaxin (CCL11) Standard ABTS ELISA Development Kit (Peprotech) and Human Growth Differentiation Factor 11 GDF11 ELISA Kit (Novatein Biosciences, Woburn, MA, USA).

3. Results

3.1. Identification of Nestin⁺/S100B⁺ Cells in the Human Heart Auricle Tissue

To localize putative adult cardiac stem cell populations within their endogenous niche, human heart auricles (LAA = left atrial appendage) (Figure 1A) were obtained during routine heart surgery. Within this heart auricle tissue, a typical morphology of three main layers was observable: the myocardium is cardiac muscle tissue, mainly cardiomyocytes that are surrounded by the epicardium on the outer surface and the endocardium on the inner surface of the heart (Figure 1B). Immunohistochemistry revealed the presence of cells positive for the neural-crest markers S100B and Nestin in the adult myocardium and not in the endocardium or epicardium (Figure 1C).

3.2. Successfully iIsolated Putative Human Cardiac Stem Cells from Heart Auricle Tissue Show High Clonal Efficiency and Capability for Cardiosphere Formation

To analyze the stem cell-marker expressing cells found in the adult human myocardium in more detail, we modified an established protocol for the isolation of human cardiomyocyte progenitor cells [12]. Explant culture resulted in the isolation of cell migrating out of tissue pieces that spontaneously formed cardiospheres. To investigate their stemness characteristics, the clonal growth of putative hCSCs was analyzed. Here, putative hCSCs revealed a clonal efficiency of 22.7%. Importantly, clonally grown cells maintained their ability to form cardiospheres under suspension culture conditions (Figure 1D).

3.3. Isolated Cells Express Known Marker Proteins of Cardiac Stem and Progenitor Cells

Characterizing putative hCSCs in more detail, we further observed a high amount of 87% to 95.6% of Sca1+ cells isolated from two distinct hCSC donors but no expression of c-kit using flow cytometry (Figure 1E–G). Multiple staining followed by flow cytometric measurement showed 92.56% of cells being double positive for CD105 and CD31 (Figure 1G), which has also been shown by Smits and colleagues [12].
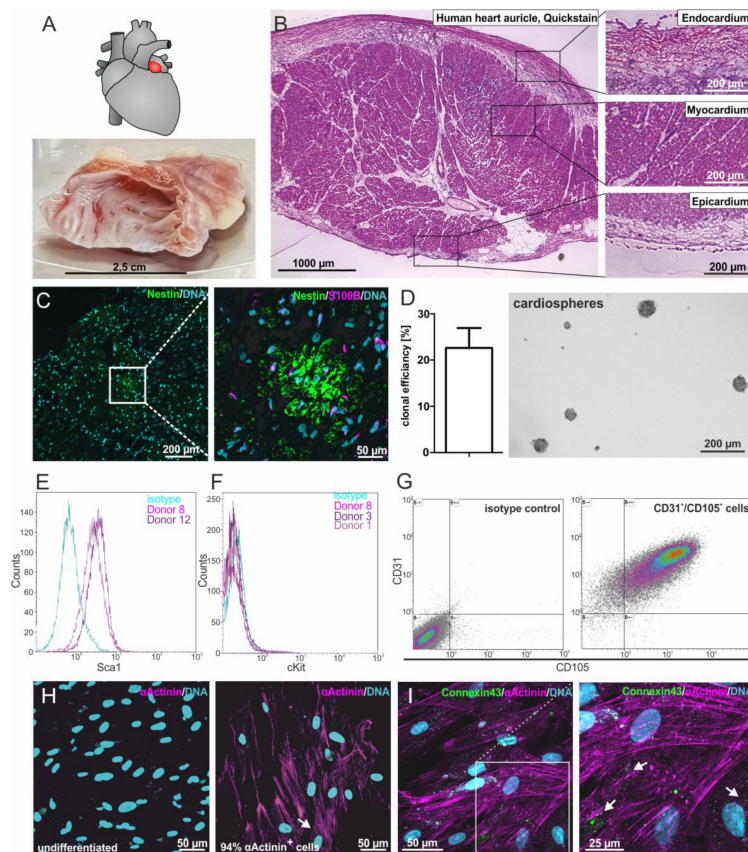

Figure 1. Isolation and characterization of adult human cardiac stem cells (hCSCs). (**A**) Human heart auricles were removed during routine heart surgery. (**B**) Heart auricle tissue consists of the three main layers: endocardium, myocardium and epicardium. (**C**) Nestin+ and S100+ cells can be found in the myocardium of the human heart auricle. (**D**) Isolated cells spontaneously form cardiospheres and possess the ability for self-renewal with a clonal efficiency of 22.7%. (**E**) Cultured cells express the cardiac stem cell marker Sca1. (**F**) Cultured cells do not express the stem cell marker cKit. (**G**) Double staining shows that cultured cells coexpress the cardiac stem cell markers CD31 and CD105. (**H**) After cardiac differentiation with biochemical cues, 94% of cells express the cardiomyocyte protein α-actinin. (**I**) After differentiation with biochemical cues, the gap junction protein Connexin43 is expressed at the surface of α-actinin+ cells, indicated by arrowheads.

3.4. HCSCs Are Able to Give Rise to Cardiomyocytes In Vitro

To investigate the cardiogenic differentiation potential of the hCSC population, we exposed the cells to TGFβ and ascorbic acid, as published by Smits and colleagues [12]. A high proportion(94%)of α-actinin+ cells were detected by immunocytochemistry, indicating a successful cardiac differentiation, whereas no α-actinin was observable in undifferentiated control cells (Figure 1H). Additionally, these cells showed the expression of the gap junction protein Connexin 43, visible as punctual structures (Figure 1I).

3.5. Blood Plasma and Blood Serum Strongly Enhance Proliferation-Inducing Effects of Blood Plasma on Adult Human Cardiac Stem Cells

To investigate potential proliferation-inducing effects of blood plasma on hCSCs, we exposed the cells to heparin-treated human blood plasma or human blood serum, which was applied to decrease the number of putative active plasma components (Figure 2A). Control cells cultured in starvation medium showed enlarged and flattened cell morphology, as would be expected of bona fide senescent cells. (Figure 2B, control). In contrast, exposure of hCSCs to human blood plasma or serum resulted in a smaller cell morphology (Figure 2B) next to strongly and significantly increased proliferation (Figure 2C). Notably, no difference was detectable between plasma and serum in the enhancing effects on the proliferation of hCSCs (Figure 2C).
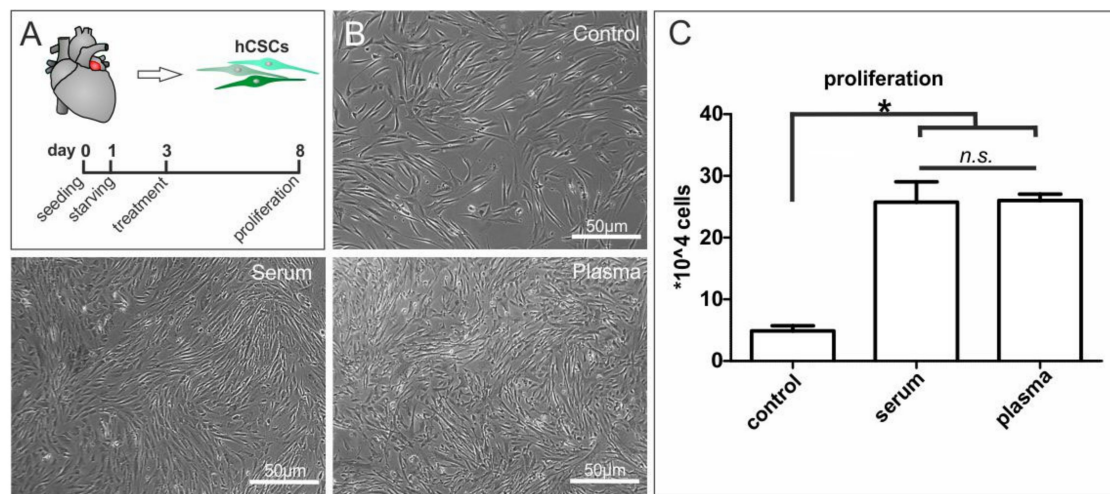

Figure 2. Application of human blood serum and human blood plasma on adult human cardiac stem cells led to increased cell proliferation. (**A**) Primary cultures of human stem cells from the adult heart auricle where exposed to blood serum, blood plasma or starvation medium. (**B**) Microscopy images of treated cells demonstrated a proliferation inducing effect of blood serum and plasma compared to untreated cells. (**C**) Serum and plasma significantly increased the proliferation of hCSCs in a similar manner. Mann-Whitney two-tailed, * $p < 0.05$ was considered significant, not significant (n.s.) $p > 0.05$.

3.6. Age and Sex of Blood Serum Donors Do Not Affect Beneficial Effects on Proliferation and Metabolism of hCSCs

Since several studies have suggested an age-dependent effect of blood plasma on stem cell behavior in the murine system [5,33], we applied serum from young (18–20 years) and old (>60 years) female and male donors to hCSCs (Figure 3A). We again observed a strongly increased proliferation of hCSCs treated with human blood serum independent to serum donor age or sex (Figure 3B). Exposure of blood serum from young and old female and male donors further resulted in significantly increased metabolism of hCSCs compared to control, but only modest variations between the serum-treated samples (Figure 3C).

3.7. Exposure of hCSCs to Blood Serum from Young Female or Male Donors Results in Significantly Enhanced Protection against Senescence Compared to Serum from Old Female Individuals

We next assessed the ability of blood serum from donors of different ages and sexes to protect hCSCs from starvation-mediated senescence by applying a senescence associated β-galactosidase (SA-β-Gal) activity assay. In comparison to control cells undergoing starvation, blood serum from young female or male donors (18–20 years) and old female or male donors (>60 years) led to significantly and strongly decreased senescence of hCSCs (Figure 3D and Figure S1B). Notably, we observed a significantly enhanced protection against senescence in hCSCs exposed to serum from young female

or male individuals compared to serum from old female donors (Figure 3D), suggesting a moderate yet significant age-dependent difference in blood-serum-mediated protection against senescence.
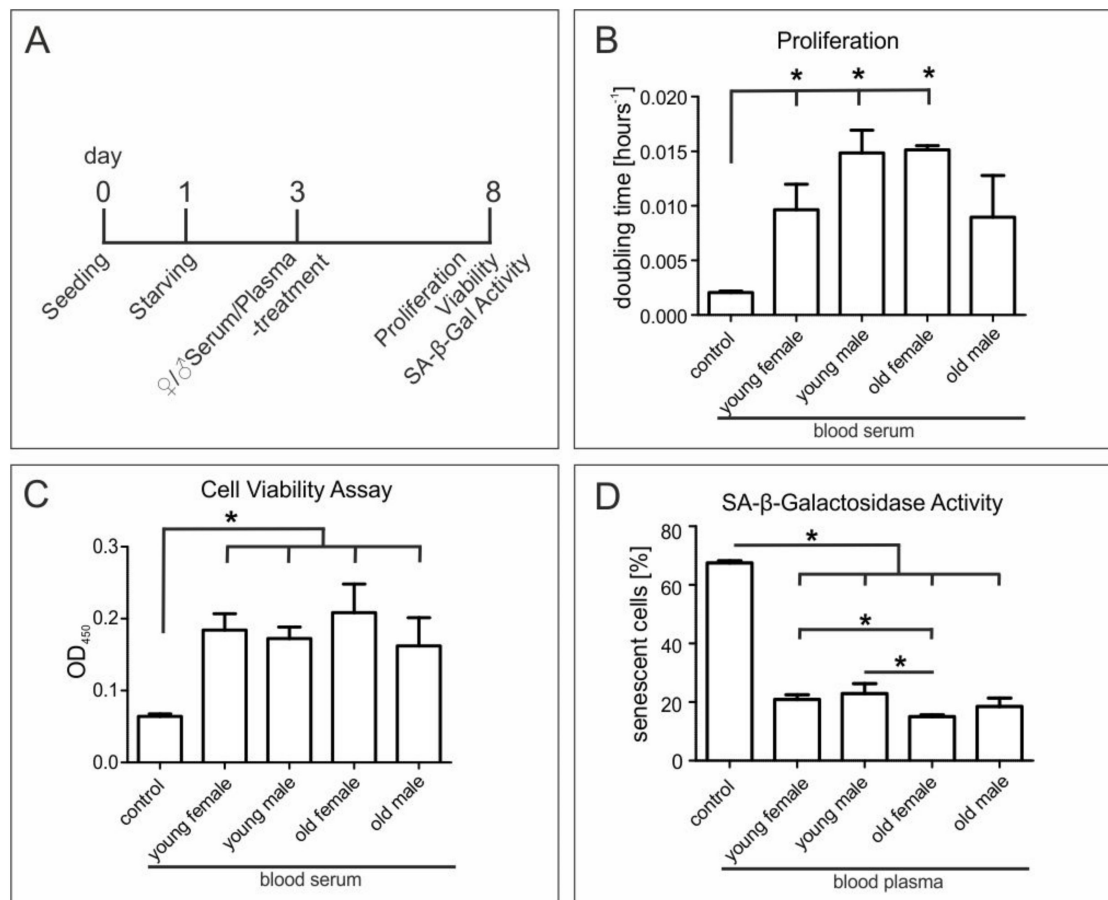

Figure 3. Application of different serum and plasma samples on adult human cardiac stem cells. (**A**) hCSCs were exposed to blood serum and blood plasma from old (>60 years) and young (<20 years) male and female donors or starvation medium. (**B**) Treatment with sera from young female, young male and old female donors significantly increased the proliferation of hCSCs. (**C**) Orangu cell viability assay to measure the metabolism of hCSCs showed increased metabolism after serum treatment but no sex or age dependency. (**D**) SA-β-Galactosidase assay showed a decrease of senescent cells after plasma treatment compared to untreated cells. Mann-Whitney two-tailed, * $p < 0.05$ was considered significant.

3.8. Young Blood Serum Enhances Differential Global Gene Expression of hCSCs

With regard to beneficial effects of blood serum on proliferation of hCSCs and the age-dependent differences observed in protection of hCSCs against senescence, we investigated the effects of blood serum from old and young male donors on global gene expression of hCSCs using RNAseq (Figure 4A). Here, we focused on the examination of potential age-dependent effects of human blood serum on the transcriptome level, since potential differences in the effects of blood serum related to the sex of the donor have not been reported so far. However, the literature frequently describes a rejuvenation phenomenon in the murine system when applying young blood/serum to older individuals.
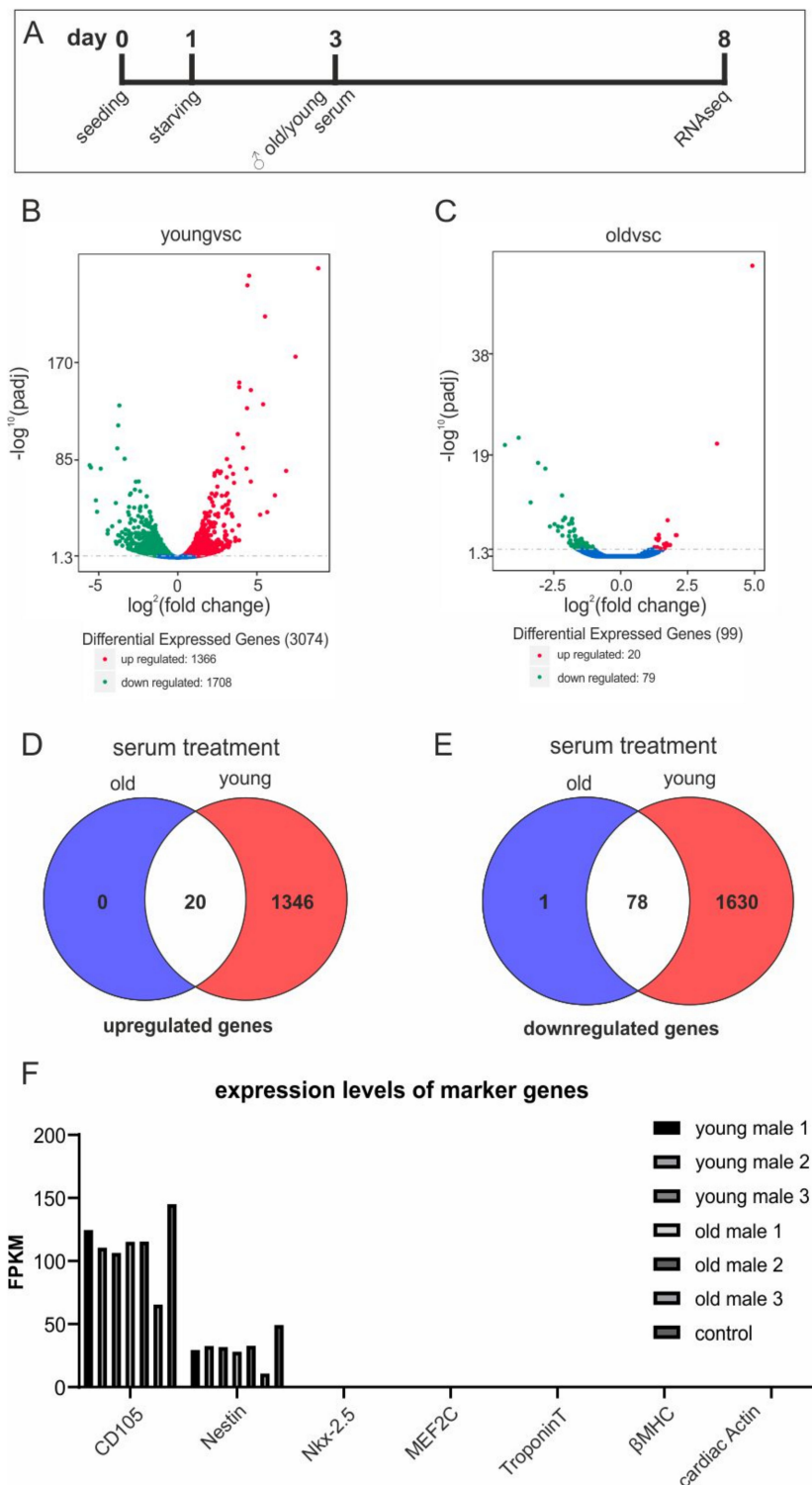
Figure 4. RNAseq showed increased differential gene expression in an age-dependent manner. (**A**) hCSCs where exposed to blood serum and blood plasma from old (>60 years) and young (<20 years) male donors or starvation medium followed by RNAseq. (**B**) Volcano plot of differential expressed genes in hCSCs treated with young serum vs. control. (**C**) Volcano plot of differential expressed genes in hCSCs treated with old serum vs. control. Red: upregulated; green: downregulated genes. A detailed list is provided in Supplementary Table S1. (**D**) Venn diagram of upregulated genes in the old and young treatment groups. (**E**) Venn diagram of downregulated genes in the old and young treatment groups.

(**F**) Gene expression levels (in fragments per kilobase million, FPKM) of selected marker genes for cardiac stem cells (CD105, Nestin) and genes that are upregulated during cardiac differentiation (Nkx-2.5, MEF2C, TroponinT, βMHC, cardiac actin). Expressions of CD105 and Nestin are not affected by serum treatment, and cardiac differentiation genes were not expressed either in the control or in the serum-treated samples.

Differential gene expression analysis between untreated and serum-treated hCSCs revealed a remarkably increased differential gene expression after application of young serum compared to control (Figure 4B) in comparison to old serum compared to control (Figure 4C). In particular, hCSCs treated with young serum showed upregulation of 1366 genes and downregulation of 1708 genes (Figure 4B), while hCSCs treated with serum from old donors differentially upregulated only 20 genes and downregulated 79 genes (Figure 4C). Both treatment groups showed an overlap of 20 upregulated genes (Figure 4D) and 78 downregulated genes (Figure 4E). Importantly, the gene expression levels of the stem cell marker Nestin and the cardiac stem cell marker CD105 remained unaffected after serum treatment. Moreover, genes that were commonly upregulated during cardiac differentiation were not expressed in serum-treated cells (Figure 4F), indicating that hCSCs keep their stem cell-like identity and do not differentiate upon serum treatment. Interestingly, treatment with young serum resulted in a significant reduction of MCP1 expression with a -1.3 fold change compared to untreated cells, whereas eotaxin and GDF11 were not differentially expressed (Supplementary Table S1). Further, IL24 could be found among the most significantly enriched transcripts after treatment with young serum with a log2fold change of +8.8 (Supplementary Table S1). The cytokines GDF11, MCP-1 and eotaxin were frequently discussed in rejuvenation experiments with old mice [34–39]. We therefore assessed the respective protein concentrations in old and young plasma samples via ELISA assays (Figure S1C). Neither increases in chemokine and cytokine levels of GDF11, MCP-1 and eotaxin nor increases in proliferation and senescence could be detected when comparing old and young plasma samples.

3.9. Global Gene Expression Profiling Indicates Age-Dependent Clusters of Blood-Serum-Treated Adult Stem Cells

Using hierarchical clustering of gene expression levels, we generated a heatmap separating the groups of untreated hCSCs and hCSCs treated with either young or old blood serum into distinct clusters. Even though the Pearson correlation analysis showed only marginal differences between the treatment groups (Figure S2), cluster analysis of differentially expressed genes resulted in clear differences along the whole transcriptome (Figure 5, Figures S3 and S4).

3.10. Gene Ontology (GO) Term Analysis Reveals Downregulation of Attachment-Associated Genes and Upregulation of Proliferation-Associated GO Terms, Including p38-MAPK

Analysis of GO Term enrichment showed beneficial effects on cell cycle and proliferation which was underlined by enrichment of the p38 MAPK pathway (P05918) as the most enriched GO-Term in samples treated with either young or old blood serum (Figure 6). In addition, the term oxidative stress response (P00046) followed as the second most enriched. Interestingly, the application of a KEGG-pathway analysis within this cluster also demonstrated amongst others, the upregulation of the KEGG-pathway glutathione metabolism (hsa00480), further highlighting a possible antioxidative effect of blood serum on hCSCs. In addition, analysis of the genes upregulated only in cells treated with young serum showed GO terms associated with DNA and protein-synthesis-like purine metabolism (P02769) or the pentose phosphate pathway (P02762), leading to enhanced proliferation (Figure 5). The p38 MAPK pathway (P05918) was also in this cluster among the significantly enriched GO terms with a 5.5-fold enrichment and in the KEGG pathways (hsa04010) (Figure 6). Interestingly, the application of GO terms and KEGG-pathway enrichment on a cluster of genes downregulated in cells treated with young serum but upregulated in cells treated with old serum led to the significant enrichment of the GO terms integrin signaling pathway (P00034) and cadherin signaling pathway (P00012) and the KEGG-pathways ECM-receptor interaction (hsa04512), adherens junction (hsa04520), focal adhesion (hsa04510) and tight junction (hsa04530), possibly indicating

degenerated exchange with the extracellular matrix (ECM) or neighboring cells or altered intercellular communication—one of the nine hallmarks of aging that were defined in 2013 [4] (Figure S4). Moreover, within this cluster we found the KEGG-pathways arrythmogenic right ventricular cardiomyopathy (hsa05412), hypertrophic cardiomyopathy (hsa05410) and dilated cardiomyopathy (hsa05414), which may indicate an age-dependent protective effect of young blood serum on hCSCs (Figure S4). In summary, GO enrichment analysis revealed the upregulation of various pathways, with p38-MAPK pathway being the most enriched GO term in genes that are highly upregulated after treatment with young serum and not regulated in the old serum group (see Figure 6). Further, p38-MAPK is also in third position (after general metabolism-associated GO terms) of the most enriched GO terms in genes that are highly upregulated after treatment with young serum and downregulated after treatment with old serum (Figure 5).
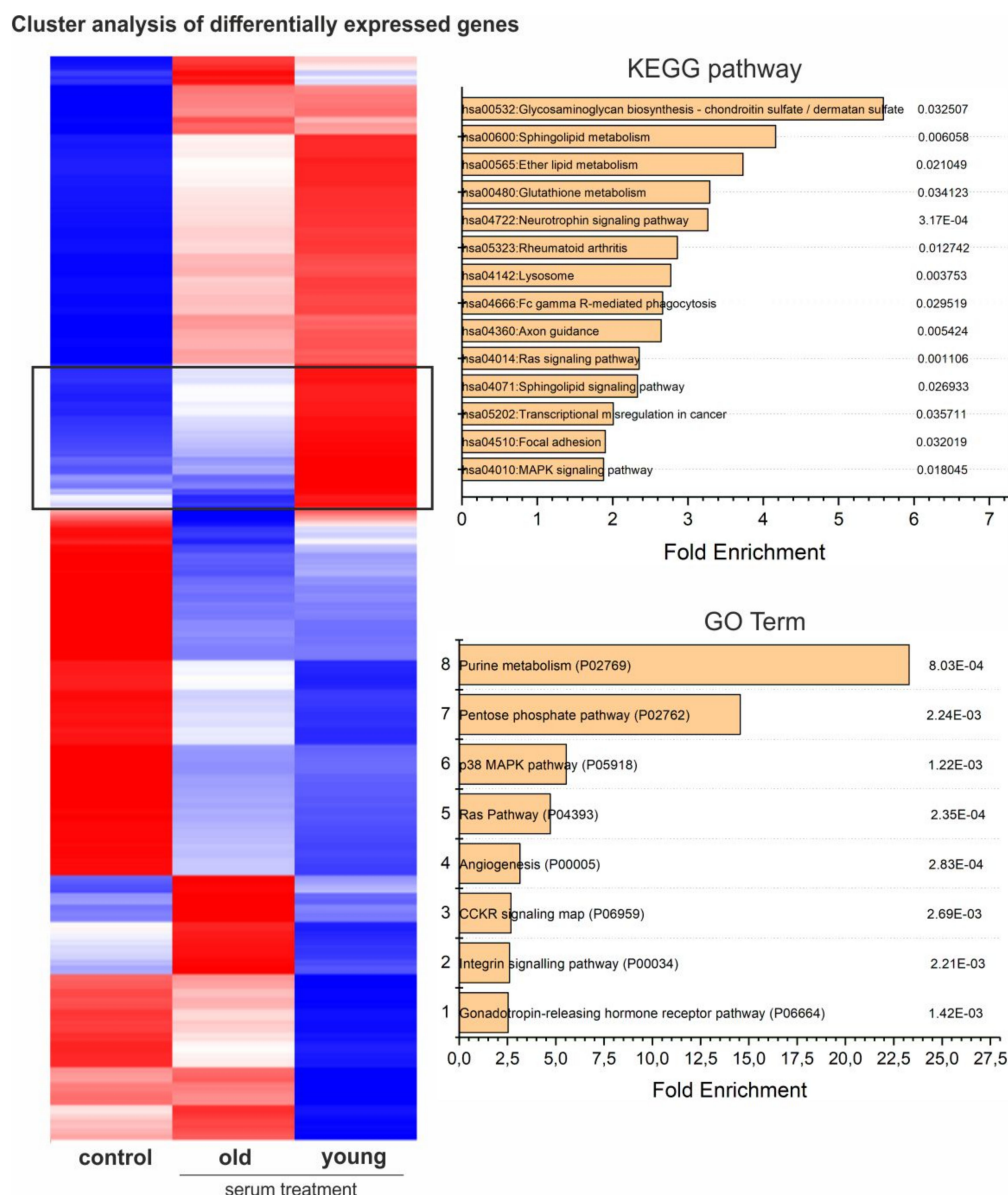

Figure 5. Heatmap of differentially expressed genes with KEGG-pathway analysis and GO-term enrichment of genes highly upregulated in hCSCs treated with young serum and downregulated in hCSCs treated with old serum and in the control (cluster marked with black box).
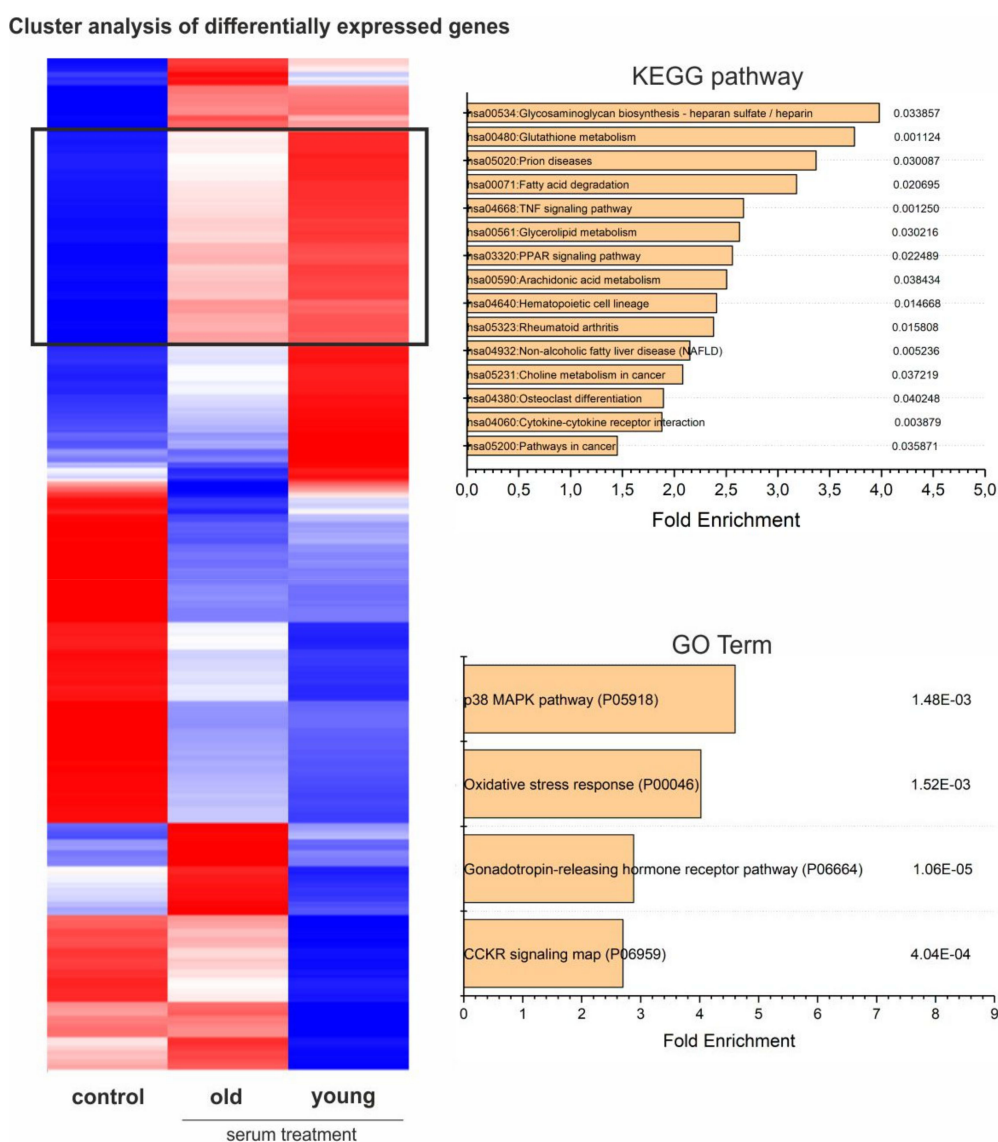
Figure 6. Heatmap of differentially expressed genes with KEGG-pathway analysis and GO-term enrichment of genes highly upregulated in hCSCs treated with young serum, slightly upregulated in hCSCs treated with old serum and downregulated in the control (cluster marked with black box).

3.11. Beneficial Effects of Blood Plasma on Proliferation and Protection of hCSCs Against Senescence Are Partially Mediated by p38 MAPK-Signaling

With regards to the up-regulation of genes associated to p38 MAPK pathway in hCSCs exposed to young serum, we were encouraged to assess its functional role in the before observed effects (Figures 2 and 3). Therefore, we applied two inhibitors of p38 MAPK (BMS-582949 and SB239063) in senescence- and proliferation assays (Figure 7A). Notably, simultaneous exposure of hCSCs to blood plasma and the p38 MAPK inhibitors BMS-582949 and SB239063 led to a strongly decreased proliferation compared to blood plasma or serum-treated hCSCs (Figure 7B,D). Accordingly, we observed a strongly elevated increase in senescence of blood plasma or serum-treated hCSCs after application of the p38 MAPK inhibitors in comparison to hCSCs solely exposed to blood plasma or serum (Figure 7C,E). These results are in line with the upregulation of p38 associated KEGG-pathways and GO terms in hCSCs treated with serum from young male donors (Figures 5 and 6) and emphasize the regulatory role of p38 MAPK in terms of blood-serum-mediated proliferation and protection against senescence.
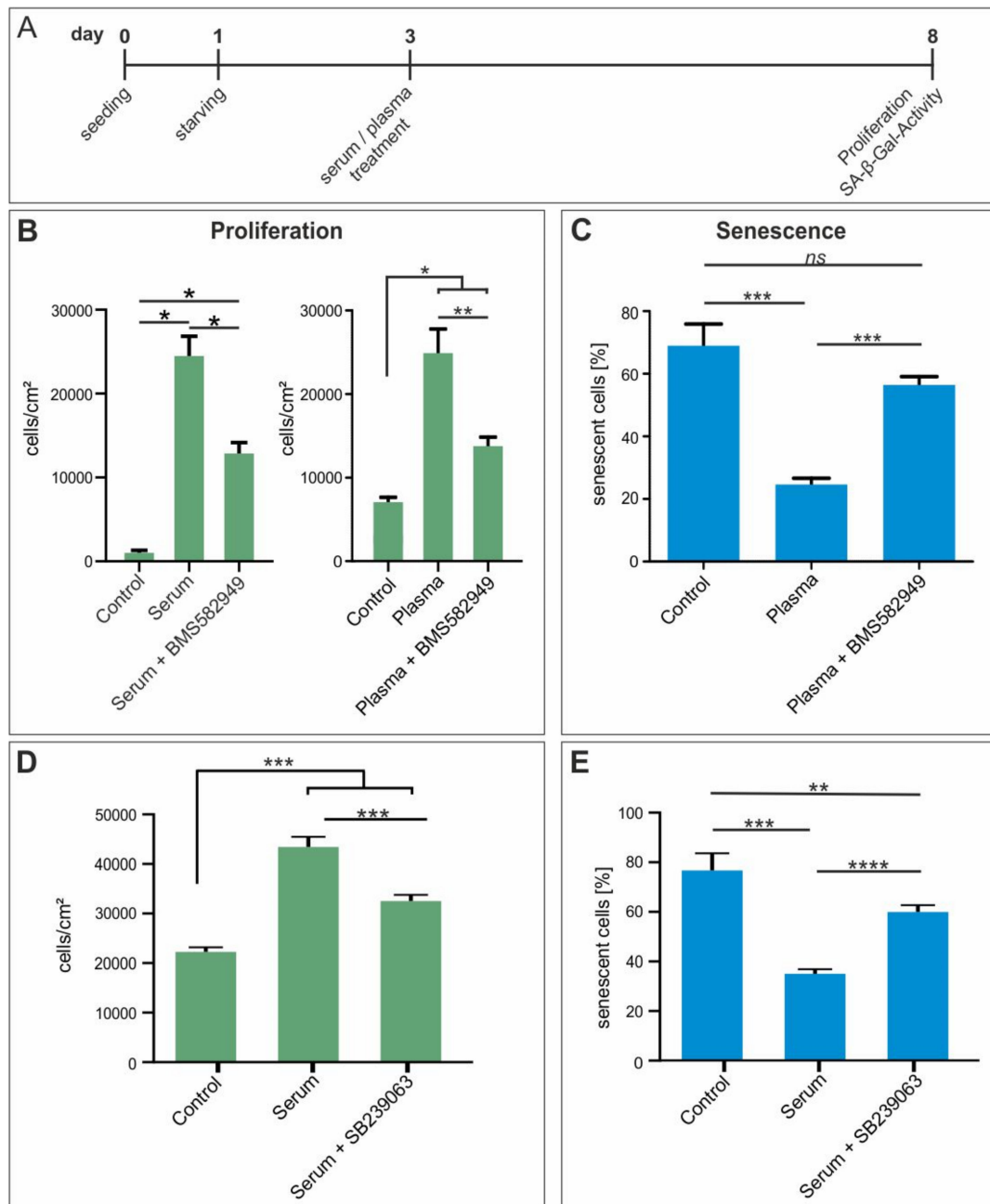
Figure 7. In vitro inhibition of p38-MAPK reversed the beneficial effect of blood plasma on proliferation and survival of hCSCs. (**A**) hCSCs where exposed to blood plasma and serum and p38 inhibitors BMS-582949 and SB239063. (**B**) Inhibition of p38 with BMS582949 led to significantly decreased proliferation compared to plasma and serum treatment alone. (**C**) Inhibition of p38 with BMS582949 led to significantly elevated SA-β-Gal activity compared to plasma treatment alone. (**D**) Inhibition of p38 with SB239063 led to significantly decreased proliferation compared to serum treatment alone. (**E**) Inhibition of p38 with SB239063 led to significantly elevated SA- β-Gal activity compared to serum treatment alone. Mann-Whitney two-tailed, * $p < 0.05$; ** $p < 0.005$; *** $p < 0.0005$; **** $p < 0.0001$ was considered significant, not significant (n.s.) $p > 0.05$.

4. Discussion

Ageing is characterized by a decline of homeostatic and regenerative capacities, at least partly caused by the exhaustion of endogenous stem cell functions [4], the accumulation of intracellular ROS and cells undergoing senescence in various tissues and organs. Prominent studies in the murine

system suggest that circulating factors play a critical role within this process [5–7]. For instance, experiments with heterochronic parabiosis in mice resulted in elevated proliferation of muscle satellite cells, liver, skin, neuronal stem cells and pancreatic β-cells [5,33,40,41]. More rejuvenation strategies targeting the cardiovascular system of aging mice have been recently reviewed by Cesselli et al. [42]. Besides, other studies provided indirect evidence by transplanting islet-cells from young or old mice into hyperglycemic recipients resulting in similar replication rates of both old and young donor cells [43]. However, a rejuvenation of aged human cells or organs by the application of a young systemic milieu could not be shown so far [8]. In the present study, we compare the effects of human blood plasma and serum of young and old donors on adult cardiac stem cells from the human heart auricle. Although the adult heart was long ago considered a terminally differentiated organ with low regenerative potential, rare populations of mouse and human cardiac stem cells (CSCs) were found that may contribute to endogenous repair mechanisms [10–12]. Although identification and isolation of adult CSCs often utilize the expression of the cell-surface marker c-kit [10,15,16], expression was also reported in non-cardiac cells [44–46] and its relevance as a cardiac stem cell marker is controversially discussed. For instance, Sultana and co-workers showed that c-kit$^+$ cells in the mouse heart are endothelial cells and not cardiac stem cells [47], and c-kit-negative stem cell populations have already been described in the human heart [11]. Interestingly, Tomita et al. reported that Nestin$^+$ NCSCs in the mouse heart give rise to cardiomyocytes in vivo [48]. Accordingly, we show here that the myocardium of the adult human heart auricle contains a population of Nestin$^+$/S100B$^+$ cardiac stem cells positive for Sca1 and CD105 but lacking c-kit-expression. Next to c-kit, the surface antigens Sca1 and CD105 are commonly used markers for human cardiac stem and progenitor cells [12]. In contrast to most studies showing co-expression of Sca1, c-kit and CD105 in human CSCs [12], we observed the presence of Sca1 and CD105 in human cardiac stem cells despite the lack of c-kit. Isolated hCSCs were able to grow clonally while maintaining their capability of sphere formation and differentiated efficiently into α-actinin$^+$ cardiomyocyte-like cells. Although the application of human blood serum, blood plasma or platelet-rich plasma on stem cell cultures has already been shown to effectively promote cell proliferation [21,22,49–53], the cardiovascular system and especially cardiac stem cells have not been investigated so far. Within this study we likewise could demonstrate an overall enhancing effect of human blood serum on adult human cardiac stem cells, while no age dependency could be detected in terms of proliferation and metabolic activity. In line with these results, other studies focusing on data analysis of red blood cell transfusions in terms of donor age and sex and the survival rates of the transfusion-recipients have not shown an age or sex-related effect [54]. Importantly, we could not detect significant changes in the gene expression levels of CD105 and Nestin upon serum-treatment, nor the expression of cardiac differentiation genes in any of the samples. These results demonstrate that hCSCs keep their stem cell-like features and do not differentiate spontaneously during exposure to blood serum. Accordingly, other adult stem cell populations were also reported to keep their characteristic gene expression and stemness characteristics when cultivated in human blood plasma [22,55].

To investigate the underlying molecular mechanisms driven by the application of blood serum, we performed RNAseq and compared the global transcriptome of hCSCs treated with either old (donor age >60 years) or young (donor age <20 years) male blood serum. This state-of-the-art technique allowed us to analyze the highly complex regulatory networks that drive proliferation of human cardiac stem cells. Here, we focused on the examination of potential age-dependent effects, since sex-specific differences were not detectable on proliferation or senescence of serum-treated hCSCs. In line with these findings, potential differences in the effects of blood serum related to the sex of the donor have not been reported so far. However, the literature frequently describes a rejuvenation phenomenon in the murine system when applying young blood/serum to old individuals [5–7]. Our present observations show that the application of young blood serum leads to an increased number of up or downregulated genes compared to the treatment with old blood serum. To the best of our knowledge, comparable transcriptomic data of human cells after exposure to serum or plasma do not exist. However, a general decline in global gene expression of aging tissues has been reported in

several studies [56–60], which is line with our present findings. In detail, the pattern of differentially expressed genes seems to be dependent on tissue type. For instance, Lipinski and colleagues showed that genes associated with autophagy are downregulated in the human brain during aging [59]. Other groups showed differential gene expression of migration and proliferation-associated genes in male skin samples with advanced age [60]. We likewise could show increased differential gene expression in hCSCs upon the treatment with young blood serum compared to the application of old blood serum. However, this seems to have no further beneficial influence on the effects on cell proliferation and viability compared to the application of old serum. We therefore suggest that both old and young serum trigger activation of pathways leading to enhanced proliferation and protection against senescence. Here, our analysis identified p38MAPK as a crucial pathway for regulating proliferation and senescence in a blood-serum-dependent manner, as discussed in detail below. In accordance to our observations, human blood serum, blood plasma or platelet-rich plasma were reported to be beneficial for proliferation of stem cells, despite the age of the plasma donors [21,22,56–60]. The highly elevated global gene expression levels after treatment of hCSCs with young blood serum compared to old serum further suggest that the application of young serum may result in cellular effects other than proliferation or protection against senescence. Considering this discrepancy in our observation, a more detailed transcriptomic analysis was necessary to understand age-related blood borne effects on cultured cells. A detailed analysis of upregulated genes after serum treatment showed significant overrepresentation of cell cycle and proliferation-enhancing GO terms, which is in line with the observed beneficial effects of blood serum on proliferation of hCSCs. Moreover, we could observe the upregulation of integrin signaling and cadherin signaling, which is also connected to proliferation in several instances [61]. In addition, a range of studies also suggest circulating pro-ageing factors with the pro-inflammatory chemokine MCP1 as one of the most popular candidates. Level of MCP1 increases with age in mice and humans and is even discussed as a biomarker for cardiac aging [34,36]. Accordingly, we could show via RNAseq that MCP1 was significantly downregulated in cells treated with young blood serum. Further, Ghosh and coworkers recently showed that levels of MCP1 in white adipose tissue in old mice were decreased upon heterochronic parabiosis with young mice and even in cell culture after conditioning with young serum [62]. In contrast to this, we detected no significant differences in the protein concentration of MCP1 between old and young plasma samples. Next to MCP1, other factors like GDF11 or eotaxin (CCL11) are also discussed as age-dependent blood borne cytokines [35,37–39]. These chemokines and cytokines were measured in moderate yet significantly higher abundances in young plasma samples compared to old plasma samples. However, our data did not show a differential expression of the corresponding genes in serum-treated hCSCs. These differences between protein concentrations in the plasma samples and gene expression levels in the treated cells may be partially explained by the only modest changes of protein contents that are not sufficient to trigger differential gene expression.

Notably, analysis of the global gene expression profile of hCSCs treated with young or old blood serum showed the upregulation and enrichment of genes in the p38-MAPK-associated GO term P05918 and KEGG-pathway hsa04010. In general, p38-MAPK signaling is understood as an inhibitor of proliferation [63] but it has also been described to enhance proliferation in a range of cell types [64,65], suggesting that the role of p38-MAPK in proliferation and senescence is strongly cell-specific. For example, in male human skin samples, MAPK signaling is upregulated along with cell proliferation in aged (>70 years) patients [60]. Further, in human breast cancer cells, p38 MAPK upregulation is associated with increased proliferation and can be inhibited by the use of the p38 inhibitor SB203580 or p38α-siRNA [64,66]. In line with these observations, inhibition of p38 significantly reversed the beneficial effects of blood serum in terms of proliferation and protection from senescence in the present study. Interestingly, we also detected the cytokine IL24 to be highly upregulated in hCSCs after treatment with young blood serum. IL24 was reported to induce p38 MAPK activation [67], suggesting a role in the upstream regulation of p38 in hCSCs in a blood-serum-dependent manner. However, other relevant signaling pathways may interact with p38 MAPK in controlling

blood-serum-mediated proliferation of hCSCs. For instance, other MAPKs, such as ERK, were described to co-regulate proliferation of stem cells together with p38 MAPK in response to stimuli such as hypoxia or proliferation-inducing drugs [68,69]. In particular, treatment of periodontal ligament stem cells with inhibitors against p38 MAPK or ERK resulted in reduced hypoxia-mediated proliferation [69]. Likewise, signaling via p38 MAPK and NF-κB was described to co-regulate proliferation of hepatic stem cells [70] and also has an essential role in the regulation of myocardial adaption to ischemia [71]. Accordingly, our present data reveal a relevant role of p38 MAPK in regulating proliferation of adult human cardiac stem cells. Regarding the reversion of the senescent phenotype after blood plasma treatment, Liu and colleagues likewise showed that young blood plasma reverses age-dependent senescence in hepatic tissues of rodents. This effect was not reported in application of old plasma [72]. Other studies also describe similar effects with young blood on various organs in heterochronic parabiotic mice [5,35,62,73,74]. However, our results show a more general protective effect of human blood plasma against senescence which is independent of age and sex. These contrasting results also demonstrate the difficulties in the transition from the murine to the human system and the highly complex regulation of the ageing process. Here, next to the investigation of age-dependent effects upon usage of human blood plasma or serum, the cell types or tissues that are addressed should also be taken into account carefully—possibly with the examination of p38-MAPK as a crucial regulator.

In summary, we demonstrate within this study the beneficial effects of blood serum on the proliferation and metabolism of adult human cardiac stem cells, which are accompanied by a decrease of senescent cells. By the application of RNAseq we were able to describe the changes in the global gene expression profiles of serum-treated hCSCs and thus successfully identified the age-dependent enhancement of p38-MAPK signaling as one of the underlying pathways that promote the blood-serum-mediated proliferation.

Supplementary Materials: The following are available online at http://www.mdpi.com/2073-4409/9/6/1472/s1. Figure S1: (A) Application of different individual serum samples in a proliferation assay. (B) Application of different individual plasma samples in a senescence assay with adult human cardiac stem cells. (C) ELISA-measurements of the plasma content of the chemokines and cytokines eotaxin 1. GDF11 and MCP-1, Figure S2: Pearson Correlation of global gene expression profiles of hCSCs treated with either young or old serum and of the starvation control, Figure S3: Heatmap of differentially expressed genes with KEGG-pathway analysis and GO-term enrichment of genes downregulated in hCSCs treated with young serum and old serum and strongly upregulated in the control, Figure S4: Heatmap of differentially expressed genes with KEGG-pathway analysis and GO-term enrichment of genes strongly downregulated in hCSCs treated with young serum and upregulated in hCSCs treated with old serum, Table S1: List of differentially expressed genes that are shown in Figure 3B,C.

Author Contributions: Conceptualization, A.L.H., C.K. (Christian Kaltschmidt) and C.K. (Cornelius Knabbe); methodology, A.L.H., K.E.S., J.H., A.-K.R. and M.M.; validation, A.L.H., I.F., J.F.W.G., J.G., C.K. (Christian Kaltschmidt) and C.K. (Cornelius Knabbe); formal analysis, A.L.H., K.E.S., J.H. and A.-K.R., J.G., C.K. (Christian Kaltschmidt), C.K. (Cornelius Knabbe), B.K.; investigation, A.L.H., K.E.S., J.H. and A.-K.R.; resources, C.K. (Christian Kaltschmidt), C.K. (Cornelius Knabbe); data curation, A.L.H., C.K. (Christian Kaltschmidt), C.K. (Cornelius Knabbe); writing—original draft preparation, A.L.H.; writing—review and editing, A.L.H., I.F., J.F.W.G., B.K., C.K. (Christian Kaltschmidt) and C.K. (Cornelius Knabbe); visualization, A.L.H., K.E.S., J.H. and A.-K.R.; supervision, I.F., J.F.W.G., B.K., C.K. (Christian Kaltschmidt) and C.K. (Cornelius Knabbe); project administration, C.K. (Christian Kaltschmidt) and C.K. (Cornelius Knabbe); funding acquisition, C.K. (Christian Kaltschmidt) and C.K. (Cornelius Knabbe). All authors have read and agreed to the published version of the manuscript.

Funding: This work was supported by the Fund for the promotion of transdisciplinary, medically relevant research cooperations in the region Ostwestfalen-Lippe.

Acknowledgments: We gratefully acknowledge the excellent technical help of Angela Kralemann-Köhler. We also thank Sebastian-Patrick Sommer, Buntaro Fujita and Thomas Pühler for providing clinical material.

Conflicts of Interest: The authors declare no conflict of interest.

References

1. Laflamme, M.A.; Murry, C.E. Heart regeneration. *Nature* **2011**, *473*, 326–335. [CrossRef] [PubMed]
2. Aguilar-Sanchez, C.; Michael, M.; Pennings, S. Cardiac Stem Cells in the Postnatal Heart: Lessons from Development. *Stem Cells Int.* **2018**, *2018*, 1247857. [CrossRef] [PubMed]

3. Franceschi, C.; Garagnani, P.; Morsiani, C.; Conte, M.; Santoro, A.; Grignolio, A.; Monti, D.; Capri, M.; Salvioli, S. The Continuum of Aging and Age-Related Diseases: Common Mechanisms but Different Rates. *Front. Med. (Lausanne)* **2018**, *5*, 61. [CrossRef] [PubMed]

4. Lopez-Otin, C.; Blasco, M.A.; Partridge, L.; Serrano, M.; Kroemer, G. The hallmarks of aging. *Cell* **2013**, *153*, 1194–1217. [CrossRef] [PubMed]

5. Conboy, I.M.; Conboy, M.J.; Wagers, A.J.; Girma, E.R.; Weissman, I.L.; Rando, T.A. Rejuvenation of aged progenitor cells by exposure to a young systemic environment. *Nature* **2005**, *433*, 760–764. [CrossRef] [PubMed]

6. Villeda, S.A.; Plambeck, K.E.; Middeldorp, J.; Castellano, J.M.; Mosher, K.I.; Luo, J.; Smith, L.K.; Bieri, G.; Lin, K.; Berdnik, D.; et al. Young blood reverses age-related impairments in cognitive function and synaptic plasticity in mice. *Nat. Med.* **2014**, *20*, 659–663. [CrossRef]

7. Castellano, J.M.; Mosher, K.I.; Abbey, R.J.; McBride, A.A.; James, M.L.; Berdnik, D.; Shen, J.C.; Zou, B.; Xie, X.S.; Tingle, M.; et al. Human umbilical cord plasma proteins revitalize hippocampal function in aged mice. *Nature* **2017**, *544*, 488–492. [CrossRef]

8. Hofmann, B. Young Blood Rejuvenates Old Bodies: A Call for Reflection when Moving from Mice to Men. *Transfus. Med. Hemother.* **2018**, *45*, 67–71. [CrossRef]

9. Sha, S.J.; Deutsch, G.K.; Tian, L.; Richardson, K.; Coburn, M.; Gaudioso, J.L.; Marcal, T.; Solomon, E.; Boumis, A.; Bet, A.; et al. Safety, Tolerability, and Feasibility of Young Plasma Infusion in the Plasma for Alzheimer Symptom Amelioration Study: A Randomized Clinical Trial. *JAMA Neurol.* **2019**, *76*, 35–40. [CrossRef]

10. Beltrami, A.P.; Barlucchi, L.; Torella, D.; Baker, M.; Limana, F.; Chimenti, S.; Kasahara, H.; Rota, M.; Musso, E.; Urbanek, K.; et al. Adult cardiac stem cells are multipotent and support myocardial regeneration. *Cell* **2003**, *114*, 763–776. [CrossRef]

11. Koninckx, R.; Daniels, A.; Windmolders, S.; Mees, U.; Macianskiene, R.; Mubagwa, K.; Steels, P.; Jamaer, L.; Dubois, J.; Robic, B.; et al. The cardiac atrial appendage stem cell: A new and promising candidate for myocardial repair. *Cardiovasc. Res.* **2013**, *97*, 413–423. [CrossRef] [PubMed]

12. Smits, A.M.; van Vliet, P.; Metz, C.H.; Korfage, T.; Sluijter, J.P.; Doevendans, P.A.; Goumans, M.J. Human cardiomyocyte progenitor cells differentiate into functional mature cardiomyocytes: An in vitro model for studying human cardiac physiology and pathophysiology. *Nat. Protoc.* **2009**, *4*, 232–243. [CrossRef] [PubMed]

13. Zaruba, M.M.; Soonpaa, M.; Reuter, S.; Field, L.J. Cardiomyogenic potential of C-kit(+)-expressing cells derived from neonatal and adult mouse hearts. *Circulation* **2010**, *121*, 1992–2000. [CrossRef] [PubMed]

14. Tallini, Y.N.; Greene, K.S.; Craven, M.; Spealman, A.; Breitbach, M.; Smith, J.; Fisher, P.J.; Steffey, M.; Hesse, M.; Doran, R.M.; et al. c-kit expression identifies cardiovascular precursors in the neonatal heart. *Proc. Natl. Acad. Sci. USA* **2009**, *106*, 1808–1813. [CrossRef]

15. Bearzi, C.; Rota, M.; Hosoda, T.; Tillmanns, J.; Nascimbene, A.; De Angelis, A.; Yasuzawa-Amano, S.; Trofimova, I.; Siggins, R.W.; Lecapitaine, N.; et al. Human cardiac stem cells. *Proc. Natl. Acad. Sci. USA* **2007**, *104*, 14068–14073. [CrossRef]

16. Urbanek, K.; Cesselli, D.; Rota, M.; Nascimbene, A.; De Angelis, A.; Hosoda, T.; Bearzi, C.; Boni, A.; Bolli, R.; Kajstura, J.; et al. Stem cell niches in the adult mouse heart. *Proc. Natl. Acad. Sci. USA* **2006**, *103*, 9226–9231. [CrossRef]

17. Moretti, A.; Caron, L.; Nakano, A.; Lam, J.T.; Bernshausen, A.; Chen, Y.; Qyang, Y.; Bu, L.; Sasaki, M.; Martin-Puig, S.; et al. Multipotent embryonic isl1+ progenitor cells lead to cardiac, smooth muscle, and endothelial cell diversification. *Cell* **2006**, *127*, 1151–1165. [CrossRef]

18. Oh, H.; Bradfute, S.B.; Gallardo, T.D.; Nakamura, T.; Gaussin, V.; Mishina, Y.; Pocius, J.; Michael, L.H.; Behringer, R.R.; Garry, D.J.; et al. Cardiac progenitor cells from adult myocardium: Homing, differentiation, and fusion after infarction. *Proc. Natl. Acad. Sci. USA* **2003**, *100*, 12313–12318. [CrossRef]

19. Eschenhagen, T.; Bolli, R.; Braun, T.; Field, L.J.; Fleischmann, B.K.; Frisen, J.; Giacca, M.; Hare, J.M.; Houser, S.; Lee, R.T.; et al. Cardiomyocyte Regeneration: A Consensus Statement. *Circulation* **2017**, *136*, 680–686. [CrossRef]

20. Vogel, J.P.; Szalay, K.; Geiger, F.; Kramer, M.; Richter, W.; Kasten, P. Platelet-rich plasma improves expansion of human mesenchymal stem cells and retains differentiation capacity and in vivo bone formation in calcium phosphate ceramics. *Platelets* **2006**, *17*, 462–469. [CrossRef]

21. Walenda, T.; Bokermann, G.; Jost, E.; Galm, O.; Schellenberg, A.; Koch, C.M.; Piroth, D.M.; Drescher, W.; Brummendorf, T.H.; Wagner, W. Serum after autologous transplantation stimulates proliferation and expansion of human hematopoietic progenitor cells. *PLoS ONE* **2011**, *6*, e18012. [CrossRef] [PubMed]

22. Greiner, J.F.; Hauser, S.; Widera, D.; Muller, J.; Qunneis, F.; Zander, C.; Martin, I.; Mallah, J.; Schuetzmann, D.; Prante, C.; et al. Efficient animal-serum free 3D cultivation method for adult human neural crest-derived stem cell therapeutics. *Eur. Cell Mater.* **2011**, *22*, 403–419. [CrossRef] [PubMed]

23. Yamaguchi, M.; Hirayama, F.; Wakamoto, S.; Fujihara, M.; Murahashi, H.; Sato, N.; Ikebuchi, K.; Sawada, K.; Koike, T.; Kuwabara, M.; et al. Bone marrow stromal cells prepared using AB serum and bFGF for hematopoietic stem cells expansion. *Transfusion* **2002**, *42*, 921–927. [CrossRef]

24. Hauser, S.; Widera, D.; Qunneis, F.; Muller, J.; Zander, C.; Greiner, J.; Strauss, C.; Luningschror, P.; Heimann, P.; Schwarze, H.; et al. Isolation of novel multipotent neural crest-derived stem cells from adult human inferior turbinate. *Stem Cells Dev.* **2012**, *21*, 742–756. [CrossRef]

25. Schneider, C.A.; Rasband, W.S.; Eliceiri, K.W. NIH Image to ImageJ: 25 years of image analysis. *Nat. Methods* **2012**, *9*, 671–675. [CrossRef] [PubMed]

26. Debacq-Chainiaux, F.; Erusalimsky, J.D.; Campisi, J.; Toussaint, O. Protocols to detect senescence-associated beta-galactosidase (SA-betagal) activity, a biomarker of senescent cells in culture and in vivo. *Nat. Protoc.* **2009**, *4*, 1798–1806. [CrossRef]

27. Dennis, G., Jr.; Sherman, B.T.; Hosack, D.A.; Yang, J.; Gao, W.; Lane, H.C.; Lempicki, R.A. DAVID: Database for Annotation, Visualization, and Integrated Discovery. *Genome Biol.* **2003**, *4*, P3. [CrossRef]

28. Mi, H.; Muruganujan, A.; Thomas, P.D. PANTHER in 2013: Modeling the evolution of gene function, and other gene attributes, in the context of phylogenetic trees. *Nucleic Acids Res.* **2013**, *41*, D377–D386. [CrossRef]

29. Mi, H.; Muruganujan, A.; Ebert, D.; Huang, X.; Thomas, P.D. PANTHER version 14: More genomes, a new PANTHER GO-slim and improvements in enrichment analysis tools. *Nucleic Acids Res.* **2019**, *47*, D419–D426. [CrossRef]

30. Mi, H.; Thomas, P. PANTHER pathway: An ontology-based pathway database coupled with data analysis tools. *Methods Mol. Biol.* **2009**, *563*, 123–140. [CrossRef]

31. Wu, J.; Mao, X.; Cai, T.; Luo, J.; Wei, L. KOBAS server: A web-based platform for automated annotation and pathway identification. *Nucleic Acids Res.* **2006**, *34*, W720–W724. [CrossRef] [PubMed]

32. Xie, C.; Mao, X.; Huang, J.; Ding, Y.; Wu, J.; Dong, S.; Kong, L.; Gao, G.; Li, C.Y.; Wei, L. KOBAS 2.0: A web server for annotation and identification of enriched pathways and diseases. *Nucleic Acids Res.* **2011**, *39*, W316–W322. [CrossRef] [PubMed]

33. Villeda, S.A.; Luo, J.; Mosher, K.I.; Zou, B.; Britschgi, M.; Bieri, G.; Stan, T.M.; Fainberg, N.; Ding, Z.; Eggel, A.; et al. The ageing systemic milieu negatively regulates neurogenesis and cognitive function. *Nature* **2011**, *477*, 90–94. [CrossRef] [PubMed]

34. Yousefzadeh, M.J.; Schafer, M.J.; Noren Hooten, N.; Atkinson, E.J.; Evans, M.K.; Baker, D.J.; Quarles, E.K.; Robbins, P.D.; Ladiges, W.C.; LeBrasseur, N.K.; et al. Circulating levels of monocyte chemoattractant protein-1 as a potential measure of biological age in mice and frailty in humans. *Aging Cell* **2018**, *17*, e12706. [CrossRef]

35. Loffredo, F.S.; Steinhauser, M.L.; Jay, S.M.; Gannon, J.; Pancoast, J.R.; Yalamanchi, P.; Sinha, M.; Dall'Osso, C.; Khong, D.; Shadrach, J.L.; et al. Growth differentiation factor 11 is a circulating factor that reverses age-related cardiac hypertrophy. *Cell* **2013**, *153*, 828–839. [CrossRef]

36. Chiao, Y.A.; Dai, Q.; Zhang, J.; Lin, J.; Lopez, E.F.; Ahuja, S.S.; Chou, Y.M.; Lindsey, M.L.; Jin, Y.F. Multi-analyte profiling reveals matrix metalloproteinase-9 and monocyte chemotactic protein-1 as plasma biomarkers of cardiac aging. *Circ. Cardiovasc. Genet.* **2011**, *4*, 455–462. [CrossRef]

37. Poggioli, T.; Vujic, A.; Yang, P.; Macias-Trevino, C.; Uygur, A.; Loffredo, F.S.; Pancoast, J.R.; Cho, M.; Goldstein, J.; Tandias, R.M.; et al. Circulating Growth Differentiation Factor 11/8 Levels Decline With Age. *Circ. Res.* **2016**, *118*, 29–37. [CrossRef]

38. Hoefer, J.; Luger, M.; Dal-Pont, C.; Culig, Z.; Schennach, H.; Jochberger, S. The "Aging Factor" Eotaxin-1 (CCL11) Is Detectable in Transfusion Blood Products and Increases with the Donor's Age. *Front. Aging Neurosci.* **2017**, *9*, 402. [CrossRef]

39. Egerman, M.A.; Cadena, S.M.; Gilbert, J.A.; Meyer, A.; Nelson, H.N.; Swalley, S.E.; Mallozzi, C.; Jacobi, C.; Jennings, L.L.; Clay, I.; et al. GDF11 Increases with Age and Inhibits Skeletal Muscle Regeneration. *Cell Metab.* **2015**, *22*, 164–174. [CrossRef]

40. Song, G.; Nguyen, D.T.; Pietramaggiori, G.; Scherer, S.; Chen, B.; Zhan, Q.; Ogawa, R.; Yannas, I.V.; Wagers, A.J.; Orgill, D.P.; et al. Use of the parabiotic model in studies of cutaneous wound healing to define the participation of circulating cells. *Wound Repair Regen.* **2010**, *18*, 426–432. [CrossRef]

41. Salpeter, S.J.; Khalaileh, A.; Weinberg-Corem, N.; Ziv, O.; Glaser, B.; Dor, Y. Systemic regulation of the age-related decline of pancreatic beta-cell replication. *Diabetes* **2013**, *62*, 2843–2848. [CrossRef] [PubMed]

42. Cesselli, D.; Aleksova, A.; Mazzega, E.; Caragnano, A.; Beltrami, A.P. Cardiac stem cell aging and heart failure. *Pharmacol. Res.* **2018**, *127*, 26–32. [CrossRef] [PubMed]

43. Chen, X.; Zhang, X.; Chen, F.; Larson, C.S.; Wang, L.J.; Kaufman, D.B. Comparative study of regenerative potential of beta cells from young and aged donor mice using a novel islet transplantation model. *Transplantation* **2009**, *88*, 496–503. [CrossRef] [PubMed]

44. Morita, N.; Yamamoto, M.; Tanizawa, T. Correlation of c-kit expression and cell cycle regulation by transforming growth factor-beta in CD34+ CD38- human bone marrow cells. *Eur. J. Haematol.* **2003**, *71*, 351–358. [CrossRef] [PubMed]

45. Rusu, M.C.; Duta, I.; Didilescu, A.C.; Vrapciu, A.D.; Hostiuc, S.; Anton, E. Precursor and interstitial Cajal cells in the human embryo liver. *Rom. J. Morphol. Embryol.* **2014**, *55*, 291–296.

46. Ilie, C.A.; Rusu, M.C.; Didilescu, A.C.; Motoc, A.G.; Mogoanta, L. Embryonic hematopoietic stem cells and interstitial Cajal cells in the hindgut of late stage human embryos: Evidence and hypotheses. *Ann Anat* **2015**, *200*, 24–29. [CrossRef]

47. Sultana, N.; Zhang, L.; Yan, J.; Chen, J.; Cai, W.; Razzaque, S.; Jeong, D.; Sheng, W.; Bu, L.; Xu, M.; et al. Resident c-kit(+) cells in the heart are not cardiac stem cells. *Nat. Commun.* **2015**, *6*, 8701. [CrossRef]

48. Tomita, Y.; Matsumura, K.; Wakamatsu, Y.; Matsuzaki, Y.; Shibuya, I.; Kawaguchi, H.; Ieda, M.; Kanakubo, S.; Shimazaki, T.; Ogawa, S.; et al. Cardiac neural crest cells contribute to the dormant multipotent stem cell in the mammalian heart. *J. Cell Biol.* **2005**, *170*, 1135–1146. [CrossRef]

49. Pandey, S.; Hickey, D.U.; Drum, M.; Millis, D.L.; Cekanova, M. Platelet-rich plasma affects the proliferation of canine bone marrow-derived mesenchymal stromal cells in vitro. *BMC Vet. Res.* **2019**, *15*, 269. [CrossRef]

50. Shen, J.; Gao, Q.; Zhang, Y.; He, Y. Autologous plateletrich plasma promotes proliferation and chondrogenic differentiation of adiposederived stem cells. *Mol. Med. Rep.* **2015**, *11*, 1298–1303. [CrossRef]

51. Shetty, P.; Bharucha, K.; Tanavde, V. Human umbilical cord blood serum can replace fetal bovine serum in the culture of mesenchymal stem cells. *Cell Biol. Int.* **2007**, *31*, 293–298. [CrossRef]

52. Witzeneder, K.; Lindenmair, A.; Gabriel, C.; Holler, K.; Theiss, D.; Redl, H.; Hennerbichler, S. Human-derived alternatives to fetal bovine serum in cell culture. *Transfus. Med. Hemother.* **2013**, *40*, 417–423. [CrossRef] [PubMed]

53. Schürmann, M.; Brotzmann, V.; Butow, M.; Greiner, J.; Höving, A.; Kaltschmidt, C.; Kaltschmidt, B.; Sudhoff, H. Identification of a Novel High Yielding Source of Multipotent Adult Human Neural Crest-Derived Stem Cells. *Stem Cell Rev.* **2018**, *14*, 277–285. [CrossRef] [PubMed]

54. Edgren, G.; Ullum, H.; Rostgaard, K.; Erikstrup, C.; Sartipy, U.; Holzmann, M.J.; Nyren, O.; Hjalgrim, H. Association of Donor Age and Sex With Survival of Patients Receiving Transfusions. *JAMA Intern. Med.* **2017**, *177*, 854–860. [CrossRef] [PubMed]

55. Greiner, J.F.; Grunwald, L.M.; Muller, J.; Sudhoff, H.; Widera, D.; Kaltschmidt, C.; Kaltschmidt, B. Culture bag systems for clinical applications of adult human neural crest-derived stem cells. *Stem Cell Res. Ther.* **2014**, *5*, 34. [CrossRef]

56. Stegeman, R.; Weake, V.M. Transcriptional Signatures of Aging. *J. Mol. Biol.* **2017**, *429*, 2427–2437. [CrossRef]

57. Peters, M.J.; Joehanes, R.; Pilling, L.C.; Schurmann, C.; Conneely, K.N.; Powell, J.; Reinmaa, E.; Sutphin, G.L.; Zhernakova, A.; Schramm, K.; et al. The transcriptional landscape of age in human peripheral blood. *Nat. Commun.* **2015**, *6*, 8570. [CrossRef]

58. Berchtold, N.C.; Cribbs, D.H.; Coleman, P.D.; Rogers, J.; Head, E.; Kim, R.; Beach, T.; Miller, C.; Troncoso, J.; Trojanowski, J.Q.; et al. Gene expression changes in the course of normal brain aging are sexually dimorphic. *Proc. Natl. Acad. Sci. USA* **2008**, *105*, 15605–15610. [CrossRef]

59. Lipinski, M.M.; Zheng, B.; Lu, T.; Yan, Z.; Py, B.F.; Ng, A.; Xavier, R.J.; Li, C.; Yankner, B.A.; Scherzer, C.R.; et al. Genome-wide analysis reveals mechanisms modulating autophagy in normal brain aging and in Alzheimer's disease. *Proc. Natl. Acad. Sci. USA* **2010**, *107*, 14164–14169. [CrossRef]

60. Haustead, D.J.; Stevenson, A.; Saxena, V.; Marriage, F.; Firth, M.; Silla, R.; Martin, L.; Adcroft, K.F.; Rea, S.; Day, P.J.; et al. Transcriptome analysis of human ageing in male skin shows mid-life period of variability and central role of NF-kappaB. *Sci. Rep.* **2016**, *6*, 26846. [CrossRef]

61. Moreno-Layseca, P.; Streuli, C.H. Signalling pathways linking integrins with cell cycle progression. *Matrix Biol.* **2014**, *34*, 144–153. [CrossRef] [PubMed]

62. Ghosh, A.K.; O'Brien, M.; Mau, T.; Qi, N.; Yung, R. Adipose Tissue Senescence and Inflammation in Aging is Reversed by the Young Milieu. *J. Gerontol. A Biol. Sci. Med. Sci.* **2019**, *74*, 1709–1715. [CrossRef]

63. Saika, S.; Okada, Y.; Miyamoto, T.; Yamanaka, O.; Ohnishi, Y.; Ooshima, A.; Liu, C.Y.; Weng, D.; Kao, W.W. Role of p38 MAP kinase in regulation of cell migration and proliferation in healing corneal epithelium. *Invest. Ophthalmol. Vis. Sci.* **2004**, *45*, 100–109. [CrossRef] [PubMed]

64. Chen, L.; Mayer, J.A.; Krisko, T.I.; Speers, C.W.; Wang, T.; Hilsenbeck, S.G.; Brown, P.H. Inhibition of the p38 kinase suppresses the proliferation of human ER-negative breast cancer cells. *Cancer Res.* **2009**, *69*, 8853–8861. [CrossRef] [PubMed]

65. Zarubin, T.; Han, J. Activation and signaling of the p38 MAP kinase pathway. *Cell Res.* **2005**, *15*, 11–18. [CrossRef] [PubMed]

66. Huth, H.W.; Santos, D.M.; Gravina, H.D.; Resende, J.M.; Goes, A.M.; de Lima, M.E.; Ropert, C. Upregulation of p38 pathway accelerates proliferation and migration of MDA-MB-231 breast cancer cells. *Oncol. Rep.* **2017**, *37*, 2497–2505. [CrossRef]

67. Tian, H.; Zhang, D.; Gao, Z.; Li, H.; Zhang, B.; Zhang, Q.; Li, L.; Cheng, Q.; Pei, D.; Zheng, J. MDA-7/IL-24 inhibits Nrf2-mediated antioxidant response through activation of p38 pathway and inhibition of ERK pathway involved in cancer cell apoptosis. *Cancer Gene Ther.* **2014**, *21*, 416–426. [CrossRef]

68. Qin, S.; Zhou, W.; Liu, S.; Chen, P.; Wu, H. Icariin stimulates the proliferation of rat bone mesenchymal stem cells via ERK and p38 MAPK signaling. *Int. J. Clin. Exp. Med.* **2015**, *8*, 7125–7133.

69. He, Y.; Jian, C.X.; Zhang, H.Y.; Zhou, Y.; Wu, X.; Zhang, G.; Tan, Y.H. Hypoxia enhances periodontal ligament stem cell proliferation via the MAPK signaling pathway. *Genet. Mol. Res.* **2016**, *15*. [CrossRef]

70. Yao, P.; Zhan, Y.; Xu, W.; Li, C.; Yue, P.; Xu, C.; Hu, D.; Qu, C.K.; Yang, X. Hepatocyte growth factor-induced proliferation of hepatic stem-like cells depends on activation of NF-kappaB. *J. Hepatol.* **2004**, *40*, 391–398. [CrossRef]

71. Maulik, N.; Sato, M.; Price, B.D.; Das, D.K. An essential role of NFkappaB in tyrosine kinase signaling of p38 MAP kinase regulation of myocardial adaptation to ischemia. *FEBS Lett.* **1998**, *429*, 365–369. [CrossRef]

72. Liu, A.; Guo, E.; Yang, J.; Yang, Y.; Liu, S.; Jiang, X.; Hu, Q.; Dirsch, O.; Dahmen, U.; Zhang, C.; et al. Young plasma reverses age-dependent alterations in hepatic function through the restoration of autophagy. *Aging Cell* **2018**, *17*, e12708. [CrossRef] [PubMed]

73. Ruckh, J.M.; Zhao, J.W.; Shadrach, J.L.; van Wijngaarden, P.; Rao, T.N.; Wagers, A.J.; Franklin, R.J. Rejuvenation of regeneration in the aging central nervous system. *Cell Stem Cell* **2012**, *10*, 96–103. [CrossRef] [PubMed]

74. Katsimpardi, L.; Litterman, N.K.; Schein, P.A.; Miller, C.M.; Loffredo, F.S.; Wojtkiewicz, G.R.; Chen, J.W.; Lee, R.T.; Wagers, A.J.; Rubin, L.L. Vascular and neurogenic rejuvenation of the aging mouse brain by young systemic factors. *Science* **2014**, *344*, 630–634. [CrossRef] [PubMed]

Original Research Report

Transcriptome Analysis Reveals High Similarities between Adult Human Cardiac Stem Cells and Neural Crest-Derived Stem Cells

Anna L. Höving, Katharina Sielemann, Johannes F. W. Greiner,
Barbara Kaltschmidt, Cornelius Knabbe* and Christian Kaltschmidt*

Transcriptome Analysis Reveals High Similarities between Adult Human Cardiac Stem Cells and Neural Crest-Derived Stem Cells

Anna L. Höving [1,2,*], **Katharina Sielemann [3,4]**, **Johannes F. W. Greiner [1]**,
Barbara Kaltschmidt [1,5], **Cornelius Knabbe [2,†]** and **Christian Kaltschmidt [1,*,†]**

1   Department of Cell Biology, Bielefeld University, 33615 Bielefeld, Germany;
     johannes.greiner@uni-bielefeld.de (J.F.W.G.); barbara.kaltschmidt@uni-bielefeld.de (B.K.)
2   Heart and Diabetes Centre NRW, Institute for Laboratory and Transfusion Medicine,
     Ruhr-University Bochum, 32545 Bad Oeynhausen, Germany; cknabbe@hdz-nrw.de
3   Genetics and Genomics of Plants, Center for Biotechnology (CeBiTec), Bielefeld University,
     33615 Bielefeld, Germany; kfrey@cebitec.uni-bielefeld.de
4   Graduate School DILS, Bielefeld Institute for Bioinformatics Infrastructure (BIBI), Bielefeld University,
     33615 Bielefeld, Germany
5   AG Molecular Neurobiology, Bielefeld University, 33615 Bielefeld, Germany
*   Correspondence: anna.hoeving@uni-bielefeld.de (A.L.H.); c.kaltschmidt@uni-bielefeld.de (C.K.)
†   These authors contributed equally to this work.

Simple Summary: The regeneration of nearly all organs of the human body mainly depends on the functionality of adult stem cell populations that reside in their respective niches and can be activated upon injuries or other damages. These stem cell populations greatly differ in their expression profile of molecular markers, which greatly influences their potential use in regenerative medicine. Neural crest-derived stem cells are a prominent subpopulation of adult stem cells and are known for their high regenerative potential. Within this study, we compared two adult human stem cell populations, namely neural crest-derived inferior turbinate stem cells from the nasal cavity and human cardiac stem cells from the heart, using global gene expression profiling. Here, we found differences that correspond to the tissue sources of origin but also similarities in the expression of markers that are associated with the neural crest. Further classifying nasal stem cells and cardiac stem cells in a broader context, we identified clear similarities between both populations and other adherent stem cell populations compared to non-adherent progenitor cells of the blood system. The analyses provided here might help to understand the differences and similarities between different adult human stem cell populations.

Abstract: For the identification of a stem cell population, the comparison of transcriptome data enables the simultaneous analysis of tens of thousands of molecular markers and thus enables the precise distinction of even closely related populations. Here, we utilized global gene expression profiling to compare two adult human stem cell populations, namely neural crest-derived inferior turbinate stem cells (ITSCs) of the nasal cavity and human cardiac stem cells (hCSCs) from the heart auricle. We detected high similarities between the transcriptomes of both stem cell populations, particularly including a range of neural crest-associated genes. However, global gene expression likewise reflected differences between the stem cell populations with regard to their niches of origin. In a broader analysis, we further identified clear similarities between ITSCs, hCSCs and other adherent stem cell populations compared to non-adherent hematopoietic progenitor cells. In summary, our observations reveal high similarities between adult human cardiac stem cells and neural crest-derived stem cells from the nasal cavity, which include a shared relation to the neural crest. The analyses provided here may help to understand underlying molecular regulators determining differences between adult human stem cell populations.

1. Introduction

Adult human stem cell (ASC) populations harbour a great potential for applications in regenerative medicine [1,2], emphasizing the importance of their identification, characterization and classification. In recent years, ASCs were described in nearly all tissues and organs of the human body [3–9]. However, these populations showed strong differences in their potential to differentiate into specialized cell types. Although most of these differences in differentiation potential were linked to developmental origin and the tissue of origin of the respective stem cell population, some tissues harbour multiple stem cell populations with highly different potentials. For instance, populations of skeletal stem cells could be found in the bone marrow next to hematopoietic stem cells and mesenchymal stem cells [10,11]. Moreover, mesenchymal stem cells with different functionalities were found in diverse tissues [12,13]. For instance, Maleki and coworkers showed that spermatogonial stem cells and Wharton's jelly-mesenchymal stem cells are all able to differentiate into the osteogenic lineage [13]. However, Riekstina and colleagues showed that adult mesenchymal stem cell populations, derived from bone marrow, adipose tissue, dermis and the heart, express different combinations of stem cell markers in vitro [12]. With regard to these differences, defining adult stem cell populations still remains challenging. On a technical level, analysis of cell surface proteins accompanied by laborious differentiation assays were commonly applied to characterize human stem cells pools [13–16]. Although this method led to the identification of a large number of cell populations, the classification of stem cell pools by marker proteins was mostly limited to the number of available fluorochromes or filters that could be used simultaneously. Addressing this challenge, the analysis of RNA sequencing (RNA-Seq) data is a widely used and powerful tool allowing the simultaneous comparison and quantification of hundreds of biomarkers and underlying signaling pathways contributing to the varying stem cell phenotypes. RNA-Seq also enables the determination of expression profiles and pathways conserved between stem cell populations from different sources, thus allowing a more precise characterization and classification.

In the present study, we used RNA-Seq to characterize and compare a very recently identified Nestin^{+}/CD105^{+} adult human cardiac stem cell population (hCSCs) [17] with neural crest-derived stem cells from the inferior turbinate of the human nose (inferior turbinate stem cells, ITSCs) [8]. Although the human heart was initially considered as a terminal differentiation organ, several populations of adult cardiac stem cells were shown to reside within the human heart. These cardiac stem cells were shown to differentiate into cardiomyocytes as well as into smooth muscle cells and endothelial cells in vitro [18–20]. We very recently extended these findings by identifying a Nestin^{+}/CD105^{+} adult hCSC population that could be isolated from the left atrial appendage (LAA) and that gave rise to cardiomyocytes in vitro [17]. Nevertheless, the in vivo contribution of CSCs to tissue repair remains elusive, partly because of the heterogeneity of the cardiac stem cell populations identified so far. The broad diversity of cardiac stem cells in terms of the described markers and properties suggests the existence of a wide range of different adult cardiac stem cell populations [21–23]. From a developmental point of view, the formation of the human heart is a complex process that is still not fully understood. A primary heart tube is formed out of the cardiogenic plates from the anterior splanchnic mesoderm after the third week of embryogenesis [24]. After a rightward looping process, the septation process follows. Here, primitive chambers are subdivided to form the cardiac atria and ventricles [24]. During septation of the outflow tract of the ventricle, the aortic orifice gets in contact with the left ventricle while the pulmonary orifice remains situated above the right ventricle. During this process, cardiac neural crest cells enter the outflow tract as condensed mesenchyme between the aortic and pulmonary orifice [24–26]. The neural crest is a transient embryonic structure that was

initially described by Wilhelm His in the development of the chick embryo as the intermediate chord appearing between the neural chord and the future ectoderm [27]. During embryonic development, neural crest stem cells migrate and give rise to a broad range of tissues including the heart, where neural crest cells populate the myocardium and contribute to myocardialization, although most of these cells disappear in later stages upon apoptosis [24,26]. However, neural crest-derived populations of cardiac stem cells have recently been described in the adult hearts of mice and zebrafishes [28–32]. In particular, El-Helou and colleagues demonstrated the presence of NCSCs in the adult rat heart via expression of Nestin [31], a characteristic NCSC-marker associated with proper self-renewal of stem cells [33,34], while Tomita and coworkers could show that Nestin$^+$ NCSCs in the mouse heart give rise to cardiomyocytes in vivo [35]. Furthermore, human congenital heart diseases like DiGeorge Syndrome, CHARGE Syndrome and Alagille Syndrome were linked to defective cardiac neural crest function [36–38], suggesting a possible contribution of neural crest-derived cardiac stem cells to normal cardiac regeneration. However, neural crest-derived stem cell populations in the human heart have not been identified so far.

Within this study, we directly compared Nestin$^+$/CD105$^+$ adult hCSCs to neural crest-derived ITSCs from the human nasal cavity using global gene expression profiling. Next to other NCSC-pools, ITSCs were reported to be positive for Nestin, S100 and p75 on the protein level and showed the ability to give rise to ectodermal as well as mesodermal cell types in vitro and in vivo [8,39–42]. Likewise, we detected the expression of the proteins Nestin, S100 and p75 in cultured hCSCs, suggesting a potential relation of hCSCs to the neural crest. Our comparison of both stem cell populations using bioinformatic tools led to the identification of 4367 differentially expressed genes (DEGs), while respective identified GO-terms of differential gene expression were associated with the tissues of origin, namely the heart and the olfactory or respiratory epithelium of the nose. Interestingly, a broad range of neural crest-associated genes was found to be expressed in both stem cell populations. We further compared the global gene expression profiles of hCSCs and ITSCs with published RNA-Seq data of adipose-derived mesenchymal stem cells (AdMSCs), CD34$^+$ hematopoietic stem cells (HSCs) [43] and cardiosphere-derived cells (CDCs) [44]. In comparison to hematopoietic stem cells, stem cell-associated GO-terms like 'tissue morphogenesis', 'vasculature development' or 'embryonic development' were upregulated in hCSCs and ITSCs, which may hint to a shared regulation of their stem cell properties. In addition, our findings may help to understand the underlying molecular kinetics determining the differences between various adult human stem cell populations.

2. Materials and Methods

2.1. Cell Isolation and Cultivation

Human cardiac stem cells were isolated and cultivated as previously described [17] according to local and international guidelines (declaration of Helsinki) after informed and written consent. Isolation and further experimental procedures were ethically approved by the ethics commission of the Ruhr-University Bochum (Faculty of Medicine, located in Bad Oeynhausen) (approval reference number eP-2016-148).

Human inferior turbinate stem cells were isolated and cultivated after informed written consent according to local and international guidelines (declaration of Helsinki) as previously described [8,45]. Isolation and further experimental procedures were ethically approved by the ethics commission of the Ärztekammer Westfalen-Lippe and the medical faculty of the Westfälische Wilhelms-Universität (Münster, Germany) (approval reference number 2012-15-fS).

2.2. Lentiviral Transduction of hCSCs

HCSCs were transduced by lentivirus with the cFUG-W plasmid. Lentivirus production was carried out in HEK293 cells with packaging plasmid Δ8.91, VSV-G envelope plasmid and cFUG-W transfer vector by calcium-phosphate precipitation. Δ8.91 and VSV-G were gifts from David

Baltimore [46]. Supernatant was harvested 48 h after transfection and lentivirus was concentrated by ultracentrifugation (50,000× *g*, 4 °C, 2 h).

2.3. Coculture of GFP-hCSCs and Primary Mouse Cardiomyocytes

Primary mouse cardiomyocytes were isolated from newborn mice according to Streejt and colleagues [47]. Prior to coculture, mouse cardiomyocytes were treated with 10 µg/mL Mitomycin C (Sigma Aldrich) according to the manufacturer's instructions. Coculture with hCSCs was carried out in DMEM-F12 with 5% horse serum (Dianova).

2.4. Immunohistochemistry and Immunocytochemistry

Cultivated cells were fixed for 20 min using 4% paraformaldehyde (PFA), washed and permeabilized in PBS with 0.02% TritonX-100 (Sigma Aldrich) and supplemented with 5% goat serum for 30 min. The applied primary antibodies were diluted in PBS as followed: rabbit anti-Nestin 1:200 (Millipore), mouse anti-S100B 1:500 (Sigma Aldrich), rabbit anti-Slug 1:100 (Cell-Signaling Technology), rabbit anti-p75 1:500 (Cell-Signaling Technology), mouse anti-β-III-tubulin 1:100 (Promega), rabbit anti-neurofilament-L 1:50 (Cell-Signaling Technology), anti-vGlut (Millipore) and anti-Synaptophysin (Millipore). They were applied for 1 h (cells) at room temperature. After three washing steps, secondary fluorochrome-conjugated antibodies (Alexa 555 anti-mouse or Alexa 488 anti-rabbit, Invitrogen, Life Technologies GmbH) were applied for 1 h at RT with a dilution ratio of 1:300. Nuclear staining was realized by incubation with 4,6-Diamidin-2-phenylindol (DAPI) (1 µg/mL, Applichem) in PBS for 15 min at RT. Finally, the samples were mounted with Mowiol (self-made). Imaging was performed using a confocal laser scanning microscope (CLSM 780, Carl Zeiss) and image processing was executed with ImageJ and CorelDRAW [48] (open source and Corel Corporation).

2.5. Induced Neuronal Differentiation

Neuronal differentiation in the isolated cells was induced following the protocol described by Müller and colleagues [39]. Briefly, cells were seeded with a density of 2×10^5 cells per 6-well in hCSC-medium. After 48 h, neural differentiation was induced with a neuronal induction medium containing 1 µM dexamethasone (Sigma Aldrich), 2 µM insulin (Sigma Aldrich), 500 µM 3-isobutyl-1-methylxanthine (Sigma Aldrich) and 200 µM indomethacin (Sigma Aldrich). Cells were fed every 2–3 days by removing half of the medium and adding the same amount of fresh prewarmed medium. After 7 days of culture, maturation of the cells was induced by adding retinoic acid (0.5 mM) (Sigma Aldrich) and N2-supplement (1x) (Gibco) over 2 days. Afterwards, retinoic acid was removed while N2 was applied until neuronal maturation at day 28. As undifferentiated control, cells were cultured in hCSC-medium as described above. After 28 days, the protein expression was analyzed by immunocytochemical staining.

2.6. Osteogenic Differentiation of hCSCs

The osteogenic differentiation of hCSCs was induced by biochemical cues according to Greiner and coworkers [45]. Briefly, cells were seeded in hCSC-medium at a density of 3×10^3 cells/cm^2. After 48 h the medium was switched to an osteogenic induction medium supplemented with 100 nM dexamethasone (Sigma Aldrich), 0.05 mM L-ascorbic acid-2-phosphate (Sigma Aldrich) and 10 mM β-glycerophosphate (Sigma Aldrich). The medium was changed every 2–3 days. After 21 days, differentiated cells were processed for RNA-Isolation as described below. For undifferentiated controls, cells were cultured in hCSC-medium as described above.

2.7. Adipogenic Differentiation of hCSCs

For adipogenic differentiation, hCSCs were cultivated in DMEM (Sigma Aldrich) containing 10% FCS (Sigma Aldrich) and plated at a density of 4×10^3 cells /cm^2. After 48 h, 1 µM dexamethasone

(Sigma Aldrich), 2 μM insulin (Sigma Aldrich), 500 μM 3-isobuthyl-1-methylxanthine (Sigma Aldrich) and 200 μM indomethacin (Sigma Aldrich) were added to the medium and cultivated for 72 h. Afterwards, the medium was switched and cells were cultivated for 4 days in DMEM containing 10% FCS and 2 μM insulin (Sigma Aldrich) to induce adipogenic differentiation. These two media were alternatingly used and changed every 4 days for 3 weeks. As undifferentiated control, cells were cultured in hCSC-medium as described above.

2.8. Quantitative PCR

The RNA isolation was performed using the NucleoSpin RNA Kit (Macherey Nagel, Bethlehem, PA, USA) according to the manufacturer's guidelines. The quality and concentration of the obtained RNA was quantified by a spectrophotometer (Thermo Fisher Scientific, Waltham, MA, USA). For cDNA synthesis, the First Strand cDNA Synthesis Kit (Thermo Fisher Scientific) was applied in accordance with the manufacturer's guidelines. qPCR was carried out using Perfecta SYBR green Supermix (quantaBio, Beverly, MA, USA) following the manufacturer's instructions with primers for *PPARG* (fwd: GGATGCAAGGGTTTCTTCCG, rev: AACAGCTTCTCCTTCTCGGC), *ON* (fwd: AAACATGGCAAGGTGTGTGA, rev: TGCATGGTCCGATGTAGTC) and *GAPDH* (fwd: CATGAGAAGTATGACAACAGCCT, rev: AGTCCTTCCACGATACCAAAGT).

2.9. RNA-Seq and Bioinformatic Analysis

RNA of cultured cells was isolated with the NucleoSpin RNA Kit (Macherey Nagel, Düren, Germany) and stabilized with RNAstable (Biomatrica, San Diego, CA, USA) for transport at room temperature. RNA was sequenced by Novogene (Beijing, China) using the Illumina Hiseq4000 platform with a paired end 150 bp strategy. RNA-Seq raw data are accessible at NCBI Gene Expression Omnibus with the accession number GSE129547. More data were downloaded from the NCBI Sequence Read Archive (SRA) with the accession numbers GSE140385 (CD34^{+} hematopoietic stem cells [43]), GSE142831 (adipose-derived mesenchymal stem cells) and GSE81827 (cardiosphere-derived cells [44]). Here, we took care to select datasets of paired end sequencing runs from the Illumina platform to minimize technical variability between the groups. From these studies, we selected the datasets of the control groups, to use only expression data of untreated cells. First, all data were processed in the same way: FastqQC (Version 0.11.19) was used for a first quality control of the raw data. Subsequently, trimming of low-quality bases and adapter clipping was performed with Trimmomatic-0.38 [49] with the following settings: PE; -phred33; ILLUMINACLIP:TruSeq3-PE.fa:2:30:10; LEADING:6; TRAILING:6; SLIDINGWINDOW:4:15; MINLEN:36. Clean reads were aligned to the *Homo sapiens* reference genome sequence (GRCh38) using STAR 2.7.3a [50] with the following parameters: runThreadN 8; limitBAMsortRAM 32000000000; –outBAMsortingThreadN 8; –outSAMtype BAM SortedByCoordinate; –outFilterMismatchNoverLmax 0.05; –outFilterMatchNminOverLread 0.8. FeatureCounts (version 2.0.0) was used to quantify the read number after mapping [51] with the following parameters: -T 4; -t gene; -g gene_id; -a Homo_sapiens.GRCh38.78.gtf. Differential gene expression analysis between two groups was performed using the DESeq2 R package [52]. Here, a publicly available script from Stephen Turner was used with slight modifications (https://gist.github.com/stephenturner/f60c1934405c127f09a6). GO-term enrichment and KEGG pathways analysis were performed using the gage package in R [53]. Here, a publicly available script from Stephen Turner was used with slight modifications (https://www.r-bloggers.com/2015/12/tutorial-rna-seq-differential-expression-pathway-analysis-with-sailfish-deseq2-gage-and-pathview/). The corresponding scripts are provided in the supplementary materials. Visualization of significantly enriched terms was performed using Graph Pad Prism 8.

3. Results

3.1. hCSCs Show a NCSC-Like Expression Pattern and Differentiate into Mesodermal and Ectodermal Derivates

For an initial comparison of hCSCs and ITSCs, we aimed to compare the marker expressions of hCSCs and ITSCs on the protein level in vitro. In a previous publication, we already showed that ITSCs express the neural crest-related stem cell markers Slug, S100, Nestin and p75 [8]. To investigate, whether hCSCs share this marker expression profile, we performed immunocytochemical stainings of cultured hCSCs and observed the presence of Slug, S100, Nestin and a slight expression of p75 proteins (Figure 1A). Notably, Slug protein seemed to be localized in the nuclear compartment, indicating its activity as a transcription factor (Figure 1A). In addition to the NCSC-like marker expression, we investigated the differentiation capacity of hCSCs in comparison to ITSCs. As already shown in a broad range of studies, ITSCs are able to differentiate very efficiently into mesodermal as well as ectodermal derivates like neurons, osteoblasts and adipocytes [8,39,40,54]. We applied these established protocols to hCSCs and detected 1–2% neuron-shaped cells positive for the neuronal markers Neurofilament, β-III-Tubulin, Synaptophysin and VGlut (Figure 1B). After directed osteogenic differentiation of hCSCs, osteonectin expression was significantly upregulated (Mann Whitney Test, $p < 0.05$) compared to an undifferentiated control (Figure 1C). HCSCs likewise successfully underwent adipogenic differentiation resulting in the significant upregulation (Mann Whitney Test, $p < 0.05$) of PPARG mRNA (Figure 1D) compared to undifferentiated controls. To investigate the differentiation of hCSCs into cardiomyocytes within a cardiomyogenic environment, we performed coculture experiments with primary neonatal beating mouse cardiomyocytes and lentiviral transduced GFP$^+$ hCSCs. After 11 days of coculture, we detected GFP$^+$ beating human cardiomyocytes next to mouse cardiomyocytes (Figure 1E, arrowheads). These observations confirmed the functionality of hCSC-derived cardiomyocytes. Notably, we already could show that hCSCs express common cardiomyocyte markers like α-actinin and Connexin43 after differentiation with biochemical cues [17]. In summary, hCSCs and ITSCs shared high similarities in the presence of marker proteins, whereas differentiation capabilities differed in dependence on the respective niche of the stem cell population (Figure S1).

3.2. Differential Gene Expression Between hCSCs and ITSCs Reflects the Particular Niches of Origin

We next extended our comparison of hCSCs and ITSCs from marker protein expression and differentiation capacities to global gene expression profiles by performing RNA-Seq of hCSCs from 4 distinct donors as well as of ITSCs from 4 different donors. A principal component analysis (PCA) showed that hCSCs and ITSCs formed distinct clusters, with PC1 explaining 49.6% of the total variance. Further, the gene expression patterns of the single hCSC donors seemed to be more heterogeneous than within ITSCs, visible by the distribution along the PC2 axis explaining 21.3% of the variance (Figure 2A). To investigate these differences in more detail, we visualized the DEGs between both groups in a volcano plot (Figure 2B). In total, 4367 genes were significantly differentially expressed ($p < 0.05$) with 2074 significantly upregulated in hCSCs ($p < 0.05$) and 2,293 significantly upregulated in ITSCs ($p < 0.05$). Interestingly, we found the genes for the transcription factors PAX3 and PAX9 to be significantly overexpressed in ITSCs (PAX3 $p \approx 7.9 \times 10^{-38}$; PAX9 $p \approx 9.1 \times 10^{-40}$). We next reduced data dimensionality by applying a KEGG pathway analysis. Here, five KEGG pathways were significantly ($q < 0.05$) upregulated in hCSCs compared to ITSCs while only the KEGG pathway hsa04740 'olfactory transduction' was significantly ($q \approx 1.1 \times 10^{-4}$) upregulated in ITSCs compared to hCSCs (Figure 2C). This may reflect the origin of the examined cell populations, however the enrichment of only six significantly up- or down regulated KEGG pathways could also demonstrate that this analysis was not appropriate to visualize the differences between hCSCs and ITSCs. We therefore analyzed the GO-term enrichment of biological processes. Among the top ten of the most significantly enriched GO-terms of genes upregulated in hCSCs, we found terms associated with cardiovascular development like

'blood vessel development' ($p \approx 1.9 \times 10^{-7}$), 'blood vessel morphogenesis' ($p \approx 3 \times 10^{-6}$) and 'heart development' ($p \approx 1.5 \times 10^{-5}$) (Figure 2D). Furthermore, the top ten of the most significantly enriched GO-terms of genes upregulated in ITSCs comprised terms like 'detection of chemical stimulus involved in sensory perception' ($p \approx 1.5 \times 10^{-4}$), 'sensory perception of chemical stimulus' ($p \approx 1.7 \times 10^{-3}$) and 'detection of chemical stimulus involved in sensory perception of smell/taste' ($p \approx 4.9 \times 10^{-3}$ and $p \approx 5.1 \times 10^{-3}$) (Figure 2D). Since hCSCs were derived from the left atrial appendage of the human heart and ITSCs were located in the inferior turbinate of the nose, these GO-terms were clearly linked to the tissue of origin of the examined stem cell populations. Remarkably, general stem cell-associated GO-terms of biological processes were not enriched when comparing global gene expression profiles of hCSCs and ITSCs, leading to the assumption that both cell populations did not differ significantly in their stem cell marker expression profiles. Further, we detected several markers for neural crest-derived stem cells [55] that were expressed in both stem cells populations (Table 1).
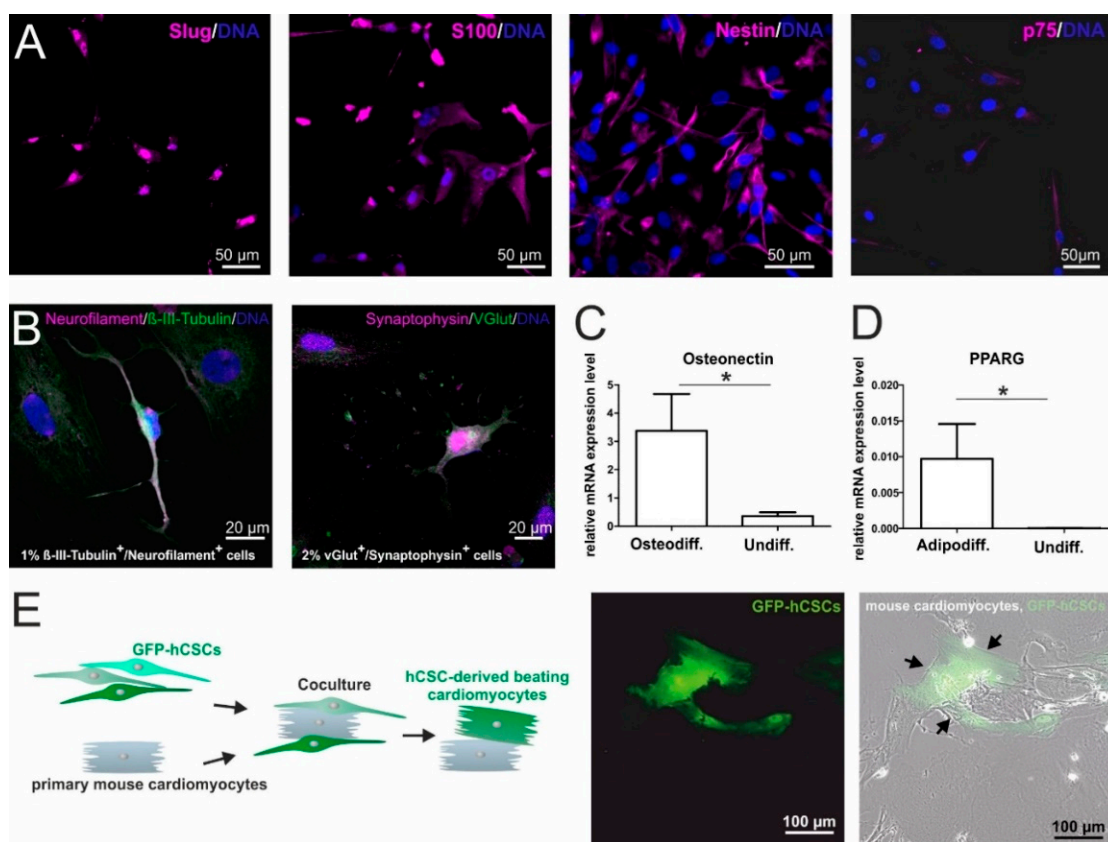

Figure 1. In vitro characterization of human cardiac stem cells (hCSCs): (**A**) Immunocytochemical stainings of cultured hCSCs showed the expression of the NCSC markers Slug, S100, Nestin and p75. (**B**) Directed differentiation of hCSCs generated Neurofilament$^+$/β-II-Tubulin$^+$ and Synaptophysin$^+$/VGlut$^+$ neuron-like cells. (**C**) Application of an osteogenic differentiation medium resulted in the upregulation of Osteonectin mRNA (Mann Whitney Test, * $p < 0.05$). (**D**) Application of an adipogenic differentiation protocol resulted in the upregulation of PPARG mRNA (Mann Whitney Test, * $p < 0.05$). (**E**) GFP$^+$ hCSCs differentiate into beating cardiomyocytes (arrowheads) upon coculture with primary mouse cardiomyocytes.

To further elucidate a potential contribution of neural crest-derived cells to adult cardiac structures and cardiac functionality, we carefully reviewed literature reporting mutations in known neural crest-associated genes expressed in ITSC and in hCSCs (Table 1). Interestingly, a wide range of the resulting defects is represented by craniofacial abnormalities as well as congenital cardiac defects such as Baraitser–Winter syndrome, oculodentodigital dysplasia, Pallister-Hall syndromes

(PHS), Alagille syndrome, Autosomal dominant form of Adams-Oliver syndrome, Hajdu Cheney Syndrome (HCS), Hirschsprung's disease, Loeys–Dietz syndrome, Saethre-Chotzen syndrome, and Kabuki syndrome.
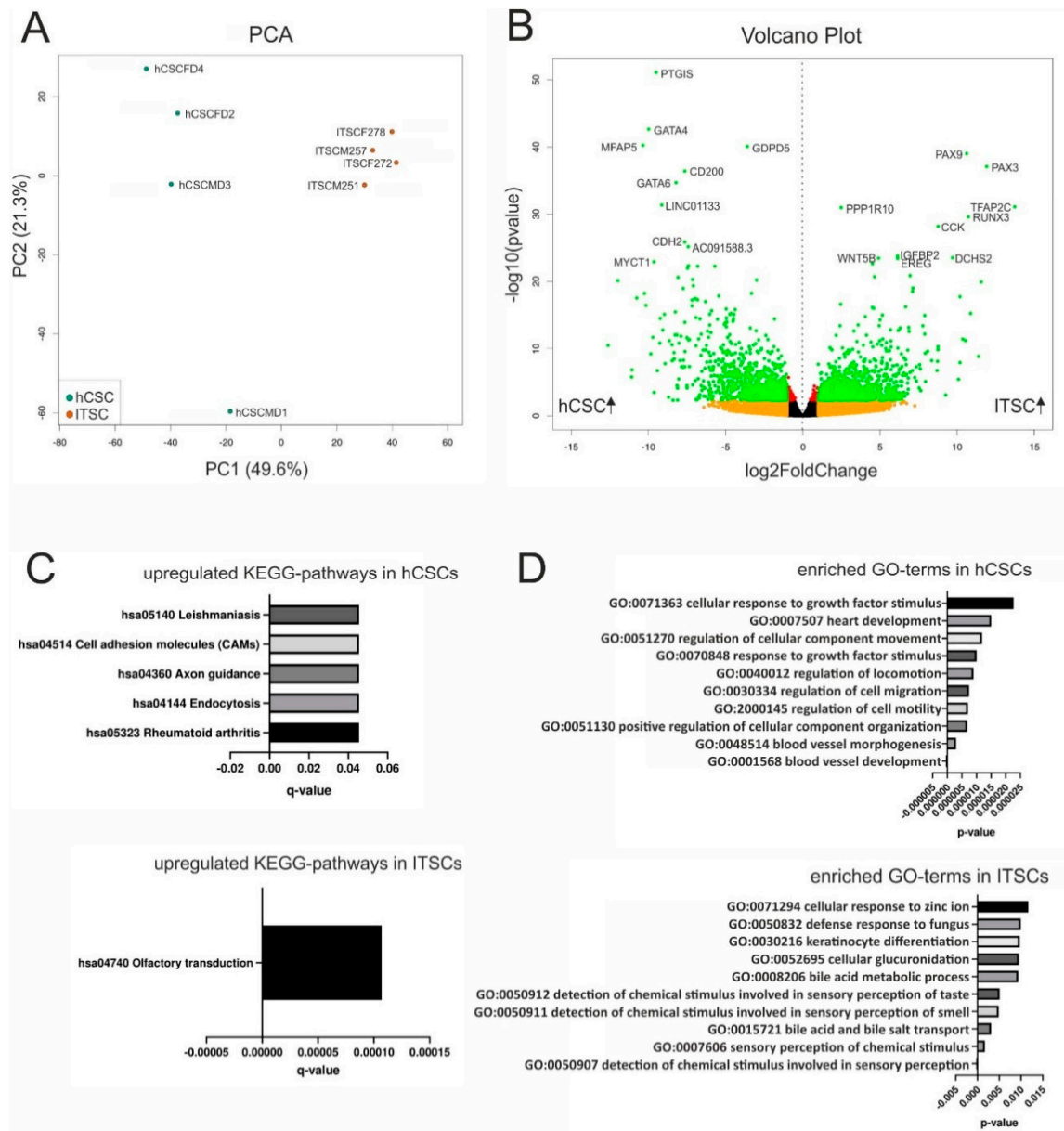

Figure 2. Differential gene expression between hCSCs and inferior turbinate stem cells (ITSCs). (**A**) Principal component analysis shows that hCSCs and ITSCs build separate clusters. (**B**) The volcano plot shows 4367 significantly DEGs (green dots). (**C**) KEGG pathway analysis reveals six pathways to be significantly ($p < 0.05$) up- or downregulated between hCSCs and ITSCs. (**D**) Top ten of the most significantly enriched GO-terms referring to biological processes.

Table 1. Diseases related to mutations in neural crest-associated genes expressed in hCSCs and ITSCs. The read counts represent the mean of four replicates of hCSCs and ITSCs respectively. The mean read count among all samples and genes was 957.

Gene	Gene-ID	Name	Defects	Mean Read Counts	Ref.
ACTB	ENSG00000075624	Baraitser–Winter syndrome	defects in the development of the brain, eyes (colomba), and other facial structures. Other defects may present as short stature, ear anormalities with hearing loss, cardiac malformations, polydactyly, renal malformations, neurologic disorders.	hCSC: 186,465; ITSC: 201,934.5	[56]
CTNNB1	ENSG00000168036	Increased tumorigenicity	mutations of the *CTNNB1* gene are frequent (40–60% of cases) in endometrioid endometrial carcinoma (EEC) but have also been detected in a broad range of other cancer types.	hCSC: 19,904.75; ITSC: 20,509.5	[57,58]
EDN1	ENSG00000078401	Recessive Auriculocondylar syndrome	micrognathia, temporomandibular joint and condyle anomalies, microstomia, prominent cheeks, and question-mark ears (QMEs).	hCSC: 1471.75; ITSC: 34.5	[59]
FZD7	ENSG00000155760	Increased tumorigeneicity	upregulated in several cancer types including intestinal tumors, hepatocellular carcinomas, gastric cancer and breast cancer and is important for progression, invasion and metastasis.	hCSC: 5757.25; ITSC: 3631	[60]
GJA1	ENSG00000152661	Oculodentodigital Dysplasia	digital malformations, craniofacial anomalies, occasionally deafness and dysplasia of the ears, abnormal dentition, rarely cardiac abnormalities.	hCSC: 40,788.5; ITSC: 6454	[61,62]
GLI3	ENSG00000106571	Greig cephalopolysyndactyly (GCPS)	polydactyly, minor craniofacial abnormalities.	hCSC: 1482.75; ITSC: 1591.25	[63,64]
		Pallister-Hall syndromes (PHS)	hypothalamic hamartoma, polydactyly, dysplastic nails, rarely congenital heart defects.		[65]
MSX1	ENSG00000163132	Wolf–Hirschhorn syndrome	mental and growth retardation, craniofacial malformations, seizures, tooth agenesis.	hCSC: 399.25; ITSC: 1250	[66,67]
		Witkop syndrome	tooth agenesis, nail dysplasia.		[66,68]
		Non-syndromic orofacial clefts	cleft lip and/or cleft palate.		[66]
NES	ENSG00000132688	Development of the heart and brain	human nestin regulates cell proliferation in the heart and brain in a transgene mouse model.	hCSC: 7872; ITSC: 17,177.5	[69]
NOTCH1	ENSG00000148400	Alagille syndrome	intrahepatic bile duct paucity and cholestasis, cardiac malformations, ophthalmological abnormalities, skeletal anomalies, characteristic facial appearance, and renal and pancreatic abnormalities.	hCSC: 6108.25; ITSC: 2544.75	[70,71]
		Aortic valve disease	valve calcification.		[72]
		Autosomal dominant form of Adams-Oliver syndrome	terminal transverse limb malformations, an absence of skin, a partial absence of skull bones. Occasionally vascular anomalies, pulmonary or portal hypertension, retinal hypervascularization, congenital heart defects in 23% of the patients.		[73,74]

Table 1. *Cont.*

Gene	Gene-ID	Name	Defects	Mean Read Counts	Ref.
NOTCH2	ENSG00000134250	Alagille syndrome	See above.	hCSC: 27,494.5; ITSC: 11,911.25	[75]
		Hajdu Cheney Syndrome (HCS)	rare disease characterized by acroosteolysis, severe osteoporosis, short stature, craniofacial defects occasionally with cleft palate, wormian bones, neurological symptoms, sometimes cardiovascular defects.		[76,77]
PAX3	ENSG00000135903	Waardenburg syndrome	heterochromia, pigmentation anomalies, varying degrees of deafness.	hCSC: 1; ITSC: 3587.5	[78]
PAX6	ENSG00000007372	Aniridia	defects in the formation of the iris (absence or hypoplasia), cornea, lens, fovea, and optic nerve	hCSC: 44.75; ITSC: 42.5	[79]
RET	ENSG00000165731	medullary thyroid carcinoma	intermediate risk	hCSC: 53; ITSC: 82	[80]
		Hirschsprung's disease	loss of neurons in the hindgut, congenital heart diseases (CHDs) are reported in 5% of the patients.		[81,82]
SMAD2	ENSG00000175387	Colorectal carcinoma	mutations in the tumor suppressors Smad2.	hCSC: 5217.25; ITSC: 5108	[83,84]
		Loeys–Dietz syndrome	defects in the connective tissue cause aortic aneurysms and arterial tortuosity, hypertelorism, and bifid/broad uvula or cleft palate.		[85]
SNAI2	ENSG00000019549	Increased tumorigeneicity	tumor growth and invasiveness in lung cancer, breast cancer progression, upregulated in colorectal carcinoma and may other cancer types.	hCSC: 3667; ITSC: 8666.75	[86–89]
SNAI1	ENSG00000124216	Increased tumorigeneicity	upregulation in breast cancer cells, ovarian cancer, and may other cancer types.	hCSC: 636.5; ITSC: 642.5	[88,90, 91]
TWIST	ENSG00000122691	Saethre-Chotzen syndrome	craniofacial malformations, mild limb deformities, occasionally hearing loss, renal abnormalities and congenital heart malformations.	hCSC: 4361.75; ITSC: 8154.75	[92,93]
KMT2D	ENSG00000167548	Kabuki	craniofacial dysmorphism, minor skeletal anomalies, persistence of fetal fingertip pads, mild-to-moderate intellectual disability, and postnatal growth deficiency. Congenital heart defects in 70% of patients with mutations in the KMT2D gene.	hCSC: 7974.5; ITSC: 6808.75	[94–96]

3.3. hCSCs and ITSCs Share Higher Similarities in Gene Expression Profiles with AdMSCs and CDCs than with HSCs

A comparison of two human stem cell populations from the adult heart (hCSCs) and the adult inferior turbinate of the nose (ITSCs) in terms of gene or protein expression as well as differentiation capacities showed differences that clearly reflected the niches or tissues of origin but no germ layer-associated differences. Therefore, we were interested in a comparison of hCSCs and ITSCs with other adult stem cell populations that were isolated and characterized independently in other labs. To compare more adult human stem cell populations on a global gene expression level, we accessed published RNA-Seq data of known human stem cell pools. Here, we took care to select datasets of paired end sequencing runs from the Illumina platform to minimize technical variability between the groups. In detail, we accessed expression data of cardiosphere-derived cells (CDC) [44], CD34+ hematopoietic stem cells (HSC) [43] and adipose-derived mesenchymal stem cells (AdMSC) (NCBI GEO-accession

number GSE142831). From these studies, we selected the datasets of the control groups, to use only expression data of untreated cells. First, all data were processed in the same way: Trimming of raw reads was performed with Trimmomatic-0.38 [49] to clip adapter sequences and low-quality bases. Subsequently, clean reads were mapped to the reference genome sequence GRCh38 using STAR-2.7.3a [50] and read counts were quantified with featureCounts [51]. The resulting data were further analyzed with the DESeq2 pipeline. Principal component analysis (PCA) revealed that all cell populations formed individual clusters along the PC1 and PC2 axes. The greatest differences existed between HSCs and all of the other stem cell populations, as PC1 explains 72.3% of the variance. However, PC2 also distributed the stem cell populations with 9.3% of the variance (Figure 3A). Interestingly, on the PC2 axis, adipose-derived MSCs and ITSCs were closer to each other than to hCSCs.
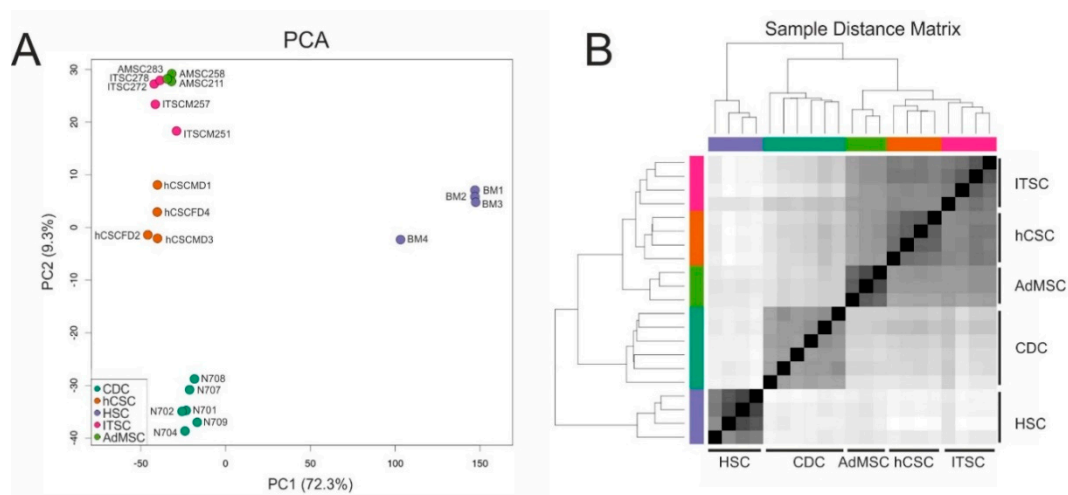
Figure 3. Comparison of global gene expression profiles of adult stem cell populations from different sources. (**A**) Principal component analysis reveals that all cell populations cluster independently. (**B**) The sample distance matrix reveals great differences between hematopoietic stem cells (HSCs) and other adult stem cell populations.

We could further confirm that the global transcriptome of cardiosphere-derived cells sequenced by Harvey and colleagues [44] shows higher similarity to, and is closer to hCSCs than to any of the other adult stem cell population. These observations indicate a shared heart stem cell-specific expression profile of hCSCs and CDCs and may allow the conclusion that minor differences visible on the PC2 axis were related to the niches of the stem cell populations. The large differences between HSCs and the other examined stem cell populations were also visible in a sample distance matrix (Figure 3B) and a hierarchical clustered heatmap of the 200 genes with the highest variance among all samples (Figure 4). Here, all cell populations clustered individually, but CS were more distinct from ITSCs, hCSCs and AdMSCs while HSCs showed the greatest differences to the other populations. A detailed list of all 200 genes is provided in Table S1.

3.4. hCSCs and ITSCs Overexpress Stem-Cell Associated Genes When Compared with HSCs

Based on the observation that hCSCs and ITSCs shared highly similar global gene expression patterns with AdMSCs and CDCs but not with HSCs, we decided to compare the transcriptomic profiles of hCSCs and ITSCs with HSCs in more detail. We therefore examined differential gene expression between the datasets of hCSCs and ITSCs compared to HSCs. A volcano plot demonstrated the significant upregulation of 7154 ($p < 0.05$) genes in hCSCs and ITSCs compared to HSCs while 8975 genes were significantly downregulated ($p < 0.05$) in this comparison (Figure 5A). We further conducted a KEGG pathway analysis. Here, we calculated overrepresented KEGG pathways and plotted the ten most significantly enriched pathways (q < 0.05). Here, the upregulated KEGG pathways

with the highest significance were 'Focal adhesion' ($q \approx 3.5 \times 10^{-7}$) and 'ECM-receptor interaction' ($q \approx 7.4 \times 10^{-6}$) (Figure 5B). Both pathways describe the adherent character of hCSCs and ITSCs either to a cell culture surface or, when grown as spheres, to other cells. Interestingly, the KEGG pathway MAPK was significantly enriched in genes that were upregulated in hCSCs and ITSCs compared to HSCs (Figure 5B). We further performed GO-term enrichment of DEGs in hCSCs and ITSCs in comparison to HSCs. The GO-terms corresponding to biological processes revealed high enrichment in stem cell- and tissue repair-associated terms like 'tissue morphogenesis' ($q \approx 1 \times 10^{-19}$), 'vasculature development' ($q \approx 2.1 \times 10^{-19}$), 'blood vessel development' ($q \approx 2 \times 10^{-18}$) and 'embryonic morphogenesis' ($q \approx 4.5 \times 10^{-16}$) (Figure 5C). In contrast, the GO-terms 'Immune response-regulating cell surface receptor signaling pathway' ($q \approx 9.1 \times 10^{-5}$), 'immune effector process' ($q \approx 1.5 \times 10^{-4}$) and 'regulation of immune response' ($q \approx 1.8 \times 10^{-4}$) were significantly downregulated in hCSCs and ITSCs compared to HSCs (Figure 5D). These data demonstrates that hCSCs and ITSCs share a transcriptional profile that is associated with stem cell properties like tissue morphogenesis, vasculature development and embryonic morphogenesis, while HSCs highly overexpress genes that are related to immune response mechanisms.
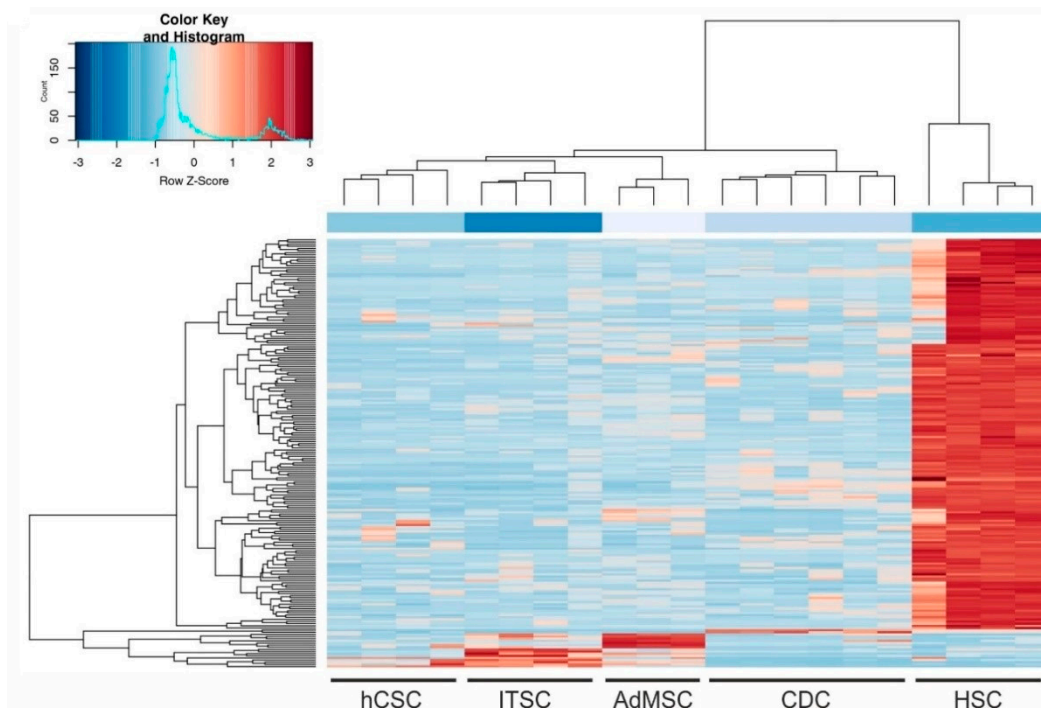

Figure 4. Hierarchically clustered heatmap of the 200 genes with the highest variance among all samples.
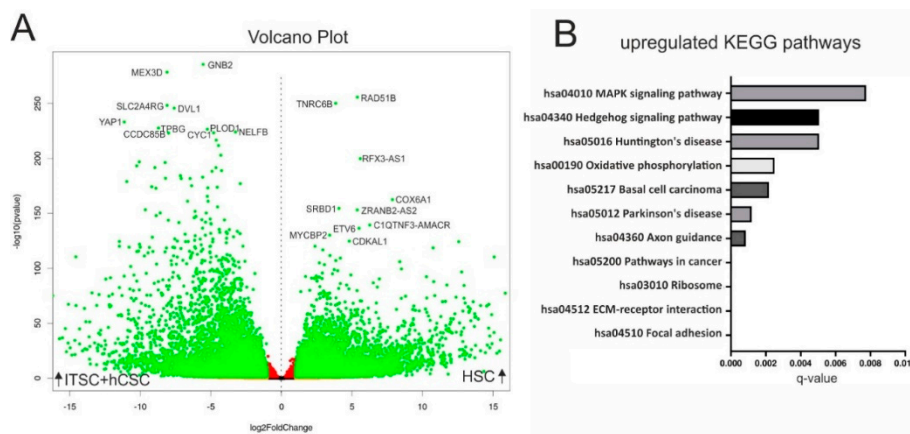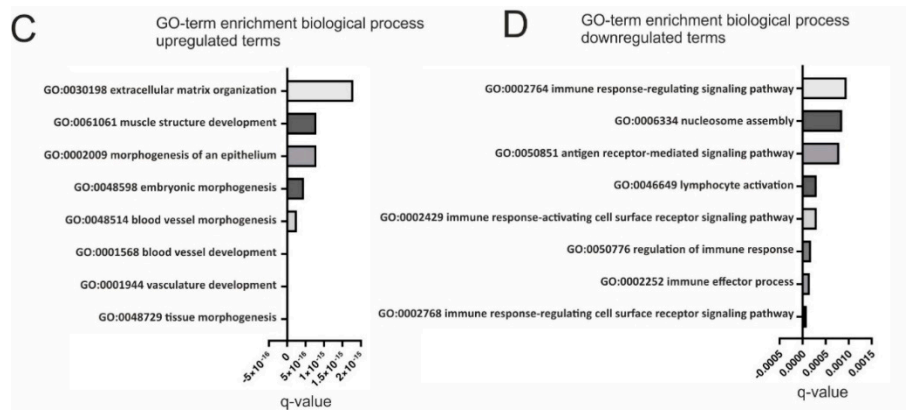

Figure 5. *Cont.*

Figure 5. Comparison of ITSCs and hCSCs with HSCs by differential gene expression analysis. (**A**) Volcano plot shows 16,129 genes to be significantly ($q < 0.05$) differentially expressed (green dots) in hCSCs and ITSCs compared to HSCs. (**B**) Top ten of the most significantly upregulated KEGG pathways in hCSCs and ITSCs ($q < 0.05$). (**C**) Top ten of the most significantly enriched GO-terms in hCSCs and ITSCs ($q < 0.05$). (**D**) Top ten of the most significantly enriched GO-terms in HSCs ($q < 0.05$).

4. Discussion

The present study describes the side-by-side comparison of two different adult human stem cell populations from the left atrial appendage of the heart and from the inferior turbinate of the nose, based on in silico and in vitro data. We detected stem cell marker proteins like Nestin, p75 and S100 in both stem cell populations, while global gene expression data revealed significant differences between the populations reflecting the particular niches of origin.

Most studies investigating cardiac stem cells focus on their potential to differentiate into cardiogenic cell types like cardiomyocytes, endothelial cells and smooth muscle cells [18,19,44,97], mainly with regard to a potential use in regenerative medicine. In general, the description of these cell populations focuses on the expression of cell surface markers like c-kit or Sca1—commonly accepted markers of cardiac stem cells. We very recently isolated a population of Sca1^{+}/cKit[−] cardiac stem cells from the adult human heart (hCSCs), which were able to give rise to α-actinin/Connexin43-positive cardiomyocytes after directed differentiation in vitro [17]. In accordance with our previous findings, hCSCs successfully differentiated into beating cardiomyocytes after exposure to a cardiomyogenic environment in the present study. Next to differentiation into cardiomyocytes, we already observed the presence of the intermediate filament Nestin in distinct spots in heart auricle tissue on protein level [17]. Within this study, we further extended these findings by the detection of Nestin also in cultured hCSCs. In the murine system, Nestin^{+} stem cells can be derived from the adult heart that give rise to neurons [31,35,98], however a neurogenic differentiation potential in human adult cardiac stem cells has not been shown so far. Here, we observed a small proportion of 1% Neurofilament[+]/β-III-Tubulin[+] and 2% Synaptophysin[+]/VGlut^{+} cells with neuron-like shape that were derived from human cardiac stem cells upon application of a defined medium. We likewise detected a shared marker expression profile of undifferentiated hCSCs with ITSCs, a known neural-crest derived adult stem cell population [8]. In addition to Nestin, the neural crest stem cell markers p75, Slug and S100 were also present in both cell populations on protein level.

The neural crest was initially described by Wilhelm His in the development of the chick embryo as the intermediate chord appearing between the neural chord and the future ectoderm [27]. After neurulation, neural crest cells migrate to a broad range of target tissues within the developing organism and give rise to various cell populations—cells of mesodermal and ectodermal type [33]. In addition, neural crest-derived cells also persist as adult stem cell populations within the adult body [8,9,99–101]. Mutations in neural crest-related genes result in severe developmental defects that are often presented in symptoms like malformations of craniofacial tissues, but also cardiac defects. Here, we provide a list of syndromes and diseases that are caused by mutations of neural

crest associated genes which are expressed in ITSCs as well as in hCSCs. Notably, ten of these defects result in craniofacial malformations and also inherited heart defects (Baraitser–Winter syndrome [56], oculodentodigital dysplasia [61,62], Pallister-Hall syndromes (PHS) [65], Alagille syndrome [75], Autosomal dominant form of Adams-Oliver syndrome [73,74], Hajdu Cheney Syndrome [76,77], Hirschsprung's disease [81,82], Loeys–Dietz syndrome [85], Saethre-Chotzen syndrome [92,93], and Kabuki syndrome [94–96]). Although a range of stem cell populations was described to be present in the human heart [6,102,103], a potential relation of these human cardiac stem cell populations to the neural crest has not been described so far. Accordingly, a potential developmental relation of cardiac stem cells to the neural crest has already been suggested in mice and rats [28,29,31,32,104]. In particular, El-Helou and colleagues demonstrated the presence of NCSCs in the adult rat heart via expression of Nestin [31], a characteristic NCSC-marker associated with proper self-renewal of stem cells [33,34], while Tomita and coworkers showed that Nestin+ NCSCs in the mouse heart give rise to cardiomyocytes in vivo [35]. Notably, similar to neural crest-derived stem cell populations residing within the head and neck region [8,9,39,105,106], hCSCs exhibited an extended differentiation capability by giving rise to cardiomyocytes, but also other mesodermal and ectodermal cell types. However, we also observed differences in the differentiation potential of both stem cell populations particularly regarding the extraordinary high differentiation capability of ITSCs into the neuronal lineage (70%) [39–41], which is only minor in hCSCs (1–2%). We suggest these differences to depend on the niches of the stem cell populations, which is in line with the GO-term enrichment analysis of DEGs in hCSCs and ITSCs.

As already postulated by Iancu and colleagues, not only the presence of single cell surface markers but rather an extensive marker profile, consisting of a combination of specific cell surface markers and global gene expression, are required to distinguish distinct cardiac and non-cardiac stem cell populations [107]. In this regard, we performed RNA-Seq to compare global transcriptional profiles of hCSCs with ITSCs. In a previous study, we showed a large difference in global gene expression between ITSCs and human embryonic stem cells using microarrays [8]. Here, RNA-Seq allowed us to detect 4367 genes that were significantly differentially expressed between hCSCs and ITSCs. Although both cell populations formed distinct clusters in a principal component analysis, the most significantly enriched GO-terms only comprised a description of the particular tissues of origin. Interestingly, GO-terms that are linked to certain germ layers of origin are not enriched among the DEGs, leading to the conclusion that hCSCs and ITSCs may share a joint developmental origin. To the best of our knowledge, analyses of RNA-Seq data comparing different stem cell populations from different laboratories are rare. Jansen and colleagues compared different mesenchymal stem cell populations side-by-side in a microarray experiment and could show that the functional status of cell populations can indeed be monitored by the transcriptomic profile [108]. However, the usability of global transcriptome data for identification of a cell population and its functional status also implies the limitation that not every mRNA is translated into a functional protein. Using next-generation sequencing, Taskiran and coworkers compared human bone marrow mesenchymal stem cells and dermal fibroblasts and identified several homeobox genes to be differentially expressed [109]. Paired box (PAX) genes are suggested to contain homeobox genes. We likewise detected the PAX genes PAX3 and PAX9 to be differentially expressed between hCSCs and ITSCs. PAX3 is known as key player in cranial neural crest development and is associated with neural crest-related diseases like Waardenburg syndrome [110], while PAX9 initiates tooth development [15,111–113].

In addition to the side-by-side analysis of hCSCs and ITSCs, we compared here for the first time the global gene expression profiles of five adult human stem cell populations from diverse niches. The principal component analysis provided here demonstrates that hCSCs, ITSCs, AdMSCs and CDCs share much more similarities with each other than with HSCs. Interestingly, adipose-derived MSCs and ITSCs were closer to each other than to hCSCs on the PC2 axis, suggesting the observed variances resulted from biological differences between the different stem cell populations rather than from the use of different library preparation protocols or sequencing platforms. The MSC

population in this study is derived from the adipose tissue while HSCs are isolated from the bone marrow. However, during development, both stem cell populations have their origin in the mesoderm. Remarkably, although HSCs and MSCs share their developmental origin in the mesoderm, their transcriptomic profiles show great differences in our analysis. Likewise, regarding differences between HSCs and MSCs, 16,129 genes were found to be differentially expressed between hCSCs and ITSCs compared to HSCs while a direct comparison of hCSCs and ITSCs revealed only 4367 DEGs. GO-term analysis demonstrated the enrichment of stem cell-associated terms like 'tissue morphogenesis', 'vasculature development', 'blood vessel development' and 'embryonic morphogenesis', while terms like 'immune response-regulating cell surface receptor signaling pathway', 'immune effector process' and 'regulation of immune response' were significantly downregulated in hCSCs and ITSCs compared to HSCs. This may indicate a similar regulation of stem cell-associated transcripts in hCSCs and ITSCs. Furthermore, our data reflect the diverging developmental potentials of HSCs and other more tissue-bound stem cell populations. The upregulation of immune-regulatory pathways and GO-terms is a known characteristic of hematopoietic stem- and progenitor cells and reflects the hematopoietic fate of these cells [114–116]. The terms 'extracellular matrix organization' and 'morphogenesis of an epithelium' upregulated in hCSCs and ITSCs compared to HSCs underline the adherent character of non-HSC populations. This linkage is further emphasized by the upregulation of the terms 'focal adhesion' and 'ECM-receptor interaction' as most significantly upregulated KEGG-pathways in hCSCs and ITSCs. Interestingly, also the term 'MAPK signaling pathway' was among these upregulated KEGG pathways. We already identified p38 MAPK as a crucial pathway mediating proliferation of blood serum-treated hCSCs [17]. The dimensionality of data that can be gained by RNA-Seq of cell populations is very large due to the high number of expressed genes. In our analysis, we detected 16,129 DEGs. This exceeds the number of proteins, which can be analyzed in comparative methods such as 2D gel or LC/MS analysis with 500–5000 proteins per sample [117–119]. However, single cell RNA-Seq (scRNA-Seq) might increase the amount of information that can be gained from such analyses. This would especially be useful for the examination of subtypes within a population [120]. In the context of the present study, we aimed to investigate the differences between distinct stem cell populations and therefore applied bulk RNA-Seq, which is a more robust and cost-effective method. Furthermore, the analysis of RNA is limited since not every expressed mRNA is related to a functional protein. The present study faces this challenge by providing both RNA-Seq data as well as a selection of stem cells markers on the protein level, accompanied by functional differentiation assays. In addition, future studies comparing the proteomes of adult stem cell populations may allow the transfer of our observations on the global transcriptome level to the functional protein level.

5. Conclusions

In summary, we provide a direct comparison of Nestin$^+$/CD105$^+$ adult hCSCs and neural crest-derived ITSCs from the human nasal cavity regarding the presence of molecular marker proteins, their differentiation capacities as well as their global transcriptomes. We show that transcriptional differences between hCSCs and ITSCs depend on their particular niches, which is also reflected on a functional level regarding their differentiation potentials. However, a potential difference in their developmental origins could not be found based on RNA-Seq data, while a broad range of neural crest-associated genes was found to be expressed in both stem cell populations, suggesting the neural crest as a developmental origin of hCSCs. We further extended these findings by the comparison of hCSCs and ITSCs with other known adult stem cell populations, identifying HSCs as a population with less stem cell-associated but more immune regulatory properties. The analyses provided here might help to understand the global transcriptional differences between different adult human stem cells populations, although our observations are limited to the mRNA level.

References

1. Liu, M.; Han, Z.C. Mesenchymal stem cells: Biology and clinical potential in type 1 diabetes therapy. *J. Cell. Mol. Med.* **2008**, *12*, 1155–1168. [CrossRef] [PubMed]

2. Barnabe-Heider, F.; Frisen, J. Stem cells for spinal cord repair. *Cell Stem Cell* **2008**, *3*, 16–24. [CrossRef] [PubMed]

3. Johansson, C.B.; Svensson, M.; Wallstedt, L.; Janson, A.M.; Frisen, J. Neural stem cells in the adult human brain. *Exp. Cell Res.* **1999**, *253*, 733–736. [CrossRef] [PubMed]

4. Pittenger, M.F.; Mackay, A.M.; Beck, S.C.; Jaiswal, R.K.; Douglas, R.; Mosca, J.D.; Moorman, M.A.; Simonetti, D.W.; Craig, S.; Marshak, D.R. Multilineage potential of adult human mesenchymal stem cells. *Science* **1999**, *284*, 143–147. [CrossRef] [PubMed]

5. De Bari, C.; Dell'Accio, F.; Tylzanowski, P.; Luyten, F.P. Multipotent mesenchymal stem cells from adult human synovial membrane. *Arthritis Rheum* **2001**, *44*, 1928–1942. [CrossRef]

6. Barile, L.; Gherghiceanu, M.; Popescu, L.M.; Moccetti, T.; Vassalli, G. Human cardiospheres as a source of multipotent stem and progenitor cells. *Stem Cells Int.* **2013**, *2013*, 916837. [CrossRef] [PubMed]

7. Pagano, S.F.; Impagnatiello, F.; Girelli, M.; Cova, L.; Grioni, E.; Onofri, M.; Cavallaro, M.; Etteri, S.; Vitello, F.; Giombini, S.; et al. Isolation and characterization of neural stem cells from the adult human olfactory bulb. *Stem Cells* **2000**, *18*, 295–300. [CrossRef]

8. Hauser, S.; Widera, D.; Qunneis, F.; Muller, J.; Zander, C.; Greiner, J.; Strauss, C.; Luningschror, P.; Heimann, P.; Schwarze, H.; et al. Isolation of novel multipotent neural crest-derived stem cells from adult human inferior turbinate. *Stem Cells Dev.* **2012**, *21*, 742–756. [CrossRef]

9. Schürmann, M.; Brotzmann, V.; Butow, M.; Greiner, J.; Höving, A.; Kaltschmidt, C.; Kaltschmidt, B.; Sudhoff, H. Identification of a Novel High Yielding Source of Multipotent Adult Human Neural Crest-Derived Stem Cells. *Stem Cell Rev.* **2018**, *14*, 277–285. [CrossRef]

10. Herzog, E.L.; Chai, L.; Krause, D.S. Plasticity of marrow-derived stem cells. *Blood* **2003**, *102*, 3483–3493. [CrossRef]

11. Chan, C.K.F.; Gulati, G.S.; Sinha, R.; Tompkins, J.V.; Lopez, M.; Carter, A.C.; Ransom, R.C.; Reinisch, A.; Wearda, T.; Murphy, M.; et al. Identification of the Human Skeletal Stem Cell. *Cell* **2018**, *175*, 43–56.e21. [CrossRef] [PubMed]

12. Riekstina, U.; Cakstina, I.; Parfejevs, V.; Hoogduijn, M.; Jankovskis, G.; Muiznieks, I.; Muceniece, R.; Ancans, J. Embryonic stem cell marker expression pattern in human mesenchymal stem cells derived from bone marrow, adipose tissue, heart and dermis. *Stem Cell Rev. Rep.* **2009**, *5*, 378–386. [CrossRef] [PubMed]

13. Maleki, M.; Ghanbarvand, F.; Reza Behvarz, M.; Ejtemaei, M.; Ghadirkhomi, E. Comparison of mesenchymal stem cell markers in multiple human adult stem cells. *Int. J. Stem Cells* **2014**, *7*, 118–126. [CrossRef] [PubMed]

14. Avinash, K.; Malaippan, S.; Dooraiswamy, J.N. Methods of Isolation and Characterization of Stem Cells from Different Regions of Oral Cavity Using Markers: A Systematic Review. *Int. J. Stem Cells* **2017**, *10*, 12–20. [CrossRef] [PubMed]

15. Bonczek, O.; Balcar, V.J.; Sery, O. PAX9 gene mutations and tooth agenesis: A review. *Clin. Genet.* **2017**, *92*, 467–476. [CrossRef] [PubMed]

16. Maurer, M.H. Proteomic definitions of mesenchymal stem cells. *Stem Cells Int.* **2011**, *2011*, 704256. [CrossRef] [PubMed]

17. Höving, A.L.; Schmidt, K.E.; Merten, M.; Hamidi, J.; Rott, A.K.; Faust, I.; Greiner, J.F.W.; Gummert, J.; Kaltschmidt, B.; Kaltschmidt, C.; et al. Blood Serum Stimulates p38-Mediated Proliferation and Changes in Global Gene Expression of Adult Human Cardiac Stem Cells. *Cells* **2020**, *9*, 1472. [CrossRef] [PubMed]

18. Beltrami, A.P.; Barlucchi, L.; Torella, D.; Baker, M.; Limana, F.; Chimenti, S.; Kasahara, H.; Rota, M.; Musso, E.; Urbanek, K.; et al. Adult cardiac stem cells are multipotent and support myocardial regeneration. *Cell* **2003**, *114*, 763–776. [CrossRef]

19. Bearzi, C.; Rota, M.; Hosoda, T.; Tillmanns, J.; Nascimbene, A.; De Angelis, A.; Yasuzawa-Amano, S.; Trofimova, I.; Siggins, R.W.; Lecapitaine, N.; et al. Human cardiac stem cells. *Proc. Natl. Acad. Sci. USA* **2007**, *104*, 14068–14073. [CrossRef]

20. Messina, E.; De Angelis, L.; Frati, G.; Morrone, S.; Chimenti, S.; Fiordaliso, F.; Salio, M.; Battaglia, M.; Latronico, M.V.; Coletta, M.; et al. Isolation and expansion of adult cardiac stem cells from human and murine heart. *Circ. Res.* **2004**, *95*, 911–921. [CrossRef]

21. Moretti, A.; Caron, L.; Nakano, A.; Lam, J.T.; Bernshausen, A.; Chen, Y.; Qyang, Y.; Bu, L.; Sasaki, M.; Martin-Puig, S.; et al. Multipotent embryonic isl1+ progenitor cells lead to cardiac, smooth muscle, and endothelial cell diversification. *Cell* **2006**, *127*, 1151–1165. [CrossRef] [PubMed]

22. Valente, M.; Nascimento, D.S.; Cumano, A.; Pinto-do, O.P. Sca-1+ cardiac progenitor cells and heart-making: A critical synopsis. *Stem Cells Dev.* **2014**, *23*, 2263–2273. [CrossRef] [PubMed]

23. Oh, H.; Bradfute, S.B.; Gallardo, T.D.; Nakamura, T.; Gaussin, V.; Mishina, Y.; Pocius, J.; Michael, L.H.; Behringer, R.R.; Garry, D.J.; et al. Cardiac progenitor cells from adult myocardium: Homing, differentiation, and fusion after infarction. *Proc. Natl. Acad. Sci. USA* **2003**, *100*, 12313–12318. [CrossRef] [PubMed]

24. Gittenberger-de Groot, A.C.; Bartelings, M.M.; Deruiter, M.C.; Poelmann, R.E. Basics of cardiac development for the understanding of congenital heart malformations. *Pediatr. Res.* **2005**, *57*, 169–176. [CrossRef]

25. Bartelings, M.M.; Wenink, A.C.; Gittenberger-De Groot, A.C.; Oppenheimer-Dekker, A. Contribution of the aortopulmonary septum to the muscular outlet septum in the human heart. *Acta Morphol. Neerl. Scand.* **1986**, *24*, 181–192.

26. Poelmann, R.E.; Mikawa, T.; Gittenberger-de Groot, A.C. Neural crest cells in outflow tract septation of the embryonic chicken heart: Differentiation and apoptosis. *Dev. Dyn.* **1998**, *212*, 373–384. [CrossRef]

27. His, W. *Untersuchungen Über die Erste Anlage des Wirbeltierleibes. Die Erste Entwicklung des Hühnchens im Ei*; Vogel: Leipzig, Germany, 1868.

28. Hatzistergos, K.E.; Takeuchi, L.M.; Saur, D.; Seidler, B.; Dymecki, S.M.; Mai, J.J.; White, I.A.; Balkan, W.; Kanashiro-Takeuchi, R.M.; Schally, A.V.; et al. cKit+ cardiac progenitors of neural crest origin. *Proc. Natl. Acad. Sci. USA* **2015**, *112*, 13051–13056. [CrossRef]

29. Leinonen, J.V.; Korkus-Emanuelov, A.; Wolf, Y.; Milgrom-Hoffman, M.; Lichtstein, D.; Hoss, S.; Lotan, C.; Tzahor, E.; Jung, S.; Beeri, R. Macrophage precursor cells from the left atrial appendage of the heart spontaneously reprogram into a C-kit+/CD45- stem cell-like phenotype. *Int. J. Cardiol.* **2016**, *209*, 296–306. [CrossRef]

30. Tang, W.; Martik, M.L.; Li, Y.; Bronner, M.E. Cardiac neural crest contributes to cardiomyocytes in amniotes and heart regeneration in zebrafish. *eLife* **2019**, *8*, e47929. [CrossRef]

31. El-Helou, V.; Beguin, P.C.; Assimakopoulos, J.; Clement, R.; Gosselin, H.; Brugada, R.; Aumont, A.; Biernaskie, J.; Villeneuve, L.; Leung, T.K.; et al. The rat heart contains a neural stem cell population; role in sympathetic sprouting and angiogenesis. *J. Mol. Cell. Cardiol.* **2008**, *45*, 694–702. [CrossRef]

32. Meus, M.A.; Hertig, V.; Villeneuve, L.; Jasmin, J.F.; Calderone, A. Nestin Expressed by Pre-Existing Cardiomyocytes Recapitulated in Part an Embryonic Phenotype; Suppressive Role of p38 MAPK. *J. Cell. Physiol.* **2017**, *232*, 1717–1727. [CrossRef] [PubMed]

33. Kaltschmidt, B.; Kaltschmidt, C.; Widera, D. Adult craniofacial stem cells: Sources and relation to the neural crest. *Stem Cell Rev.* **2012**, *8*, 658–671. [CrossRef] [PubMed]

34. Park, D.; Xiang, A.P.; Mao, F.F.; Zhang, L.; Di, C.G.; Liu, X.M.; Shao, Y.; Ma, B.F.; Lee, J.H.; Ha, K.S.; et al. Nestin is required for the proper self-renewal of neural stem cells. *Stem Cells* **2010**, *28*, 2162–2171. [CrossRef] [PubMed]

35. Tomita, Y.; Matsumura, K.; Wakamatsu, Y.; Matsuzaki, Y.; Shibuya, I.; Kawaguchi, H.; Ieda, M.; Kanakubo, S.; Shimazaki, T.; Ogawa, S.; et al. Cardiac neural crest cells contribute to the dormant multipotent stem cell in the mammalian heart. *J. Cell Biol.* **2005**, *170*, 1135–1146. [CrossRef]

36. Pauli, S.; Bajpai, R.; Borchers, A. CHARGEd with neural crest defects. *Am. J. Med. Genet. C Semin. Med. Genet.* **2017**, *175*, 478–486. [CrossRef]

37. Wurdak, H.; Ittner, L.M.; Lang, K.S.; Leveen, P.; Suter, U.; Fischer, J.A.; Karlsson, S.; Born, W.; Sommer, L. Inactivation of TGFbeta signaling in neural crest stem cells leads to multiple defects reminiscent of DiGeorge syndrome. *Genes Dev.* **2005**, *19*, 530–535. [CrossRef]

38. Humphreys, R.; Zheng, W.; Prince, L.S.; Qu, X.; Brown, C.; Loomes, K.; Huppert, S.S.; Baldwin, S.; Goudy, S. Cranial neural crest ablation of Jagged1 recapitulates the craniofacial phenotype of Alagille syndrome patients. *Hum. Mol. Genet.* **2012**, *21*, 1374–1383. [CrossRef]

39. Müller, J.; Ossig, C.; Greiner, J.F.; Hauser, S.; Fauser, M.; Widera, D.; Kaltschmidt, C.; Storch, A.; Kaltschmidt, B. Intrastriatal transplantation of adult human neural crest-derived stem cells improves functional outcome in parkinsonian rats. *Stem Cells Transl. Med.* **2015**, *4*, 31–43. [CrossRef]

40. Ruiz-Perera, L.M.; Greiner, J.F.W.; Kaltschmidt, C.; Kaltschmidt, B. A Matter of Choice: Inhibition of c-Rel Shifts Neuronal to Oligodendroglial Fate in Human Stem Cells. *Cells* **2020**, *9*, 1037. [CrossRef]

41. Ruiz-Perera, L.M.; Schneider, L.; Windmoller, B.A.; Muller, J.; Greiner, J.F.W.; Kaltschmidt, C.; Kaltschmidt, B. NF-kappaB p65 directs sex-specific neuroprotection in human neurons. *Sci. Rep.* **2018**, *8*, 16012. [CrossRef]

42. Greiner, J.F.; Gottschalk, M.; Fokin, N.; Buker, B.; Kaltschmidt, B.P.; Dreyer, A.; Vordemvenne, T.; Kaltschmidt, C.; Hutten, A.; Kaltschmidt, B. Natural and synthetic nanopores directing osteogenic differentiation of human stem cells. *Nanomedicine* **2019**, *17*, 319–328. [CrossRef] [PubMed]

43. Sinnakannu, J.R.; Lee, K.L.; Cheng, S.; Li, J.; Yu, M.; Tan, S.P.; Ong, C.C.H.; Li, H.; Than, H.; Anczukow-Camarda, O.; et al. SRSF1 mediates cytokine-induced impaired imatinib sensitivity in chronic myeloid leukemia. *Leukemia* **2020**, *34*, 1787–1798. [CrossRef] [PubMed]

44. Harvey, E.; Zhang, H.; Sepulveda, P.; Garcia, S.P.; Sweeney, D.; Choudry, F.A.; Castellano, D.; Thomas, G.N.; Kattach, H.; Petersen, R.; et al. Potency of Human Cardiosphere-Derived Cells from Patients with Ischemic Heart Disease Is Associated with Robust Vascular Supportive Ability. *Stem Cells Transl. Med.* **2017**, *6*, 1399–1411. [CrossRef] [PubMed]

45. Greiner, J.F.; Hauser, S.; Widera, D.; Muller, J.; Qunneis, F.; Zander, C.; Martin, I.; Mallah, J.; Schuetzmann, D.; Prante, C.; et al. Efficient animal-serum free 3D cultivation method for adult human neural crest-derived stem cell therapeutics. *Eur. Cells Mater.* **2011**, *22*, 403–419. [CrossRef]

46. Lois, C.; Hong, E.J.; Pease, S.; Brown, E.J.; Baltimore, D. Germline transmission and tissue-specific expression of transgenes delivered by lentiviral vectors. *Science* **2002**, *295*, 868–872. [CrossRef]

47. Sreejit, P.; Kumar, S.; Verma, R.S. An improved protocol for primary culture of cardiomyocyte from neonatal mice. *Vitr. Cell. Dev. Biol. Anim.* **2008**, *44*, 45–50. [CrossRef]

48. Schneider, C.A.; Rasband, W.S.; Eliceiri, K.W. NIH Image to ImageJ: 25 years of image analysis. *Nat. Methods* **2012**, *9*, 671–675. [CrossRef]

49. Bolger, A.M.; Lohse, M.; Usadel, B. Trimmomatic: A flexible trimmer for Illumina sequence data. *Bioinformatics* **2014**, *30*, 2114–2120. [CrossRef]

50. Dobin, A.; Davis, C.A.; Schlesinger, F.; Drenkow, J.; Zaleski, C.; Jha, S.; Batut, P.; Chaisson, M.; Gingeras, T.R. STAR: Ultrafast universal RNA-seq aligner. *Bioinformatics* **2013**, *29*, 15–21. [CrossRef]

51. Liao, Y.; Smyth, G.K.; Shi, W. featureCounts: An efficient general purpose program for assigning sequence reads to genomic features. *Bioinformatics* **2014**, *30*, 923–930. [CrossRef]

52. Love, M.I.; Huber, W.; Anders, S. Moderated estimation of fold change and dispersion for RNA-seq data with DESeq2. *Genome Biol.* **2014**, *15*, 550. [CrossRef] [PubMed]

53. Luo, W.; Friedman, M.S.; Shedden, K.; Hankenson, K.D.; Woolf, P.J. GAGE: Generally applicable gene set enrichment for pathway analysis. *BMC Bioinform.* **2009**, *10*, 161. [CrossRef] [PubMed]

54. Hofemeier, A.D.; Hachmeister, H.; Pilger, C.; Schurmann, M.; Greiner, J.F.; Nolte, L.; Sudhoff, H.; Kaltschmidt, C.; Huser, T.; Kaltschmidt, B. Label-free nonlinear optical microscopy detects early markers for osteogenic differentiation of human stem cells. *Sci. Rep.* **2016**, *6*, 26716. [CrossRef] [PubMed]

55. Thomas, S.; Thomas, M.; Wincker, P.; Babarit, C.; Xu, P.; Speer, M.C.; Munnich, A.; Lyonnet, S.; Vekemans, M.; Etchevers, H.C. Human neural crest cells display molecular and phenotypic hallmarks of stem cells. *Hum. Mol. Genet.* **2008**, *17*, 3411–3425. [CrossRef]

56. Cuvertino, S.; Stuart, H.M.; Chandler, K.E.; Roberts, N.A.; Armstrong, R.; Bernardini, L.; Bhaskar, S.; Callewaert, B.; Clayton-Smith, J.; Davalillo, C.H.; et al. ACTB Loss-of-Function Mutations Result in a Pleiotropic Developmental Disorder. *Am. J. Hum. Genet.* **2017**, *101*, 1021–1033. [CrossRef]

57. Gao, C.; Wang, Y.; Broaddus, R.; Sun, L.; Xue, F.; Zhang, W. Exon 3 mutations of CTNNB1 drive tumorigenesis: A review. *Oncotarget* **2018**, *9*, 5492–5508. [CrossRef]

58. Polakis, P. Wnt signaling and cancer. *Genes Dev.* **2000**, *14*, 1837–1851. [CrossRef]

59. Gordon, C.T.; Petit, F.; Kroisel, P.M.; Jakobsen, L.; Zechi-Ceide, R.M.; Oufadem, M.; Bole-Feysot, C.; Pruvost, S.; Masson, C.; Tores, F.; et al. Mutations in endothelin 1 cause recessive auriculocondylar syndrome and dominant isolated question-mark ears. *Am. J. Hum. Genet.* **2013**, *93*, 1118–1125. [CrossRef]

60. Phesse, T.; Flanagan, D.; Vincan, E. Frizzled7: A Promising Achilles' Heel for Targeting the Wnt Receptor Complex to Treat Cancer. *Cancers* **2016**, *8*, 50. [CrossRef]

61. Debeer, P.; Van Esch, H.; Huysmans, C.; Pijkels, E.; De Smet, L.; Van de Ven, W.; Devriendt, K.; Fryns, J.P. Novel GJA1 mutations in patients with oculo-dento-digital dysplasia (ODDD). *Eur. J. Med. Genet.* **2005**, *48*, 377–387. [CrossRef]

62. Paznekas, W.A.; Boyadjiev, S.A.; Shapiro, R.E.; Daniels, O.; Wollnik, B.; Keegan, C.E.; Innis, J.W.; Dinulos, M.B.; Christian, C.; Hannibal, M.C.; et al. Connexin 43 (GJA1) mutations cause the pleiotropic phenotype of oculodentodigital dysplasia. *Am. J. Hum. Genet.* **2003**, *72*, 408–418. [CrossRef] [PubMed]

63. Matissek, S.J.; Elsawa, S.F. GLI3: A mediator of genetic diseases, development and cancer. *Cell Commun. Signal.* **2020**, *18*, 54. [CrossRef] [PubMed]

64. Duncan, P.A.; Klein, R.M.; Wilmot, P.L.; Shapiro, L.R. Greig cephalopolysyndactyly syndrome. *Am. J. Dis. Child.* **1979**, *133*, 818–821. [CrossRef] [PubMed]

65. Kang, S.; Graham, J.M., Jr.; Olney, A.H.; Biesecker, L.G. GLI3 frameshift mutations cause autosomal dominant Pallister-Hall syndrome. *Nat. Genet.* **1997**, *15*, 266–268. [CrossRef]

66. Liang, J.; Von den Hoff, J.; Lange, J.; Ren, Y.; Bian, Z.; Carels, C.E. MSX1 mutations and associated disease phenotypes: Genotype-phenotype relations. *Eur. J. Hum. Genet.* **2016**, *24*, 1663–1670. [CrossRef]

67. Nieminen, P.; Kotilainen, J.; Aalto, Y.; Knuutila, S.; Pirinen, S.; Thesleff, I. MSX1 gene is deleted in Wolf-Hirschhorn syndrome patients with oligodontia. *J. Dent. Res.* **2003**, *82*, 1013–1017. [CrossRef]

68. Jumlongras, D.; Bei, M.; Stimson, J.M.; Wang, W.F.; DePalma, S.R.; Seidman, C.E.; Felbor, U.; Maas, R.; Seidman, J.G.; Olsen, B.R. A nonsense mutation in MSX1 causes Witkop syndrome. *Am. J. Hum. Genet.* **2001**, *69*, 67–74. [CrossRef]

69. Liu, J.; Ji, X.; Li, Z.; Zheng, H.; Zheng, W.; Jia, J.; Shen, H.; Zhang, Q.; An, J. Nestin overexpression promotes the embryonic development of heart and brain through the regulation of cell proliferation. *Brain Res.* **2015**, *1610*, 1–11. [CrossRef]

70. Gridley, T. Notch signaling and inherited disease syndromes. *Hum. Mol. Genet.* **2003**, *12*, R9–R13. [CrossRef]

71. Krantz, I.D.; Piccoli, D.A.; Spinner, N.B. Alagille syndrome. *J. Med. Genet.* **1997**, *34*, 152–157. [CrossRef]

72. Garg, V.; Muth, A.N.; Ransom, J.F.; Schluterman, M.K.; Barnes, R.; King, I.N.; Grossfeld, P.D.; Srivastava, D. Mutations in NOTCH1 cause aortic valve disease. *Nature* **2005**, *437*, 270–274. [CrossRef] [PubMed]

73. Masek, J.; Andersson, E.R. The developmental biology of genetic Notch disorders. *Development* **2017**, *144*, 1743–1763. [CrossRef] [PubMed]

74. Southgate, L.; Sukalo, M.; Karountzos, A.S.V.; Taylor, E.J.; Collinson, C.S.; Ruddy, D.; Snape, K.M.; Dallapiccola, B.; Tolmie, J.L.; Joss, S.; et al. Haploinsufficiency of the NOTCH1 Receptor as a Cause of Adams-Oliver Syndrome With Variable Cardiac Anomalies. *Circ. Cardiovasc. Genet.* **2015**, *8*, 572–581. [CrossRef] [PubMed]

75. McDaniell, R.; Warthen, D.M.; Sanchez-Lara, P.A.; Pai, A.; Krantz, I.D.; Piccoli, D.A.; Spinner, N.B. NOTCH2 mutations cause Alagille syndrome, a heterogeneous disorder of the notch signaling pathway. *Am. J. Hum. Genet.* **2006**, *79*, 169–173. [CrossRef] [PubMed]

76. Canalis, E.; Zanotti, S. Hajdu-Cheney syndrome: A review. *Orphanet J. Rare Dis.* **2014**, *9*, 200. [CrossRef] [PubMed]

77. Sargin, G.; Cildag, S.; Senturk, T. Hajdu-Cheney syndrome with ventricular septal defect. *Kaohsiung J. Med. Sci.* **2013**, *29*, 343–344. [CrossRef]

78. Kumar, S.; Rao, K. Waardenburg syndrome: A rare genetic disorder, a report of two cases. *Indian J. Hum. Genet.* **2012**, *18*, 254–255. [CrossRef]

79. Lima Cunha, D.; Arno, G.; Corton, M.; Moosajee, M. The Spectrum of PAX6 Mutations and Genotype-Phenotype Correlations in the Eye. *Genes* **2019**, *10*, 1050. [CrossRef]

80. Mian, C.; Sartorato, P.; Barollo, S.; Zane, M.; Opocher, G. RET codon 609 mutations: A contribution for better clinical managing. *Clinics* **2012**, *67* (Suppl. 1), 33–36. [CrossRef]

81. Tuo, G.; Pini Prato, A.; Derchi, M.; Mosconi, M.; Mattioli, G.; Marasini, M. Hirschsprung's Disease and Associated Congenital Heart Defects: A Prospective Observational Study from a Single Institution. *Front. Pediatrics* **2014**, *2*, 99. [CrossRef]

82. Robertson, K.; Mason, I.; Hall, S. Hirschsprung's disease: Genetic mutations in mice and men. *Gut* **1997**, *41*, 436–441. [CrossRef] [PubMed]

83. Xu, J.; Attisano, L. Mutations in the tumor suppressors Smad2 and Smad4 inactivate transforming growth factor beta signaling by targeting Smads to the ubiquitin-proteasome pathway. *Proc. Natl. Acad. Sci. USA* **2000**, *97*, 4820–4825. [CrossRef] [PubMed]

84. Eppert, K.; Scherer, S.W.; Ozcelik, H.; Pirone, R.; Hoodless, P.; Kim, H.; Tsui, L.C.; Bapat, B.; Gallinger, S.; Andrulis, I.L.; et al. MADR2 maps to 18q21 and encodes a TGFbeta-regulated MAD-related protein that is functionally mutated in colorectal carcinoma. *Cell* **1996**, *86*, 543–552. [CrossRef]

85. Schepers, D.; Tortora, G.; Morisaki, H.; MacCarrick, G.; Lindsay, M.; Liang, D.; Mehta, S.G.; Hague, J.; Verhagen, J.; van de Laar, I.; et al. A mutation update on the LDS-associated genes TGFB2/3 and SMAD2/3. *Hum. Mutat.* **2018**, *39*, 621–634. [CrossRef]

86. Zhou, W.; Gross, K.M.; Kuperwasser, C. Molecular regulation of Snai2 in development and disease. *J. Cell Sci* **2019**, *132*, jcs235127. [CrossRef]

87. Shih, J.Y.; Yang, P.C. The EMT regulator slug and lung carcinogenesis. *Carcinogenesis* **2011**, *32*, 1299–1304. [CrossRef]

88. de Herreros, A.G.; Peiro, S.; Nassour, M.; Savagner, P. Snail family regulation and epithelial mesenchymal transitions in breast cancer progression. *J. Mammary Gland. Biol. Neoplasia* **2010**, *15*, 135–147. [CrossRef]

89. De Craene, B.; Berx, G. Regulatory networks defining EMT during cancer initiation and progression. *Nat. Rev. Cancer* **2013**, *13*, 97–110. [CrossRef]

90. Wang, Y.; Shi, J.; Chai, K.; Ying, X.; Zhou, B.P. The Role of Snail in EMT and Tumorigenesis. *Curr. Cancer Drug Targets* **2013**, *13*, 963–972. [CrossRef]

91. Kurrey, N.K.; Jalgaonkar, S.P.; Joglekar, A.V.; Ghanate, A.D.; Chaskar, P.D.; Doiphode, R.Y.; Bapat, S.A. Snail and slug mediate radioresistance and chemoresistance by antagonizing p53-mediated apoptosis and acquiring a stem-like phenotype in ovarian cancer cells. *Stem Cells* **2009**, *27*, 2059–2068. [CrossRef]

92. Kress, W.; Schropp, C.; Lieb, G.; Petersen, B.; Busse-Ratzka, M.; Kunz, J.; Reinhart, E.; Schafer, W.D.; Sold, J.; Hoppe, F.; et al. Saethre-Chotzen syndrome caused by TWIST 1 gene mutations: Functional differentiation from Muenke coronal synostosis syndrome. *Eur. J. Hum. Genet.* **2006**, *14*, 39–48. [CrossRef] [PubMed]

93. Pelc, A.; Mikulewicz, M. Saethre-Chotzen syndrome: Case report and literature review. *Dent. Med. Probl.* **2018**, *55*, 217–225. [CrossRef] [PubMed]

94. Adam, M.P.; Banka, S.; Bjornsson, H.T.; Bodamer, O.; Chudley, A.E.; Harris, J.; Kawame, H.; Lanpher, B.C.; Lindsley, A.W.; Merla, G.; et al. Kabuki syndrome: International consensus diagnostic criteria. *J. Med. Genet.* **2019**, *56*, 89–95. [CrossRef] [PubMed]

95. Digilio, M.C.; Gnazzo, M.; Lepri, F.; Dentici, M.L.; Pisaneschi, E.; Baban, A.; Passarelli, C.; Capolino, R.; Angioni, A.; Novelli, A.; et al. Congenital heart defects in molecularly proven Kabuki syndrome patients. *Am. J. Med. Genet. A* **2017**, *173*, 2912–2922. [CrossRef]

96. Shpargel, K.B.; Mangini, C.L.; Xie, G.; Ge, K.; Magnuson, T. The KMT2D Kabuki syndrome histone methylase controls neural crest cell differentiation and facial morphology. *Development* **2020**, *147*, dev187997. [CrossRef]

97. Torella, D.; Ellison, G.M.; Mendez-Ferrer, S.; Ibanez, B.; Nadal-Ginard, B. Resident human cardiac stem cells: Role in cardiac cellular homeostasis and potential for myocardial regeneration. *Nat. Clin. Pr. Cardiovasc Med.* **2006**, *3* (Suppl. 1), S8–S13. [CrossRef]

98. El-Helou, V.; Dupuis, J.; Proulx, C.; Drapeau, J.; Clement, R.; Gosselin, H.; Villeneuve, L.; Manganas, L.; Calderone, A. Resident nestin+ neural-like cells and fibers are detected in normal and damaged rat myocardium. *Hypertension* **2005**, *46*, 1219–1225. [CrossRef]

99. Widera, D.; Grimm, W.D.; Moebius, J.M.; Mikenberg, I.; Piechaczek, C.; Gassmann, G.; Wolff, N.A.; Thevenod, F.; Kaltschmidt, C.; Kaltschmidt, B. Highly efficient neural differentiation of human somatic stem cells, isolated by minimally invasive periodontal surgery. *Stem Cells Dev.* **2007**, *16*, 447–460. [CrossRef]

100. Sieber-Blum, M.; Grim, M. The adult hair follicle: Cradle for pluripotent neural crest stem cells. *Birth Defects Res. Part. CEmbryo Today Rev.* **2004**, *72*, 162–172. [CrossRef]

101. Toma, J.G.; Akhavan, M.; Fernandes, K.J.; Barnabe-Heider, F.; Sadikot, A.; Kaplan, D.R.; Miller, F.D. Isolation of multipotent adult stem cells from the dermis of mammalian skin. *Nat. Cell Biol.* **2001**, *3*, 778–784. [CrossRef]

102. Smits, A.M.; van Vliet, P.; Metz, C.H.; Korfage, T.; Sluijter, J.P.; Doevendans, P.A.; Goumans, M.J. Human cardiomyocyte progenitor cells differentiate into functional mature cardiomyocytes: An in vitro model for studying human cardiac physiology and pathophysiology. *Nat. Protoc.* **2009**, *4*, 232–243. [CrossRef] [PubMed]

103. Koninckx, R.; Daniels, A.; Windmolders, S.; Mees, U.; Macianskiene, R.; Mubagwa, K.; Steels, P.; Jamaer, L.; Dubois, J.; Robic, B.; et al. The cardiac atrial appendage stem cell: A new and promising candidate for myocardial repair. *Cardiovasc. Res.* **2013**, *97*, 413–423. [CrossRef] [PubMed]

104. Engleka, K.A.; Manderfield, L.J.; Brust, R.D.; Li, L.; Cohen, A.; Dymecki, S.M.; Epstein, J.A. Islet1 derivatives in the heart are of both neural crest and second heart field origin. *Circ. Res.* **2012**, *110*, 922–926. [CrossRef] [PubMed]

105. Clewes, O.; Narytnyk, A.; Gillinder, K.R.; Loughney, A.D.; Murdoch, A.P.; Sieber-Blum, M. Human epidermal neural crest stem cells (hEPI-NCSC)–characterization and directed differentiation into osteocytes and melanocytes. *Stem Cell Rev.* **2011**, *7*, 799–814. [CrossRef] [PubMed]

106. Dupin, E.; Sommer, L. Neural crest progenitors and stem cells: From early development to adulthood. *Dev. Biol.* **2012**, *366*, 83–95. [CrossRef]

107. Iancu, C.B.; Iancu, D.; Rentea, I.; Hostiuc, S.; Dermengiu, D.; Rusu, M.C. Molecular signatures of cardiac stem cells. *Rom. J. Morphol. Embryol.* **2015**, *56*, 1255–1262.

108. Jansen, B.J.; Gilissen, C.; Roelofs, H.; Schaap-Oziemlak, A.; Veltman, J.A.; Raymakers, R.A.; Jansen, J.H.; Kogler, G.; Figdor, C.G.; Torensma, R.; et al. Functional differences between mesenchymal stem cell populations are reflected by their transcriptome. *Stem Cells Dev.* **2010**, *19*, 481–490. [CrossRef]

109. Taskiran, E.Z.; Karaosmanoglu, B. Transcriptome analysis reveals differentially expressed genes between human primary bone marrow mesenchymal stem cells and human primary dermal fibroblasts. *Turk. J. Biol* **2019**, *43*, 21–27. [CrossRef]

110. Greiner, J.F.W.; Merten, M.; Kaltschmidt, C.; Kaltschmidt, B. Sexual dimorphisms in adult human neural, mesoderm-derived, and neural crest-derived stem cells. *Febs Lett.* **2019**, *593*, 3338–3352. [CrossRef]

111. Wong, S.W.; Han, D.; Zhang, H.; Liu, Y.; Zhang, X.; Miao, M.Z.; Wang, Y.; Zhao, N.; Zeng, L.; Bai, B.; et al. Nine Novel PAX9 Mutations and a Distinct Tooth Agenesis Genotype-Phenotype. *J. Dent. Res.* **2018**, *97*, 155–162. [CrossRef]

112. Tremblay, P.; Kessel, M.; Gruss, P. A transgenic neuroanatomical marker identifies cranial neural crest deficiencies associated with the Pax3 mutant Splotch. *Dev. Biol.* **1995**, *171*, 317–329. [CrossRef] [PubMed]

113. Boudjadi, S.; Chatterjee, B.; Sun, W.; Vemu, P.; Barr, F.G. The expression and function of PAX3 in development and disease. *Gene* **2018**, *666*, 145–157. [CrossRef] [PubMed]

114. Terskikh, A.V.; Miyamoto, T.; Chang, C.; Diatchenko, L.; Weissman, I.L. Gene expression analysis of purified hematopoietic stem cells and committed progenitors. *Blood* **2003**, *102*, 94–101. [CrossRef] [PubMed]

115. Solaimani Kartalaei, P.; Yamada-Inagawa, T.; Vink, C.S.; de Pater, E.; van der Linden, R.; Marks-Bluth, J.; van der Sloot, A.; van den Hout, M.; Yokomizo, T.; van Schaick-Solerno, M.L.; et al. Whole-transcriptome analysis of endothelial to hematopoietic stem cell transition reveals a requirement for Gpr56 in HSC generation. *J. Exp. Med.* **2015**, *212*, 93–106. [CrossRef] [PubMed]

116. Li, P.; Wu, M.; Lin, Q.; Wang, S.; Chen, T.; Jiang, H. Key genes and integrated modules in hematopoietic differentiation of human embryonic stem cells: A comprehensive bioinformatic analysis. *Stem Cell Res.* **2018**, *9*, 301. [CrossRef] [PubMed]

117. Zhang, Z. Retention time alignment of LC/MS data by a divide-and-conquer algorithm. *J. Am. Soc. Mass Spectrom.* **2012**, *23*, 764–772. [CrossRef] [PubMed]

118. Tautenhahn, R.; Bottcher, C.; Neumann, S. Highly sensitive feature detection for high resolution LC/MS. *BMC Bioinform.* **2008**, *9*, 504. [CrossRef] [PubMed]

119. Roche, S.; Delorme, B.; Oostendorp, R.A.; Barbet, R.; Caton, D.; Noel, D.; Boumediene, K.; Papadaki, H.A.; Cousin, B.; Crozet, C.; et al. Comparative proteomic analysis of human mesenchymal and embryonic stem cells: Towards the definition of a mesenchymal stem cell proteomic signature. *Proteomics* **2009**, *9*, 223–232. [CrossRef] [PubMed]

120. Chen, G.; Ning, B.; Shi, T. Single-Cell RNA-Seq Technologies and Related Computational Data Analysis. *Front. Genet.* **2019**, *10*, 317. [CrossRef] [PubMed]

Publisher's Note: MDPI stays neutral with regard to jurisdictional claims in published maps and institutional affiliations.

Original Research Report *under review*

Human blood serum induces p38-MAPK-dependent migration dynamics of adult human cardiac stem cells – Single-cell analysis via a microfluidic-based cultivation platform

Anna L. Höving*, Julian Schmitz*, Kazuko Schmidt, Johannes Greiner, Cornelius Knabbe, Barbara Kaltschmidt, Alexander Grünberger, Christian Kaltschmidt

Human blood serum induces p38-MAPK-dependent migration dynamics of adult human cardiac stem cells – Single-cell analysis via a microfluidic-based cultivation platform

Anna L. Höving [1,2] # *, **Julian Schmitz** [3] #, **Kazuko Schmidt** [1,2], **Johannes Greiner** [1], **Cornelius Knabbe** [2], **Barbara Kaltschmidt** [1,4], **Alexander Grünberger** [3], **Christian Kaltschmidt** [1]

[1] Department of Cell Biology, Faculty of Biology, Bielefeld University, 33615 Bielefeld, Germany
[2] Heart and Diabetes Centre NRW, Institute for Laboratory and Transfusion Medicine, Ruhr-University Bochum, 32545 Bad Oeynhausen, Germany
[3] Multiscale Bioengineering, Faculty of Technology, Bielefeld University, 33615 Bielefeld, Germany
[4] Molecular Neurobiology, Faculty of Biology, Bielefeld University, 33615 Bielefeld, Germany
* Correspondence: anna.hoeving@uni-bielefeld.de
# These authors contributed equally to this manuscript

Simple Summary: Adult human stem cells possess the ability to contribute to endogenous regeneration processes of injured tissue by migration to the specific locations. For stem cell-based clinical applications it is highly important to gain knowledge about the migration behavior of adult human stem cells and the underlying molecular mechanisms of this ability. Human blood serum has already shown to have beneficial effects on other regenerative capacities of adult human stem cells. Within this study we tested the effect of human blood serum on the migration behavior of stem cells from the human heart. We used a microfluidic cultivation device, which allowed us to monitor the living cells and their movement behavior in real time. After addition of human blood serum, the heart stem cells increased their speed of movement and covered distance. Further, we observed that this effect can be diminished by inhibition of a specific kinase p38-MAPK. Thus, our data suggest beneficial effects of human blood serum on adult human heart stem cells in dependence on p38-MAPK. Our study contributes to a deeper understanding of the dynamics of stem cell migration and introduces a new system to monitor stem cell movement in real time.

Abstract: Migratory capabilities of adult human stem cells are vital for assuring endogenous tissue regeneration and stem cell-based clinical applications. Although human blood serum was already shown to be beneficial for cell migration and proliferation, little is known about its impact on the migratory behavior of cardiac stem cells and underlying signaling pathways. Within this study, we investigated the effects of human blood serum on primary human cardiac stem cells (hCSCs) from the adult heart auricle. On technical level, we took advantage of a microfluidic cultivation platform, which allowed us to characterize cell morphologies and track migration of single hCSCs via live cell imaging over a period of up to 48 h. Our findings show a significantly increased migration distance and speed of hCSCs after treatment with human serum compared to control. Exposure of blood serum-stimulated hCSCs to the p38 mitogen-activated protein kinase (p38-MAPK)-inhibitor SB239063 resulted in significantly decreased migration.
In summary, we demonstrate human blood serum as a strong inducer of adult human cardiac stem cell migration in dependence on p38-MAPK-signalling. Our findings further emphasize the great potential of microfluidic cultivation devices for assessing spatio-temporal migration dynamics of adult human stem cells on single cell level.

Keywords: cardiac stem cells; single-cell analysis; p38-MAPK; cell morphology; stem cell migration; microfluidics; human blood serum.

1. Introduction

Adult human stem cells (ASCs) can be found in various tissues of the human body where they remain as quiescent cells in their respective niches and -upon activation- contribute to tissue renewal and regeneration [1]. To reach the exact locations of damaged tissue, ASCs often exhibit a migratory behavior, referred to as homing [2]. The underlying mechanisms of this process are well described: migration requires a deformation of the cell shape, which is achieved by reorganization of the actin cytoskeleton. Here, a highly orchestrated cascade of actin polymerization drives the formation of protrusions and the adhesion to a substrate or extracellular matrix (ECM) at the leading zone of cell movement [3].

In recent years, various stimuli have been identified that induce or inhibit migratory behavior in diverse cell populations. Next to mechanical factors like sheer stress, matrix stiffness or mechanical strain [4-7], a range of chemokines, cytokines and growth factors is involved in the regulation of stem cell migration behavior [8].

The application of human blood plasma and serum is a therapeutic approach chosen in cases of impaired wound healing [9], coagulopathy [10], and liver cirrhosis [11]. Moreover, the use of convalescent plasma is currently under discussion as treatment option in the COVID-19 pandemic [12,13]. *In vitro* cultivation of adult human stem cells with human blood plasma or serum has demonstrated increased proliferation and viability [14-17]. Mishima and coworkers have shown increased migration of human articular chondrocytes and MSCs in response to 5 %, 10 % and 20 % fetal bovine serum (FBS) [18]. Human keratinocytes were demonstrated to respond to human serum treatment with increased migration in dependence on activation of p38 mitogen-activated protein kinase (p38-MAPK) [19]. In contrast, human serum inhibited the migration of human fetal skin fibroblasts and fetal lung fibroblasts [20,21]. These data demonstrate that the effect of human serum on cell migration strongly depends on the cell type. In this context, the influence of human blood serum on the migration behavior of adult human stem cells is only poorly described. In the present study, we assessed potential effects of blood serum on migration of adult human cardiac stem cells.

Adult human cardiac stem cells (hCSCs) were first described in 2007 as multipotent population residing from the adult human myocardium [22]. However, their *in vivo* contribution to cardiac regeneration remains unclear and is highly discussed [23]. Therefore, investigations that describe the migratory behavior of adult human cardiac stem cells could be an important contribution to the current knowledge of cardiac stem cell behavior. Very recently, we identified a human cardiac stem cell population that is derived from the left atrial appendage of the adult heart [14,24]. These cells express common cardiac stem cell markers like Sca1 but also markers that are associated to the neural crest. Likewise, their differentiation potential extends the cardiogenic lineage to a differentiation capacity into the adipogenic, neurogenic and osteogenic derivates. We therefore concluded these cells to be a novel neural crest-derived cell population isolated from the adult heart. Best to our knowledge, little is known about homing and migration of adult cardiac stem cells. However, we already could show that human blood plasma and serum have beneficial effects on hCSC viability in terms of inducing cell proliferation and protection from senescence. Moreover, we showed p38-MAPK pathway to be highly important in this process [14]. The p38-MAPK pathway has been described as an important player in the regulation of migration in various cell types [25-29]. Recently, Dubon and colleagues showed that p38-MAPK mediated the migrative response of murine MSC-like ST2-cells to TGF- β1 [25]. P38-MAPK was also shown to be crucial for human umbilical cord blood-

derived MSC migration [26]. Within this study, we aimed to investigate the effects of human blood serum on hCSC migration and a potential role of p38-MAPK within this process.

On technical level, experiments assessing cell migration are mainly carried out to date as scratch wound assays or compartmentalization of the cultivation wells with transwell inserts [8]. These assays are often limited to an end-point determination of entire populations concerning migration distance or direction and do not allow any insights into single-cell behavior. Further, standard cell culture dishes or flasks only operate in batch-mode, thus cells experience changing environmental conditions during the experiment. Facing this challenge, a range of microfluidic approaches has been developed [30-32]. In comparison to classic assays, microfluidic concepts feature several benefits for cultivating and analyzing stem cell migration. Most prominent in the field of microfluidics is the utilization of polydimethylsiloxane (PDMS)-based devices, which facilitate the application of microscopic live cell imaging because of their optical transparency and ease of use [33,34]. When compartmented, single-cell growth and motility is restricted to selected positions on the microfluidic device so that time-lapse microscopy results in a high spatio-temporal resolution of cellular behavior [35]. Decreasing the experimental scale from milliliter to nanoliter furthermore reduces the needed volume of a sample and the reagent consumption, making microfluidic approaches especially beneficial in case of expensive reagents or rare samples like patient cells [36]. Since most microfluidic devices are operated in perfusion-mode, they come with a high level of environmental control resulting in constant cultivation conditions or even allow dynamic changes between different conditions [37]. Based on their design, most devices enable a vast degree of parallelization and thus a high experimental throughput [38]. Different approaches aiming at scaling down conventional scratch or compartmentalization assays to microscale by either inserting a wound into a pre-grown monolayer or sparing distinct areas from being confluently overgrown can be found in literature [39,40]. Additionally, microfluidic setups with defined experimental compartments e.g., growth chambers or migration channels, where -contrary to monolayers- single cells are applied to study cellular migration, have been reported. However, spatio-temporal tracking of single cells was limited to experimental periods below 12 h [7,41-43].

Within this study, single-cell behavior of primary adult human cardiac stem cells (hCSCs) inside a previously introduced microfluidic cultivation device [44] was tracked and analyzed for up to 120 h under controlled environmental conditions. We here provide an overview of different cell morphologies during migration, cell division or cell death. We further traced the migration distance and speed of hCSCs in dependence on human blood serum for up to 48 h. After application of human blood serum, the distance as well as the migration speed of hCSCs was significantly increased compared to untreated cells. Moreover, we demonstrated a p38-dependent activation of migratory behavior upon serum treatment. The here presented method offers the possibility to directly track the response of primary adult human stem cells in terms of their spatio-temporal migration dynamics and morphology upon treatment with different stimuli.

2. Materials and Methods

2.1. Isolation and cultivation of human cardiac stem cells

Adult human cardiac stem cells (hCSCs) were derived from left atrial appendages that were isolated during routine heart surgery according to local and international guidelines (declaration of Helsinki) after informed and written consent. Isolation and further experimental procedures were ethically approved by the ethics commission of the Ruhr-University Bochum (Faculty of Medicine, located in Bad Oeynhausen) (approval reference number eP-2016-148). Isolation and cultivation of hCSCs was carried out as described before [14,24]. After precultivation and expansion of hCSCs in a T25 cell culture flask (Sarstedt AG and Co., Nürmbrecht, Germany), cells were detached using Trypsin-EDTA (Sigma Aldrich, St.-Louis, MO, USA) and a suspension of approx. 10^6 cells/mL was prepared for loading onto a microfluidic cultivation device. After successful seeding of hCSCs in the cultivation chambers, cells were allowed to attach to the surface for 24 h in hCSC-medium containing DMEM/F12 (Sigma Aldrich) supplemented with 10 % fetal calf serum (VWR, Radnor, PA, USA), 10 mg/mL penicillin/streptomycin (Sigma Aldrich), 200 mM L-glutamine (Sigma-Aldrich), 5 ng/mL basic fibroblast growth factor (bFGF) (Peprotech, Hamburg, Germany) and 10 ng/mL epidermal growth factor (EGF) (Peprotech) (Fig. 1). In the starvation period, the medium was switched to starvation-medium consisting of DMEM/F12 (Sigma Aldrich) supplemented with 10 mg/mL penicillin/streptomycin (Sigma Aldrich), 200 mM L-glutamine (Sigma-Aldrich), 5 ng/mL basic fibroblast growth factor (bFGF) (Peprotech, Hamburg, Germany) and 10 ng/mL epidermal growth factor (EGF) (Peprotech) for 24 h. In the treatment phase, starvation medium was supplemented with either 10 % human blood serum or 10 % human serum and 50 µM p38-MAPK-inhibitor SB239063 (Medchemexpress, Sollentuna, Sweden) in accordance to our previous study [14]. Blood plasma was collected from routine blood donation service from healthy individual donors. For the isolation of serum from fresh frozen plasma (FFP), 20% $CaCl_2$ was added in a ratio of 1:50 and incubated at 4 °C overnight. After centrifugation at 1920 RCF for 20 min, blood serum was harvested from the supernatant.

Figure 1: Consecutive cultivation conditions of hCSCs in the microfluidic cultivation device.

2.2. Microfluidics

The applied microfluidic PDMS-glass cultivation device was fabricated in a multiple-step procedure as described before [44]. Using photolithographic techniques, a silicon wafer was fabricated in clean room facilities. In a following soft lithography step, PDMS base and curing agent (SYLGARD 184 Silicone Elastomer, Dow Corning Corporation, USA) were mixed in a 10:1 ratio and PDMS chips were molded from the wafer. After an intermediate cleaning step, the PDMS chip and a glass substrate were surface-activated via oxygen plasma and covalently bonded to each other. Microfluidic cultivation of single hCSC cells was performed on an automated inverted microscope (Nikon Eclipse Ti2, Nikon Instruments, Germany) for multiple days. To assure steady cultivation conditions a microscope incubator system (Cage incubator, OKO Touch, Okolab S.R.L., Italy) and additional CO_2 incubation chamber (H201-K-FRAME GS35-M, Okolab S.R.L.) were applied, guaranteeing a constant cultivation temperature of 37 °C and an atmosphere of 5 % CO_2. Time-lapse images of relevant positions were taken periodically to monitor cellular morphology and migration behavior via phase-contrast microscopy, applying a 40x objective (NIS Elements AR 5.20.01 Software, Nikon Instruments).

By manually flushing the microfluidic cultivation device with cell suspension, hCSCs were seeded into the respective cultivation chambers until loading was sufficient. Subsequently, single-use syringes containing cultivation medium were connected via PTFE tubing to the microfluidic chip and medium supply with a constant flow rate of 2 μL/min was established by the use of low-pressure syringe pumps (neMESYS, CETONI, Germany).

2.3. Data analysis

Following up microfluidic single-cell cultivation, microscope images were exported as 8-bit TIFF images and processed with ImageJ/Fiji software to create videos [45]. The manual tracking plugin was used to visualize the migration paths of the cells and the corresponding data were statistically analyzed with Prism software (GraphPad Software, San Diego, CA, USA).

3. Results

3.1. Successful cultivation of human cardiac stem cells in a microfluidic cultivation device

To access the ability of hCSCs to survive and proliferate in a microfluidic cultivation device, the already established MaSC platform [44] was adapted to the cultivation and analysis of single adult cardiac stem cells.

The applied device consists of four parallel-arranged independent cultivation arrays (Fig. 2A) which simultaneously enable four different experiments. For seeding hCSCs into the device, we prepared a solution of approx. 10^6 cells/mL in hCSC-medium. Cell suspension was flushed into each array through the outlet by means of a 1 mL single-use syringe and cells were seeded into the respective cultivation chambers by manually moving the solution back and forth through the adjacent supply channels (Fig. 2B). Since there is no flow inside the chambers, single cells entered the chambers randomly. Following successful loading, pumping periphery was connected to the devices' inlets and the flow-through was collected in a waste tube, which then was connected to the arrays' outlets. Due to a constant perfusion of the microfluidic device with a flow rate of 2 μL/min, seeded cells were continuously supplied with fresh hCSC-medium guaranteeing consistent cultivation conditions. Mass transport inside the chambers with a dimension of 200 x 200 μm (200 x 350 μm) and a height of 8 μm is almost exclusively diffusive. Flow inside the chamber is additionally restricted by the difference in height between the cultivation chambers and the supply channel (Fig. 2C). Therefore, hCSC cells were not exposed to any shear stress inside the cultivation chambers. Positions of cell containing chambers were marked in the software and the microscope was programmed to record images of each position in a pre-set interval (Fig. 2 D). Here, we detected a high number of cells attached to the PDMS-surface, which were migrating and proliferating (Fig. 2 E) (supplemental video S1).
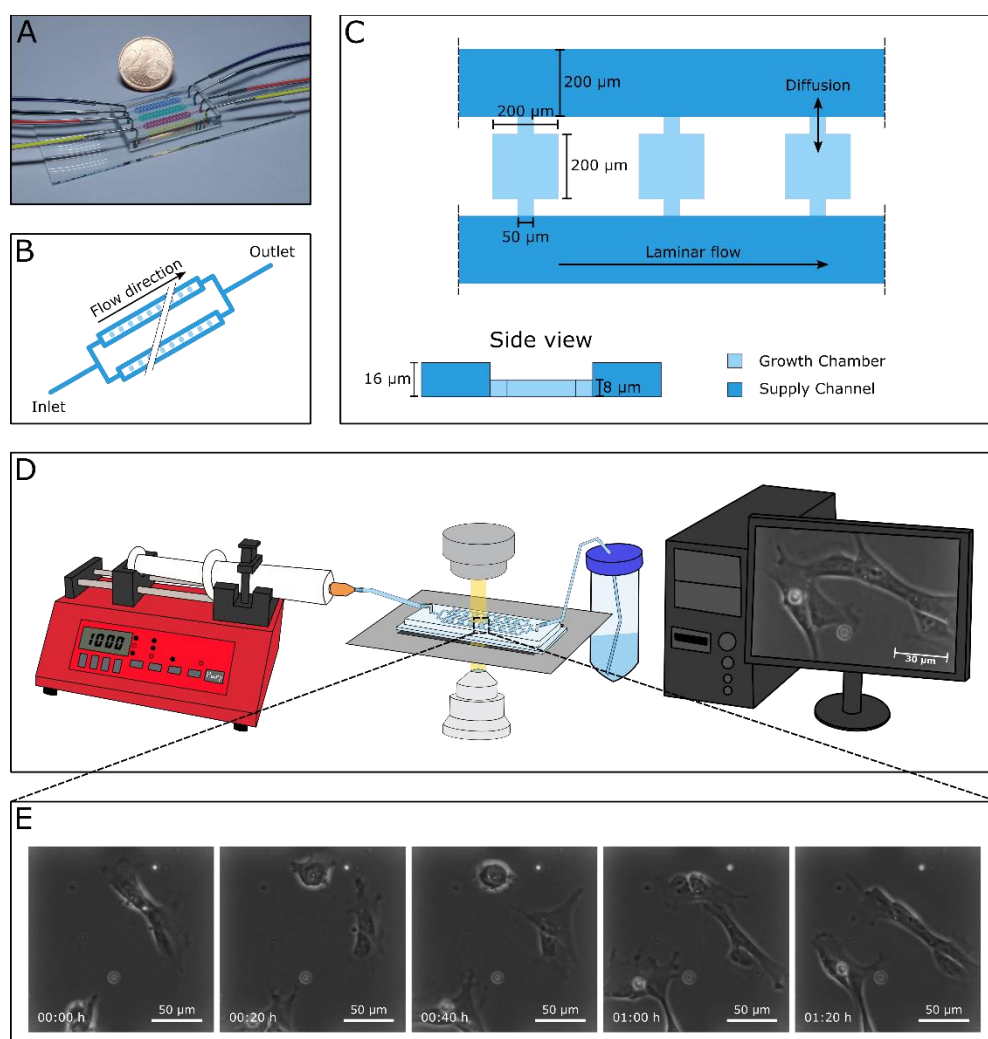
223

Figure 2: Chip design and working principle of the experimental setting. A) Microfluidic cultiva-
tion device consisting of four cultivation arrays for the analysis of hCSC cells. B) Schematic figure
of one cultivation array. Each array includes four parallel supply channels with 30 cultivation
chambers between two of them, resulting in a total number of 60 chambers per array. C) Three
exemplary cultivation chambers with an area of 200 x 200 μm and a height of 8 μm. The adjacent
supply channels with a width of 200 μm are twice as high. Mass transport from supply channel
into the cultivation chambers is almost exclusively diffusive. D) Experimental setup showing the
syringe pump for steady medium supply, the microfluidic cultivation device mounted onto an
inverted microscope, and the computer-assisted automated live cell imaging. E) Time-lapse image
sequence illustrating cellular behavior of single hCSC cells.

3.2. Migrating hCSCs exhibit diverse morphologies and migration patterns

During cultivation in the microfluidic device and accompanying image acquisition
of single cells, we were able to observe various morphologies and migration behavior such
as a mesenchymal-like shape (Fig. 3 A) or ameboid-like migration along the walls of the
cultivation chambers (Fig. 3 B). Further, some migrating cells also exhibited a flattened
morphology with pseudopodia or lamellipodia in the leading zone (Fig. 3 C). These dif-
ferent morphologies were presented alternately by the same individual cells, making the
underlying mechanisms and signaling pathways highly interesting for future studies. We
further detected temporary cell-cell-contacts between neighboring cells by the formation
of stretches reaching out to the other cells and the subsequent withdraw of these stretches
(Fig. 3 D) (supplemental video S2). Especially in the attachment phase and for cells ex-
posed to serum in the treatment phase, we could detect events of cytokinesis where a cell
first exhibited a sphere-like morphology followed by the formation of a cleavage furrow

and the stretching of the two daughter cells to a flattened shape with leading zone lamel- 247
lipodia migrating away from each other (Fig. 3 E) (supplemental video S3). Events of cell 248
death were visible in each treatment group but especially in the group of cells treated with 249
serum-free medium. Dying cells formed a rounded shape with disheveled margins result- 250
ing in lysis or release of the cytoplasm (Fig. 3 F) (supplemental video S4). Although we 251
could not analyze these morphologies and events in a quantitative manner, we here sum- 252
marize exemplary images and schemes of these different events and morphologies to pre- 253
sent for the first time an overview of the different morphologies of adult human cardiac 254
stem cells during *in vitro* cultivation. 255
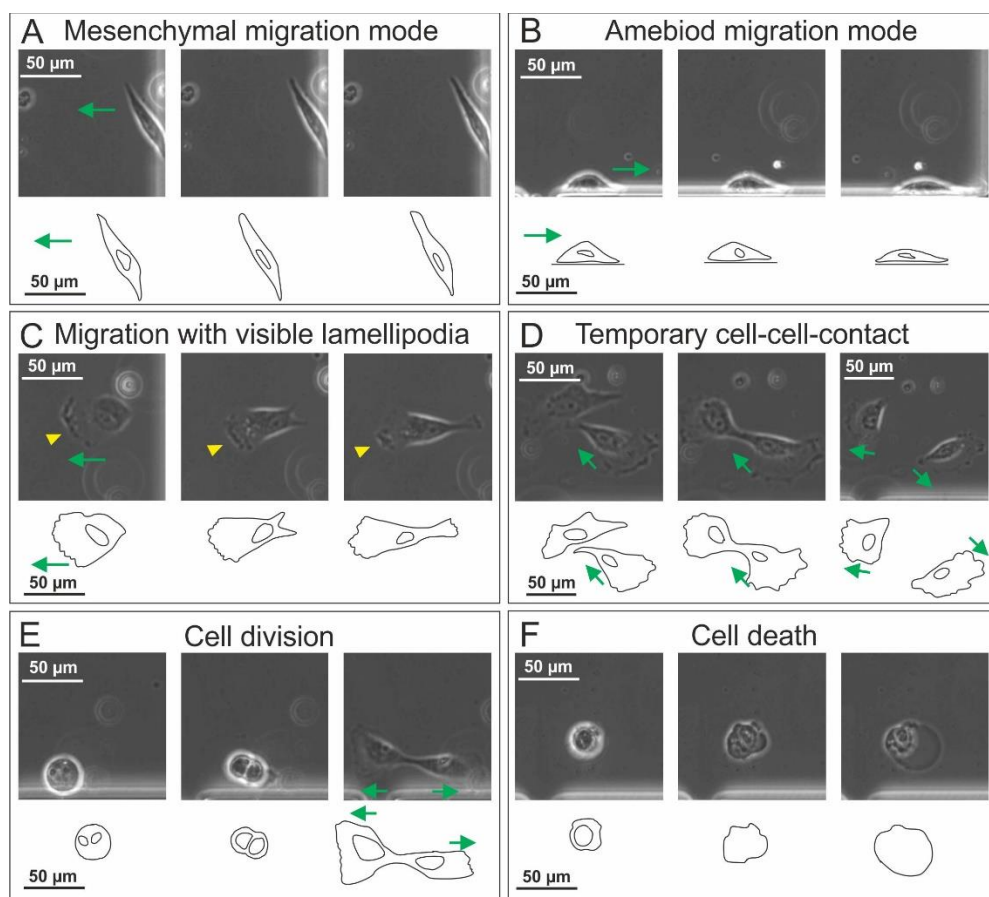
256

257

Figure 3: Examples of different morphologies, behavior and rare events occurring during cultiva- 258
tion of hCSCs in a microfluidic chip. A) Mesenchymal migration mode. B) Ameboid-like migration 259
behavior of hCSCs attached to the chamber's walls. C) Lamellipodia visible in the leading zone of 260
migrating cells (yellow arrowheads). D) Neighboring cells form temporary cell-cell-contacts. E) 261
hCSCs undergo mitosis while forming a sphere-shaped morphology followed by a flattened mor- 262
phology of the daughter cells migrating away from each other. F) Cell death of hCSCs is repre- 263
sented by a sphere-like structure where cytoplasm is leaking. Green arrows indicate the direction 264
of cell migration. 265

3.3. Human blood serum enhances the migration distance and speed of hCSCs 266

We next applied a starvation phase of 24 h by switching the syringe connected to the 267
arrays' inlets from FCS-containing hCSC-medium to serum-free medium. Here, hCSCs 268
remained viable and attached to the surface. In the following treatment period, the sy- 269
ringes with the medium of one array were switched to medium containing 10 % human 270
blood serum. *In vitro* cultivation of adult human stem cells with human blood plasma or 271
serum has demonstrated increased proliferation and viability [14-17]. To investigate a po- 272
tential effect of human serum on hCSC migration, we here tracked the covered path of 273
single cells that were cultivated under exposure to blood serum or to control medium in 274

our microfluidic device. We captured images of marked positions every 15 min and ana- 275
lyzed these data using the manual tracking plugin of ImageJ [45]. HCSCs showed migra- 276
tion behavior in the cultivation chambers under each cultivation condition, although the 277
migration activity of serum treated hCSCs was highly increased (Fig. 4 A, B) (supple- 278
mental video S5). The resulting data allowed us to statistically compare the migration dis- 279
tance and velocity of the two treatment groups. The covered track of serum-treated hCSCs 280
was significantly longer than of hCSCs treated with serum-free medium (Fig. 4 C). Fur- 281
ther, serum treatment significantly increased the velocity of migrating hCSCs compared 282
to untreated hCSCs (Fig. 4 D). These results encouraged us to functionally analyze puta- 283
tive underlying pathways involved in the blood serum-mediated increase of hCSC-migra- 284
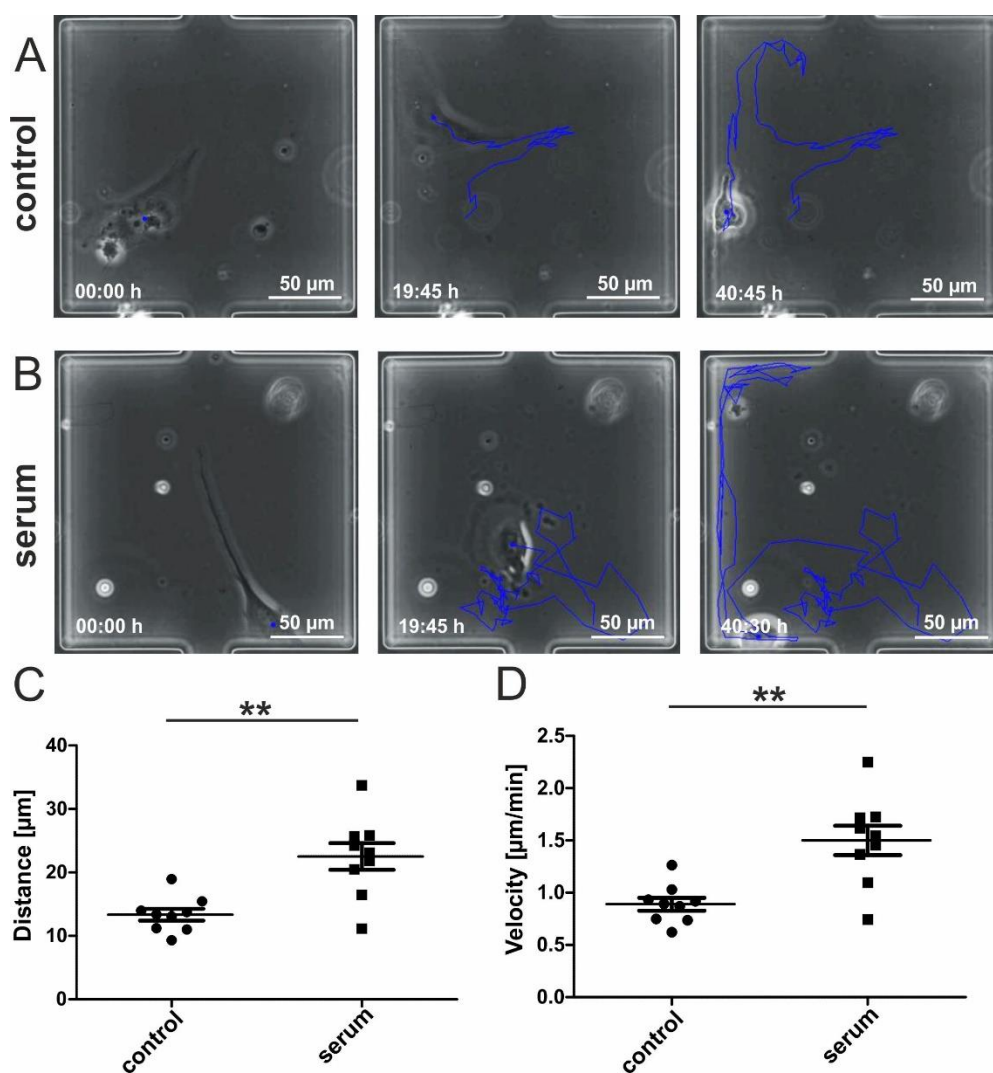tion. 285
286

Figure 4: Human blood serum enhances migration behavior of hCSCs. A) Exemplary images of 288
hCSCs cultivated without serum directly after medium switch, after 19:45 h and after 40:45 h. The 289
blue line indicates the migration path. B) Exemplary images of hCSCs cultivated with human 290
blood serum directly after medium switch, after 19:45 h and after 40:30 h. The blue line indicates 291
the migration path. C) Migration distance of hCSCs is significantly increased by the application of 292
human serum. D) Migration velocity of hCSCs is significantly increased by the application of hu- 293
man serum. 294

3.4. Inhibition of p38-MAPK leads to decreased migration of blood-serum stimulated hCSCs 295

We recently described a blood serum-mediated effect on hCSC proliferation and se- 296
nescence which is party mediated by p38-signaling [14]. These data motivated us to test a 297

possible influence of p38-MAPK on the blood serum mediated migration of hCSCs. We therefore performed a microfluidic experiment where p38-MAPK-inhibitor SB239063 was applied to hCSCs along with human blood serum. Cells cultivated in serum-free medium exhibited a moderate migration track (Fig. 5 A), while the application of human serum led to increased migration (Fig. 5 B). Interestingly, cells cultivated in the presence of human blood serum and the p38-MAPK-inhibitor showed almost no migration accompanied by a mesenchymal-like morphology (Fig. 5 C) (supplemental video S6). Quantitative assessment of the covered tracks showed a significant increase in the migrated distance of serum-treated hCSCs compared to untreated cells. This effect was reversed after co-admission of the p38-MAPK-inhibitor SB239063, which resulted in a significantly decreased migration distance of hCSCs compared to their serum-treated counterparts (Fig. 5 D). We likewise observed the strong increase in migration velocity of serum-treated hCSCs (compared to untreated cells) to be significantly reduced by additional inhibition of p38-MAPK (Fig. 5 E).
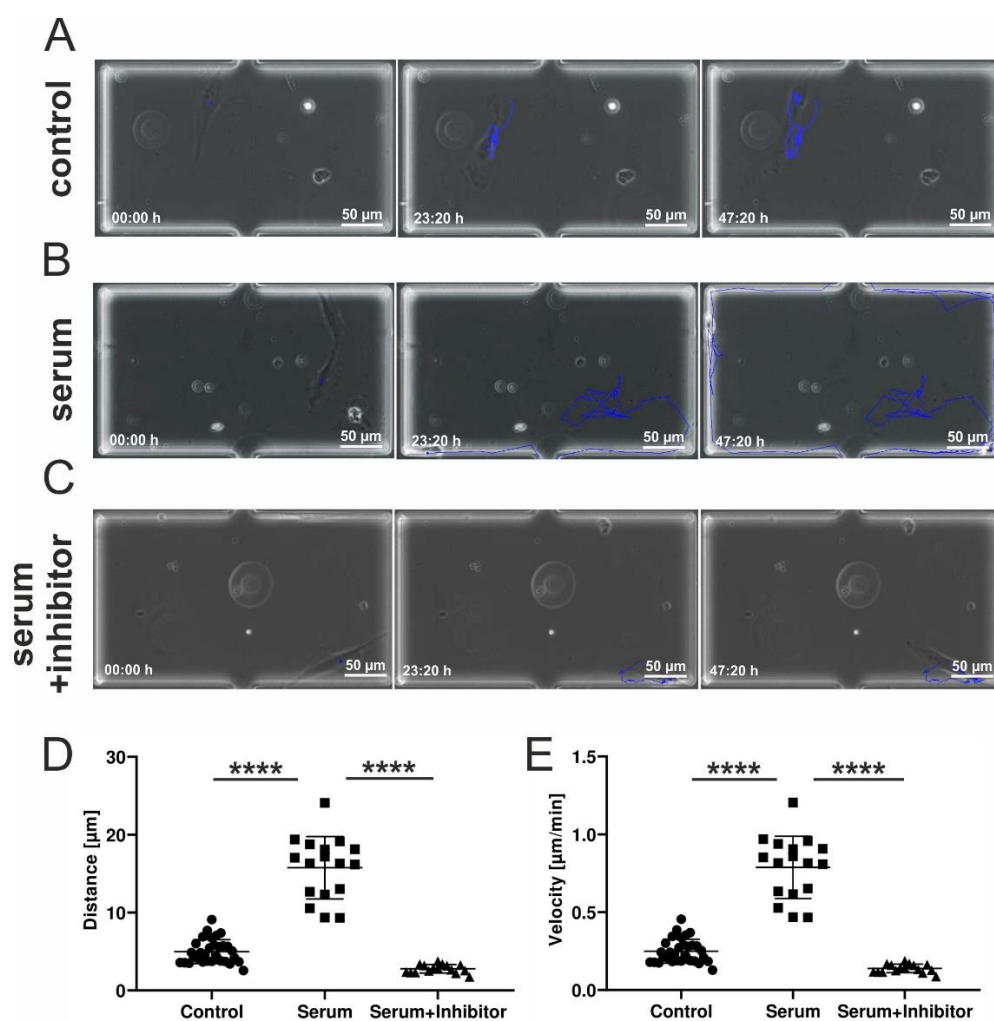

Figure 5: Increased migration behavior of hCSCs after application of human blood serum is dependent on p38-MAPK signaling. A) Exemplary images of hCSCs cultivated without serum directly after medium switch, after 23:20 h and after 47:20 h. The blue line indicates the migration path. B) Exemplary images of hCSCs cultivated with human blood serum directly after medium switch, after 23:20 h and after 47:20 h. The blue line indicates the migration path. C) Exemplary images of hCSCs cultivated with human blood serum and p38-MAPK-inhibitor SB239063 directly after medium switch, after 23:20 h and after 47:20 h. The blue line indicates the migration path. D) Migration distance of hCSCs is significantly increased by the application of human serum. This effect is reversed by the inhibition of p38. E) Migration velocity of hCSCs is significantly increased by the application of human serum. This effect is reversed by inhibition of p38.

4. Discussion

The present study describes the beneficial effects of human blood serum on human cardiac stem cell migration by implementing a microfluidic single cell cultivation tool. We particularly observed a significant increase of hCSC migration distance and speed upon exposure to human blood serum. On mechanistic level, we demonstrated the beneficial effects of human serum to be reversable by inhibition of p38-MAPK signaling.

During cultivation in the microfluidic device, we observed a range of different morphologies like mesenchymal or ameboid-like cell shapes. HCSCs also presented fan-like lamellipodia at the leading edges. These observations are in line with a range of studies describing the mechanisms of actin polymerization leading to protrusions and integrin attachment to the cultivation surface [3]. Accordingly, we recently detected an upregulation of genes associated to the KEGG pathways 'focal adhesion' and 'ECM-receptor interaction' in untreated hCSCs compared to non-adherent human hematopoietic stem cells [24]. Within this study, single hCSCs demonstrated a high plasticity by switching between the different morphologies during cultivation. This mode switching was also observed in human fibroblasts and discussed to be associated with the speed or directionality of migrating cells and may be dependent on external cues such as the composition of the extracellular matrix (ECM) or soluble signaling factors [46-48]. However, in absence of changing external cues, also internal cues were discussed to be responsible for migration mode switching [46]. Our established microfluidic platform further allowed us to observe distinct events like cell division and cell death. Dying cells showed disheveled margins with blebs around the surface. These blebs are commonly observed in apoptotic cells before tying off apoptotic bodies as a result of ROCK1 cleavage and actomyosin contraction leading to delamination of the plasma membrane from the cytoskeleton membrane [30,49,50].

Next to a detailed description of the diverse morphologies of hCSCs during cultivation, we investigated the migration behavior in dependence on human blood serum. Recently, we described increased proliferation and decreased senescence of human serum-treated hCSCs [14]. Here, we extended these findings by showing a significantly increased migration distance and velocity of hCSCs after application of human serum. In accordance to our data, a serum-dependent migration was also reported in human articular chondrocytes and MSCs cultivated in 5 %, 10 % and 20 % fetal bovine serum [18]. In contrast, migration of human fetal skin fibroblasts and fetal lung fibroblasts was demonstrated to be inhibited after application of human blood serum [20,21]. These contradicting data strongly indicate a cell type-dependent response to human serum treatment. In this regard, we demonstrate for the first time the beneficial effects of human serum on the migration of adult human cardiac stem cells in the present study.

To gain functional insights into the increase in cell migration distance and velocity in human serum treated hCSCs, we applied the p38-MAPK-inhibitor SB239063 together with serum in our microfluidic cultivation system. Here, p38-inhibition led to a reversal of serum-induced migration, strongly indicating a participation of p38-signaling in this process. In accordance with our observations, the p38-MAPK pathway has been shown to be important for migration in a range other cell types. For instance, Dubon and coworkers showed increased migration of murine MSC-like ST2-cells as response to TGF-β1-treatment that was mediated by p38-MAPK [25]. Further, human umbilical cord blood-derived MSCs migration was reported to be directed by p38-MAPK [26]. Hamanoue and colleagues described a p38-dependent migration of mouse neural stem cells [27]. Other groups reported p38-activation in highly proliferating and migrating MDA-MB-231 breast cancer cells [28] or p38-induced alterations in actin architecture and corresponding migration of human umbilical vein endothelial cells (HUVECs) [29]. Further, human serum treatment led to increased migration of human keratinocytes which was accompanied with p38-MAPK activation [19]. Interestingly, a global gene expression analysis of blood serum-treated hCSCs showed the KEGG pathway 'focal adhesion' being significantly enriched along with 'MAPK signaling pathway'. Further, the GO-terms 'p38 MAPK-pathway' and 'Integrin Signaling pathway' were found to be enriched in serum treated hCSCs

compared to untreated hCSCs [14]. These data strongly indicate a central role of p38-MAPK signaling in serum-dependent hCSC-migration and may enable new potential therapeutic approaches to enhance cardiac regeneration in heart failure patients.

In comparison to the most prominently employed *in vitro* cell migration assays namely scratch wound assays or compartmentalization of the cultivation wells i.e., with transwell inserts [8], the microfluidic approach presented in this study comes with multiple benefits. Common end-point determination of migrated cells, leaving the meantime dynamics in migration direction or morphology undetected, are replaced by highly time resolved analysis, due to the application of live cell imaging [37]. Owing to the chamber-based design of our device, not only population averages can be investigated but also single-cell behavior is accessible for several days thus extending previously reported experimental durations of max. 12 h [7,41]. Especially in case of cellular response to certain stimuli like human serum the presented method proved to provide valuable insights into single-cell decisions which would have stayed masked using typical average end-point measurements. Therefore, heterogeneity within a cell population that has often been described in primary adult stem cells before [51-53] becomes approachable. Additionally, steady perfusion of the microfluidic cultivation device guarantees full environmental control and makes single-cell analysis under changing cultivation conditions possible.

5. Conclusions

In summary, this study demonstrates a beneficial effect of human blood serum on the migration behavior of an adult human cardiac stem cell in a p38-MAPK-dependent manner. We further provide a microfluidic-based cultivation method facilitating the measurement of primary human stem cell migration. Next to an overview of different morphologies of hCSCs during *in vitro* migration, we show that human serum significantly enhances hCSC migration distance and speed. Application of a specific inhibitor of p38-MAPK completely reversed this effect, strongly suggesting that the activation of hCSC migration by human serum is mediated by p38-signaling. The here presented method offers the possibility to directly track the response of primary adult human stem cells in terms of their spatio-temporal migration dynamics and morphology upon treatment with different stimuli. In addition, our data give valuable insights into the role of blood serum on cardiac stem cell migration and the underlying molecular networks.

Supplementary Materials: The following are available online at www.mdpi.com/xxx/s1, Video S1: successful cultivation of hCSCs in a microfluidic chip, Video S2: temporary cell-cell-contacts between adjacent cells, Video S3: cytokinesis, Video S4: cell death, Video S5: human serum increases hCSC migration behavior, Video S6: p38-MAPK-inhibitor reverses blood serum-mediated hCSC-migration.

References

1.   Goodell, M.A.; Nguyen, H.; Shroyer, N. Somatic stem cell heterogeneity: diversity in the blood, skin and intestinal stem cell compartments. *Nat Rev Mol Cell Biol* **2015**, *16*, 299-309, doi:10.1038/nrm3980.

2.   Liesveld, J.L.; Sharma, N.; Aljitawi, O.S. Stem cell homing: From physiology to therapeutics. *Stem Cells* **2020**, *38*, 1241-1253, doi:10.1002/stem.3242.

3.   Ridley, A.J.; Schwartz, M.A.; Burridge, K.; Firtel, R.A.; Ginsberg, M.H.; Borisy, G.; Parsons, J.T.; Horwitz, A.R. Cell migration: integrating signals from front to back. *Science* **2003**, *302*, 1704-1709, doi:10.1126/science.1092053.

4.   Yuan, L.; Sakamoto, N.; Song, G.; Sato, M. Migration of human mesenchymal stem cells under low shear stress mediated by mitogen-activated protein kinase signaling. *Stem Cells Dev* **2012**, *21*, 2520-2530, doi:10.1089/scd.2012.0010.

5.   Liang, X.; Huang, X.; Zhou, Y.; Jin, R.; Li, Q. Mechanical Stretching Promotes Skin Tissue Regeneration via Enhancing Mesenchymal Stem Cell Homing and Transdifferentiation. *Stem Cells Transl Med* **2016**, *5*, 960-969, doi:10.5966/sctm.2015-0274.

6.   Raab, M.; Swift, J.; Dingal, P.C.; Shah, P.; Shin, J.W.; Discher, D.E. Crawling from soft to stiff matrix polarizes the cytoskeleton and phosphoregulates myosin-II heavy chain. *J Cell Biol* **2012**, *199*, 669-683, doi:10.1083/jcb.201205056.

7.   Saxena, N.; Mogha, P.; Dash, S.; Majumder, A.; Jadhav, S.; Sen, S. Matrix elasticity regulates mesenchymal stem cell chemotaxis. *J Cell Sci* **2018**, *131*, doi:10.1242/jcs.211391.

8.   Fu, X.; Liu, G.; Halim, A.; Ju, Y.; Luo, Q.; Song, A.G. Mesenchymal Stem Cell Migration and Tissue Repair. *Cells* **2019**, *8*, doi:10.3390/cells8080784.

9.   Carter, M.J.; Fylling, C.P.; Parnell, L.K. Use of platelet rich plasma gel on wound healing: a systematic review and meta-analysis. *Eplasty* **2011**, *11*, e38.

10.   Heim, M.U.; Meyer, B.; Hellstern, P. Recommendations for the use of therapeutic plasma. *Curr Vasc Pharmacol* **2009**, *7*, 110-119, doi:10.2174/157016109787455671.

11.   Rassi, A.B.; d'Amico, E.A.; Tripodi, A.; da Rocha, T.R.F.; Migita, B.Y.; Ferreira, C.M.; Carrilho, F.J.; Farias, A.Q. Fresh frozen plasma transfusion in patients with cirrhosis and coagulopathy: Effect on conventional coagulation tests and thrombomodulin-modified thrombin generation. *J Hepatol* **2020**, *72*, 85-94, doi:10.1016/j.jhep.2019.09.008.

12.   Duan, K.; Liu, B.; Li, C.; Zhang, H.; Yu, T.; Qu, J.; Zhou, M.; Chen, L.; Meng, S.; Hu, Y., et al. Effectiveness of convalescent plasma therapy in severe COVID-19 patients. *Proc Natl Acad Sci U S A* **2020**, *117*, 9490-9496, doi:10.1073/pnas.2004168117.

13.   Rajendran, K.; Krishnasamy, N.; Rangarajan, J.; Rathinam, J.; Natarajan, M.; Ramachandran, A. Convalescent plasma transfusion for the treatment of COVID-19: Systematic review. *J Med Virol* **2020**, *92*, 1475-1483, doi:10.1002/jmv.25961.

14.   Höving, A.L.; Schmidt, K.E.; Merten, M.; Hamidi, J.; Rott, A.K.; Faust, I.; Greiner, J.F.W.; Gummert, J.; Kaltschmidt, B.; Kaltschmidt, C., et al. Blood Serum Stimulates p38-Mediated Proliferation and Changes in Global Gene Expression of Adult Human Cardiac Stem Cells. *Cells* **2020**, *9*, doi:10.3390/cells9061472.

15. Greiner, J.F.; Hauser, S.; Widera, D.; Muller, J.; Qunneis, F.; Zander, C.; Martin, I.; Mallah, J.; Schuetzmann, D.; Prante, C., et al. Efficient animal-serum free 3D cultivation method for adult human neural crest-derived stem cell therapeutics. *Eur Cell Mater* **2011**, *22*, 403-419, doi:10.22203/ecm.v022a30.

16. Pandey, S.; Hickey, D.U.; Drum, M.; Millis, D.L.; Cekanova, M. Platelet-rich plasma affects the proliferation of canine bone marrow-derived mesenchymal stromal cells in vitro. *BMC Vet Res* **2019**, *15*, 269, doi:10.1186/s12917-019-2010-x.

17. Shen, J.; Gao, Q.; Zhang, Y.; He, Y. Autologous plateletrich plasma promotes proliferation and chondrogenic differentiation of adiposederived stem cells. *Mol Med Rep* **2015**, *11*, 1298-1303, doi:10.3892/mmr.2014.2875.

18. Mishima, Y.; Lotz, M. Chemotaxis of human articular chondrocytes and mesenchymal stem cells. *J Orthop Res* **2008**, *26*, 1407-1412, doi:10.1002/jor.20668.

19. Henry, G.; Li, W.; Garner, W.; Woodley, D.T. Migration of human keratinocytes in plasma and serum and wound re-epithelialisation. *Lancet* **2003**, *361*, 574-576, doi:10.1016/S0140-6736(03)12510-X.

20. Kondo, H.; Yonezawa, Y.; Ito, H. Inhibitory effects of human serum on human fetal skin fibroblast migration: migration-inhibitory activity and substances in serum, and its age-related changes. *In Vitro Cell Dev Biol Anim* **2000**, *36*, 256-261, doi:10.1290/1071-2690(2000)036<0256:IEOHSO>2.0.CO;2.

21. Kondo, H.; Nomaguchi, T.A.; Yonezawa, Y. Effects of serum from human subjects of different ages on migration in vitro of human fibroblasts. *Mech Ageing Dev* **1989**, *47*, 25-37, doi:10.1016/0047-6374(89)90004-3.

22. Bearzi, C.; Rota, M.; Hosoda, T.; Tillmanns, J.; Nascimbene, A.; De Angelis, A.; Yasuzawa-Amano, S.; Trofimova, I.; Siggins, R.W.; Lecapitaine, N., et al. Human cardiac stem cells. *Proc Natl Acad Sci U S A* **2007**, *104*, 14068-14073, doi:10.1073/pnas.0706760104.

23. Eschenhagen, T.; Bolli, R.; Braun, T.; Field, L.J.; Fleischmann, B.K.; Frisen, J.; Giacca, M.; Hare, J.M.; Houser, S.; Lee, R.T., et al. Cardiomyocyte Regeneration: A Consensus Statement. *Circulation* **2017**, *136*, 680-686, doi:10.1161/CIRCULATIONAHA.117.029343.

24. Höving, A.L.; Sielemann, K.; Greiner, J.F.W.; Kaltschmidt, B.; Knabbe, C.; Kaltschmidt, C. Transcriptome Analysis Reveals High Similarities between Adult Human Cardiac Stem Cells and Neural Crest-Derived Stem Cells. *Biology (Basel)* **2020**, *9*, doi:10.3390/biology9120435.

25. Dubon, M.J.; Yu, J.; Choi, S.; Park, K.S. Transforming growth factor beta induces bone marrow mesenchymal stem cell migration via noncanonical signals and N-cadherin. *J Cell Physiol* **2018**, *233*, 201-213, doi:10.1002/jcp.25863.

26. Ryu, C.H.; Park, S.A.; Kim, S.M.; Lim, J.Y.; Jeong, C.H.; Jun, J.A.; Oh, J.H.; Park, S.H.; Oh, W.I.; Jeun, S.S. Migration of human umbilical cord blood mesenchymal stem cells mediated by stromal cell-derived factor-1/CXCR4 axis via Akt, ERK, and p38 signal transduction pathways. *Biochem Biophys Res Commun* **2010**, *398*, 105-110, doi:10.1016/j.bbrc.2010.06.043.

27. Hamanoue, M.; Morioka, K.; Ohsawa, I.; Ohsawa, K.; Kobayashi, M.; Tsuburaya, K.; Akasaka, Y.; Mikami, T.; Ogata, T.; Takamatsu, K. Cell-permeable p38 MAP kinase promotes migration of adult neural stem/progenitor cells. *Sci Rep* **2016**, *6*, 24279, doi:10.1038/srep24279.

28. Huth, H.W.; Santos, D.M.; Gravina, H.D.; Resende, J.M.; Goes, A.M.; de Lima, M.E.; Ropert, C. Upregulation of p38 pathway accelerates proliferation and migration of MDA-MB-231 breast cancer cells. *Oncol Rep* **2017**, *37*, 2497-2505, doi:10.3892/or.2017.5452.

29. McMullen, M.E.; Bryant, P.W.; Glembotski, C.C.; Vincent, P.A.; Pumiglia, K.M. Activation of p38 has opposing effects on the proliferation and migration of endothelial cells. *J Biol Chem* **2005**, *280*, 20995-21003, doi:10.1074/jbc.M407060200.

30. Lindström, S.; Andersson-Svahn, H. Overview of single-cell analyses: microdevices and applications. *Lab Chip* **2010**, *10*, 3363-3372, doi:10.1039/c0lc00150c.

31. van Noort, D.; Ong, S.M.; Zhang, C.; Zhang, S.; Arooz, T.; Yu, H. Stem cells in microfluidics. *Biotechnol Prog* **2009**, *25*, 52-60, doi:10.1002/btpr.171.

32. Zhang, Q.; Austin, R.H. Applications of Microfluidics in Stem Cell Biology. *Bionanoscience* **2012**, *2*, 277-286, doi:10.1007/s12668-012-0051-8.

33. Halldorsson, S.; Lucumi, E.; Gomez-Sjoberg, R.; Fleming, R.M.T. Advantages and challenges of microfluidic cell culture in polydimethylsiloxane devices. *Biosens Bioelectron* **2015**, *63*, 218-231, doi:10.1016/j.bios.2014.07.029.

34. Berthier, E.; Young, E.W.; Beebe, D. Engineers are from PDMS-land, Biologists are from Polystyrenia. *Lab Chip* **2012**, *12*, 1224-1237, doi:10.1039/c2lc20982a.

35. Lecault, V.; White, A.K.; Singhal, A.; Hansen, C.L. Microfluidic single cell analysis: from promise to practice. *Curr Opin Chem Biol* **2012**, *16*, 381-390, doi:10.1016/j.cbpa.2012.03.022.

36. Wu, H.W.; Lin, C.C.; Lee, G.B. Stem cells in microfluidics. *Biomicrofluidics* **2011**, *5*, 13401, doi:10.1063/1.3528299.

37. Schmitz, J.; Noll, T.; Grunberger, A. Heterogeneity Studies of Mammalian Cells for Bioproduction: From Tools to Application. *Trends Biotechnol* **2019**, *37*, 645-660, doi:10.1016/j.tibtech.2018.11.007.

38. Lecault, V.; Vaninsberghe, M.; Sekulovic, S.; Knapp, D.J.; Wohrer, S.; Bowden, W.; Viel, F.; McLaughlin, T.; Jarandehei, A.; Miller, M., et al. High-throughput analysis of single hematopoietic stem cell proliferation in microfluidic cell culture arrays. *Nat Methods* **2011**, *8*, 581-586, doi:10.1038/nmeth.1614.

39. Zhang, M.; Li, H.; Ma, H.; Qin, J. A simple microfluidic strategy for cell migration assay in an in vitro wound-healing model. *Wound Repair Regen* **2013**, *21*, 897-903, doi:10.1111/wrr.12106.

40. van der Meer, A.D.; Vermeul, K.; Poot, A.A.; Feijen, J.; Vermes, I. A microfluidic wound-healing assay for quantifying endothelial cell migration. *Am J Physiol Heart Circ Physiol* **2010**, *298*, H719-725, doi:10.1152/ajpheart.00933.2009.

41. Zhang, Y.; Wen, J.; Zhou, L.; Qin, L. Utilizing a high-throughput microfluidic platform to study hypoxia-driven mesenchymal-mode cell migration. *Integr Biol (Camb)* **2015**, *7*, 672-680, doi:10.1039/c5ib00059a.

42. Menon, N.V.; Chuah, Y.J.; Phey, S.; Zhang, Y.; Wu, Y.; Chan, V.; Kang, Y. Microfluidic Assay To Study the Combinatorial Impact of Substrate Properties on Mesenchymal Stem Cell Migration. *ACS Appl Mater Interfaces* **2015**, *7*, 17095-17103, doi:10.1021/acsami.5b03753.

43. Schwarz, J.; Bierbaum, V.; Merrin, J.; Frank, T.; Hauschild, R.; Bollenbach, T.; Tay, S.; Sixt, M.; Mehling, M. A microfluidic device for measuring cell migration towards substrate-bound and soluble chemokine gradients. *Sci Rep* **2016**, *6*, 36440, doi:10.1038/srep36440.

44. Schmitz, J.; Tauber, S.; Westerwalbesloh, C.; von Lieres, E.; Noll, T.; Grunberger, A. Development and application of a cultivation platform for mammalian suspension cell lines with single-cell resolution. *Biotechnol Bioeng* **2020**, 10.1002/bit.27627, doi:10.1002/bit.27627.

45. Schindelin, J.; Arganda-Carreras, I.; Frise, E.; Kaynig, V.; Longair, M.; Pietzsch, T.; Preibisch, S.; Rueden, C.; Saalfeld, S.; Schmid, B., et al. Fiji: an open-source platform for biological-image analysis. *Nat Methods* **2012**, *9*, 676-682, doi:10.1038/nmeth.2019.

46. Petrie, R.J.; Yamada, K.M. At the leading edge of three-dimensional cell migration. *J Cell Sci* **2012**, *125*, 5917-5926, doi:10.1242/jcs.093732.

47. Petrie, R.J.; Gavara, N.; Chadwick, R.S.; Yamada, K.M. Nonpolarized signaling reveals two distinct modes of 3D cell migration. *The Journal of cell biology* **2012**, *197*, 439-455, doi:10.1083/jcb.201201124.

48. Friedl, P.; Wolf, K. Plasticity of cell migration: a multiscale tuning model. *J Cell Biol* **2010**, *188*, 11-19, doi:10.1083/jcb.200909003.

49. Zhang, Y.; Chen, X.; Gueydan, C.; Han, J. Plasma membrane changes during programmed cell deaths. *Cell Res* **2018**, *28*, 9-21, doi:10.1038/cr.2017.133.

50. Kerr, J.F.; Wyllie, A.H.; Currie, A.R. Apoptosis: a basic biological phenomenon with wide-ranging implications in tissue kinetics. *Br J Cancer* **1972**, *26*, 239-257, doi:10.1038/bjc.1972.33.

51. Dulken, B.W.; Leeman, D.S.; Boutet, S.C.; Hebestreit, K.; Brunet, A. Single-Cell Transcriptomic Analysis Defines Heterogeneity and Transcriptional Dynamics in the Adult Neural Stem Cell Lineage. *Cell Rep* **2017**, *18*, 777-790, doi:10.1016/j.celrep.2016.12.060.

52. Bryder, D.; Rossi, D.J.; Weissman, I.L. Hematopoietic stem cells: the paradigmatic tissue-specific stem cell. *Am J Pathol* **2006**, *169*, 338-346, doi:10.2353/ajpath.2006.060312.

53. Suslov, O.N.; Kukekov, V.G.; Ignatova, T.N.; Steindler, D.A. Neural stem cell heterogeneity demonstrated by molecular phenotyping of clonal neurospheres. *Proc Natl Acad Sci U S A* **2002**, *99*, 14506-14511, doi:10.1073/pnas.212525299.

Original Research Report

Identification of a Novel High Yielding Source of Multipotent Adult Human Neural Crest-Derived Stem Cells

Matthias Schürmann, Viktoria Brotzmann, Marlena Bütow, Johannes Greiner, Anna Höving, Christian Kaltschmidt, Barbara Kaltschmidt, Holger Sudhoff

CrossMark

Identification of a Novel High Yielding Source of Multipotent Adult Human Neural Crest-Derived Stem Cells

Matthias Schürmann[1] · Viktoria Brotzmann[1] · Marlena Bütow[1] · Johannes Greiner[2] · Anna Höving[2] ·
Christian Kaltschmidt[2] · Barbara Kaltschmidt[2,3] · Holger Sudhoff[1]

Abstract

Due to their extraordinarily broad differentiation potential and persistence during adulthood, adult neural crest-derived stem cells (NCSCs) are highly promising candidates for clinical applications, particularly when facing the challenging treatment of neurodegenerative diseases or complex craniofacial injuries. Successful application of human NCSCs in regenerative medicine and pharmaceutical research mainly relies on the availability of sufficient amounts of tissue for cell isolation procedures. Facing this challenge, we here describe for the first time a novel population of NCSCs within the middle turbinate of the human nasal cavity. From a surgical point of view, high amounts of tissue are routinely and easily removed during nasal biopsies. Investigating the presence of putative stem cells in obtained middle turbinate tissue by immunohistochemistry, we observed Nestin$^+$/p75^{NTR+}/S100$^+$/α smooth muscle actin (αSMA)$^-$ cells, which we successfully isolated and cultivated in vitro. Cultivated middle turbinate stem cells (MTSCs) kept their expression of neural crest and stemness markers Nestin, p75^{NTR} and S100 and showed the capability of sphere formation and clonal growth, indicating their stem cell character. Application of directed in vitro differentiation assays resulted in successful differentiation of MTSCs into osteogenic and neuronal cell types. Regarding the high amount of tissue obtained during surgery as well as their broad differentiation capability, MTSCs seem to be a highly promising novel neural crest stem cell population for applications in cell replacement therapy and pharmacological research.

Keywords NCSCs · Human · Nasal cavity · Middle turbinate · Neural crest · Adult stem cells

Introduction

In the adult human body, the renewal of organs as well as the repair of tissue upon injury relies on adult stem cells (ASCs) [1], which are located within distinct niches controlling proliferation and differentiation behavior [2, 3]. Among the

broad range of adult human stem cells, neural crest-derived stem cells (NCSCs) remain as highly promising candidates for clinical applications in terms of their extraordinarily broad differentiation potential [4–7]. Identified by Wilhelm His in 1868 as the "Zwischenstrang" (intermediate chord) in the developing chicken embryo, the neural crest is a transient cell population located between the neural tube and the future ectoderm [8, 9]. Following neurulation, neural crest cells migrate towards different parts of the body, where they contribute to tissue development but also reside as dormant stem cells during adulthood [4, 10, 11]. Emphasizing their therapeutic potential, Tabakow and coworkers described the autologous transplantation of cranial NCSCs in a patient with a transected spinal cord to result in functional regeneration of supraspinal connections, including partial recovery of voluntary movement of the lower extremities [12]. Common sources of cranial NCSCs particularly include the skin [4, 10], dental pulp [13] and the nasal cavity. Here, olfactory ensheathing cells (OECs) located in the olfactory bulb or the

✉ Holger Sudhoff
holger.sudhoff@rub.de

1 Department of Otolaryngology, Head and Neck Surgery, Klinikum Bielefeld, Teutoburger Straße 50, 33604 Bielefeld, Germany

2 Department of Cell Biology, University of Bielefeld, 33615 Bielefeld, Germany

3 AG Molecular Neurobiology, University of Bielefeld, 33615 Bielefeld, Germany

lamina propria of olfactory mucosa of the middle and superior turbinate are a commonly known NCSC-population. Although restricted in terms of their accessibility [14] and complexity of surgery [15], OECs were reported to recover animal models of spinal cord injury and Parkinson's disease [16, 17] and even a transected spinal cord in a patient [12]. Next to OECs residing in the olfactory bulb and superior turbinates, we reported the presence of a novel population of nasal NCSCs in inferior turbinate tissue in 2012 [11]. Inferior turbinate stem cells (ITSCs) showed a broad differentiation potential in vitro, namely into mesodermal and ectodermal cell types [7, 11, 18, 19]. In vivo, transplantation of ITSCs into Parkinsonian rats led to functional recovery of the Parkinson's disease phenotype [7]. Next to potential clinical applications, ITSCs were successfully used as a model system for pharmacological research in terms of treating inflammatory diseases of the upper respiratory tract [20]. Although these findings emphasize the suitability of adult human NCSCs isolated from the nasal cavity for clinical applications, gaining sufficient amounts of tissue remains as a crucial step for clinical applications.

Facing this challenge, here we describe for the first time a novel population of NCSCs within the middle turbinate of the human nasal cavity. From a surgical point of view, middle turbinate tissue can be obtained easily and without severe side-effects for the patients. In addition, high amounts of tissue are routinely removed and can be used directly for NCSC-isolation. We observed the presence of Nestin[+]/p75[NTR+]/S100[+]/αSMA^{−} cells within middle turbinate tissue, which we successfully isolated and cultivated in vitro. Cultivated middle turbinate stem cells (MTSCs) kept their expression of neural crest and stemness markers Nestin, p75[NTR], S100 and showed the capability of sphere formation and clonal growth. Their multipotent differentiation capability was proven by the application of directed in vitro differentiation assays. Due to availability of considerable amounts of middle turbinate tissue through nasal surgery as well as their broad differentiation potential, MTSCs appear as a promising novel neural crest stem cell population for applications in pharmacological research and cell replacement therapy.

Materials and Methods

Cell Isolation and Cultivation

Middle turbinate tissue was obtained from patients during routine nasal surgery at Klinikum Bielefeld Mitte (Bielefeld, Germany) after informed written consent according to local and international guidelines (Bezirksregierung Detmold/Münster). After surgical removal, biopsies were cut into small pieces, treated with Collagenase (0.375 U / ml in PBS, NB4, SERVA Electrophoresis GmbH) for at least 1 h

at 37 °C and were finally mechanically dissociated. Afterwards cells were centrifuged at 300 x g for 10 min and the pellet was resuspended in stem cell medium consisting of DMEM/F-12 medium (Sigma–Aldrich) containing Penicillin, Streptomycin, Amphotericin B (Sigma–Aldrich), a basic fibroblast growth factor (bFGF, 40 ng / ml, Peprotech), an epidermal growth factor (EGF 20 ng / ml; Peprotech) and B27 supplement (Gibco, Life Technologies). For initial expansion, the suspension was seeded in surface treated T-25 cell culture flasks (Sarstedt AG & Co.) with stem cell medium containing 10% human blood plasma. After reaching confluence, the cells were released from the blood plasma matrix by treatment with Collagenase for 1 h at 37 °C and cultivated in stem cell medium supplemented with heparin (2 μg / ml, Sigma–Aldrich) in T-25 low adhesion cell culture flasks (Sarstedt) at 37 °C and 5% CO_2 in a humidified incubator. For further cultivation, cells were again seeded in surface treated T-25 cell culture flasks (Sarstedt AG & Co.) in stem cell medium containing 10% human blood plasma. The medium was changed all two to three days, passaging was performed by treatment with collagenase.

Human mesenchymal stem cells (hMSCs) were isolated from lipoaspirates obtained from suitable donors during adipose tissue augmentationat Klinikum Bielefeld Mitte (Bielefeld, Germany) after informed written consent according to local and international guidelines (Bezirksregierung Detmold/Münster). Briefly, lipoaspirates were treated with Collagenase (0.375 U / ml in PBS, NB4, SERVA Electrophoresis GmbH) for 30 min at 37 °C followed by centrifugation for 10 min at 300 x g. After discarding the supernatant, pelleted cells were seeded at a density of 20,000 cell / cm^2 in DMEM containing 10% FCS (Sigma–Aldrich) and cultivated at 37 °C and 5% CO_2. Purity of the isolated hMSCs-populations was validated by expression of characteristic MSC-markers (data not shown).

Immunohistochemistry and Immunocytochemistry

Cryosections of the middle turbinate tissue or cultivated cells were fixed for 20 min using 4% paraformaldehyde (PFA), washed and permeabilized in PBS with TritonX-100 (tissue: 0.2%, cells: 0.02%, Applichem) and supplemented with 5% goat serum for 30 min. The applied primary antibodies were diluted in PBS as followed: mouse anti-Nestin 1:200 (Millipore), rabbit anti-S100B 1:100 (Dako), rabbit anti-p75 1:500 (Cell-Signaling Technology), mouse anti-αSMA 1:50 (Sigma–Aldrich), mouse anti-β-III-tubulin 1:100 (Promega) and rabbit neurofilament-L 1:50 (Cell-Signaling Technology). They were applied for 1 h (cells) or for 2 h (sections), both at RT. After three washing steps, secondary fluorochrome-conjugated antibodies (Alexa 555

anti-mouse or Alexa 488 anti-rabbit, Invitrogen, Life Technologies GmbH) were applied for 1 h at RT with a dilution ratio of 1:300. Nuclear staining was realized by incubation with 4,6-Diamidin-2-phenylindol (DAPI) (1 μg/ml) in PBS for 15 min at RT. Finally, the samples were mounted with mowiol. Imaging was performed using a confocal laser scanning microscope (CLSM 780, Carl Zeiss) and image processing was executed with imagej (open source).

Reverse Transcriptase PCR

The RNA isolation was performed utilizing the innuPREP RNA Mini Kit (Analytic Jena AG) according to the manufacturer's guidelines. The quality and concentration of the obtained RNA was quantified by a nanophotometer (Implen GmbH). For cDNA synthesis, the M-MuLV RT DNA-Polymerase (Bio-Budget Technologies GmbH) was applied in accordance to the manufacturer's guidelines. PCR was executed with the 5 x Hot-Start Taq PCR-Mastermix (Bio-Budget Technologies GmbH) according to manufacturer's guidelines with primers for Nestin (fw: CAGCGTTGG AACAGAGGTTG, rev: GCTGGCACAGGTGTCTCA AG), p75^{NTR} (fw: TGAGTGCTGCAAAGCCTGCAA, rev: TCTCATCCTGGTAGTAGCCGT), SNAIL (fw: CCCAAT CGGAAGCCTAACTA, rev: GGACAGAGTCCCAGATGA GC), S100 (fw: GGGAGACAAGCACAAGCTGAAGA, rev: TCAAAGAACTCGTGGCAGGCAGTA), CD105 (fw: CGGGTCTCAAGACCAGGAAG, rev: GGGGCCTGGGGT ACTCA), CD106 (fw: GGACCACATCTACGCTGACAA, rev: CTCCAGAGGGCCACTCAAAT), CD90 (fw: TGA GGACACAGACCAGAGGAA, rev: TGTTTGAGATGT TGTGCGGG), CD45 (fw: TCTAATGAAAGAGTGAGA GTGGACG, rev: AACCAATTCTGGTGTCTGCCT) and GAPDH (fw: CTGCACCACCAACTGCTTAG, rev: GTC TTCTGGGTGGCAGTGAT).

Real-Time PCR

For qPCR (quantitative real-time polymerase chain reaction) myBudged 5x EvaGreen QPCR-Mix (Biobudged Technologies GmbH, Krefeld, Germany) was applied according to manufactures guidelines after RNA isolation and cDNA synthesis as described above. All reactions were done as technical triplicates, primer sequences for were GCAGAAGCT CTCGATGGACA (CD13 fw), CAGATCTGCTGCCCTGTT GA (CD13 rev), CCGTGCAAATCCCACAACAC (CD29 fw), TTGTCAGTCCCTGGCATGAA (CD29 rev), CTT TGCACCAAGTGTCGAGTG (CD73 fw), TCTGGAACC CATCTCCACCA (CD73 rev), TGAGGACACAGACCA GAGGAA (CD90 fw) and TGTTTGAGATGTTGTGCGGG (CD90 rev). The MIC qPCR cycler (Bio Molecular Systems, San Francisco, USA) was used for product detection. Glyceraldehyde 3-phosphate dehydrogenase (GAPDH, fw: CTG CACCACCAACTGCTTAG, rev: GTCTTCTGGGTGGCA GTGAT) expression was utilized for normalisation of cycle threshold values. GraphPad Prism (GraphPad Software, La Jolla, USA) was used for graphics and statistical analysis.

Flow Cytometry

Cultivated MTSCs were harvested by centrifugation after treatment with Collagenase and subsequently stained with PE-coupled anti-CD271 antibody (Miltenyi Biotec, Bergisch Gladbach, Germany) according to manufacturer's guidelines. hMSCs were dissociated likewise and labeled with PE-coupled anti-CD105 PE-coupled antibody (Miltenyi Biotec). For isotype controls, MTSCs and hMSCs were stained with PE-coupled IgG1 control antibody. Analysis was done using Gallios Flow Cytometer (Beckmann Coulter Inc., Brea, CA, United States), while Kaluza Acquisition Software (Beckmann Coulter Inc.) served for subsequent data acquisition and statistical analysis.

Clonal Density Assay

To ascertain the capability of self-renewal of isolated cells, cultivation under standard culture conditions in a limited dilution assay was performed. Briefly, the cell suspension was diluted to 1 cell / 100 μl in stem cell medium containing 10% human blood plasma and seeded into U-bottom 96-well plates. After two hours, the wells were microscopically inspected for the presence of single cells using an Olympus CKX41 microscope (Olympus Deutschland GmbH). The clonal growth of cells was observed once a week for 21 days.

Differentiation Into Osteoblasts

The osteogenic differentiation of MTSCs was induced by biochemical cues according to Greiner and coworkers [18]. Briefly, cells were seeded in DMEM containing 10% FCS (Sigma–Aldrich) at a density of 3×10^3 cells / cm^2. After 48 h the medium was switched to an osteogenic induction medium supplemented with 100 nM dexamethasone (Sigma–Aldrich), 0.05 mM L-ascorbic acid-2-phosphate (Sigma–Aldrich) and 10 mM β-glycerophosphate (Sigma–Aldrich). The medium was changed every two to three days. After 21 days differentiated cells were processed for the detection of ALP activity and the Alizarin red S staining as described below.

ALP Detection with Alizarin Red Staining

For the detection of alkaline phosphatase (ALP) activity, differentiated cells were briefly fixed for 2 min with 4% PFA, washed with ddH$_2$O and incubated with a 1:1:2 mixture of Water, Naphthol AS-MX phosphate alkaline solution (Sigma

Aldrich) and fast red violet lb staining solution (0.7 mg/ml in ddH$_2$O, Sigma Aldrich) for 5 min at RT, washed again with ddH$_2$O and mounted with mowiol.

For detection of calcium deposits maturated cells were fixed for 20 min with 4% PFA and briefly washed with PBS followed by a thorough washing with ddH$_2$O. Subsequently, a staining solution of 1% Alizarin red S (Waldeck) in ddH$_2$O with a pH of 4.3 was applied for 5 min at RT followed by rinsing with ddH$_2$O.

Induced Neuronal Differentiation

Neuronal differentiation in the isolated cells was induced following the protocol described by Müller and colleagues [7]. Briefly, cells were seeded with a density of 5×10^4 cells per 12-well in DMEM (Sigma–Aldrich) containing 10% FCS (Sigma–Aldrich). After 48 h, neural differentiation was induced with a neuronal induction medium containing 1 μM dexamethasone (Sigma–Aldrich), 2 μM insulin (Sigma–Aldrich), 500 μM 3-isobutyl-1-methylxanthine (Sigma–Aldrich) and 200 μM indomethacin (Sigma–Aldrich). The medium was changed every two to three days. After 28 days, the protein expression was analyzed by immunocytochemical staining as described above.

Adipogenic Differentiation of MSCs

For adipogenic differentiation, MSCs were cultivated in DMEM (Sigma–Aldrich) containing 10% FCS (Sigma–Aldrich) and plated at a density of 4×10^3 cells / cm². After 48 h, 1 μm dexamethasone (Sigma–Aldrich), 2 μM insulin (Sigma–Aldrich), 500 μM 3-isobuthyl-1-methylxanthine (Sigma–Aldrich) and 200 μM indomethacin (Sigma–Aldrich) were added to the medium and cultivated for 72 h. Afterwards the medium was switched and cells were cultivated for 4 days in DMEM containing 10% FCS and 2 μM insulin (Sigma–Aldrich) to induce adipogenic differentiation. These two media were alternatingly used and changed every 4 days for 3 weeks. Subsequently cells were fixed in 4% PFA for 10 min and stained with Oil red O (Sigma–Aldrich).

Results

Identification of a Cell Population Expressing Distinct Neural Crest-Derived Stem Cell Markers in Middle Turbinate Tissue

To investigate the potential presence of a stem cell population in middle turbinate tissue (Fig. 1a), *concha nasalis mediae* were obtained from patients during routine nasal surgery. Notably, tissue pieces of up to 4 cm length were

gained routinely and without severely affecting respiration and olfactory sensing. Using immunohistochemical stainings, we observed cells co-expressing the characteristic NCSC-markers Nestin and p75^{NTR} as well as Nestin and S100B in the lamina propria of human middle turbinate tissue (Fig. 1b, c arrows). On the contrary, cells positive for the OEC-maker α-smooth muscle actin (α-SMA, [21]) (Fig. 1d, e arrowheads) were found to be solely located adjacent to those expressing p75^{NTR} and S100B (Fig. 1d, e, arrows). Since we found no α-SMA$^+$/p75^{NTR+}/S100B$^+$ cell in the examined areas of middle turbinate tissue, we proposed the presence of a novel NCSC-population clearly distinguishable from olfactory escheating cells also located within in the *concha nasalis mediae*.

Successful Isolation of Sphere-Forming Putative Stem Cells from Middle Turbinate tissue

Since cells positive for the NCSC-markers Nestin, p75^{NTR} and S100B were detectable in the middle turbinate, we applied an established protocol for NCSC-isolation [11]. Mechanical disintegration and enzymatic digestion of the tissue followed by exposure to a serum-free culture medium comprising FGF and EGF resulted in formation of neurospheres (Fig. 2a), a common characteristic of NCSCs. We successfully isolated putative middle turbinate stem cells (MTSCs) from eleven donors, six of them being male and five female with an age variing from 13 to 74 years. All isolated cell populations showed the potential to form neurospheres under serum free-conditions in a gender and age independend manner. Subsequently to this initial isolation step, we were able to efficiently expand the cells in a human blood plasma-derived 3D fibrin matrix. Blood plasma-cultivated MTSCs showed a long-shaped morphology accompanied by an increased proliferative behavior (Fig. 2b, data not shown).

Isolated Middle Turbinate Stem Cells Express Characterisitc Neural Crest and Stemness Markers

Analyzing the expression pattern of the isolated sphere-forming cells, we investigated markers characterstic for neural crest stem cells by RT-PCR. Here, MTSCs showed expression of the NCSC marker Nestin as well as the neural crest markers p75^{NTR}, S100B and Snail (Fig. 2c). In contrast, real-time PCR revealed strongly reduced expression levels of the MSC-marker CD90 in comparison to human MSCs (Fig. 2c), which we isolated from lipoaspirates and characterized in terms of expression profile and differentiation capability (Fig. S1). The observed reduction in CD90 expression in comparison to hMSCs distinguishes the here discovered stem cell population from CD90$^+$ olfactory ectomesenchymal stem cells (OE-MSCs) [21].
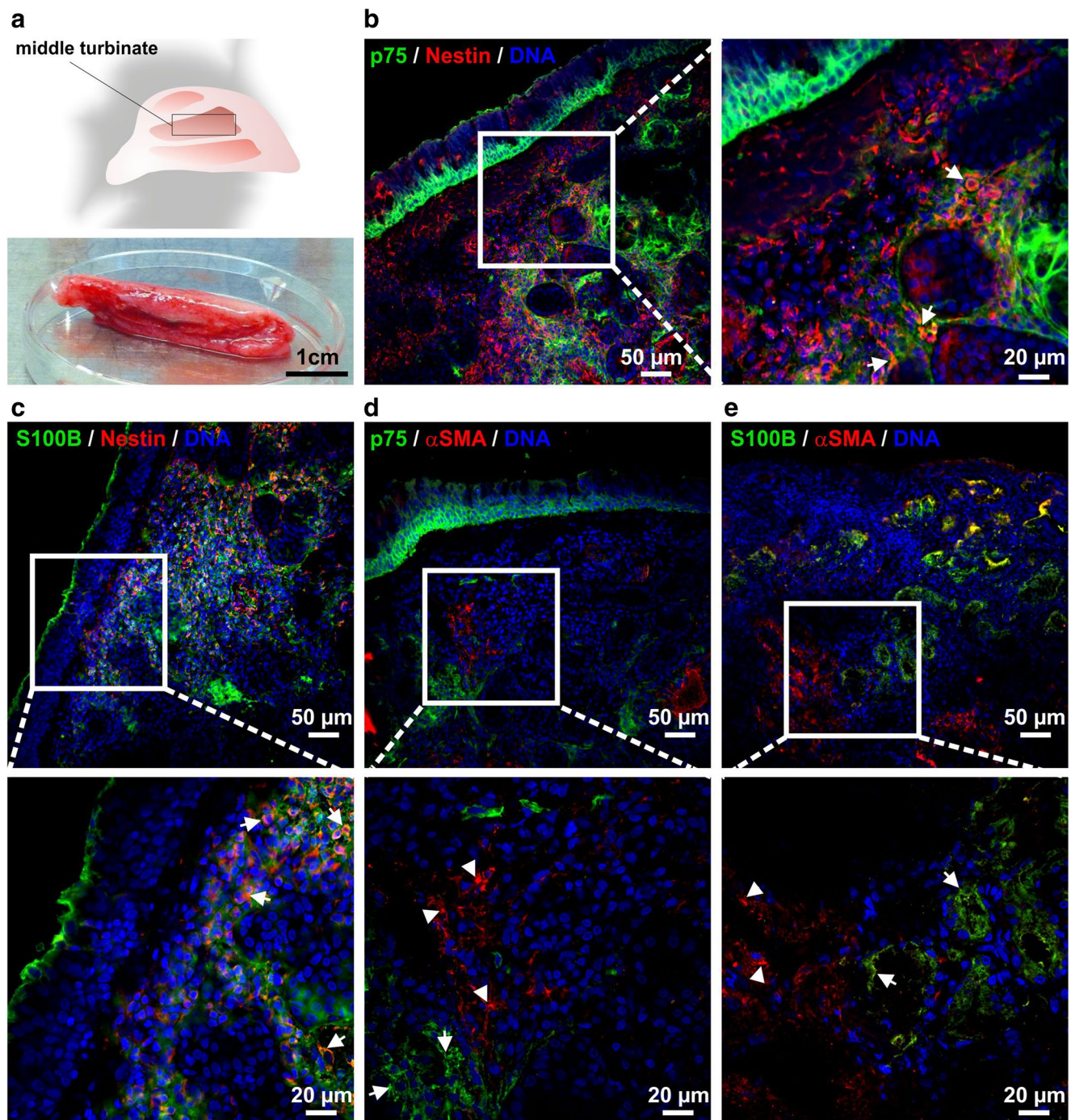
Fig. 1 Middle turbinate tissue contains cells coexressing markers characteristic for neural crest-derived stem cell. Schematic view of the middle turbinate located in the nasal cavity. Large amount of middle turbinate tissue extracted during routine surgical procedure **a**. Immunohistochemical staining revealed the presence of cells co-expressing Nestin and p75^{NTR} **b** as well as Nestin and S100B **c** within the lamina propria of middle turbinate tissue. Further immunohisto-chemical analysis detected no co-expression of p75^{NTR} **d** or S100B **e** with αSMA in cells residing in the middle turbinate

Immunocytochemical analysis further validated expression of the NCSCs markers on protein level. In particular, MTSCs cultivated as neurospheres or in an adherent manner were positive for Nestin and S100B as well as Nestin and p75^{NTR} (Fig. 2d, e). In summary, these findings indicate the successful isolation of Nestin^{+}/S100^{+}/p75^{NTR+} NCSCs, which we initially observed to be present within human middle turbinate tissue.

Fig. 2 **Successfully isolation of sphere-forming Nestin⁺/S100⁺/p7 5^NTR+ neural crest-derived stem cells from the middle turbinate**. Isolated middle turbinate stem cells (MTSCs) were able to form neurospheres under serum-free conditions (**a**) and could be efficiently expanded in a human blood plasma-derived fibrin matrix (**b**). RT-PCR showed characteristic expression of the NCSC-markers Nestin, SNAIL, S100B and p75^NTR, but strongly reduced level of the CD90 in comparison to hMSCs (**c**)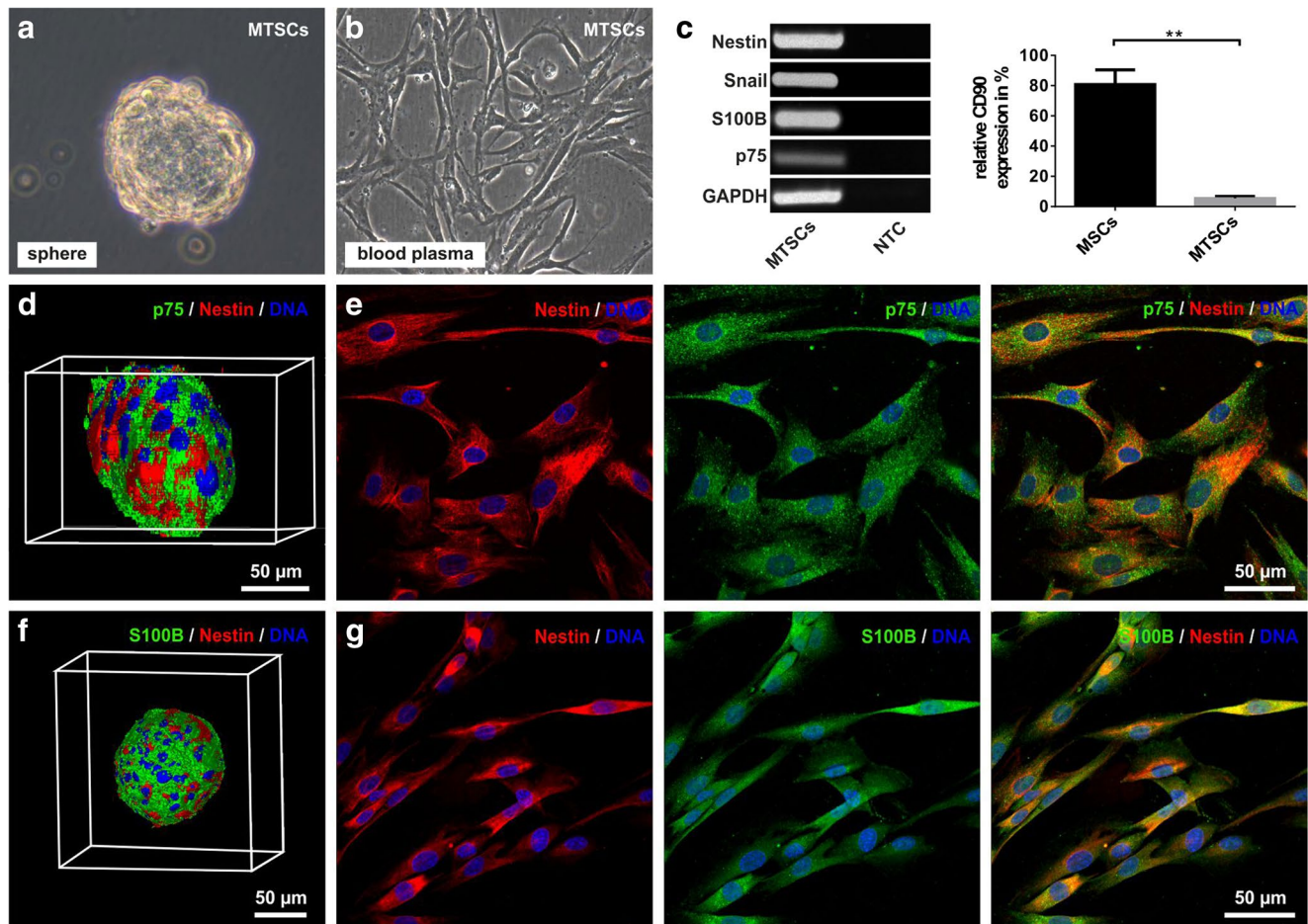. Immunocytochemical stainings exhibited co-expression of Nestin/p75^NTR (**d**) and Nestin/S100B (**e**) in the isolated MTSCs cultivated as neurospheres or under adherent conditions (**≤0.01, unpaired t-test; one-tailed, confidence interval: 95%)

MTSCs Reveal an Extraordinary High Clonal Efficiency and Capability to Differentiate into Mesodermal and Ectodermal Derivates

Investigating the stemness characteristics of MTSCs, a limited dilution assay was applied to analyze the ability of MTSCs to grow in a clonal manner. Here, single seeded MTSCs efficiently gave rise to daughter cells with an extraordinary high clonal efficiency of > 75% (Fig. 3a). Further determining their capability to differentiate, MTSCs were exposed to biochemical cues described to induce a differentiation of NSCs into osteogenic derivates [18]. In contrast to cells solely exposed to FCS-containing medium, MTSCs gave rise to early osteogenic cell types marked by an enhanced activity of the alkaline phosphatase (ALP) within the first week after induction (Fig. 3b). Further differentiation and *in-vitro* maturation of MTSC-derived osteogenic cells was validated by the detection

of alizarin red S-stained calcium deposits after three weeks of culture (Fig. 3c). Next to differentiation into the mesodermal lineage, we applied a neuronal induction medium [7] for directed differentiation of MTSCs into neuron-like cell types. After 28 days of directed differentiation, cells co-expressing the neuronal markers β−III tubulin and neurofilament–L were observable, indicating a successful differentiation of MTSCs into neuron-like cells (Fig. 3d). Given the successful differentiation into derivates of two different germ layers, our findings indicate MTSCs to be a multipotent stem cell population

Discussion

The present study describes for the first time the identification of a novel population of human adult neural crest-derived stem cells in the middle turbinate of the human
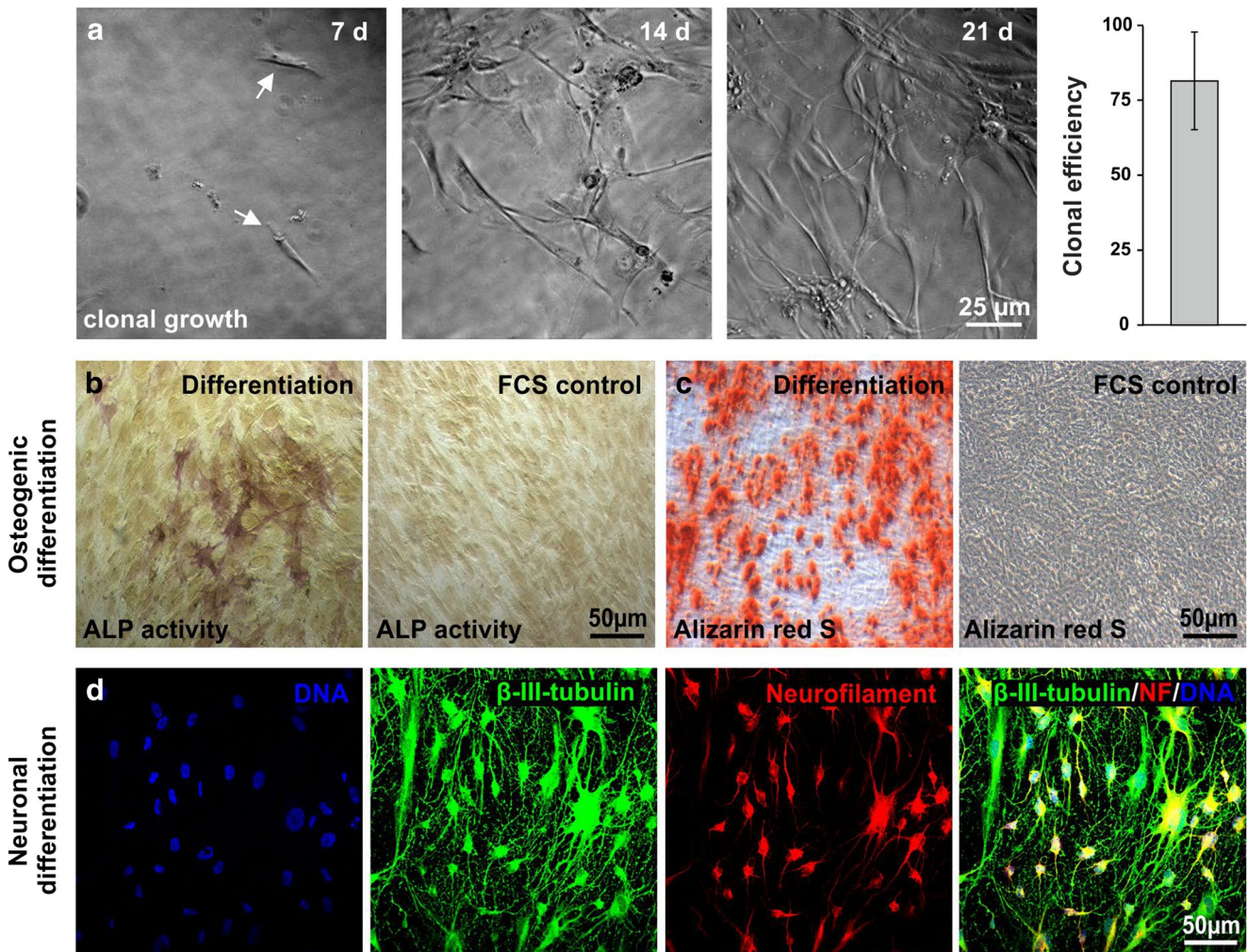
Fig. 3 Cultivated MTSCs Show an Extraordinary High Clonal Efficiency and Capability to Differentiate Into Mesodermal and Ectodermal derivates. MTSCs were able to grow clonally with an efficiency of >75% in a limited dilution assay a. In contrast to MTSCs cultivated solely in FCS-containing medium, exposure of MTSCs to a directed osteogenic differentiation medium led to activation of alkaline phosphatase (ALP) after one week b and formation of Alizarin red S-positive calcium apatite deposits after three weeks c. Cultivation of MTSCs following a neurogenic differentiation protocol for three weeks led to the presence of MTSC-derived neuron-like cells types co-expressing β−III tubulin and neurofilament-L d

nasal cavity. Nestin$^+$/S100$^+$/p75^{NTR+} NCSCs residing within human middle turbinate tissue were successfully isolated and cultivated in vitro, where they revealed a broad differentiation potential and high clonal efficiency.

Middle turbinates located above the middle meatus mainly function as a diffusor to enable a better smelling with the olfactory mucosa mainly located in the superior turbinate [22]. Within the human nasal cavity, olfactory ensheathing cells (OECs) are known to be located in the middle and to a greater extend in the superior turbinate as well as within the olfactory bulb [6, 15, 17, 23]. Emphasizing the potential of adult nasal stem cells in clinical applications, transplantation of OECs was described to result in functional recovery of animal models of spinal cord injury and Parkinson's disease [16, 17, 23]. In 2014,

Tabakow and colleagues even described the functional regeneration of a transected spinal cord in a patient after autologous OB-OEC-transplantation. In particular, the authors observed partial recovery of sensation and voluntary movements of the lower extremities as well as improved trunk stability in the patient, without occurrence of persistent unilateral anosmia [12]. Investigating the developmental origin of OECs in detail, Barraud and colleagues applied genetic lineage tracing in mice to show that OECs do not arise from the olfactory epithelium, but from the neural crest [24]. Next to expression of characteristic NCSC-markers like Nestin [25] p75^{NTR} [23] and S100 [15], OECs were shown to express α-SMA in vivo [26]. In contrast, Nestin$^+$/S100$^+$/p75^{NTR+} NCSCs identified in the present study within middle turbinate tissue lacked

co-expression of α-SMA, clearly distinguishing this novel NCSC-population from OECs.

Next to OECs, olfactory ectomesenchymal stem cells (OE-MSCs) were identified within the lamina propria of the human olfactory mucosa of the human nasal cavity [21]. Transplantation of OE-MSCs into mice with chemically induced hippocampal lesion restored neuroplasticity by differentiation into neurons and stimulating endogenous neurogenesis in vivo [27]. Closely related to bone marrow stem cells, OE-MSCs were shown to express markers characteristic for the bone marrow niche like CD90 [21]. Although sharing a similar developmental potential with OE-MSCs in terms of differentiation into neuronal and osteogenic subtypes, MTSCs revealed strongly reduced expression levels of CD90 in comparison to human MSCs in vitro. Our findings therefore suggest MTSCs and OE-MSCs to be different stem cell populations residing in a similar but not identical niche.

Next to NCSC populations residing within the olfactory epithelium of the middle and superior turbinates, stem cells isolated from the inferior turbinate likewise reveal a neural crest origin accompanied by an extraordinary broad differentiation potential in vitro [11] Greiner, 2011 #18} [19] and in vivo [7]. Unfortunately, a total turbinectomy of the inferior turbinate impairs the air conditioning capacity of the nasal cavity significantly compared to the total middle turbinectomy [28], and may in rare cases also result in an empty nose syndrome [29]. Although not severely impairing the air conditioning capacity, OECs mainly derived from the superior turbinate or olfactory bulb are sometimes more restricted in terms of complexity of surgery [15] and accessibility [14]. In contrast to these both tissue sources middle turbinate tissue applied in the present study is routinely obtained in high amounts during nasal surgery indicated due to turbinate hyperplasia without severely affecting respiration and olfactory sensing [28, 29]. Notably, such high amounts of middle turbinate tissue can be directly used for isolation of large numbers of MTSCs. Given the necessity to expand adult stem cells after their isolation in vitro to gain sufficient amounts of cells for transplantation into the patient, initial isolation of large quantities of MTSCs emphasizes the potential suitability of this novel stem cell population for clinical applications. In addition to these benefits of the here identified NCSC-source, MTSCs were successfully cultivated within a 3D-fibrin matrix derived from human blood plasma. Being the key player in the coagulation cascade of proteins during wound healing, fibrin is broadly used in clinical sealant [30] or adhesive for skin transplantation [31] and was already shown to be beneficial for graft survival [32]. Accordingly, fibrin matrices were described to be suitable for cultivating hMSC [33] and NCSCs [18] as well as differentiating adipose-derived stem cells [34]. Using the 3D-culture technique applied in the present study, we recently described the expansion of NCSCs from the inferior turbinate in a completely closable and clinically accredited cultivation system based on fluoroethylenepropylene bags. Here, NCSCs kept their highly proliferative character, while maintaining their capability to differentiate into mesodermal and ectodermal cell types [35]. Accordingly, our findings suggest a similar potential expansion system for MTSCs. Since the here described successful cultivation of MTSCs still exhibited high clonal efficiency and a broad differential potential. Especially the differential potential into the neuronal lineage supports the neural crest origin.

In summary, we describe here for the first time a new source of human adult neural crest-derived stem cells within the nasal cavity. Given the high amounts of routinely obtained middle turbinate tissue combined with a broad differentiation potential and high clonal efficiency, MTSCs seem to be an ideal candidate for applications in pharmacological research and regenerative medicine. Here, MTSCs may be applied for treating complex injuries after severe accidents or tumor therapy.

Compliance with Ethical Standards

References

1. Wagers, A. J., & Weissman, I. L. Plasticity of adult stem cells. *Cell 2004;116*:639 – 48.
2. Schofield, R. (1978). The relationship between the spleen colony-forming cell and the haemopoietic stem cell. *Blood Cells, 4*, 7–25.
3. Collins, C. A., Olsen, I., Zammit, P. S., et al. (2005). Stem cell function, self-renewal, and behavioral heterogeneity of cells from the adult muscle satellite cell niche. *Cell, 122*, 289–301.
4. Clewes, O., Narytnyk, A., Gillinder, K. R., Loughney, A. D., Murdoch, A. P., & Sieber-Blum, M. Human epidermal neural crest stem cells (hepi-ncsc)-characterization and directed differentiation into osteocytes and melanocytes. *Stem Cell Reviews* 2011.
5. Dupin, E., & Sommer, L. (2012). Neural crest progenitors and stem cells: from early development to adulthood. *Developmental Biology, 366*, 83–95.
6. Murrell, W., Feron, F., Wetzig, A., et al. (2005). Multipotent stem cells from adult olfactory mucosa. *Developmental Dynamics, 233*, 496–515.
7. Müller, J., Ossig, C., Greiner, J. F., et al. (2015). Intrastriatal transplantation of adult human neural crest-derived stem cells improves functional outcome in Parkinsonian rats. *Stem Cells Translational Medicine, 4*, 31–43.014.
8. His, W. (1868). *Untersuchungen über die erste Anlage des Wirbeltierleibes. Die erste Entwicklung des Hühnchens im Ei*. Leipzig: Vogel.

9. Kaltschmidt, B., Kaltschmidt, C., & Widera, D. (2012). Adult craniofacial stem cells: sources and relation to the neural crest. *Stem Cell Reviews, 8*, 658 – 71.

10. Toma, J. G., Akhavan, M., Fernandes, K. J., et al. (2001). Isolation of multipotent adult stem cells from the dermis of mammalian skin. *Nature Cell Biology, 3*, 778 – 84.

11. Hauser, S., Widera, D., Qunneis, F., et al. (2012). Isolation of novel multipotent neural crest-derived stem cells from adult human inferior turbinate. *Stem Cells and Development, 21*, 742 – 56.

12. Tabakow, P., Raisman, G., Fortuna, W., et al. Functional regeneration of supraspinal connections in a patient with transected spinal cord following transplantation of bulbar olfactory ensheathing cells with peripheral nerve bridging. *Cell Transplantation* 2014.

13. Arthur, A., Rychkov, G., Shi, S., Koblar, S. A., & Gronthos, S. (2008). Adult human dental pulp stem cells differentiate toward functionally active neurons under appropriate environmental cues. *Stem Cells, 26*, 1787–1795.

14. Nakashima, T., Kimmelman, C. P., & Snow, J. B. Jr. (1984). Structure of human fetal and adult olfactory neuroepithelium. *Archives of Otolaryngology, 110*, 641–646.

15. Feron, F., Perry, C., Cochrane, J., et al. (2005). Autologous olfactory ensheathing cell transplantation in human spinal cord injury. *Brain, 128*, 2951–2960.

16. Murrell, W., Wetzig, A., Donnellan, M., et al. (2008). Olfactory mucosa is a potential source for autologous stem cell therapy for Parkinson's disease. *Stem Cells, 26*, 2183–2192.

17. Mackay-Sim, A. (2005). Olfactory ensheathing cells and spinal cord repair. *The Keio Journal of Medicine, 54*, 8–14.

18. Greiner, J. F., Hauser, S., Widera, D., et al. (2011). Efficient animal-serum free 3D cultivation method for adult human neural crest-derived stem cell therapeutics. *European Cell & Materials, 22*, 403 – 19.

19. Hofemeier, A. D., Hachmeister, H., Pilger, C., et al. (2016). Label-free nonlinear optical microscopy detects early markers for osteogenic differentiation of human stem cells. *Scientific Reports, 6*, 26716.

20. Muller, J., Greiner, J. F., Zeuner, M., et al. (2016). 1,8-Cineole potentiates IRF3-mediated antiviral response in human stem cells and in an ex vivo model of rhinosinusitis. *Clinical Science (London), 130*, 1339–1352.

21. Delorme, B., Nivet, E., Gaillard, J., et al. (2010). The human nose harbors a niche of olfactory ectomesenchymal stem cells displaying neurogenic and osteogenic properties. *Stem Cells and Development, 19*, 853 – 66.

22. Damm, M., Vent, J., Schmidt, M., et al. (2002). Intranasal volume and olfactory function. *Chemical Senses, 27*, 831–839.

23. Barnett, S. C., Alexander, C. L., Iwashita, Y., et al. (2000). Identification of a human olfactory ensheathing cell that can effect transplant-mediated remyelination of demyelinated CNS axons. *Brain, 123*(Pt 8), 1581–1588.

24. Barraud, P., Seferiadis, A. A., Tyson, L. D., et al. (2010)Neural crest origin of olfactory ensheathing glia. *Proceedings of the National Academy of Sciences of the United States of America ;107*:21040–5.

25. Viktorov, I. V., Savchenko, E. A., & Chekhonin, V. P. (2007). Spontaneous neural differentiation of stem cells in culture of human olfactory epithelium. *Bulletin of Experimental Biology and Medicine, 144*, 596–601.

26. Jahed, A., Rowland, J. W., McDonald, T., Boyd, J. G., Doucette, R., & Kawaja, M. D. (2007). Olfactory ensheathing cells express smooth muscle alpha-actin in vitro and in vivo. *The Journal of Comparative Neurology, 503*, 209 – 23.

27. Nivet, E., Vignes, M., Girard, S. D., et al. (2011). Engraftment of human nasal olfactory stem cells restores neuroplasticity in mice with hippocampal lesions. *The Journal of Clinical Investigation, 121*, 2808–2820.

28. Dayal, A., Rhee, J. S., & Garcia, G. J. (2016). Impact of middle versus inferior total turbinectomy on nasal aerodynamics. *Otolaryngology–Head and Neck Surgery: Official Journal of American Academy of Otolaryngology-Head and. Neck Surgery, 155*, 518 – 25.

29. Scheithauer, M. O. (2010). Surgery of the turbinates and "empty nose" syndrome. *GMS Current Topics Otorhinolaryngol Head Neck Surgery, 9*, Doc03.

30. Modi, P., & Rahamim, J. (2005). Fibrin sealant treatment of splenic injuries during oesophagectomy. *European Journal Cardiothoracic Surgery, 28*, 167–168.

31. Dahlstrom, K. K., Weis-Fogh, U. S., Medgyesi, S., Rostgaard, J., & Sorensen, H. The use of autologous fibrin adhesive in skin transplantation. *Plastic and Reconstructive Surgery* 1992;89:968 – 72; discussion 73 – 6.

32. Gerard, C., Forest, M. A., Beauregard, G., Skuk, D., & Tremblay, J. P. (2012). Fibrin gel improves the survival of transplanted myoblasts. *Cell Transplantation, 21*(1), 127 – 37.

33. Ho, W., Tawil, B., Dunn, J. C., & Wu, B. M. (2006). The behavior of human mesenchymal stem cells in 3D fibrin clots: dependence on fibrinogen concentration and clot structure. *Tissue Engineering, 12*, 1587–1595.

34. Peterbauer-Scherb, A., Danzer, M., Gabriel, C., van Griensven, M., Redl, H., & Wolbank, S. (2012). In vitro adipogenesis of adipose-derived stem cells in 3D fibrin matrix of low component concentration. *Journal Tissue of Engineering and Regenerative Medicine, 6*, 434 – 42.

35. Greiner, J. F., Grunwald, L. M., Muller, J., et al. (2014). Culture bag systems for clinical applications of adult human neural crest-derived stem cells. *Stem Cell Research & Therapy, 5*, 34.

Original Research Report

Nanopore Sequencing reveals global Transcriptome Signatures of mitochondrial and ribosomal Gene Expressions in various human Cancer Stem-like Cell Populations

Kaya E. Witte*, Oliver Hertel*, Beatrice A. Windmöller, Laureen P. Helweg, Anna L. Höving, Cornelius Knabbe, Tobias Busche, Johannes F. W. Greiner, Jörn Kalinowski, Thomas Noll, Fritz Mertzlufft, Morris Beshay, Jesco Pfitzenmaier, Barbara Kaltschmidt, Christian Kaltschmidt, Constanze Banz-Jansen* and Matthias Simon*

Article

Nanopore Sequencing Reveals Global Transcriptome Signatures of Mitochondrial and Ribosomal Gene Expressions in Various Human Cancer Stem-like Cell Populations

Kaya E. Witte [1,2,*,†], Oliver Hertel [3,4,†], Beatrice A. Windmöller [1,2], Laureen P. Helweg [1,2], Anna L. Höving [1,5], Cornelius Knabbe [2,5], Tobias Busche [4], Johannes F. W. Greiner [1,2], Jörn Kalinowski [4], Thomas Noll [3,4], Fritz Mertzlufft [2,6], Morris Beshay [2,7], Jesco Pfitzenmaier [2,8], Barbara Kaltschmidt [1,2,9], Christian Kaltschmidt [1,2], Constanze Banz-Jansen [2,10,‡] and Matthias Simon [2,11,‡]

[1] Department of Cell Biology, Faculty of Biology, University of Bielefeld, Universitätsstrasse 25, 33699 Bielefeld, Germany; Beatrice.windmoeller@uni-bielefeld.de (B.A.W.); l.helweg@uni-bielefeld.de (L.P.H.); Anna.hoeving@uni-bielefeld.de (A.L.H.); Johannes.greiner@uni-bielefeld.de (J.F.W.G.); Barbara.kaltschmidt@uni-bielefeld.de (B.K.); C.Kaltschmidt@uni-bielefeld (C.K.)

[2] Forschungsverbund BioMedizin Bielefeld, OWL (FBMB e.V.), Maraweg 21, 33699 Bielefeld, Germany; cknabbe@hdz-nrw.de (C.K.); fritz.mertzlufft@evkb.de (F.M.); Morris.Beshay@evkb.de (M.B.); Jesco.Pfitzenmaier@evkb.de (J.P.); Constanze.Banz-Jansen@evkb.de (C.B.-J); Matthias.Simon@evkb.de (M.S.)

[3] Department of Cell Culture Technology, Faculty of Technology, University of Bielefeld, Universitätsstrasse 25, 33699 Bielefeld, Germany; oliver.hertel@uni-bielefeld.de (O.H.); Thomas.Noll@uni-bielefeld.de (T.N.)

[4] Center for Biotechnology-CeBiTec, University of Bielefeld, Universitätsstrasse 27, 33699 Bielefeld, Germany; tbusche@cebitec.uni-bielefeld.de (T.B.); joern@cebitec.uni-bielefeld.de (J.K.)

[5] Heart and Diabetes Centre NRW, Institute for Laboratory and Transfusion Medicine, Ruhr-University Bochum, 32545 Bad Oeynhausen, Germany

[6] Scientific Director of the Protestant Hospital of Bethel Foundation, University Medical School OWL at Bielefeld, Bielefeld University, Campus Bielefeld-Bethel, Maraweg 21, 33699 Bielefeld, Germany

[7] Department for Thoracic Surgery and Pneumology, Protestant Hospital of Bethel Foundation, University Medical School OWL at Bielefeld, Bielefeld University, Campus Bielefeld-Bethel, Burgsteig 13, 33699 Bielefeld, Germany

[8] Department of Urology and Center for Computer-assisted and Robotic Urology, Protestant Hospital of Bethel Foundation, University Medical School OWL at Bielefeld, Bielefeld University, Campus Bielefeld-Bethel, Burgsteig 13, 33699 Bielefeld, Germany

[9] Molecular Neurobiology, Faculty of Biology, Bielefeld University, Universitätsstrasse 25, 33699 Bielefeld, Germany

[10] Department of Gynecology and Obstetrics, and Perinatal Center, Protestant Hospital of Bethel Foundation, University Medical School OWL at Bielefeld, Bielefeld University, Campus Bielefeld-Bethel, Burgsteig 13, 33699 Bielefeld, Germany

[11] Department of Neurosurgery and Epilepsy Surgery, Protestant Hospital of Bethel Foundation, University Medical School OWL at Bielefeld, Bielefeld University, Campus Bielefeld-Bethel, Burgsteig 13, 33699 Bielefeld, Germany

* Correspondence: Kaya.friedrich@uni-bielefeld.de; Tel.: +49-521-106-5629

† Authors contributed equally as co-first authors.

‡ Authors contributed equally as co-last authors.

Simple Summary: Cancer is the leading cause of death in the industrialized world. In particular, so-called cancer stem cells (CSCs) play a crucial role in disease progression, as they are known to contribute to tumor growth and metastasis. Thus, CSCs are heavily investigated in a broad range of cancers. Nevertheless, global transcriptomic profiling of CSC populations derived from different tumor types is rare. We established three CSC populations from tumors in the uterus, brain, lung, and prostate and assessed their global transcriptomes using nanopore full-length cDNA sequencing, a new technique to assess insights into global gene profile. We observed common expression in all CSCs for distinct genes encoding proteins for organelles, such as ribosomes, mitochondria, and proteasomes. Additionally, we detected high expressions of inflammation- and immunity-related genes. Conclusively, we observed high similarities between all CSCs independent of their tumor of origin, which may build the basis for identifying novel therapeutic strategies targeting CSCs.

Abstract: Cancer stem cells (CSCs) are crucial mediators of tumor growth, metastasis, therapy resistance, and recurrence in a broad variety of human cancers. Although their biology is increasingly investigated within the distinct types of cancer, direct comparisons of CSCs from different tumor types allowing comprehensive mechanistic insights are rarely assessed. In the present study, we isolated CSCs from endometrioid carcinomas, glioblastoma multiforme as well as adenocarcinomas of lung and prostate and assessed their global transcriptomes using full-length cDNA nanopore sequencing. Despite the expression of common CSC markers, principal component analysis showed a distinct separation of the CSC populations into three clusters independent of the specific type of tumor. However, GO-term and KEGG pathway enrichment analysis revealed upregulated genes related to ribosomal biosynthesis, the mitochondrion, oxidative phosphorylation, and glycolytic pathways, as well as the proteasome, suggesting a great extent of metabolic flexibility in CSCs. Interestingly, the GO term "NF-kB binding" was likewise found to be elevated in all investigated CSC populations. In summary, we here provide evidence for high global transcriptional similarities between CSCs from various tumors, which particularly share upregulated gene expression associated with mitochondrial and ribosomal activity. Our findings may build the basis for identifying novel therapeutic strategies targeting CSCs.

Keywords: cancer stem cells; endometrioid carcinoma; glioblastoma multiforme; lung adenocarcinoma; prostate adenocarcinoma; nanopore sequencing; mitochondrion; ribosome

1. Introduction

Cancer stem cells (CSCs) are increasingly noticed to initiate tumor growth and to drive metastasis and tumor recurrence in a broad range of human cancers (reviewed in [1]). Within the highly heterogeneous tumor cell mass, CSCs represent only a small subpopulation [2] (reviewed in [3]), but possess stem-like properties like self-renewal, asymmetric division and multi-lineage differentiation [4–7] (reviewed in [1]). Moreover, CSCs remain hidden in the body of the patients until their reactivation by various stimuli leads to the regeneration of the tumor or to the formation of metastasis [8]. These characteristics facilitate the role of CSCs as major drivers of tumor formation and progression. From a therapeutic point of view, their quiescent-like state makes CSCs highly resistant to chemotherapeutic agents, while the low expression of major histocompatibility class I molecules enables the escape from immune surveillance by cytotoxic T-cells [9–11]. To gain a deeper understanding of CSC biology and potential treatment options, global transcriptional profiling has become a state-of-the-art tool during the recent years [12]. However, direct comparisons of CSCs from different tumor types are rarely assessed, although these may allow the identification of comprehensive mechanisms present in CSCs independent to the type of the tumor. In the present study, we isolated CSCs from endometrioid carcinomas, glioblastoma multiforme, as well as adenocarcinomas of lung and prostate, and assessed their global transcriptomes by nanopore RNA sequencing (RNA-Seq) to identify such potential common regulators and mechanisms.

Endometrial cancer is one of the most common sex-specific malignant diseases in women worldwide. Annually, about 320,000 women are diagnosed with endometrial cancer. Especially in high-income countries, the incidence of endometrial cancer is high, at 5.9% [13]. Major risk factors are obesity, physical inactivity, and elevated estrogen levels in postmenopausal women [14,15]. In Europe and North America, endometrial cancer is the most frequent cancer of the female genital tract. However, it is mainly presented with postmenopausal bleeding and therefore in most cases diagnosed at an early stage. Nevertheless, it is more and more emphasized that a small subpopulation of tumor stem-like cells with clonogenic, self-renewing, differentiating and tumorigenic properties are responsible for the production of endometrial carcinoma cells [4]. Additionally, endometrial

CSCs seem to play a role in chemoresistance of endometrial carcinomas, as increased expression of CSC markers were shown to enrich resistance to cisplatin, placlitaxel and doxorubicin [16].

Being the most common primary brain tumor, glioblastoma multiforme (GBM) possesses a high cellular heterogeneity and aggressiveness accompanied by an extensive invasiveness and inevitable recurrence, resulting in an average survival time of less than 15 months [6,17–19]. As a description of the cellular composition, GBM tumors contain a relatively rare glioblastoma stem-like cell (GSC) population, which is able to self-renew and repopulate the whole tumor building [20]. GSCs can be found within the tumor infiltrating zone and therefore contribute prominently to a subsequent tumor recurrence [21]. On the contrary, differentiated GBM cells are considered as the main contributor to the tumor mass development [20,22–26]. In a therapeutic context, Happold and coworkers analyzed GSCs and described NF-κB RELA as a positive regulator of O6-methylguanine-DNA methyltransferase (MGMT) [27]. Of note, *MGMT* promoter hypermethylation has proven an important predictive biomarker for benefit from alkylating chemotherapy as well as a powerful prognostic factor in gliomas [28,29].

Lung cancer is the leading cause of cancer-related deaths worldwide. According to its histological differentiation, it is classified into small-cell lung cancer and non-small cell lung cancer (NSCLC), which is the most frequent form with an incidence of about 80% [30]. In the last few years, target therapy or immune therapy has been gaining popularity. Nevertheless, the overall prognosis of NSCLC is bad, with a five-year survival rate of only 15% [31]. A meta-analysis evaluating the effect of CSC markers on the clinicopathological characteristics of lung cancer revealed a significant association with poor differentiation and metastasis [32]. Accordingly, CSCs were reported to be responsible for therapy resistance and tumor growth as well as metastasis in lung cancer [5]. Moreover, lung cancer stem-like cells (LCSCs) were shown to be regulated by NF-κB [33], as already mentioned for GSCs.

Prostate cancer (PCa) is the most common sex-specific cancer within industrialized countries as well as the second leading cause of cancer deaths (10%) in men [34]. PCas are described as having an epithelial origin and an almost exclusive occurrence as an acinar adenocarcinoma [35]. PCa mainly occurs in the elderly, from the age of at least 65 years, and can be detected using prostate-specific antigen-testing, enabling early stage detection [36]. The overall mortality is only reduced by performing a radically prostatectomy [37]. Relating to further therapeutic options, luminal epithelial stem cells could be revealed as the origin of PCa via lineage tracing in mice [38]. In context with CSCs, prostate tumor spheres, originating from prostate cancer stem-like cells (PCSCs), were also shown to express a constitutive NF-κB signaling and inherent increased IL-6 levels [39].

Here, we established cultures of CSCs and analyzed three of each cancer type via RNA-Seq on global transcriptome level. We used the recently developed nanopore sequencing technology (reviewed in [40]) and a protocol for generating full length cDNA to identify common regulators and mechanisms present in CSCs independent to the tumor origin.

2. Materials and Methods

2.1. Cancer Stem–like Cell Population Establishment and Cultivation

Cancer tissue samples used to isolate CSCs were obtained during surgical resection and were kindly provided by the Forschungsverbund BioMedizin Bielefeld/OWL (FBMB e.V.) at the Protestant Hospital of Bethel Foundation (Bielefeld, Germany) after assuring routine histopathological analysis. Primary tumor samples were collected from each tumor type, including three endometrioid carcinomas, three glioblastomas, and three adenocarcinomas of the lung and prostate, respectively. Informed consent according to local and international guidelines was signed by all patients and further experimental procedures were ethically approved (Ethics committee Münster, Germany, 2017-522-f-S).

Samples were transferred into ice-cold Dulbecco's phosphate buffered saline (PBS; Sigma Aldrich, Munich, Germany) and for further processing transported to the University of Bielefeld. Tumor tissue was mechanically disintegrated followed by enzymatic digestion with collagenase for 2 h at 37 °C as described previously [41,42]. The minced tissue was cultured on gelatin (bovine skin-derived, type B; Sigma Aldrich)-coated culture dishes in CSC-selective medium composed of Dulbecco's modified Eagle's medium/Ham's F-12 (Sigma Aldrich) with the addition of 2 mM L-glutamine (Sigma Aldrich), penicillin/streptomycin (100 μg/mL; Sigma Aldrich), epidermal growth factor (EGF; 20 ng/mL; MiltenyiBiotec, Bergisch Gladbach, Germany), basic fibroblast growth factor-2 (bFGF-2; 40 ng/mL; Miltenyi Biotec), B27 supplement (Gibco, Thermo Fisher Scientific, Bremen, Germany) and 10% FCS (Sigma Aldrich). Enrichment of CSCs was achieved via serial trypsin treatment, as described by Walia et al. and Morata-Tarifa et al. [43,44]. Briefly, cells isolated by explant culture (passage 0) were washed with PBS and subsequently treated for 5 min with trypsin (Sigma Aldrich). Detached cells were transferred into a new gelatin pre-coated culture dish. Trypsinization and transfer of the cells were repeated every 48 to 72 h, at least for three cycles to assure stem-like characteristics in adherently grown and fibroblast-shaped cancer cells. For cultivation of free-floating spheres, CSC populations from endometrioid carcinoma and glioblastoma multiforme were cultured without the addition of serum for several days in regular growth medium supplemented with 4 μg/mL heparin (Sigma Aldrich).

2.2. Immunocytochemistry

For immunocytochemical staining of adherent CSC populations, cells were seeded at the top of sterilized coverslips with 15,000-30,000 cells per 4 cm^2 in 24-well plates with 0.5 mL growth medium and cultured initially for 48 to 72 h until cells reached 70–80% confluency. CSCs were fixed for 10 min with 4% para-formaldehyde in PBS. Blocking of free binding sides and permeabilization were performed with PBT solution, including 0.02% Triton-X-100 (Sigma Aldrich) and 5% goat serum (DIANOVA, Hamburg Germany) in PBS for 30 min. Next, three washing steps with PBS were performed as well as an incubation with primary antibodies for 1 h at room temperature (RT). Used antibodies for this study: anti-CD44 (1:400; 156-3C11; Cell Signaling, Frankfurt am Main, Germany), anti-CD133 (1:100; NB120-16518; NovusBio, Bio-Techne, Wiesbaden-Nordenstadt, Germany), anti-Nestin (1:200; MAB5326; Merck) and anti-MYC (10 μg/mL; Y69; Abcam, Cambridge, UK). After further washing steps, secondary fluorochrome-conjugated antibodies (Alexa Fluor 555 and -488 dyes; 1:300; goat anti-mouse and goat anti-rabbit; Life Technologies) were applied for 1 h at RT, protected from light. Nuclear staining were performed by using 4′,6-diamidino-2-phenylindole (DAPI; 1 μg/mL; Sigma Aldrich) for 10 min. Before CSC populations were embedded in Mowiol 4-88 (Carl Roth GmbH, Karlsruhe, Germany) upside down on the top of microscope slides, another washing step was performed. For fluorescence imaging, a confocal laser-scanning microscope (LSM 780; Carl Zeiss, Jena, Germany) was used.

For immunostaining of CSC spheres, free-floating cultured cells were fixed in 4% para-formaldehyde for 2 h, were further embedded in paraffin and sectionalized in 4 μm sections. Resulting slices were deparaffinized and rehydrated with xylol (Sigma Aldrich) as well as via ethanol in different steps. After reconditioning of the epitope with citrate buffer (pH 6), slices were washed in PBS and blocking of free binding sides were performed via incubation with 0.02% Triton-X 100, 10% appropriative serum and 1% bovine serum albumin (Sigma Aldrich) also in PBS for at least 2 h at RT. Next, incubation with primary antibodies was performed over night at 4 °C by using: anti-CD44 (1:50), anti-CD133 (1:100) and anti-MYC (10 μg/mL). Slices were washed three times with PBS and incubated for 1 h at RT with the Alexa Fluor 555 and −488 secondary fluorochrome-conjugated antibodies (1:300). Nuclear staining by using DAPI (1 μg/mL) as well as fluorescence imaging were processed equally to immunocytochemistry of adherently cultured CSCs.

2.3. RNA Isolation and Sequencing

RNA from 1×10^6 cultured CSCs of each population and cancer type were isolated by using the NucleoSpin® RNA Plus kit (Macherey-Nagel, Düren, Germany) according to manufacturer's guidelines. Quality and concentration of isolated RNAs were assessed via nanodrop ultraviolet spectrophotometry. Total RNA samples with RNA Integrity Numbers (RIN) > 9.5 were used to convert full-length RNA molecules that are both capped and polyadenylated to cDNA using the TeloPrime Full-Length cDNA Amplification Kit V2 (Lexogen, Vienna, Austria). Amplified full length cDNAs were then used to prepare Oxford Nanopore Technologies (ONT) compatible libraries using the Ligation Sequencing Kit LSK109 with the Native Barcoding Kit NBD104 (ONT, Oxford, UK), which were run on three R9.4 flowcells on the ONT system GridION. Base calling and demultiplexing were performed using Guppy v3.1.5.

2.4. Preprocessing and Genome Alignment

Fastq files containing reads that passed the quality filtering were concatenated according to their barcodes from each flowcell. Since the three flowcells showed high correlation on gene count level, technical triplicates were merged accordingly. Sequencing adapters were trimmed using porechop v0.2.4 [45]. Trimming was checked using FastQC v0.11.9 [46]. Trimmed reads were aligned to the human RefSeq genome GRCh38.p13 [47,48] using minimap 2 [49]with the arguments -ax splice -p 0.99. Alignment files were converted to bam format using samtools v1.10.2 [50]. The bam files were quality checked using AlignQC v2.0.5 [51] samtools v1.10.2 [50]. As the alignments showed up to 15% trans-chimeric reads, which most likely resulted from the library preparation, those reads were removed from the alignments. Therefore, the chimera.bed file from the AlignQC output were converted to exclusion lists. Bam files were sorted using samtools v1.10.2 [50] and filtered using the FilterSamReads module of Picard Toolkit (http://broadinstitute.github.io/picard/) with the exclusion lists and the arguments --FILTER excludeReadList --SORT_ORDER. Mismatches and small indels were corrected using TranscriptClean [52] with the human RefSeq genome GRCh38.p13 [47]. These high-quality alignments were used as input for the estimation of gene abundances.

2.5. Gene Abundance Estimation and Enrichment Analysis

Mapped reads were assigned to genes and counted by the featureCounts module of the R/Bioconductor [53] package Rsubread v2.0.1 [54] with the arguments countMultiMappings = TRUE, fraction = TRUE, isLongRead = TRUE. The gtf file of the human RefSeq genome GRCh38.p13 [47] was used as external annotation. From genes with multiple integrations but the same exon structure, only one was retained, because they shared the same multimapping reads. These raw counts were grouped by the CSC populations and preprocessed using the R/Bioconductor package edgeR v3.28.1. [55,56]. Lowly expressed genes were filtered using the filterByExpr function with default arguments. Normalization factors were calculated using the trimmed mean of M-values method [57]. Differentially expressed genes (DEGs) were identified by an ANOVA-like testing using the generalized linear models with the quasi-likelihood F-test (glmQLFTest). The threshold of DEGs was set as p value < 0.05. Principle component analysis (PCA) was conducted using the R/Bioconductor package PCAtools v1.2.0 [58]. Heatmaps were created using the heatmap.2 function of the R package gplots v3.1.1 [59]. Correlation analysis was conducted using the R package Hmisc package [60]. Functional enrichment of GO-terms of genes expressed in all 12 CSC populations were calculated using the PANTHER classification system [61], while the DAVID database [62,63] served for calculating functional enriched KEGG pathways. Significantly (modified Fisher Exact p-value; $p < 0.05$) enriched GO-terms and pathways were visualized with Prism software (GraphPad Software, San Diego, CA, USA).

3. Results

3.1. Correlative Analysis of Characteristic Markers in Cancer Stem-like Cells from Endometrioid Carcinomas, Glioblastoma Multiforme, Lung- and Prostate Adenocarcinomas

In this study, 12 different CSC populations from four different carcinoma types were established. Carcinoma types included three endometrial carcinomas, three glioblastomas as well as three adenocarcinomas of the lung and the prostate, respectively. All female donors of the endometrial cancer stem-like cell populations (ECSCs) suffered from endometrioid carcinomas of the corpus uteri ranging WHO grade I-II and were aged between 72 and 86 years. Donors of GSCs were two males (42 and 69 years old) and one female (60 years old), all revealing glioblastoma multiforme. Glioblastomas of the donors of GSCs_a and GSCs_c revealed no mutation for the isocitrate dehydrogenase (NADP(+)) 1 (*IDH1*), whereas in the glioblastoma of the donor of GSCs_b *IDH1* was mutated. Additionally, *MGMT* promoter methylation status differed between the three donors, as glioblastomas of the donors of GSCs_a and GSCs_b depicted *MGMT* promoter methylation in contrast to the glioblastoma of donor GSCs_c. LCSC populations were derived from three relatively young female patients (aged between 49 and 61 years) all diseased with adenocarcinomas. Analysis of clinically relevant mutations revealed an epidermal growth factor receptor (*EGFR*) mutation for the donor of LCSCs_a as well as tumor tissue of the donor of LCSCs_c showed mutations in the genes for the KRAS proto-oncogene (*KRAS*) and serine/threonine kinase 11 (*STK11*). The three PCSCs were isolated from male patients aged between 57 and 72 years all suffering from acinar adenocarcinomas with WHO grade II, III and V (Table 1).

Table 1. Cell population-specific donor information.

Donor of Cell Population	Tumor Typing/Characterization	WHO Grade	Sex	Age
ECSCs_a	Endometrioid carcinoma of the corpus uteri	GII	female	72
ECSCs_b	Endometrioid carcinoma of the corpus uteri	GI	female	83
ECSCs_c	Endometrioid carcinoma of the corpus uteri with invasion of the outer half of the myometrium and invasion of the cervix uteri	GII	female	86
GSCs_a	Primary glioblastoma multiforme, *IDH1* wildtype with *MGMT* promoter methylation	GIV	female	60
GSCs_b	Secondary glioblastoma multiforme, *IDH1* mutation with *MGMT* promoter methylation	GIV	male	42
GSCs_c	Primary glioblastoma multiforme, *IDH1* wildtype without *MGMT* promoter methylation	GIV	male	69
LCSCs_a	Highly metastatic adenocarcinoma of the lung, *EGFR* mutation	n.a.	female	50
LCSCs_b	Multifocal adenocarcinoma of the lung	GII	female	61
LCSCs_c	Adenocarcinoma of the lung, *KRAS* and *STK11* mutation	GII	female	49
PCSCs_a	Acinar adenocarcinoma	GIII	male	71
PCSCs_b	Acinar adenocarcinoma	GII	male	57
PCSCs_c	Locally advanced acinar adenocarcinoma	GV	male	72

All cancer populations were cultured as adherently growing cells within stem cell-selective media after passing serial trypsin treatment, for enrichment of the respective CSC-population. Here, we used chemically defined medium containing EGF and bFGF-2, in accordance with the isolation of colorectal cancer stem-like cells as well as of adult human stem cells from the nasal cavity and the heart auricle [42,64–67]. In contrast with the successful isolation of human stem cells from the nasal cavity as free-floating spheres [64,65], adoption of the reported isolation process for human CSCs from solid tumors resulted in an unsatisfactory low culture efficacy and low growth rates. Therefore, we utilized an alternative method to enrich primary isolated CSCs, namely via differential trypsinization [42,44]. In accordance with a range of previous studies, we obtained trypsin-sensitive CSC populations with low attachment capability by culturing with 10% FCS [42–44,66,67]. Representative images of one of the successfully isolated CSC populations derived from endometrioid carcinomas, glioblastomas, lung and prostate adenocarcinomas revealed similar morphology independently of the origin of parental tumor tissues (Figure 1B–E). In accordance with the observations by Walia et al. and Elble et al., cultured CSCs depicted a fibroblast-like and spindle-shaped morphology after selection with dif-

ferential trypsin treatment [43]. To confirm the stem-like phenotype of isolated CSC populations, we determined the presence of characteristic CSC markers on protein level using immunocytochemistry. Notably, high levels of CD44, CD133, Nestin and MYC protein were detectable in adherently grown CSC populations from all tumor types as well as in spheres derived from ECSC_b and GSC_c (Figures S1 and S2 and Figure 2). Immunocytochemistry further revealed co-expressions of CD44 and CD133 as well as Nestin in isolated CSCs, independently to the tumor origin (Figure 2A and Figures S2 and S3). The proto-oncogene MYC was also detectable on protein level independent to the parental tumor tissue, particularly with a nuclear localization (Figure 2B and Figure S4). As an internal negative control and evaluation of the unique stem-like characteristics of isolated CSCs, human dermal fibroblasts (HDFs) were additionally immunocytochemically stained for CD44, CD133, Nestin and MYC. Here, HDFs showed no signs of CSC markers on protein level (Figure S5), emphasizing the CSC-like character of our isolated cell populations.
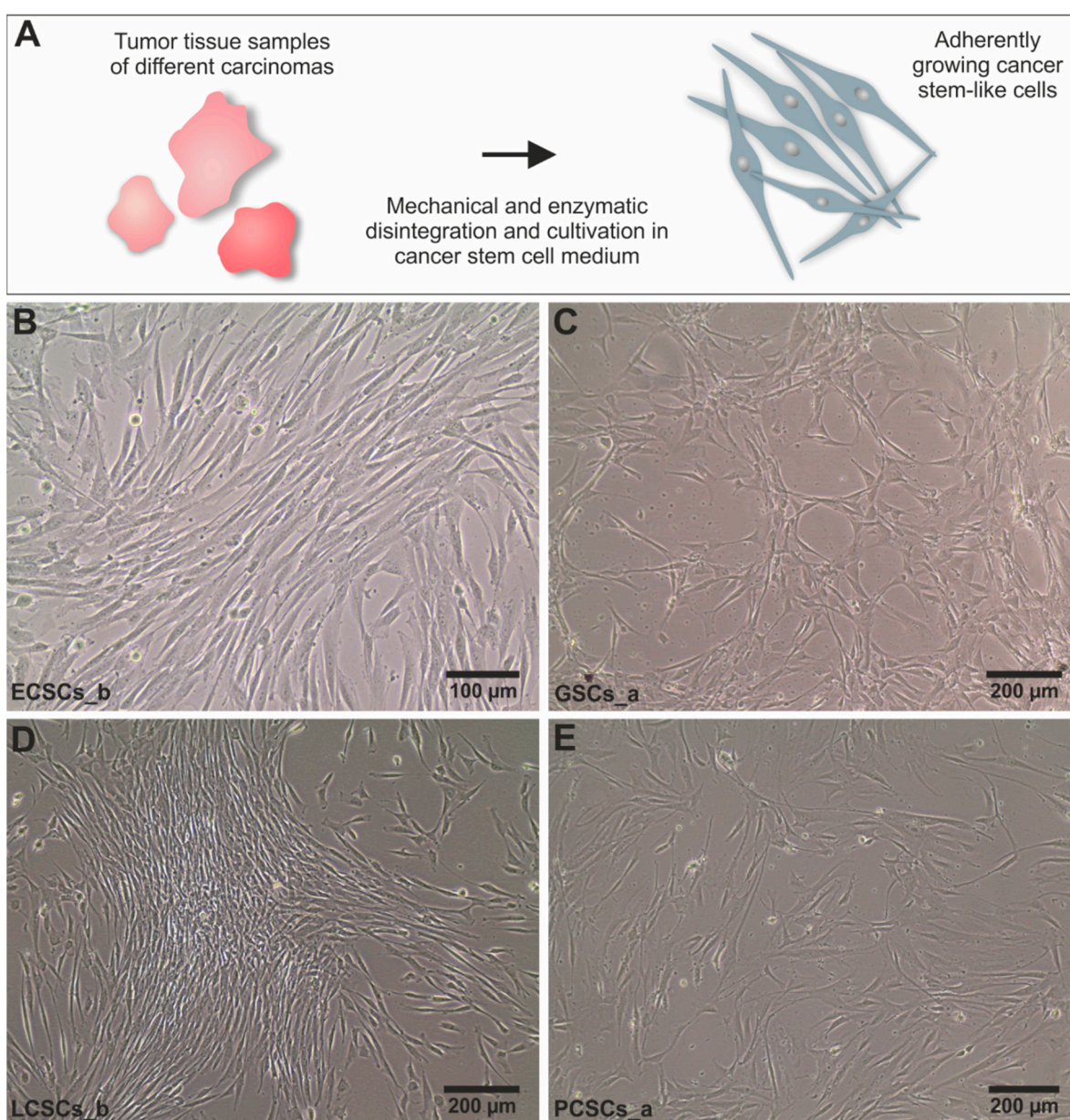
Figure 1. Isolation of cancer stem-like cell populations of four different types of carcinomas. (**A**) Schematic illustration of the isolation of cancer-stem-like cells out of primary tumor tissue. Representative pictures of adherently grown primary

cancer stem-like cells derived from parental tumor tissue of (**B**) endometrial cancer stem-like cells b (ECSCs_b), (**C**) glioblastoma stem-like cells a (GSCs_a), (**D**) lung cancer stem-like cells b (LCSCs_b) and (**E**) prostate cancer stem-like cells a (PCSCs_a).
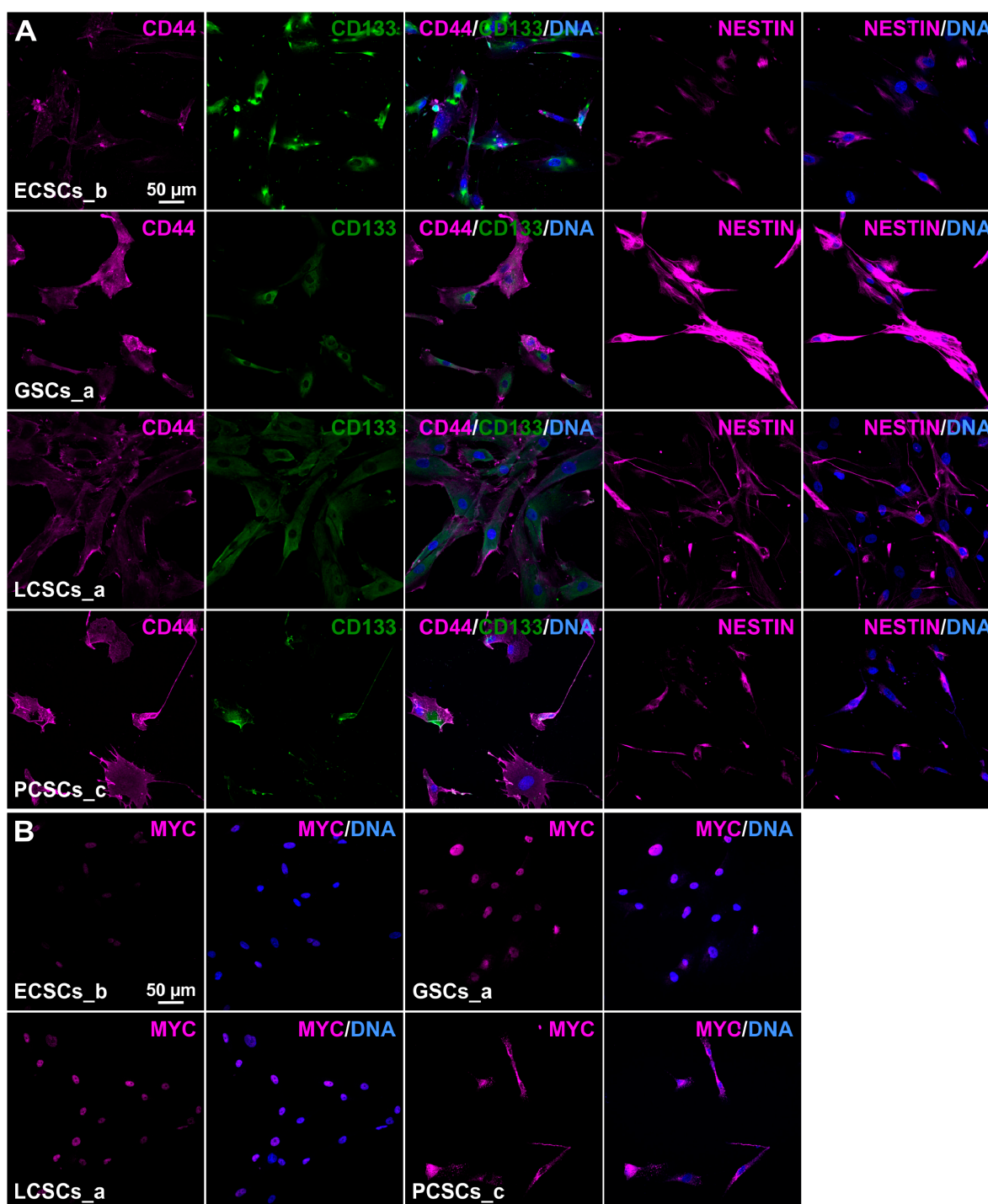
Figure 2. Immunocytochemistry of adherently grown cancer stem-like cell populations. (**A**) Representative immunostainings of co-expressed cancer stem cell (CSC) markers CD44/CD133 as well as Nestin, localized within the cytoplasm. (**B**) Exemplary depicted MYC expressions from one of each CSC population showed high frequencies of nuclear localizations of the analyzed protein. DAPI served in all cases for nuclear counterstaining.

For in-depth analysis of the gene expression of the 12 isolated CSC populations nanopore cDNA sequencing was used. Full-length cDNA sequencing was conducted using three R9.4 flowcells on the ONT system GridION. Only reads that passed the default quality criteria of the Guppy basecaller were further investigated. All sequencing runs yielded

10,627,235 reads (11.2 Gbp of sequence) with a mean read length of 1056 bp and a mean quality score of 21.3. Reads were aligned to the human genome (hg38) using minimap2 [49]. We observed a read alignment rate of 99.2% and an error rate of 7.3%, which was reduced to 0.69% using TranscriptClean [52] for correction. To check the reproducibility of gene counts between the technical triplicates, fastq files from the different flowcells were preprocessed, mapped, corrected, and quantified separately. Subsequent analysis showed strong correlation between respective flowcells (mean Spearman correlation co-efficient ϱ = 0.94). All datasets were processed similarly and gene expression of specific CSC markers was investigated firstly. CSC marker *CD44* was ubiquitously expressed in all 12 CSC populations. Analysis of the co-expression of *CD44* with further CSC markers revealed expression of MYC proto-oncogene (*MYC*) in all CSC populations, except for ECSCs_c. Here, especially LCSCs_a and GSCs_c showed high expression of *MYC* (Figure 3A). Further quantification depicted *Nestin* expression in LCSCs_a, _c, PCSCs_a, _c as well as in GSCs_a and ECSCs_b (Figure 3B). Pluripotency marker Kruppel-like factor 4 (*KLF4*) and aldehyde dehydrogenase 1 (*ALDH1*) were only expressed in three of 12 CSC populations each, as *KLF4* was only observable in GSCs_b, _c and PCSCs_c and *ALDH1* in LCSCs_b, _c as well as in PCSCs_c (Figure 3C,D). In CSC populations PCSCs_a and GSCs_b, expression of epithelial cell adhesion molecule (*EPCAM*) was detectable (Figure 3E). Additionally, PCSCs_c and ECSCs_b expressed ATP binding cassette subfamily G member 2 (*ABCG2*) (Figure 3F). On the contrary, we did not observe any expression of CSC markers Prominin-1 (*CD133*), SRY-box transcription factor 2 (*SOX2*), POU class 5 homeobox 1 (*OCT4*) and MYCN proto-oncogene in the here analyzed CSCs cultivated and sequenced as described above. In summary, all isolated CSC populations expressed the CSC marker *CD44*. Expression of further CSC markers was more heterogeneous, except for the expression level of *MYC*, which could be detected in 11 of 12 CSC populations. *Nestin*, *KLF4*, *ALDH1*, *EPCAM* as well as *ABCG2* expression was incongruous, with no clear relation to the four different parental tumor groups.
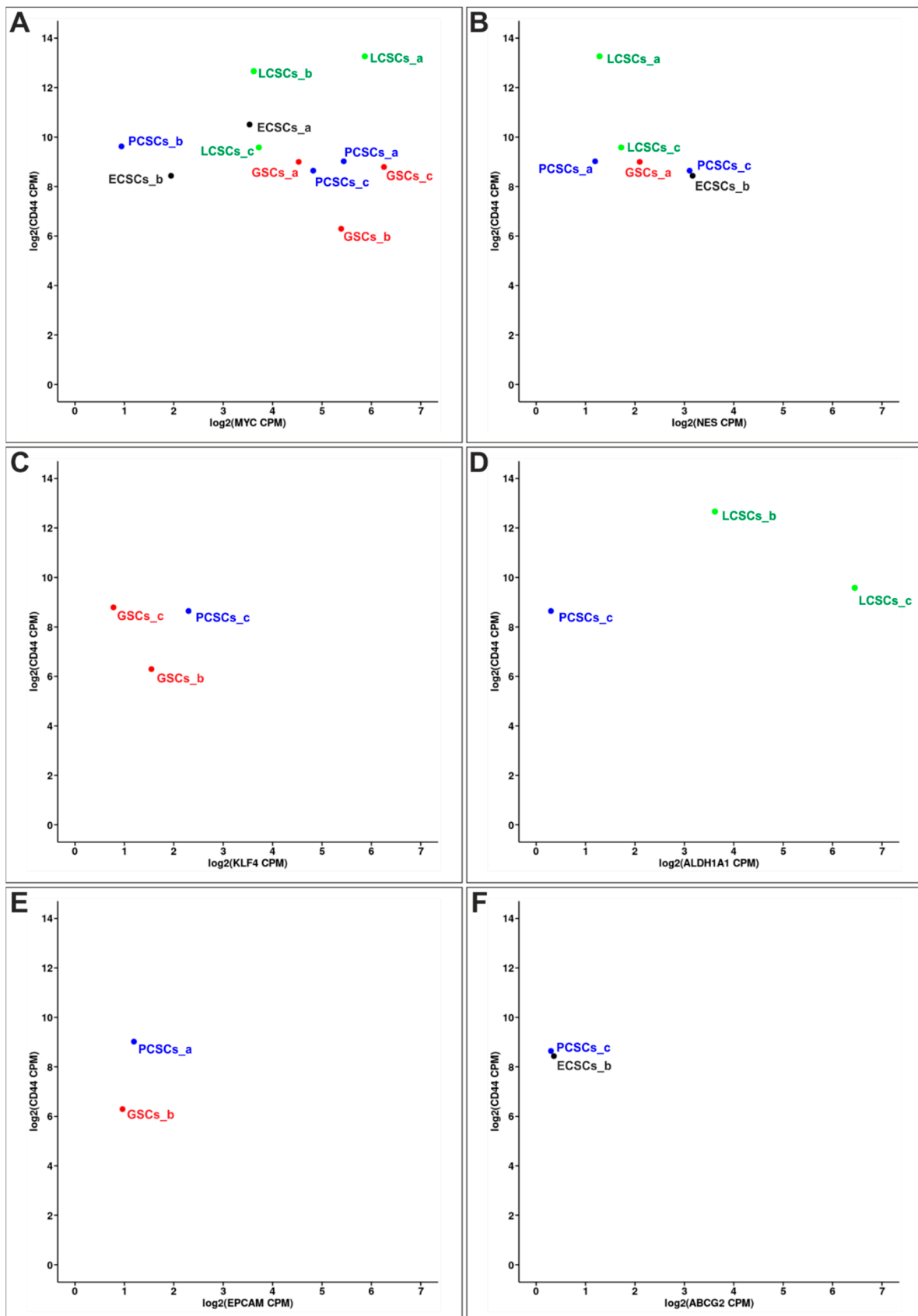
Figure 3. Correlated expression of CD44 with various other cancer stem cell (CSC) markers in different CSC populations. For each analysis, biological replicates depicted the mean of merged technical triplicates. (**A**) All CSC populations expressed CSC marker *CD44* and MYC proto-oncogene (*MYC*), except for endometrial cancer stem-like cell population c (ECSCs_c), which only expressed *CD44*. (**B**) CSC marker *Nestin* was expressed in lung cancer stem-like cells (LCSCs)_a

and _c, prostate cancer stem-like cells (PCSCs)_a and _c as well as in glioblastoma stem-like cells (GSCs)_a and ECSCs_b. (**C**) Pluripotency marker Kruppel like factor 4 (*KLF4*) was expressed in GSCs_b, GSCs_c and in PCSCs_c as well as (**D**) aldehyde dehydrogenase 1 (*ALDH1*) could be detected in LCSCs_b, LCSCs_c and PCSCs_c. (**E**) Epithelial cell adhesion molecule (*EPCAM*) was only observed in PCSCs_a and GSCs_b. (**F**) Expression of the ATP binding cassette subfamily G member 2 (*ABCG2*) gene could only be detected in PCSCs_c and ECSCs_b.

3.2. Global Gene Expression Analysis of Cancer Stem–like Cell Populations Reveals Distinct Clusters

After analysis of the expression of known CSC markers, global gene expression of the 12 isolated CSC populations was investigated. Similarly, processed datasets were used for PCA, revealing three dominant clusters among the 12 populations (Figure 4). Here, cluster one comprises all three ECSC populations and PCSCs_b. However, variances between the populations could be seen within this cluster, too. Second and biggest cluster consisted of all LCSC populations, the two remaining PCSC populations and two GSC populations. Within this cluster, LCSCs_a and LCSCs_b revealed less variances in comparison to LCSCs_c, which was clustered next to GSCs_a and GSCs_c. GSCs_b clustered independently, with the highest variance of PC1 between the group of LCSCs_a and LCSCs_b, in comparison with GSCs_b. PC2 differed with a variance of 23.73% with the greatest variation between ECSCs_c and GSCs_b (Figure 4).
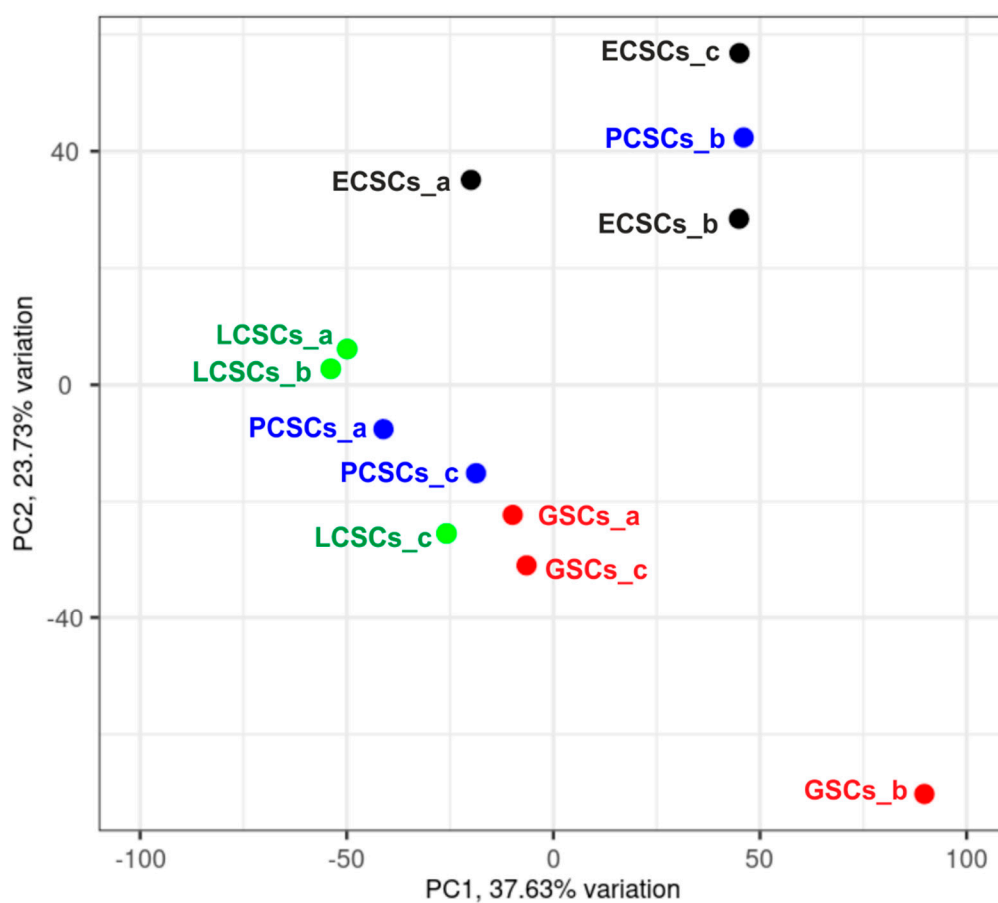
Figure 4. Comparison of gene expression profiles from different primary cancer stem-like cell (CSC) populations. Principal component analysis reveals two predominant clusters of CSCs, independently of the parental tumor types. Within the first cluster all three endometrial cancer stem-

like cells (ECSCs) are present and one of the three prostate cancer stem-like cell (PCSCs) populations. The second cluster comprises the two remaining PCSCs, all three lung cancer-derived stem-like cell populations (LCSCs) as well as glioblastoma stem-like cells a (GSCs_a) and GSCs_c. The population of GSCs_b clustered independently.

The large variance between the different CSC populations as well as patient-specific variations within the four distinct groups of endometrioid carcinomas, glioblastomas, and adenocarcinomas of lung and prostate, were also visible in a hierarchical clustered heatmap of the 200 top expressed genes (for all detected genes see Figure S6). Distribution of up- and down-regulated genes of the top 200 expressed genes followed the Gaussian distribution (Figure 5, for the 200 top expressed genes, which were not significantly regulated see Figure S7). Notably, tumor type-specific clustering was not observable. However, cross-group clustering emerged with GSCs_a, GSCs_c, LCSCs_c, and PCSCs_c forming one pattern. A second pattern could be seen for PCSCs_a, ECSCs_a, LCSCs_a and LCSCs_b. Further, ECSCs_b, PCSCs_b and ECSCs_c seemed to build one cluster-group (Figure 5). GSCs_b clustered independently, as already shown within the PCA (Figures 4 and 5). Of note, major histocompatibility complex class I A (*HLA-A*), major histocompatibility complex class I B (*HLA-B*) and interleukin 1 beta (*IL1B*) were detected in the top 200 expressed genes among the CSC populations.

Figure 5. Hierarchically clustered heatmap of the 200 top expressed logarithmic gene counts within all 12 cancer stem-like cell (CSC) populations. RNA samples of different CSCs are arranged according to their corresponding expression profiles.

Next to the general clustering, it has been noticed that especially genes involved in ribosome biosynthesis have occurred more frequently (Figure 6A–B). Here, 20 different genes encoding for ribosomal proteins that are components of the 60S subunit can be found. Further, 14 genes involved in the protein synthesis of the 40S subunit of the ribosome are clustered under the 200 top expressed genes. Nevertheless, expression levels of genes relevant for the ribosome biosynthesis differed between the 12 CSC populations.

Particularly striking was the high expression of diverse genes encoding for components of the 40S and 60S subunit in GSCs_b (Figure 6B). Additionally, PCSCs_b and ECSCs_c revealed high expression of ribosomal biosynthesis associated genes (Figure 6A). Among the enriched genes relevant for ribosome biosynthesis, we found distinct genes been highly expressed in GSCs_b (Figure 6A), while PCSCs_b and ECSCs_c showed other genes upregulated for ribosome biosynthesis (Figure 6B). As already shown within the dot plots, CSC marker *CD44* was ubiquitously expressed in all 12 CSC populations. Nevertheless, differences between the populations could be seen with LCSCs_a and LCSCs_b, revealing the highest expression (Figure 6A). Conspicuously, three genes of the S100 family are comprised within the top expressed genes among the 12 CSC populations, including *S100A13*, *S100A10* and *S100A6* (Figure 6A).
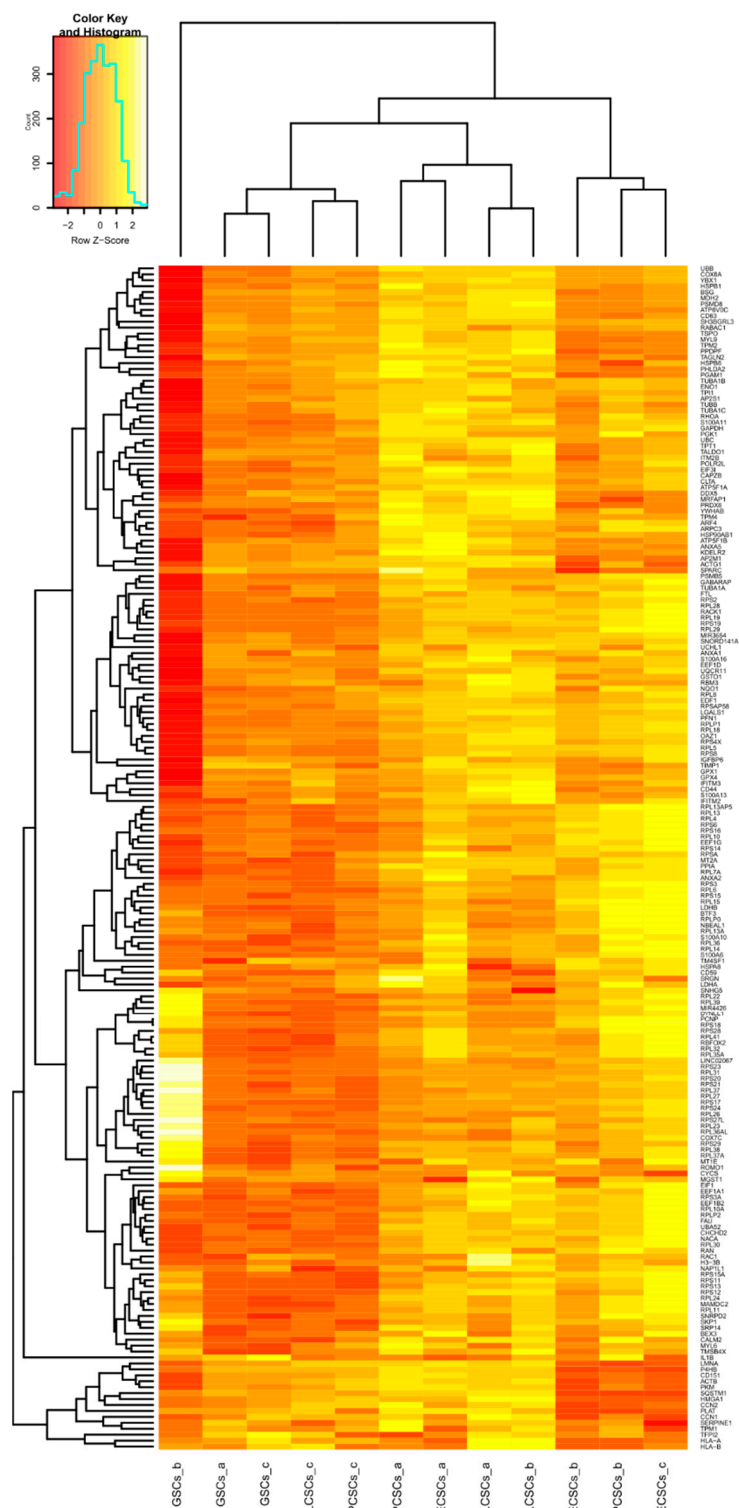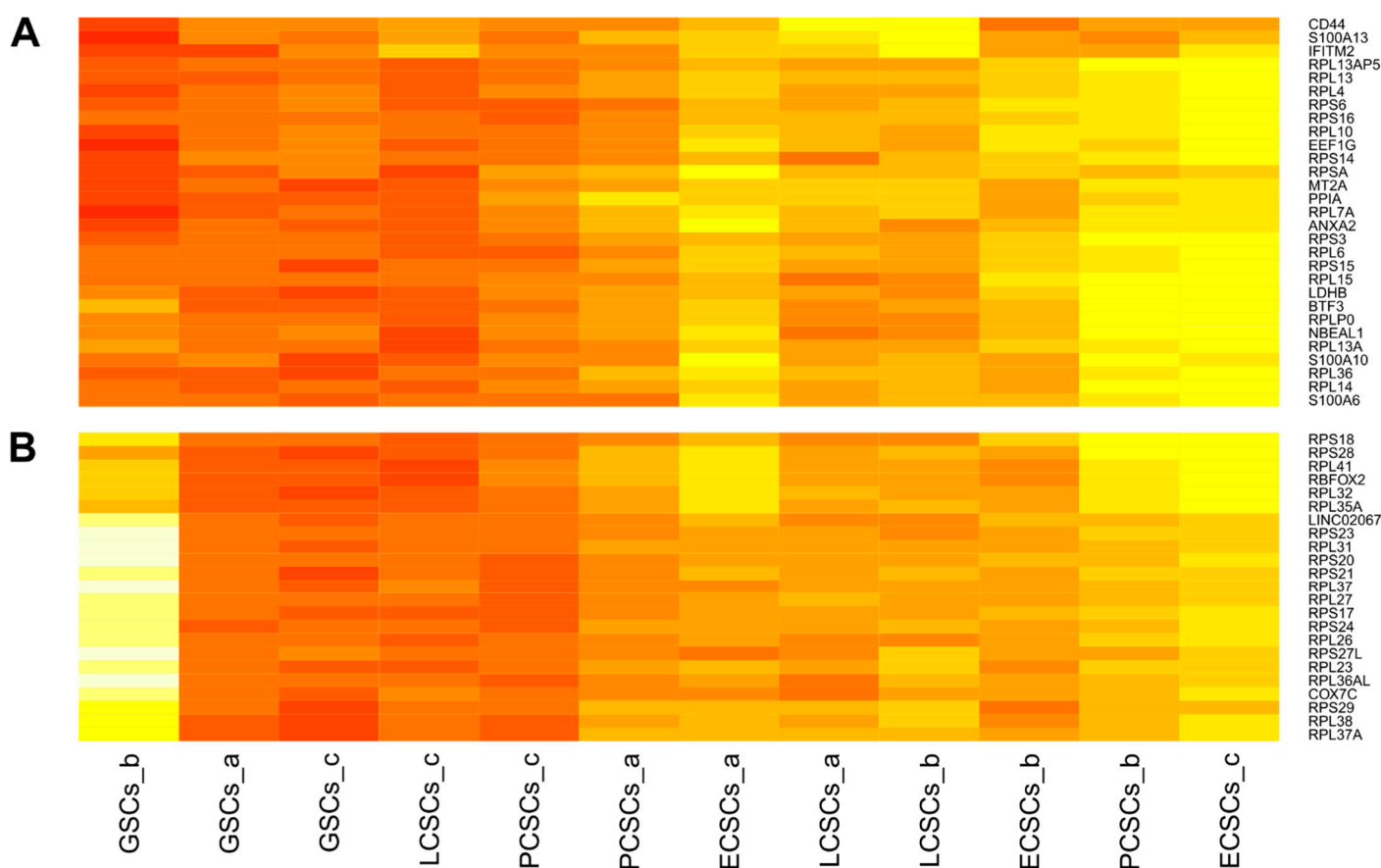

Figure 6. Two extracts of the hierarchically clustered heatmap of the 200 top expressed genes within all 12 cancer stem-like cell (CSC) populations. (**A**) Expressions of ribosomal biosynthesis associated genes were upregulated in endometrioid cancer stem-like cells c (ECSCs_c) and in prostate cancer stem-like cells b (PCSCs_b). Genes encoding for the S100 family were significantly expressed in all CSCs. (**B**) Expression levels of further genes relevant for ribosome biosynthesis differed between analyzed CSC populations, whereas glioblastoma stem-like cells b (GSCs_b) depicted the highest levels of genes responsible for the 40S and 60S subunit.

3.3. KEGG Pathway and GO-term Analysis Reveal Broad Similarities between the Cancer Stem-like Cell Populations

For an unbiased detailed analysis of the transcriptomic profiles of the 12 CSC populations, we performed a KEGG pathway analysis (Figure 7, Table S1). Here, five of the top enriched pathways were significantly overrepresented in all CSC populations and plotted together ($p < 0.05$). Next to the gene pathway responsible for "Ribosome", which owns the strongest significance ($p = 1.9 \times 10^{-41}$), also "Oxidative phosphorylation" ($p = 0.013$) and "Non-alcoholic fatty liver disease" ($p = 0.015$) displayed highly enriched pathways. Surprisingly, two unexpected signaling pathways were also significantly overrepresented,

namely the genes associated with "Parkinson's disease" (p = 0.004) and "Alzheimer's disease" (p = 0.005).
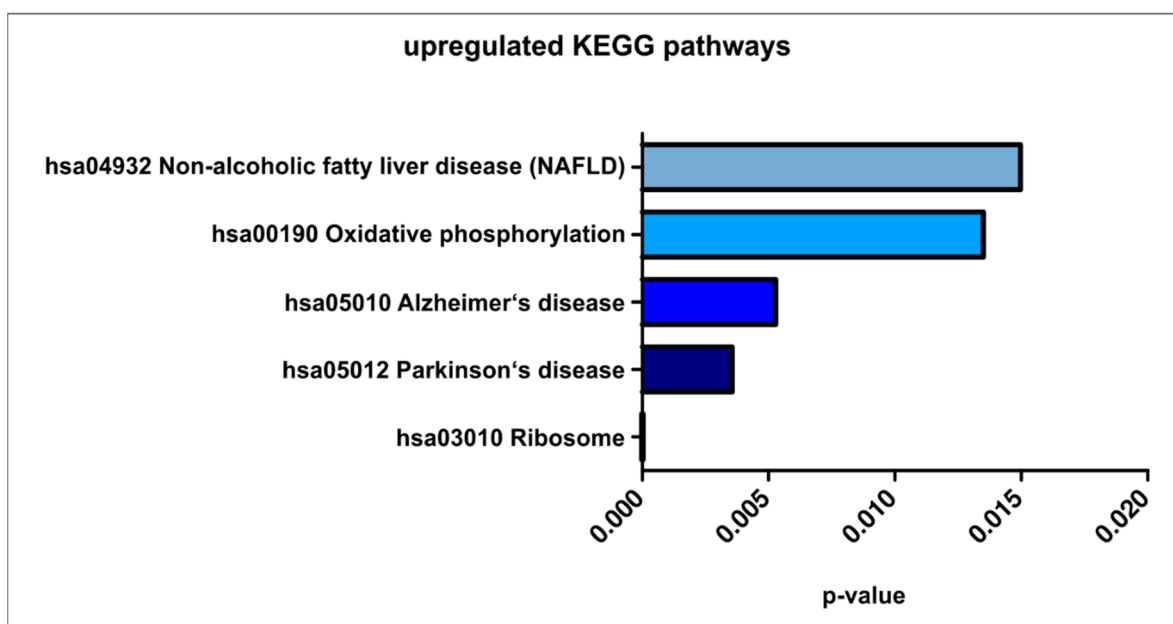
Figure 7. Top five upregulated KEGG pathways within the 12 investigated primary cancer stem-like cell populations ($p < 0.05$).

We further conducted GO-term enrichment analysis for a more specific insight into similarly upregulated terms from biological processes, cellular components and molecular functions (Figure 8). For enriched GO-terms relating to biological processes, the top ten terms were depicted in accordance with their fold enrichments (Figure 8A, Table S2). Here, genes involved in the glycolytic pathways (fructose and glycose) were highly enriched (see "methylglyoxal metabolic process"). Further, GO-terms "formation of cytoplasmic translation initiation complex" fitting to the enriched genes in ribosomal biosynthesis and "protein deneddylation" involved in ubiquitin-mediated proteasomal degradation were upregulated. Accordingly, GO-terms relating to the cellular components (Figure 8B, Table S3) showed six-fold upregulated genes involved in "translation preinitiation complex", "proteasome core complex, alpha-subunit complex" and "cytosolic large ribosomal subunit". Ribosome associated GO-terms were likewise found among the terms related to molecular function, such as "7S RNA binding", "5S rRNA binding" and "structural constituent of ribosome". Further, genes related to "peroxiredoxin activity" were highest enriched (Figure 8C). Additionally, "NF-κB binding" was found to be upregulated in all CSC populations (Table S4).
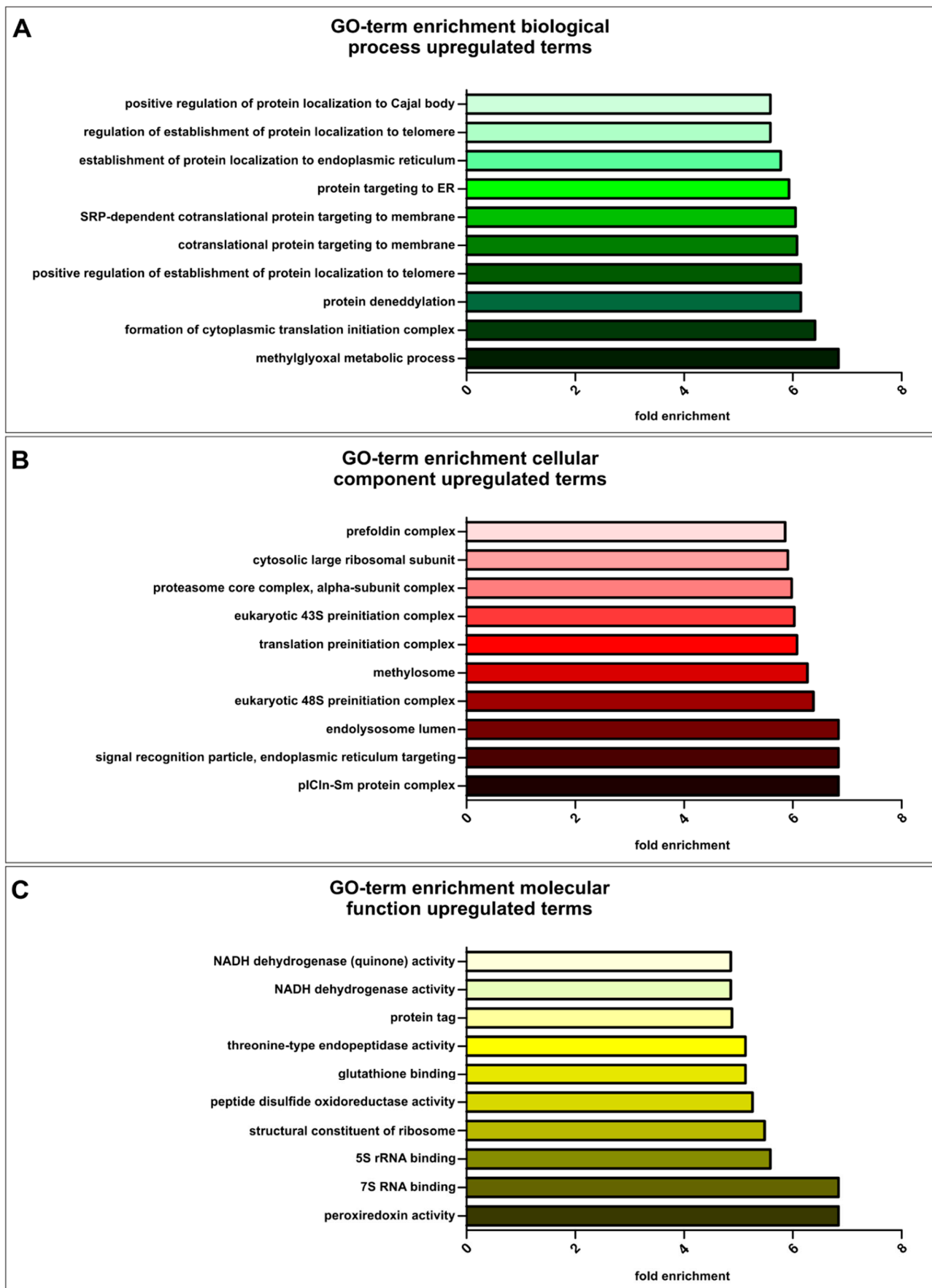
Figure 8. Gene ontology (GO)-term enrichment analysis of all 12 cancer stem-like cell populations, including all populations of endometrial-, glioblastoma-, lung- and prostate cancer stem-like cells, respectively. (**A**) Visualization of the top

ten fold enriched GO-terms involved in biological processes ($p < 2.00 \times 10^{-3}$). (**B**) Top ten of the fold enriched GO-terms concerning cellular components ($p < 1.38 \times 10^{-3}$). (**C**) Representation of fold enriched GO-terms associated with molecular functions ($p < 2.65 \times 10^{-4}$).

4. Discussion

In the present study, we report for the first time global transcriptional differences and similarities of CSCs from various tumors including glioblastoma multiforme, non-small cell lung carcinoma, endometrial carcinoma, and prostate carcinoma. We found the transcripts of all investigated CSC-populations to share significantly upregulated genes associated with the mitochondrion, proteasome, and ribosome (Figure 9).
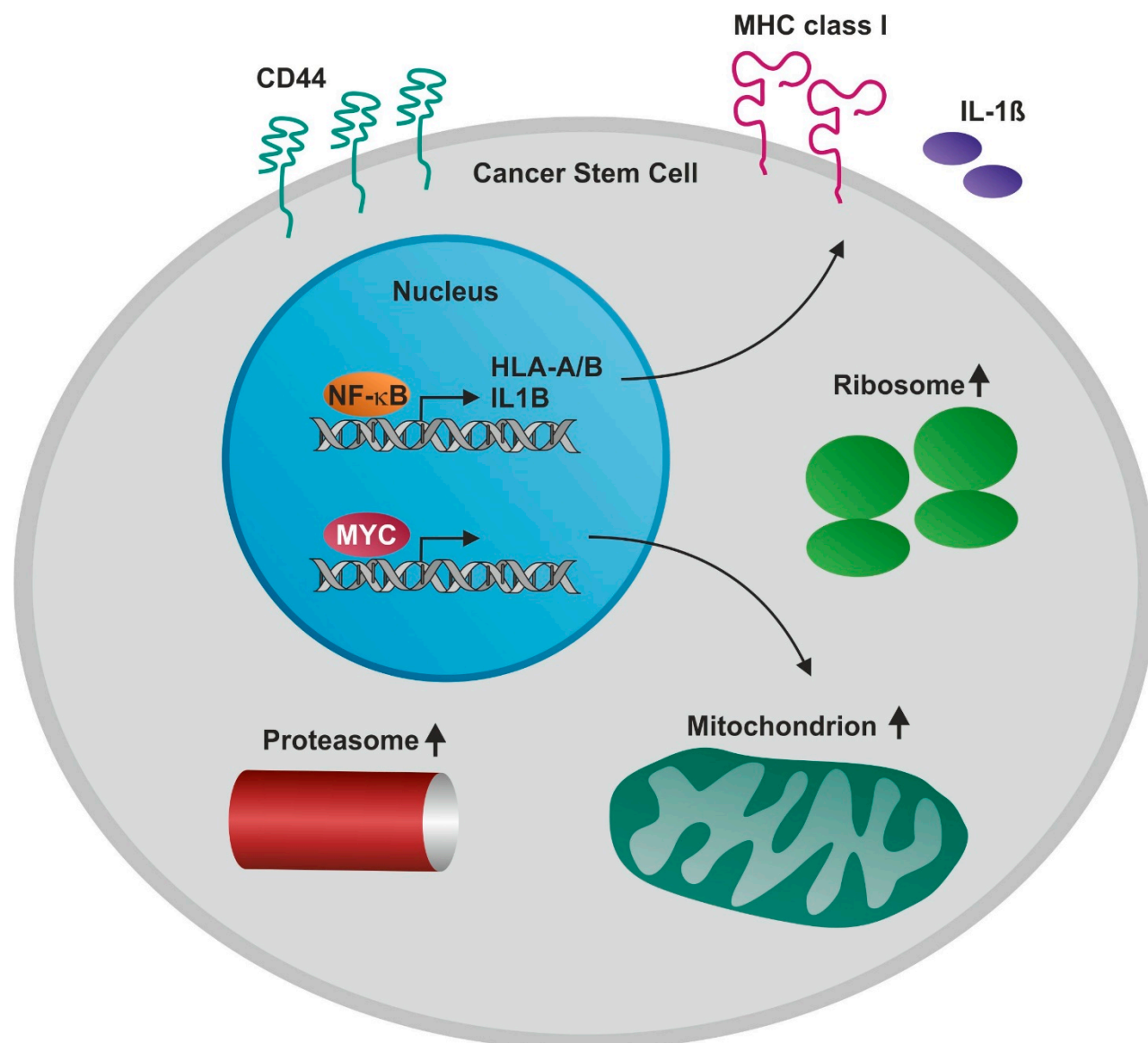
Figure 9. Schematic view on biological processes with enriched genes in CD44-positive cancer stem-like cells (CSCs) from glioblastoma, lung, endometrial and prostate cancer. Genes associated with the mitochondrion, proteasome, ribosome as well as *NF-κB* and *MYC* genes were highly enriched in all CSC populations.

In 1924, Otto Warburg and co-workers published a seminal paper on aerobic glycolysis in rat tumor cells and sections derived from human tumors [68]. The Warburg effect described an increased rate of glucose fermentation leading to lactic acid by tumor cells, even under aerobic conditions [69]. Eight-seven years later, the Warburg effect was included in the list of general hallmarks of cancer. Tumor cells are able to reprogram the

energy metabolism to aerobic glycolysis independent to mitochondrial function to produce adenosine triphosphate (ATP) [70]. However, a tumor is increasingly recognized to consist of a highly heterogeneous cell mass, with the rare cell type of CSCs driving metastasis, invasiveness, therapeutic resistance and recurrence of the tumor (reviewed in [71]). Here, we determined the global transcriptomes of CSCs propagated in vitro. Extending the findings of Warburg, these cells seem to have high metabolic plasticity and might use mitochondria for oxidative phosphorylation. In this line, gene enrichment analysis of the genes expressed in CSCs in comparison to the human genome showed a more than five-fold enrichment of expressed genes involved in mitochondria and oxidative phosphorylation. Accordingly, the amount of metabolic flexibility allowing the switch from oxidative phosphorylation to aerobic glycolysis was reported for CSCs (reviewed in [72]). In particular, a recent study investigated whether the metabolic state (especially the Warburg effect) of GSCs differs from the bulk of the tumor cells with a newly developed imaging system [73]. Vlashi and coworkers reported that monolayer cultures of GSCs produce about 20% less ATP than neurosphere cultures. Of note, another study showed high expressions of CD133 and Nestin in cultured GSC spheres but not in non-sphere GSC monolayers, cultured in 10% FBS [74]. In our study, we detected no difference in the expression of CSC markers in sphere cultures in comparison to adherently grown CSC populations. This might be due to a different experimental strategy used here, as we selected CSCs by differential trypsinization and cultured adherent populations with 10% serum supplemented with B27, bFGF-2 and EGF. Using specific inhibitors for oxidative phosphorylation and aerobic glycolysis, the authors suggested that ATP in both monolayer and neurosphere cultures was mainly produced by glycolysis and oxidative phosphorylation. Inhibition of glycolysis could be compensated through increased oxidative phosphorylation and vice versa. However, the authors conclude that the GSC-metabolism mainly relies on oxidative phosphorylation, which is in line to the here observed enrichment in genes involved in mitochondria and oxidative phosphorylation. Of note, mutations in *IDH1* and *IDH2* genes were shown to reprogram the metabolism of cancer cells to produce the onco-metabolite D-2-hydroxyglutarate and cells with mutations might be additionally dependent on lactate (see for review [75]). In our analysis, CSCs from a secondary GBM showing an *IDH1* mutation (see Figure 4, GSCs_b) did not cluster with the other analyzed GBM-derived CSCs without *IDH1* mutation because of significant changes in global gene expression.

Otto Warburg had many important contributions to biochemistry, such as the discovery of the 'oxygen-transferring ferment of respiration' (cytochrome-c oxidase complex), leading to him receiving the Nobel Prize in physiology or medicine, 1931. We found expressed genes enriched, which might be important for oxidative phosphorylation in mitochondria, such as NADH dehydrogenase activity, proton-transporting ATP synthase activity and cytochrome-c oxidase activity. Since respiratory chain activity leads to constant production of the reactive oxygen intermediate (ROS) it might not be surprising to find enrichment of genes, which code for antioxidant activity such as peroxiredoxin activity, glutathione binding and glutathione peroxidase activity. Some of the ROS produced might result in NF-κB binding. Other organelles containing enriched genes include ribosomes and 26 proteasomes. Indeed, oxidative phosphorylation in mitochondria have been identified as hallmark of CSC metabolism (reviewed in [76]). We also analyzed the expression of general CSC markers (Figure S7). Of special interest might be our recent observation of MYC, as a potential regulator of survival in colon carcinoma-specific CSCs (see [42]). In our study, we could detect MYC expressions in each investigated CSC population. Furthermore, published cancer surface markers CD44 and CD59, as well as the insulin-like growth factor binding protein 2 (IGFBP2), were expressed in all analyzed CSCs. In this context, Chen and Ding demonstrated gradually increased CD59 expression levels in different breast- and lung parental cancer cell lines and further observed that the absence of CD59 resulted in a completely suppression of tumorigenesis in vivo [77]. These results were investigated within sphere cultures, whereas we also detected CD59 within

our adherently cultured CSC populations, further substantiating stem-like characteristics in our CSC models. Next, gene expressions for ribosomal proteins like *RPLP1*, *RPS27L*, *RPL14* and *RPL21* as well as the nuclear encoded and mitochondrial localized protein *COX8A* were detected after transcriptomic analysis. Finally, genes involved in cell cycle regulation and tumor growth like *CDK16*, *CDC20* and the Ras homologue enriched in brain (*RHEB)* were ubiquitously expressed in our established CSCs. In this context, RHEB is commonly known to function in human carcinogenesis [78]. In more detail, Tian and co-workers reported the inhibition of cell proliferation and initiation of apoptosis in colorectal cancer cells via silencing of the *RHEB* gene [79].

We have previously shown that the guanine exchange factor (GEF) pleckstrin homology and RhoGEF domain containing G5 (*PLEKHG5*) plays an essential role in the formation of autolysosomes in glioblastoma cells and induces the transcription factor NF-κB [80]. However, in the present dataset we could not detect any expression of *PLEKHG5*. With respect to a recently proposed role of NF-κB in cancer and CSCs (reviewed in [1,81]), we searched for evidence of activated NF-κB in this transcriptome dataset. We detected highly enriched genes involved in the GO-term "NF-κB binding". However, out of all five DNA-binding subunits, only the expression of *RELA* in all CSC samples was detectable. Furthermore, expression of interleukin 6 and tumor necrosis factor-alpha was not detectable in CSCs, whereas we observed NF-κB target gene expression of *IL1B*, *HLA-A* as well as *HLA-B* in all CSC population. We therefore conclude that further experiments might be necessary to provide conclusive data on the role of NF-κB in CSCs.

We further demonstrate high amounts of ribosome-associated gene expressions in CSCs independent of the tumor type. These data suggest a mechanism of ribosome-enrichment for oxidative phosphorylation in CSCs. On the mechanistic level, RNA polymerase III (Pol III) may transcribe the ribosomal 5S rRNA and the 5.8S, 18S as well as 28S rRNAs are known to arise from the processing of a common precursor rRNA (47S) transcribed by the Pol I. Accordingly, altered ribosome components were discussed to play a significant role in CSCs [82]. There is additional evidence that ribosome biosynthesis and protein synthesis might be directed by transcription factor *MYC* (reviewed in [83]). Proteasome-related transcription was enriched by more than a factor of six in CSCs, although investigations with fluorogenic proteasome substrates suggest a low activity of proteasomal protein degradation in CSCs of breast cancer and glioma [84].

Limitations: on a technical level, this study relies on in vitro protein and transcriptomic data generated with newly developed nanopore sequencing. Although we generally achieved full-length transcript data using this technology, read depth is not as high as in standard Illumina approaches, but seems to be sufficiently sensitive to detect differences and similarities between CSC populations. However, due to the performed read depth, we cannot exclude the possibility of missing low abundant transcripts as transcription factors.

5. Conclusions

From our transcriptomic analysis, we conclude that the here used CSC populations could be divided into three clusters independent of the parental tumor. Nevertheless, we detected conserved expressions of the CSC markers CD44, Nestin, and MYC on mRNA and protein level as well as transcriptional expression of *CD59*. Moreover, GO-term and KEGG pathway enrichment analysis revealed upregulated genes related to ribosomal biosynthesis, the mitochondrion, oxidative phosphorylation, and glycolytic pathways as well as to the proteasome, suggesting the great extent of metabolic flexibility in CSCs. Taken together, transcriptomic analysis might pave the way for future pathway-directed therapies such as targeting mitochondria and 80S ribosomes, together with the already established proteasome. However, further in vitro and in vivo studies are necessary to overcome potential limitations of the study and for specific target discovery.

References

1. Kaltschmidt, C.; Banz-Jansen, C.; Benhidjeb, T.; Beshay, M.; Förster, C.; Greiner, J.; Hamelmann, E.; Jorch, N.; Mertzlufft, F.; Pfitzenmaier, J.; et al. A Role for NF-κB in Organ Specific Cancer and Cancer Stem Cells. *Cancers* **2019**, *11*, 655, doi:10.3390/cancers11050655.
2. Lapidot, T.; Sirard, C.; Vormoor, J.; Murdoch, B.; Hoang, T.; Caceres-Cortes, J.; Minden, M.; Paterson, B.; Caligiuri, M.A.; Dick, J.E. A cell initiating human acute myeloid leukaemia after transplantation into SCID mice. *Nature* **1994**, *367*, 645–648, doi:10.1038/367645a0.
3. Meacham, C.E.; Morrison, S.J. Tumour heterogeneity and cancer cell plasticity. *Nature* **2013**, *501*, 328–337, doi:10.1038/nature12624.
4. Hubbard, S.A.; Friel, A.M.; Kumar, B.; Zhang, L.; Rueda, B.R.; Gargett, C.E. Evidence for cancer stem cells in human endometrial carcinoma. *Cancer Res.* **2009**, *69*, 8241–8248, doi:10.1158/0008-5472.CAN-08-4808.

5. Eramo, A.; Lotti, F.; Sette, G.; Pilozzi, E.; Biffoni, M.; Di Virgilio, A.; Conticello, C.; Ruco, L.; Peschle, C.; Maria, R. de. Identification and expansion of the tumorigenic lung cancer stem cell population. *Cell Death Differ.* **2008**, *15*, 504–514, doi:10.1038/sj.cdd.4402283.

6. Bayin, N.S.; Modrek, A.S.; Placantonakis, D.G. Glioblastoma stem cells: Molecular characteristics and therapeutic implications. *World J. Stem Cells* **2014**, *6*, 230–238, doi:10.4252/wjsc.v6.i2.230.

7. Kasper, S. Exploring the origins of the normal prostate and prostate cancer stem cell. *Stem Cell Rev.* **2008**, *4*, 193–201, doi:10.1007/s12015-008-9033-1.

8. Sultan, M.; Coyle, K.M.; Vidovic, D.; Thomas, M.L.; Gujar, S.; Marcato, P. Hide-and-seek: The interplay between cancer stem cells and the immune system. *Carcinogenesis* **2017**, *38*, 107–118, doi:10.1093/carcin/bgw115.

9. Marsden, C.G.; Wright, M.J.; Pochampally, R.; Rowan, B.G. Breast tumor-initiating cells isolated from patient core biopsies for study of hormone action. *Methods Mol. Biol.* **2009**, *590*, 363–375, doi:10.1007/978-1-60327-378-7_23.

10. Singh, S.K.; Clarke, I.D.; Terasaki, M.; Bonn, V.E.; Hawkins, C.; Squire, J.; Dirks, P.B. Identification of a cancer stem cell in human brain tumors. *Cancer Res.* **2003**, *63*, 5821–5828.

11. Di Tomaso, T.; Mazzoleni, S.; Wang, E.; Sovena, G.; Clavenna, D.; Franzin, A.; Mortini, P.; Ferrone, S.; Doglioni, C.; Marincola, F.M.; et al. Immunobiological characterization of cancer stem cells isolated from glioblastoma patients. *Clin. Cancer Res.* **2010**, *16*, 800–813, doi:10.1158/1078-0432.CCR-09-2730.

12. Li, X.; Larsson, P.; Ljuslinder, I.; Öhlund, D.; Myte, R.; Löfgren-Burström, A.; Zingmark, C.; Ling, A.; Edin, S.; Palmqvist, R. Ex Vivo Organoid Cultures Reveal the Importance of the Tumor Microenvironment for Maintenance of Colorectal Cancer Stem Cells. *Cancers* **2020**, *12*, 923, doi:10.3390/cancers12040923.

13. Torre, L.A.; Bray, F.; Siegel, R.L.; Ferlay, J.; Lortet-Tieulent, J.; Jemal, A. Global cancer statistics, 2012. *CA Cancer J. Clin.* **2015**, *65*, 87–108, doi:10.3322/caac.21262.

14. Renehan, A.G.; Roberts, D.L.; Dive, C. Obesity and cancer: Pathophysiological and biological mechanisms. *Arch. Physiol. Biochem.* **2008**, *114*, 71–83, doi:10.1080/13813450801954303.

15. Nevadunsky, N.S.; van Arsdale, A.; Strickler, H.D.; Moadel, A.; Kaur, G.; Levitt, J.; Girda, E.; Goldfinger, M.; Goldberg, G.L.; Einstein, M.H. Obesity and age at diagnosis of endometrial cancer. *Obstet. Gynecol.* **2014**, *124*, 300–306, doi:10.1097/AOG.0000000000000381.

16. Ding, D.-C.; Liu, H.-W.; Chang, Y.-H.; Chu, T.-Y. Expression of CD133 in endometrial cancer cells and its implications. *J. Cancer* **2017**, *8*, 2142–2153, doi:10.7150/jca.18869.

17. Desai, R.; Suryadevara, C.M.; Batich, K.A.; Farber, S.H.; Sanchez-Perez, L.; Sampson, J.H. Emerging immunotherapies for glioblastoma. *Expert Opin. Emerg. Drugs* **2016**, *21*, 133–145, doi:10.1080/14728214.2016.1186643.

18. Delgado-López, P.D.; Corrales-García, E.M. Survival in glioblastoma: A review on the impact of treatment modalities. *Clin. Transl. Oncol.* **2016**, *18*, 1062–1071, doi:10.1007/s12094-016-1497-x.

19. Almeida, N.D.; Klein, A.L.; Hogan, E.A.; Terhaar, S.J.; Kedda, J.; Uppal, P.; Sack, K.; Keidar, M.; Sherman, J.H. Cold Atmospheric Plasma as an Adjunct to Immunotherapy for Glioblastoma Multiforme. *World Neurosurg.* **2019**, *130*, 369–376, doi:10.1016/j.wneu.2019.06.209.

20. Lathia, J.D.; Mack, S.C.; Mulkearns-Hubert, E.E.; Valentim, C.L.L.; Rich, J.N. Cancer stem cells in glioblastoma. *Genes Dev.* **2015**, *29*, 1203–1217, doi:10.1101/gad.261982.115.

21. Glas, M.; Rath, B.H.; Simon, M.; Reinartz, R.; Schramme, A.; Trageser, D.; Eisenreich, R.; Leinhaas, A.; Keller, M.; Schildhaus, H.-U.; et al. Residual tumor cells are unique cellular targets in glioblastoma. *Ann. Neurol.* **2010**, *68*, 264–269, doi:10.1002/ana.22036.

22. Schneider, M.; Ströbele, S.; Nonnenmacher, L.; Siegelin, M.D.; Tepper, M.; Stroh, S.; Hasslacher, S.; Enzenmüller, S.; Strauss, G.; Baumann, B.; et al. A paired comparison between glioblastoma "stem cells" and differentiated cells. *Int. J. Cancer* **2016**, *138*, 1709–1718, doi:10.1002/ijc.29908.

23. Bonavia, R.; Inda, M.-d.-M.; Cavenee, W.; Furnari, F. Heterogeneity Maintenance in Glioblastoma: A social network. *Cancer Res.* **2011**, *71*, 4055–4060, doi:10.1158/0008-5472.CAN-11-0153.

24. Yan, K.; Yang, K.; Rich, J.N. The Evolving Landscape of Brain Tumor Cancer Stem Cells. *Curr. Opin. Neurol.* **2013**, *26*, 701–707, doi:10.1097/WCO.0000000000000032.

25. Suvà, M.L.; Rheinbay, E.; Gillespie, S.M.; Patel, A.P.; Wakimoto, H.; Rabkin, S.D.; Riggi, N.; Chi, A.S.; Cahill, D.P.; Nahed, B.V.; et al. Reconstructing and reprogramming the tumor-propagating potential of glioblastoma stem-like cells. *Cell* **2014**, *157*, 580–594, doi:10.1016/j.cell.2014.02.030.

26. Seymour, T.; Nowak, A.; Kakulas, F. Targeting Aggressive Cancer Stem Cells in Glioblastoma. *Front. Oncol.* **2015**, *5*, doi:10.3389/fonc.2015.00159.

27. Happold, C.; Stojcheva, N.; Silginer, M.; Weiss, T.; Roth, P.; Reifenberger, G.; Weller, M. Transcriptional control of O6 -methylguanine DNA methyltransferase expression and temozolomide resistance in glioblastoma. *J. Neurochem.* **2018**, *144*, 780–790, doi:10.1111/jnc.14326.

28. Stupp, R.; Mason, W.P.; van, d.B.M.; Weller, M.; Fisher, B.; Taphoorn, M.J.; Belanger, K.; Brandes, A.A.; Marosi, C.; Bogdahn, U.; et al. Radiotherapy plus concomitant and adjuvant temozolomide for glioblastoma. *N. Engl. J. Med.* **2005**, *352*, doi:10.1056/NEJMoa043330.

29. Hegi, M.E.; Diserens, A.-C.; Gorlia, T.; Hamou, M.-F.; de Tribolet, N.; Weller, M.; Kros, J.M.; Hainfellner, J.A.; Mason, W.; Mariani, L.; et al. MGMT gene silencing and benefit from temozolomide in glioblastoma. *N. Engl. J. Med.* **2005**, *352*, 997–1003, doi:10.1056/NEJMoa043331.

30. Ruiz-Ceja, K.A.; Chirino, Y.I. Current FDA-approved treatments for non-small cell lung cancer and potential biomarkers for its detection. *Biomed. Pharmacother.* **2017**, *90*, 24–37, doi:10.1016/j.biopha.2017.03.018.

31. Schild, S.E.; Tan, A.D.; Wampfler, J.A.; Ross, H.J.; Yang, P.; Sloan, J.A. A new scoring system for predicting survival in patients with non-small cell lung cancer. *Cancer Med.* **2015**, *4*, 1334–1343, doi:10.1002/cam4.479.

32. Tan, Y.; Chen, B.; Xu, W.; Zhao, W.; Wu, J. Clinicopathological significance of CD133 in lung cancer: A meta-analysis. *Mol. Clin. Oncol.* **2014**, *2*, 111–115, doi:10.3892/mco.2013.195.

33. Zakaria, N.; Yusoff, N.M.; Zakaria, Z.; Lim, M.N.; Baharuddin, P.J.N.; Fakiruddin, K.S.; Yahaya, B. Human non-small cell lung cancer expresses putative cancer stem cell markers and exhibits the transcriptomic profile of multipotent cells. *BMC Cancer* **2015**, *15*, 84, doi:10.1186/s12885-015-1086-3.

34. Siegel, R.L.; Miller, K.D.; Jemal, A. Cancer statistics, 2019. *CA Cancer J. Clin.* **2019**, *69*, 7–34, doi:10.3322/caac.21551.

35. Li, J.; Wang, Z. The pathology of unusual subtypes of prostate cancer. *Chin. J. Cancer Res.* **2016**, *28*, 130–143, doi:10.3978/j.issn.1000-9604.2016.01.06.

36. Schröder, F.H.; Hugosson, J.; Roobol, M.J.; Tammela, T.L.J.; Zappa, M.; Nelen, V.; Kwiatkowski, M.; Lujan, M.; Määttänen, L.; Lilja, H.; et al. Screening and prostate cancer mortality: Results of the European Randomised Study of Screening for Prostate Cancer (ERSPC) at 13 years of follow-up. *Lancet* **2014**, *384*, 2027–2035, doi:10.1016/S0140-6736(14)60525-0.

37. Bill-Axelson, A.; Holmberg, L.; Garmo, H.; Taari, K.; Busch, C.; Nordling, S.; Häggman, M.; Andersson, S.-O.; Andrén, O.; Steineck, G.; et al. Radical Prostatectomy or Watchful Waiting in Prostate Cancer—29-Year Follow-up. *N. Engl. J. Med.* **2018**, *379*, 2319–2329, doi:10.1056/NEJMoa1807801.

38. Wang, X.; Kruithof-de Julio, M.; Economides, K.D.; Walker, D.; Yu, H.; Halili, M.V.; Hu, Y.-P.; Price, S.M.; Abate-Shen, C.; Shen, M.M. A luminal epithelial stem cell that is a cell of origin for prostate cancer. *Nature* **2009**, *461*, 495–500, doi:10.1038/nature08361.

39. Rajasekhar, V.K.; Studer, L.; Gerald, W.; Socci, N.D.; Scher, H.I. Tumour-initiating stem-like cells in human prostate cancer exhibit increased NF-κB signalling. *Nat. Commun.* **2011**, *2*, 162–, doi:10.1038/ncomms1159.

40. Cao, Y.; Li, W.; Chu, X.; Wu, K.; Liu, H.; Liu, D. Research progress and application of nanopore sequencing technology. *Sheng Wu Gong Cheng Xue Bao* **2020**, *36*, 811–819, doi:10.13345/j.cjb.190368.

41. Windmöller, B.A.; Greiner, J.F.W.; Förster, C.; Wilkens, L.; Mertzlufft, F.; Am Schulte Esch, J.; Kaltschmidt, B.; Kaltschmidt, C.; Beshay, M. A typical carcinoid of the lung—A case report with pathological correlation and propagation of the cancer stem cell line BKZ1 with synaptophysin expression. *Medicine* **2019**, *98*, e18174, doi:10.1097/MD.0000000000018174.

42. Schulte am Esch, J.; Windmöller, B.A.; Hanewinkel, J.; Storm, J.; Förster, C.; Wilkens, L.; Krüger, M.; Kaltschmidt, B.; Kaltschmidt, C. Isolation and Characterization of Two Novel Colorectal Cancer Cell Lines, Containing a Subpopulation with Potential Stem-Like Properties: Treatment Options by MYC/NMYC Inhibition. *Cancers* **2020**, *12*, 2582, doi:10.3390/cancers12092582.

43. Walia, V.; Elble, R.C. Enrichment for breast cancer cells with stem/progenitor properties by differential adhesion. *Stem Cells Dev.* **2010**, *19*, 1175–1182, doi:10.1089/scd.2009.0430.

44. Morata-Tarifa, C.; Jiménez, G.; García, M.A.; Entrena, J.M.; Griñán-Lisón, C.; Aguilera, M.; Picon-Ruiz, M.; Marchal, J.A. Low adherent cancer cell subpopulations are enriched in tumorigenic and metastatic epithelial-to-mesenchymal transition-induced cancer stem-like cells. *Sci. Rep.* **2016**, *6*, 18772, doi:10.1038/srep18772.

45. Wick, R.R.; Judd, L.M.; Gorrie, C.L.; Holt, K.E. Completing bacterial genome assemblies with multiplex MinION sequencing. *Microb. Genom.* **2017**, *3*, e000132, doi:10.1099/mgen.0.000132.

46. Andrews, S. *FastQC: A Quality Control Tool for High Throughput Sequence Data*; Bioinformatics; Babraham: Cambridge, UK, 2010.

47. Schneider, V.A.; Graves-Lindsay, T.; Howe, K.; Bouk, N.; Chen, H.-C.; Kitts, P.A.; Murphy, T.D.; Pruitt, K.D.; Thibaud-Nissen, F.; Albracht, D.; et al. Evaluation of GRCh38 and de novo haploid genome assemblies demonstrates the enduring quality of the reference assembly. *Genome Res.* **2017**, *27*, 849–864, doi:10.1101/gr.213611.116.

48. O'Leary, N.A.; Wright, M.W.; Brister, J.R.; Ciufo, S.; Haddad, D.; McVeigh, R.; Rajput, B.; Robbertse, B.; Smith-White, B.; Ako-Adjei, D.; et al. Reference sequence (RefSeq) database at NCBI: Current status, taxonomic expansion, and functional annotation. *Nucleic Acids Res.* **2016**, *44*, D733–D745, doi:10.1093/nar/gkv1189.

49. Li, H. Minimap2: Pairwise alignment for nucleotide sequences. *Bioinformatics* **2018**, *34*, 3094–3100, doi:10.1093/bioinformatics/bty191.

50. Li, H.; Handsaker, B.; Wysoker, A.; Fennell, T.; Ruan, J.; Homer, N.; Marth, G.; Abecasis, G.; Durbin, R. The Sequence Alignment/Map format and SAMtools. *Bioinformatics* **2009**, *25*, 2078–2079, doi:10.1093/bioinformatics/btp352.

51. Weirather, J.L.; de Cesare, M.; Wang, Y.; Piazza, P.; Sebastiano, V.; Wang, X.-J.; Buck, D.; Au, K.F. Comprehensive comparison of Pacific Biosciences and Oxford Nanopore Technologies and their applications to transcriptome analysis. *F1000Resarch* **2017**, *6*, 100, doi:10.12688/f1000research.10571.2.

52. Wyman, D.; Mortazavi, A. TranscriptClean: Variant-aware correction of indels, mismatches and splice junctions in long-read transcripts. *Bioinformatics* **2018**, *35*, 340–342, doi:10.1093/bioinformatics/bty483.

53. Huber, W.; Carey, V.J.; Gentleman, R.; Anders, S.; Carlson, M.; Carvalho, B.S.; Bravo, H.C.; Davis, S.; Gatto, L.; Girke, T.; et al. Orchestrating high-throughput genomic analysis with Bioconductor. *Nat. Methods* **2015**, *12*, 115–121, doi:10.1038/nmeth.3252.

54. Liao, Y.; Smyth, G.K.; Shi, W. The R package Rsubread is easier, faster, cheaper and better for alignment and quantification of RNA sequencing reads. *Nucleic Acids Res.* **2019**, *47*, e47, doi:10.1093/nar/gkz114.

55. Robinson, M.D.; McCarthy, D.J.; Smyth, G.K. edgeR: A Bioconductor package for differential expression analysis of digital gene expression data. *Bioinformatics* **2010**, *26*, 139–140, doi:10.1093/bioinformatics/btp616.

56. McCarthy, D.J.; Chen, Y.; Smyth, G.K. Differential expression analysis of multifactor RNA-Seq experiments with respect to biological variation. *Nucleic Acids Res.* **2012**, *40*, 4288–4297, doi:10.1093/nar/gks042.

57. Robinson, M.D.; Oshlack, A. A scaling normalization method for differential expression analysis of RNA-seq data. *Genome Biol.* **2010**, *11*, R25, doi:10.1186/gb-2010-11-3-r25.

58. Blighe, K. *PCAtools: Everything Principal Components Analysis: Everything Principal Components Analysis*; PCAtools: London, UK, 2019.

59. Warnes, G.; Bolker, B.; Bonebakker, L.; Gentleman, R.; Huber, W.; Liaw, A.; Lumley, T.; Maechler, M.; Magnusson, A.; Moeller, S.; et al. *gplots: Various R Programming Tools for Plotting Data*; Publisher: city, state abbreviation (if CA/USA), country, 2020.

60. Harrell Frank, E., Jr. With contributions from Dupont, Charles and many others. In *Hmisc: Harrell Miscellaneous*; R package version; 2020.

61. Mi, H.; Ebert, D.; Muruganujan, A.; Mills, C.; Albou, L.-P.; Mushayamaha, T.; Thomas, P.D. PANTHER version 16: A revised family classification, tree-based classification tool, enhancer regions and extensive API. *Nucleic Acids Res.* **2021**, *49*, D394–D403, doi:10.1093/nar/gkaa1106.

62. Huang, D.W.; Sherman, B.T.; Lempicki, R.A. Systematic and integrative analysis of large gene lists using DAVID bioinformatics resources. *Nat. Protoc.* **2009**, *4*, 44–57, doi:10.1038/nprot.2008.211.

63. Huang, D.W.; Sherman, B.T.; Lempicki, R.A. Bioinformatics enrichment tools: Paths toward the comprehensive functional analysis of large gene lists. *Nucleic Acids Res.* **2009**, *37*, 1–13, doi:10.1093/nar/gkn923.

64. Greiner, J.F.W.; Hauser, S.; Widera, D.; Müller, J.; Qunneis, F.; Zander, C.; Martin, I.; Mallah, J.; Schuetzmann, D.; Prante, C.; et al. Efficient animal-serum free 3D cultivation method for adult human neural crest-derived stem cell therapeutics. *Eur. Cells Mater.* **2011**, *22*, 403–419, doi:10.22203/ecm.v022a30.

65. Hauser, S.; Widera, D.; Qunneis, F.; Müller, J.; Zander, C.; Greiner, J.; Strauss, C.; Lüningschrör, P.; Heimann, P.; Schwarze, H.; et al. Isolation of novel multipotent neural crest-derived stem cells from adult human inferior turbinate. *Stem Cells Dev.* **2012**, *21*, 742–756, doi:10.1089/scd.2011.0419.

66. Höving, A.L.; Schmidt, K.E.; Merten, M.; Hamidi, J.; Rott, A.-K.; Faust, I.; Greiner, J.F.W.; Gummert, J.; Kaltschmidt, B.; Kaltschmidt, C.; et al. Blood Serum Stimulates p38-Mediated Proliferation and Changes in Global Gene Expression of Adult Human Cardiac Stem Cells. *Cells* **2020**, *9*, 1472, doi:10.3390/cells9061472.

67. Höving, A.L.; Sielemann, K.; Greiner, J.F.W.; Kaltschmidt, B.; Knabbe, C.; Kaltschmidt, C. Transcriptome Analysis Reveals High Similarities between Adult Human Cardiac Stem Cells and Neural Crest-Derived Stem Cells. *Biology* **2020**, *9*, 435, doi:10.3390/biology9120435.

68. Warburg, O.; Posener, K.; Negelein, E. Über den Stoffwechsel der Carcinomzelle. *Biochem. Zeitschr.* **1924**, *152*, 309–344.

69. Warburg, O. On respiratory impairment in cancer cells. *Science* **1956**, *124*, 269–270.

70. Hanahan, D.; Weinberg, R.A. Hallmarks of cancer: The next generation. *Cell* **2011**, *144*, 646–674, doi:10.1016/j.cell.2011.02.013.

71. Zhao, Y.; Dong, Q.; Li, J.; Zhang, K.; Qin, J.; Zhao, J.; Sun, Q.; Wang, Z.; Wartmann, T.; Jauch, K.W.; et al. Targeting cancer stem cells and their niche: Perspectives for future therapeutic targets and strategies. *Semin. Cancer Biol.* **2018**, *53*, 139–155, doi:10.1016/j.semcancer.2018.08.002.

72. García-Heredia, J.M.; Carnero, A. Role of Mitochondria in Cancer Stem Cell Resistance. *Cells* **2020**, *9*, 1693, doi:10.3390/cells9071693.

73. Vlashi, E.; Lagadec, C.; Vergnes, L.; Matsutani, T.; Masui, K.; Poulou, M.; Popescu, R.; Della Donna, L.; Evers, P.; Dekmezian, C.; et al. Metabolic state of glioma stem cells and nontumorigenic cells. *Proc. Natl. Acad. Sci. USA* **2011**, *108*, 16062–16067, doi:10.1073/pnas.1106704108.

74. Yuan, X.; Curtin, J.; Xiong, Y.; Liu, G.; Waschsmann-Hogiu, S.; Farkas, D.L.; Black, K.L.; Yu, J.S. Isolation of cancer stem cells from adult glioblastoma multiforme. *Oncogene* **2004**, *23*, 9392–9400, doi:10.1038/sj.onc.1208311.

75. Dang, L.; Yen, K.; Attar, E.C. IDH mutations in cancer and progress toward development of targeted therapeutics. *Ann. Oncol.* **2016**, *27*, 599–608, doi:10.1093/annonc/mdw013.

76. Sancho, P.; Barneda, D.; Heeschen, C. Hallmarks of cancer stem cell metabolism. *Br. J. Cancer* **2016**, *114*, 1305–1312, doi:10.1038/bjc.2016.152.

77. Chen, J.; Ding, P.; Li, L.; Gu, H.; Zhang, X.; Zhang, L.; Wang, N.; Gan, L.; Wang, Q.; Zhang, W.; et al. CD59 Regulation by SOX2 Is Required for Epithelial Cancer Stem Cells to Evade Complement Surveillance. *Stem Cell Rep.* **2017**, *8*, 140–151, doi:10.1016/j.stemcr.2016.11.008.

78. Lu, Z.H.; Shvartsman, M.B.; Lee, A.Y.; Shao, J.M.; Murray, M.M.; Kladney, R.D.; Fan, D.; Krajewski, S.; Chiang, G.G.; Mills, G.B.; et al. Mammalian target of rapamycin activator RHEB is frequently overexpressed in human carcinomas and is critical and sufficient for skin epithelial carcinogenesis. *Cancer Res.* **2010**, *70*, 3287–3298, doi:10.1158/0008-5472.CAN-09-3467.

79. Tian, Y.; Shen, L.; Li, F.; Yang, J.; Wan, X.; Ouyang, M. Silencing of RHEB inhibits cell proliferation and promotes apoptosis in colorectal cancer cells via inhibition of the mTOR signaling pathway. *J. Cell. Physiol.* **2020**, *235*, 442–453, doi:10.1002/jcp.28984.

80. Witte, K.E.; Slotta, C.; Lütkemeyer, M.; Kitke, A.; Coras, R.; Simon, M.; Kaltschmidt, C.; Kaltschmidt, B. PLEKHG5 regulates autophagy, survival and MGMT expression in U251-MG glioblastoma cells. *Sci. Rep.* **2020**, *10*, 21858, doi:10.1038/s41598-020-77958-3.

81. Kaltschmidt, B.; Greiner, J.F.W.; Kadhim, H.M.; Kaltschmidt, C. Subunit-Specific Role of NF-κB in Cancer. *Biomedicines* **2018**, *6*, 44, doi:10.3390/biomedicines6020044.

82. Bastide, A.; David, A. The ribosome, (slow) beating heart of cancer (stem) cell. *Oncogenesis* **2018**, *7*, 34, doi:10.1038/s41389-018-0044-8.

83. Van Riggelen, J.; Yetil, A.; Felsher, D.W. MYC as a regulator of ribosome biogenesis and protein synthesis. *Nat. Rev. Cancer* **2010**, *10*, 301–309, doi:10.1038/nrc2819.

84. Vlashi, E.; Kim, K.; Lagadec, C.; Della Donna, L.; McDonald, J.T.; Eghbali, M.; Sayre, J.W.; Stefani, E.; McBride, W.; Pajonk, F. In vivo imaging, tracking, and targeting of cancer stem cells. *J. Natl. Cancer Inst.* **2009**, *101*, 350–359, doi:10.1093/jnci/djn509.

Review article *accepted for publication*

Between fate choice and self-renewal - Heterogeneity of adult neural crest-derived stem cells

Anna L. Höving*, Beatrice A. Windmöller*, Cornelius Knabbe, Barbara Kaltschmidt, Christian Kaltschmidt and Johannes F.W. Greiner

1 Between fate choice and self-renewal - Heterogeneity of adult neural
2 crest-derived stem cells

3 **Anna L. Höving[1,2†], Beatrice A. Windmöller[1,3†], Cornelius Knabbe[2,3], Barbara Kaltschmidt[1,3,4],**
4 **Christian Kaltschmidt[1,3] and Johannes F.W. Greiner[1,3,*]**

5 [1] Department of Cell Biology, University of Bielefeld, 33615 Bielefeld, Germany

6 [2] Institute for Laboratory- and Transfusion medicine, Heart and Diabetes Centre NRW, Ruhr
7 University Bochum, 32545 Bad Oeynhausen, Germany

8 [3] Forschungsverbund BioMedizin Bielefeld FBMB e.V., Maraweg 21, Bielefeld, Germany

9 [4] AG Molecular Neurobiology, University of Bielefeld, 33615 Bielefeld, Germany

10 †These authors contributed equally to this work and share first authorship.

11 *** Correspondence:**
12 Johannes F.W. Greiner
13 johannes.greiner@uni-bielefeld.de

14 **Keywords: Adult stem cells, Neural crest-derived stem cells, heterogeneity, single cell analysis,**
15 **fate choice, neural crest**

16 **Abstract**

17 Stem cells of the neural crest (NC) vitally participate to embryonic development, but also remain in
18 distinct niches as quiescent neural crest-derived stem cell (NCSC) pools into adulthood. Although
19 NCSC-populations share a high capacity for self-renewal and differentiation resulting in promising
20 preclinical applications within the last two decades, inter- and intrapopulational differences exist in
21 terms of their expression signatures and regenerative capability. Differentiation and self-renewal of
22 stem cells in developmental and regenerative contexts are partially regulated by the niche or culture
23 condition and further influenced by single cell decision processes, making cell-to-cell variation and
24 heterogeneity critical for understanding adult stem cell populations.
25 The present review summarizes current knowledge of the cellular heterogeneity within NCSC-
26 populations located in distinct craniofacial and trunk niches including the nasal cavity, olfactory bulb,
27 oral tissues or skin. We shed light on the impact of intrapopulational heterogeneity on fate
28 specifications and plasticity of NCSCs in their niches *in vivo* as well as during *in vitro* culture. We
29 further discuss underlying molecular regulators determining fate specifications of NCSCs, suggesting
30 a regulatory network including NF-κB and NC-related transcription factors like SLUG and SOX9
31 accompanied by Wnt- and MAPK-signaling to orchestrate NCSC stemness and differentiation.
32 In summary, adult NCSCs show a broad heterogeneity on the level of the donor and the donors' sex,
33 the cell population and the single stem cell directly impacting their differentiation capability and fate
34 choices *in vivo* and *in vitro*. The findings discussed here emphasize heterogeneity of NCSCs as a crucial
35 parameter for understanding their role in tissue homeostasis and regeneration and for improving their
36 applicability in regenerative medicine.

37 **1 Introduction: Intrapopulational heterogeneity of adult stem cells**

38 Adult stem cells (ASCs) are undifferentiated cells capable of self-renewal as well as multi-lineage
39 differentiation and are located in a broad range of niches throughout the human body (Rochat et al.,
40 1994; Johansson et al., 1999; Pittenger et al., 1999; Messina et al., 2004; Hauser et al., 2012; Höving
41 et al., 2020b). By giving rise to a variety of specialized cell types, ASCs not only participate to normal
42 adult tissue homeostasis and endogenous regeneration processes upon injury or inflammation, but also
43 harbor an enormous potential for applications in regenerative medicine. Differentiation and self-
44 renewal of stem cells in developmental and regenerative contexts are partially regulated by the niche
45 or culture condition and further influenced by single cell decision processes. Cell-to-cell variation and
46 heterogeneity can thus be considered as fundamental and intrinsic characteristics of adult stem cell
47 populations. Utilization of bulk samples thus not only limits the degree of resolution of cell type
48 definitions but can also mask crucial information about subcellular heterogeneity within stem cell
49 populations and their lineage choices (Moignard and Gottgens, 2016; Griffiths et al., 2018). In this
50 regard, first observations of heterogeneity within a defined cell population were reported by Fleming
51 and colleagues. In this pioneering study, the authors described functional heterogeneity within a
52 phenotypically defined Thy1.1^{lo}/lin$^-$/Sca-1$^+$ multipotent hematopoietic stem cell (HSC) population
53 which was associated with the cell cycle status. In detail, murine Thy1.1^{lo}/lin$^-$/Sca-1$^+$ cells in the G0/G1
54 phase showed significantly higher capacities for radioprotection and long-term multilineage
55 reconstitution of peripheral blood after injection into lethally irradiated recipient mice compared to
56 Thy1.1^{lo}/lin$^-$/Sca-1$^+$ cells in the S/G2/M phase (Fleming et al., 1993). Following this pioneering work,
57 single cell technologies have been developed rapidly in recent years to dissect cellular heterogeneity
58 and identify subpopulations even within a "homogenous" stem cell population, providing deeper
59 insight into their behavior and biological function (Fletcher et al., 2017; Gadye et al., 2017; Joost et
60 al., 2018). For HSCs, recent single cell observations ranged from reporting heterogeneity of HSCs
61 within the bone marrow (Moignard et al., 2013; Yu et al., 2016), for instance regarding the cell-cycle
62 status of pre-HSCs (Zhou et al., 2016), up to providing the regulatory landscape of human
63 hematopoietic differentiation on single cell level (Buenrostro et al., 2018). For long time,
64 transplantation assays did not reveal functional differences but the observed diversity at transcriptional
65 and epigenetic level may provide information to engineer HSCs for clinical applications and emphasize
66 the importance of single cell measurements (Yu et al., 2016; Zhou et al., 2016; Buenrostro et al., 2018).
67 Very recently, Rodriguez-Fraticelli and colleagues combined single cell transcriptome analysis with
68 functional transplantation assays and discovered the transcription factor Tcf15 to be crucial for the
69 regulation of HSC long-term regenerative capacity *in vivo* (Rodriguez-Fraticelli et al., 2020). Next to
70 well-studied HSCs, single cell analysis was successfully applied to investigate the differentiation
71 dynamics of primary human skeletal muscle myoblasts (Trapnell et al., 2014) and neural stem cells
72 (NSCs). Here, Suslov and colleagues as well as Dulken and coworkers reported intra-clonal
73 heterogeneity and cell-lineage diversity in NSCs cultured as neurospheres (Suslov et al., 2002; Dulken
74 et al., 2017), initiating a discussion regarding their applicability as a model system. Mesenchymal stem
75 cells (MSCs) were likewise observed to show not only functional and molecular differences between
76 clones, but also intra-clonal heterogeneity and cell-to-cell variations (reviewed in (McLeod and Mauck,
77 2017). For instance, Freeman and coworkers utilized single cell RNA-sequencing (scRNA-seq) to
78 demonstrate unique profiles of lineage priming in individual bone marrow-derived MSC. Although
79 multipotency-associated transcriptional profiles were consistently observed, single MSCs showed
80 varying levels of genes associated with differentiation and immunomodulation, which could not be
81 ascribed to proliferation state or other cellular processes (Freeman et al., 2015). The possibility to
82 define intercellular heterogeneity via single cell analysis becomes thus more and more evident to
83 understand cell-to-cell variations within a tissue or a distinct population of cells and stem cells.

84   Determining the identities of ASCs at single cell resolution will improve our insights into lineage
85   choices and underlying regulatory networks in endogenous tissue regeneration as well as in the context
86   of cell-intrinsic sexual dimorphisms (Fig. 1). In addition, the systematic investigation of cellular
87   heterogeneity in ASC-based model systems like cultured stem cell-derived spheroids may broaden the
88   applicability of ASCs in drug development and regenerative medicine (Fig. 1).
89   Among the broad range of ASCs in their diverse niches, adult neural crest-derived stem cells (NCSCs)
90   reveal a particularly broad differentiation potential (see also chapter 3) and are therefore highly
91   promising candidates for studying heterogeneity of stem cell populations and fate decisions. This
92   review will summarize current tools for analyzing gene expression profiles of single (neural crest-
93   derived) stem cells via scRNA-seq and discuss recent observations of single cell heterogeneity in
94   mammalian NCSC-populations located in distinct craniofacial and trunk niches including the nasal
95   cavity, olfactory bulb, carotid body, cornea of the eye, oral tissues, craniofacial and trunk skin, dorsal
96   root ganglia, sciatic nerve, bone marrow, heart and gut . We will further assess underlying molecular
97   regulators orchestrating fate specifications and stemness of NCSCs.

98   **2   Technical excursion: State of the art tools and challenges of analyzing single stem cells**

99   The major challenge in performing single stem cell experiments lies in the extremely low amount of
100   starting material that can be isolated from one single cell. This little starting material can lead to a loss
101   of information in the resulting cDNA libraries as well as to a phenomenon called drop-out, if a gene is
102   expressed in a cell but not detected in RT-PCR or scRNA-seq (Kumar et al., 2017). On the contrary,
103   fluctuations in the transcription rates of a gene (termed as transcriptional noise) occur based on random
104   distributions of extremely low intracellular concentrations of the acting molecules (McAdams and
105   Arkin, 1999; Kumar et al., 2017). To gain a deeper insight into cellular heterogeneity, the analysis of
106   a large quantity of single cells is necessary making high throughput methods inevitable. Next to
107   appropriate sample acquisition (reviewed in (Saliba et al., 2014)), various strategies and platforms for
108   analyzing gene expression of single stem cells have been established in the last years (see Fig. 2). As
109   an image-based method, RNA-fluorescence *in situ* hybridization (FISH) utilizes fluorescently labeled
110   oligonucleotides that hybridize to their complementary counterparts in a fixed cell. Thus, mRNA
111   molecules can be visualized as diffraction limited spots providing information about their spatial
112   distribution within the cell. However, the potential number of simultaneously assayed genes is
113   restricted by the availability of microscope filters but can be increased to a certain extend by
114   combinatorial and sequential barcoding (Lubeck and Cai, 2012; Lubeck et al., 2014; Moffitt et al.,
115   2016). For in-depth analyses, global gene expression profiling by scRNA-Seq harbors the potential to
116   discriminate thousands of transcripts (biomarkers) and their expression levels. One first scRNA-seq
117   technique was SMARTseq/SMARTseq2 (switching mechanism at 5' end of the RNA transcript),
118   which enables the generation of full-length cDNA transcripts of one single cell (Ramsköld et al., 2012;
119   Picelli et al., 2014). However, prior to the application of SMARTseq methods, single cells have to be
120   prepared by either FACS or single cell dilution limiting the amount of analyzed single cells. Rosenberg
121   and colleagues developed spilt-pool ligation-based transcriptome sequencing (SPLiT-seq), which
122   applies four rounds of combinatorial barcoding to a suspension of formaldehyde-fixed cells (Rosenberg
123   et al., 2018). Sequential barcoding of the mRNA results in more than 21 million of possible barcode
124   combinations starting from 96 individual cells enabling high-grade multiplexing in a single sequencing
125   run and reducing costs to 0.1 USD per cell. However, the workflow prior to sequencing requires a
126   range of pipetting steps, which is time-consuming and limits the number of simultaneously analyzed
127   cells. Microfluidic-based systems are working with nanoliter-scale volumes allowing substantial
128   reduction of the rate of external contaminations (Blainey and Quake, 2011). Additionally, the small
129   volumes avoid an excessive dilution of the input RNA as well as concomitant potential bias from pre-

130   amplification steps and technical variability (Wu et al., 2014). Linking microfluidic systems and
131   droplet barcoding strategies currently represents the leading edge of single cell research (Klein et al.,
132   2015; Macosko et al., 2015; Zilionis et al., 2016; Zheng et al., 2017). Here, individual (stem) cells are
133   trapped in a nanoliter-scale droplet containing barcoding oligonucleotide primers as well as reverse
134   transcriptase (RT)- and lysis reagents. Inside the droplet, a single cell is lysed followed by mRNA-
135   barcoding during RT-reaction. Barcoded single cell mRNAs are pooled and prepared cDNA libraries
136   can be processed for sequencing. Due to the initial barcoding, the information derived from a pool of
137   cells can be separated *in silico* to create expression profiles of the corresponding cells (Klein et al.,
138   2015; Zilionis et al., 2016; Zheng et al., 2017). With regard to nanoliter-scale working-volumes and
139   pooling of labeled single cell mRNA, the linkage of microfluidic systems and droplet barcoding
140   strategies allows a significant decrease in the respective amount of required reagents and therefore a
141   dramatic reduction of costs per sequenced cell (Klein et al., 2015; Ziegenhain et al., 2017). Currently,
142   the platforms Drop-seq (Macosko et al., 2015), inDrop (Klein et al., 2015; Zilionis et al., 2016) and
143   10X Genomics Chromium (Zheng et al., 2017) are most widely applied for microfluidic-based
144   generation of single cell libraries followed by scRNA-seq. In a recent side-by-side comparison by
145   Zhang and coworkers, all systems were shown to be satisfactory efficient in detection of transcripts.
146   The authors concluded 10X to be a reasonable and safe option for a wide range of applications, while
147   Drop-seq being more cost-efficient for abundant samples and inDrop being the best choice for detecting
148   low-abundance transcripts or for establishing custom protocols (Zhang et al., 2019). Although the
149   sorting of a cell population of interest prior to sequencing is not supported and the analysis of distinct
150   small cell populations is thus exacerbated, microfluidic systems are well-suited to address the challenge
151   of scRNA-seq of stem cells in a cost-efficient manner. Regarding the techniques introduced above, the
152   following chapters will discuss single cell data reporting heterogeneity in neural crest-derived stem
153   cell populations and underlying regulatory networks.

154   **3   Adult neural crest-derived stem cells – From individual developmental drivers to mediators**
155   **of regeneration during adulthood**

156   The neural crest (NC) was described the first time by Wilhelm His in 1868 as the intermediate chord
157   (''Zwischenstrang'') between the neural tube and the future ectoderm in the developing chick embryo
158   (His, 1868). During neurulation, premigratory neural crest cells arise from the neural plate border and
159   undergo epithelial to mesenchymal transition (EMT) after formation of the neural tube (Fig. 3A).
160   Following EMT, neural crest cells migrate out of their niche and give rise to a broad variety of
161   ectodermal and mesenchymal cell types, thereby fundamentally contributing to embryonic
162   development (Dupin and Sommer, 2012; Kaltschmidt et al., 2012; Etchevers et al., 2019). According
163   to their position on the anteroposterior axis, migration behavior and differentiation potential, migrating
164   NC cells are divided into cranial, vagal (including cardiac), trunk and sacral NC cells (Yntema and
165   Hammond, 1954; Le Douarin and Teillet, 1974; Noden, 1975; 1978a) (reviewed by (Rothstein et al.,
166   2018)). Cranial NC cells firstly undergo EMT and form a range of craniofacial cell types and tissues
167   such as peripheral nerves, melanocytes, thyroid cells, teeth and most of the craniofacial skeleton
168   (Johnston, 1966; Noden, 1978a; b; Baker et al., 1997) (see reviews from (Graham et al., 2004;
169   Kaltschmidt et al., 2012; Rocha et al., 2020)for overview) (Fig. 3A). Vagal NC cells give rise to enteric
170   neurons and glia forming the enteric nervous system of the foregut and stomach, while an anterior
171   localized subset, the cardiac NC cells, contributes to septation of the outflow tract in the developing
172   heart (Phillips et al., 1987; Burns and Douarin, 1998). Trunk NC cells were reported to differentiate
173   into sensory and sympathetic ganglia, melanocytes and the adrenal medulla (Fig. 3A). Sacral NC cells,
174   which have only been identified in amniotes so far, colonize the gut after their vagal counterparts to

175 form enteric glia and neurons innervating the hindgut (Yntema and Hammond, 1954; Le Douarin and
176 Teillet, 1973; Epstein et al., 1994) (see review from (Rothstein et al., 2018) for overview). Notably,
177 NC cells not only give rise to distinct cell types in the developing tissues, but even guide patterning
178 and differentiation of their target tissues during embryogenesis (Rios et al., 2011; Faure et al., 2015).
179 For instance, in the avian system, the cephalic neural crest (CNC) has been shown to control
180 development of the forebrain and midbrain. Here, the CNC regulates the shaping and size of the pre-
181 otic brain by the expression of bone morphogenetic protein (BMP) antagonists like Gremlin and
182 Noggin (Creuzet, 2009). Accordingly, mutations in key transcription factors regulating migration and
183 differentiation of NC cells, like SLUG, SOX10, SNAIL, or TWIST lead to NC maldevelopment and
184 specific disease phenotypes. Amongst others, these so-called neurocristopathies (Bolande, 1974)
185 particularly include tumors as melanoma, neuroblastoma or neurofibroma, malformations like cleft lip
186 or palate, heart malformations and craniofacial defects (Kabuki syndrome) as well as Hirschsprung's
187 disease, Waardenburg syndrome or Charcot–Marie–Tooth disease (Bolande, 1974; Wilkie and
188 Morriss-Kay, 2001; Amiel et al., 2008; Vega-Lopez et al., 2018; Greiner et al., 2019a). Interestingly,
189 certain neurocristopathies like Hirschsprung's disease, Waardenburg syndrome, melanoma or
190 meningioma were reported to occur in a sex-specific manner (reviewed in (Greiner et al., 2019a)).
191 While Hirschsprung's disease, Waardenburg syndrome and melanoma were described to have a
192 prevalence in males (Amiel et al., 2008; Karimkhani et al., 2017), meningiomas occur twice as often
193 in female individuals (Korhonen et al., 2006), emphasizing the potential heterogeneity between
194 embryonic NC populations of distinct sexes (reviewed in (Greiner et al., 2019a)). In addition, Lignell
195 and coworkers revealed heterogeneity even within embryonic NC stem cell populations in the chick
196 dorsal neural tube by demonstrating the presence of distinct premigratory and early migratory neural
197 crest populations in the developing dorsal midbrain. These observations emphasize the heterogeneity
198 of cells located in the neural crest stem cell niche and provide hints for spatially and transcriptionally
199 distinct subpopulations at single cell resolution (Lignell et al., 2017).
200 Beyond their tremendous role in embryogenesis, neural crest stem cells also remain in distinct niches
201 as quiescent stem cell pools into adulthood (Sieber-Blum and Grim, 2004; Widera et al., 2007; Dupin
202 and Sommer, 2012; Hauser et al., 2012). These neural crest-derived stem cells can be found in various
203 tissues of the adult human body, for example the bone marrow (Coste et al., 2017), skin (Toma et al.,
204 2001), heart (Höving et al., 2020b), cornea (Katikireddy et al., 2016), hair follicles (Clewes et al.,
205 2011), dental pulp (Waddington et al., 2009), palatum (Widera et al., 2009) or the respiratory and
206 olfactory epithelium of the nasal cavity (Murrell et al., 2008; Hauser et al., 2012; Schurmann et al.,
207 2017). Adult NCSCs are known to possess a high capacity for self-renewal as well as an extended
208 multipotency, revealed by an extraordinary high differentiation potential particularly into
209 mesenchymal and ectodermal cell types *in vitro* and *in vivo* (Fig. 3B)(Murrell et al., 2008; Shakhova
210 and Sommer, 2008; Müller et al., 2015; Hofemeier et al., 2016; Greiner et al., 2019b). Common
211 characteristics of NCSCs further include expression of the intermediate filament Nestin and NC-
212 associated markers like SOX9, SOX10, SLUG, SNAIL or TWIST as well as the capacity to form
213 neurospheres *in vitro* (Nieto et al., 1994; Lothian and Lendahl, 1997; Southard-Smith et al., 1998; del
214 Barrio and Nieto, 2002; Spokony et al., 2002; Kim et al., 2003; Soldatov et al., 2019). Their broad
215 differentiation and migration capability and accessibility in the adult human organism make NCSCs
216 promising candidates for pharmacological research (Matigian et al., 2010; Rodrigues et al., 2014;
217 Müller et al., 2016) and regenerative medicine (Barnett et al., 2000; Tabakow et al., 2014; Müller et
218 al., 2015). Here, NCSCs were reported to functionally recover animal models of Parkinson's disease
219 or spinal cord injury (Barnett et al., 2000; Murrell et al., 2008; Müller et al., 2015). Tabakow and
220 coworkers impressively demonstrated the functional regeneration of supraspinal connections in a
221 patient with transected spinal cord. Next to peripheral nerve bridging, the authors transplanted
222 autologous olfactory ensheathing cells, a population of NCSCs located in the olfactory bulb, resulting
223 in partial recovery of voluntary movement of the lower extremities (Tabakow et al., 2014).

224   Despite similarities in their clinical applicability and common characteristics, distinct populations of
225   human NCSCs differ in their expression profiles and differentiation potential with particular regard to
226   their tissue of origin (Höving et al., 2020b). In addition to differences between distinct populations of
227   adult NCSCs, several very recent studies even point towards a cellular heterogeneity within respective
228   NCSC-pools (Fig. 3C)(Young et al., 2016)(see table 1 for overview). The following chapters will focus
229   on these heterogeneities in terms of NCSC-identities, fate decision and underlying regulatory networks.

4   Fate specifications and heterogeneity of NCSCs from the nasal cavity and olfactory bulb

231   The mammalian nasal cavity and olfactory bulb (OB) are well-known to harbor distinct niches for adult
232   neural crest-derived stem cells. Amongst others, these NCSC-populations include horizontal basal cells
233   (HBCs) and olfactory ensheathing cells (OECs) residing in olfactory mucosa of the middle and superior
234   turbinate (OECs and HBCs) and as well as the olfactory bulb (OECs) (Barnett et al., 2000; Murrell et
235   al., 2008; Barraud et al., 2010; Suzuki et al., 2013; Tabakow et al., 2014). Further, olfactory
236   ectomesenchymal stem cells (OE-MSC) within the lamina propria of the human olfactory mucosa were
237   shown to express a range of neural as well as mesenchymal markers (Delorme et al., 2010). In addition,
238   neural crest-derived stem cells were described to be located in the respiratory epithelium of the inferior
239   turbinate (inferior turbinate stem cells, ITSCs) (Hauser et al., 2012) and in the lamina propria of middle
240   turbinate tissue (middle turbinate stem cells, MTSCs) (Schurmann et al., 2017). Assessment of the
241   heterogeneity of these stem cell populations is increasingly enabling promising insights into the control
242   of fate decisions and lineage restrictions of mammalian stem cells and adult mammalian regeneration.
243   In this regard, Fletcher and coworkers recently investigated a detailed map of lineage choices for HBCs
244   in the murine postnatal olfactory epithelium using scRNA-seq combined with lineage tracing *in vivo*.
245   Interestingly, an initial lineage trajectory of quiescent HBCs into either sustentacular cells via direct
246   fate conversion or globose basal cells (GBCs) was reported to occur prior to cell division. For olfactory
247   neurogenesis ensuring tissue homeostasis, GBCs proliferate and give rise to microvillous cells and
248   olfactory sensory neurons, but also to Bowman's gland. The authors further identified canonical Wnt-
249   signaling as a major regulator driving the route of HBCs from quiescence to neuronal differentiation
250   by promoting neuronal fate choices (Fletcher et al., 2017). Within the injured mouse olfactory
251   epithelium, quiescent HBCs were shown to be activated and adopt a proliferative and transient state,
252   which was found to be unique to injury (Gadye et al., 2017). Self-renewal of proliferating transient
253   HBCs was reported to result in a resting HBC-population as well as in further enlargement of the
254   transient HBC-population. Transient HBCs differentiated into the neuronal lineage via GBCs and
255   microvillous cells towards mature olfactory sensory neurons with Sox2 being essential for transition
256   from the activated to neuronal progenitor states. In contrast to non-injury conditions in tissue
257   homeostasis (Fletcher et al., 2017), regeneration of sustentacular cells was demonstrated to involve
258   proliferation of HBCs, although sustentacular cells likewise differentiated directly from the transient
259   HBCs. Notably, activated single HBCs revealed a highly heterogeneous gene expression indicating a
260   heterogeneity within the transient state of HBCs leading to designation of lineage commitment (Gadye
261   et al., 2017). Using scRNA-Seq of 28,726 single cells, Durante and coworkers very recently provided
262   evidence for ongoing robust neurogenesis in the human olfactory epithelium under non-injury
263   conditions contributing to sensing of smell. Next to a high ratio of immature to mature neurons,
264   KRT5^{+}/SOX2^{+} HBCs were frequently observed to possess a rounded, reactive-like morphology. The
265   authors thus suggested the stemness state of HBCs in the OE of middle-aged humans to be similar to
266   injury-induced epithelial reconstitution in rodents (Durante et al., 2020). Next to heterogeneity of
267   NCSCs in the olfactory epithelium *in vivo*, Huang and colleagues reported differential migration
268   behavior of distinct single murine OECs. Here, the distinct OEC-subpopulations defined the respective
269   mode of migration as well as underlying distribution of the cytoskeleton (Huang et al., 2008).

270   Nearly a decade ago, we identified a population of NCSCs in the respiratory epithelium of the human
271   inferior turbinate (Hauser et al., 2012). Inferior turbinate stem cells (ITSCs) could be propagated *in*
272   *vitro* as free-floating neurospheres or within human blood plasma-derived 3D fibrin matrix. *In vitro*
273   cultivated ITSCs showed the ability to self-renew and differentiate into mesenchymal derivates like
274   adipocytes or osteoblasts, but also efficiently gave rise to glutamatergic and dopaminergic neurons
275   (Greiner et al., 2011; Müller et al., 2015; Ruiz-Perera et al., 2018; Greiner et al., 2019b; Ruiz-Perera et
276   al., 2020). Despite this commonly shared differentiation potential, ITSCs also revealed heterogeneities
277   in their behavior during differentiation. In particular, we recently observed differences in
278   neuroprotection of ITSC-derived glutamatergic neurons against oxidative stress in dependence on the
279   sex of the stem cell donor. ITSC-derived neurons from female donors showed increased oxidative
280   stress-induced neuronal death but also an elevated neuroprotection after stimulation of the transcription
281   factor nuclear factor 'kappa- light-chain-enhancer' of activated B cells (NF-κB) compared to their male
282   counterparts (Ruiz-Perera et al., 2018). The observed differences in neuroprotection were accompanied
283   by the presence of a sexually dimorphic protective gene expression program (Ruiz-Perera et al., 2018),
284   suggesting further heterogeneities in differentiation behavior of ITSCs. In addition, we observed
285   donor-dependent differences in the amount of p75^{NTR}-positive stem cells in their niche within the
286   inferior turbinate. Here, freshly dissociated tissue from individual donors showed 9.78% to even
287   26.50% of p75^{NTR}-positive ITSCs depending on the donor. On single cell level, assessment of self-
288   renewal in tertiary ITSC clones revealed different ratios of ITSC-derived ectodermal to mesenchymal
289   progeny dependent on the distinct single stem cell (Greiner et al., 2011; Hauser et al., 2012), as
290   schematically depicted in Fig. 3C. Accordingly, recent qPCR-analysis following SMART-Seq2 of
291   single self-renewing ITSCs emphasized the heterogeneity between individual stem cells on gene
292   expression level. In particular, we observed great differences in expression levels of NCSC-markers
293   SLUG, SNAIL and Nestin between single ITSCs (Fig. 4A). Immunocytochemistry validated the
294   heterogeneous amounts of nuclear localized SLUG protein, indicating variations in the presence and
295   activity of SLUG depending on the individual stem cell state (Fig. 4B, see also chapter 9). Since
296   spontaneous differentiation of ITSCs was not observable under the applied culture conditions in our
297   previous studies (Greiner et al., 2011; Hauser et al., 2012), we strongly suggest intrinsic differences
298   between stem cell states to account for this heterogeneity. Interestingly, activation of SLUG is
299   commonly noticed to regulate and determine stemness states of adult stem cells (Guo et al., 2012; Tang
300   et al., 2016). The heterogeneous expression of major NCSC-markers like Nestin and regulatory
301   transcription factors like SLUG may thus be directly associated to the observed differences in
302   differentiation potentials between single ITSCs, as already described for NCSCs located in the oral
303   cavity ((Young et al., 2016), see below).

304   **5   Heterogeneity of NCSCs in the oral cavity**

305   Next to the nasal cavity, neural crest-derived stem cells are present within oral tissues for instance as
306   periodontal ligament stem cells (PDLSCs) (Widera et al., 2007; Huang et al., 2009; Kawanabe et al.,
307   2010), dental pulp stem cells (DPSCs) (Gronthos et al., 2000; Stevens et al., 2008)(reviewed in (Sloan
308   and Waddington, 2009; Kaltschmidt et al., 2012)), human oral mucosa stem cells (hOMS) (Marynka-
309   Kalmani et al., 2010) and progenitor cells in the lamina propria of the oral mucosa (OMLP-PC) (Davies
310   et al., 2010), or oral stromal stem cells (Boddupally et al., 2016). Although expression of neural crest-
311   associated markers in PDLSCs seems to be heterogeneous in dependence to the culture system, several
312   studies reported successful differentiation into a range of ectodermal and mesenchymal derivates
313   (Widera et al., 2007; Huang et al., 2009). However, single cell-derived PDLSC-clones were
314   demonstrated to differ in their differentiation capability ranging from clones with multilineage potential
315   to sole osteoprogenitors (Singhatanadgit et al., 2009).

316 Next to periodontal ligament, dental tissues particularly including the dental pulp are developmentally
317 derived from the neural crest (Chai et al., 2000). Human DPSCs were reported to be positive for the
318 NCSC-marker Nestin (Arthur et al., 2008) and to form dentin and dental pulp tissue *in vivo*, but are
319 also able to give rise to osteoblasts, chondrocytes, adipocytes and even to NC-related melanocytes and
320 functionally active neurons (Gronthos et al., 2000; Arthur et al., 2008; Stevens et al., 2008; Jiang et al.,
321 2019). In accordance with our own observations in human ITSCs, single cell-derived clonal cultures
322 of murine DPSCs revealed highly heterogeneous gene expression levels of Nestin between individual
323 stem cell clones. Notably, DPSCs showing high Nestin expression differentiated into neuron-like or
324 oligodendrocyte-like derivates, while Nestin^{low}-DPSCs lacked this capacity (Young et al., 2016). In
325 line with these findings, Kobayashi and coworkers recently characterized differences in proliferation,
326 differentiation potential and gene expression between fifty human dental pulp stem cell clones.
327 Although the characteristic DPSC-markers STRO-1 and CD146 were co-expressed in nearly all DPSC
328 clones, individual DPSCs showed great differences in their differentiation capacities into odontogenic,
329 adipogenic and chondrogenic derivates (Kobayashi et al., 2020). Likewise, Jiang and colleagues
330 observed successful differentiation of a human DPSC clone into the osteogenic, adipogenic and
331 chondrogenic lineage, while two distinct clones from the same parental population only revealed
332 osteogenic differentiation capacity (Jiang et al., 2019). In this line, Gronthos and coworkers reported
333 *in vivo* generation of ectopic dentin by nine out of twelve individual single-colony-derived DPSCs. On
334 the contrary, three out of twelve clonally grown DPSCs revealed only a limited capability of forming
335 dentin, indicating great heterogeneity between individual DPSCs regarding their differentiation
336 capability (Gronthos et al., 2000). On technical level, heterogeneity of human DPSCs was recently
337 shown to be assessable by single-cell Raman spectroscopy (SCRM). Alraies and coworkers utilized
338 SCRM to discriminate subpopulations of DPSCs from human third molars and established SCRM-
339 fingerprints defining highly proliferative/multipotent and low proliferative/unipotent DPSCs (Alraies
340 et al., 2019). This highly promising technique may enable selective noninvasive screening of DPSCs
341 in the future and further validates the heterogeneity between individual NC-derived DPSCs.
342 Determining the molecular basis for the commonly observed differences in proliferative behavior,
343 Alraies and colleagues identified a relation between proliferative heterogeneity of DPSCs and
344 differences in telomere lengths and CD271 expression, suggesting variations in human dental pulp
345 stem cell ageing (Alraies et al., 2017).

346 **6   Heterogeneity of NCSCs in the carotid body and cornea of the eye**

347 Located in the bifurcation of the carotid artery, the carotid body (CB) is the main arterial chemoreceptor
348 sensing oxygen (Lopez-Barneo et al., 2001) and was reported to contain cells of neural crest origin in
349 1973 by Pearse and coworkers (Pearse et al., 1973). NCSCs were discovered to be present in the adult
350 rat CB by Pardal and coworkers and revealed the capacity to form spheres and give rise to dopaminergic
351 neurons and mesenchymal cell in vitro (Pardal et al., 2007). Strikingly, the authors demonstrated CB-
352 NCSCs to remain in a quiescent glia-like cell state until activation by hypoxia, which in turn resulted
353 in a phenotype switch towards Nestin-positive NCSCs undergoing neurogenesis in vivo (Pardal et al.,
354 2007; Platero-Luengo et al., 2014). Next to contributing to neurogenesis in the CB during persistent
355 hypoxia, the group around López-Barneo further reported murine CB-NCSCs to efficiently give rise
356 to endothelial cells directly contributing to hypoxia-induced angiogenesis (Annese et al., 2017). These
357 promising data emphasize the enormous plasticity of adult NCSCs commonly described to undergo
358 mesenchymal or ectodermal rather than endothelial differentiation. Although investigations of their
359 plasticity still remain to be investigated in human CB-NCSCs, the data provided by the López-Barneo
360 group further indicate a niche-dependent heterogeneity of NCSCs in terms of their differentiation
361 potential, which is in accordance to our own very recent findings (Höving et al., 2020b).

362 Next to the carotid body, the oral and nasal cavity as well as the olfactory bulb, the human eye likewise
363 harbors craniofacial NCSCs. In this regard, Yoshida and coworkers demonstrated the presence of
364 NCSCs positive for Nestin, SOX9, TWIST, SLUG and SNAIL in the adult murine cornea. Such NC-
365 derived corneal precursors (COPs) revealed the capacity to differentiate into keratocytes, adipocytes
366 and chondrocytes, while only showing a minor potential to undergo neuronal differentiation (Yoshida
367 et al., 2006). NCSCs expressing Nestin, SOX9, SNAIL, SLUG and TWIST were further reported to
368 be located in the murine corneal limbus (Brandl et al., 2009). ABCB5-positive human limbal stem cells
369 (LSCs) capable of restoring the corneal epithelium upon transplantation into LSC-deficient mice
370 (Ksander et al., 2014) are likewise suggested to be of neural crest origin (reviewed in (Gonzalez et al.,
371 2018)). However, although the limbal niche is commonly known to harbor NC-derived limbal stromal
372 fibroblasts (Gage et al., 2005) and melanocytes, its complexity and heterogeneity challenges the
373 determination of the identity and developmental origin of LSCs (reviewed in (Gonzalez et al., 2018)).
374 In addition, NCSC-markers were observed to be expressed in neural crest-derived progenitors isolated
375 from the adult human corneal endothelium, which revealed the capacity to undergo differentiation into
376 the neuronal lineage and the corneal endothelium itself (Katikireddy et al., 2016). As discussed above,
377 the complexity of this already highly heterogeneous microenvironment accompanied by the lack of
378 single cell data regarding potential human corneal/limbal NCSCs so far likewise challenges the
379 assessment of NCSC-heterogeneity in the limbal and corneal niche.

380 **7 Heterogeneous expression patterns and plasticity of NCSCs in the craniofacial and trunk**
381 **skin**

382 The human craniofacial skin is known to harbor two distinct populations of NCSCs, namely skin-
383 derived precursors (SKPs) (Toma et al., 2001; Fernandes et al., 2004) and epidermal neural crest stem
384 cells (EPI-NCSCs) located within the bulge of hair follicles (Sieber-Blum et al., 2004). Next to their
385 presence in the craniofacial region, EPI-NCSCs were also identified within the trunk region of the
386 human body (Clewes et al., 2011). While SKPs were reported to express Nestin, SNAIL, SLUG,
387 TWIST and SOX9 (Toma et al., 2001; Fernandes et al., 2004), EPI-NCSCs were shown to lack
388 expression of Slug, Snail and Twist. On the contrary, EPI-NCSCs were shown to display expression
389 of Msx2 and SOX10 (Sieber-Blum et al., 2004; Hu et al., 2006), emphasizing the transcriptional
390 heterogeneity of NCSCs even between bulk populations located close to each other. Interestingly, an
391 assessment of the adult murine epidermis on single level by Joost and coworkers suggested that self-
392 renewing cells in the adult hair follicle lack a distinct stemness gene expression signature. On the
393 contrary, self-renewing cells shared a common basal gene expression signature accompanied by
394 characteristic spatial signatures segregating the cell populations in relation to their location during
395 tissue homeostasis (Joost et al., 2016). Two years later, Joost and colleagues analyzed hair follicle
396 bulge stem cells positive for LGR5, a marker for NCSCs in the oral cavity (Boddupally et al., 2016),
397 on single cell level to asses transcriptional adaptations during wound healing in mice (Joost et al.,
398 2018). Interestingly, LGR5-positive hair follicle bulge stem cells gradually activated an interfollicular
399 epidermis stem cell-like gene expression signature even before migrating out of the bulge towards the
400 lesion. These findings suggest a great cellular plasticity of single LGR5-positive hair follicle bulge
401 stem cells allowing rapid transcriptional adaptations during wound healing (Joost et al., 2018).
402 Accordingly, EPI-NCSCs were also described to show great cellular plasticity (Sieber-Blum et al.,
403 2004; Hu et al., 2006; Hu et al., 2010) but no reports addressing their intrapopulational heterogeneity
404 are available so far. Single SKPs from human foreskin were shown to give rise to mesenchymal and
405 ectodermal cell types like neurons or smooth muscle cells (Toma et al., 2001), although Dai and
406 coworkers suggested SKP-spheres to contain a heterogeneous mixture of stem and progenitor cells

407 (Dai et al., 2018). These suggestions are in accordance with our own observations regarding the
408 different ratios of single ITSC-derived ectodermal to mesenchymal progeny (Greiner et al., 2011;
409 Hauser et al., 2012)(see also chapter 4 and Fig. 3C) as well as the heterogeneous expression of NC-
410 markers in ITSCs (Fig. 4).

411 **8 Heterogeneity of trunk NCSCs in the dorsal root ganglia, sciatic nerve, bone marrow, heart**

412 **and gut**

413 Trunk NCSC populations can be found in the gut, bone marrow, sciatic nerve, dorsal root ganglia and
414 the heart (Kruger et al., 2002; Mosher et al., 2007; Nagoshi et al., 2008; Coste et al., 2017; Höving et
415 al., 2020a; Höving et al., 2020b). For instance, clonally grown colonies of $p75^+$ NCSC from the
416 postnatal rat gut showed multilineage potential containing neurons, glia, and myofibroblasts (Kruger
417 et al., 2002). Nagoshi and coworkers compared mouse NCSCs from bone marrow, dorsal root ganglia
418 and whisker pad and detected tissue source-dependent differentiation capacities. Compared with
419 whisker pad- and bone marrow-derived NCSCs, dorsal root ganglia-derived NCSCs showed a higher
420 degree of sphere formation and increased expression of p75, Nestin, SOX10 and Musashi1
421 accompanied by increased differentiation capacity into neurons, glia and myofibroblasts (Nagoshi et
422 al., 2008). Morrison and colleagues isolated $p75^+$ NCSC from the rat fetal sciatic nerve. These cells
423 possessed the capacity to expand on clonal level and to differentiate into neurons, Schwann cells and
424 myofibroblasts. Moreover, the neurotrophin receptor p75 and the peripheral myelin protein P0 were
425 utilized to isolate subpopulations of cells with varying developmental potentials. Notably, high
426 expression of p75 compared with a lack of P0 was accompanied by a high frequency (60 %) of
427 multipotent clones giving rise to neurons, Schwann cells and myofibroblasts while $p75^+P0^+$ cells
428 showed only a frequency of 28 % of multipotent clones. In addition, clonal cultured p75- cells were
429 only able to differentiate into myofibroblasts independent of the expression of P0 (Morrison et al.,
430 1999). These results suggest p75 to be one of the major markers for self-renewing, multipotent NCSCs.
431 Accordingly, we detected higher proliferation rates in $p75^+$ subpopulations of ITSCs compared to p75-
432 ITSCs (Hauser et al., 2012). Moreover, a recent study from Coste and colleagues identified a
433 $Nestin^+/SOX9^+/TWIST^+$ NCSC population in the human bone marrow with the ability to follow neural
434 crest migration pathways after transplantation into chick embryos (Coste et al., 2017). Populations of
435 NCSCs in the adult heart were firstly described in mice and zebrafish (Tomita et al., 2005; El-Helou et
436 al., 2008; Hatzistergos et al., 2015; Leinonen et al., 2016; Meus et al., 2017; Tang et al., 2019).
437 Recently, we identified a $Nestin^+/cKit^-$ stem cell population in the human heart (human cardiac stem
438 cells, hCSCs) with NCSC properties, giving rise to neuron-like cells, adipocytes and cardiomyocytes
439 (Höving et al., 2020a; Höving et al., 2020b). However, in a direct comparison with ITSCs as cranial
440 NC-derivates we observed a relatively minor potential of hCSCs to undergo neuronal differentiation
441 (Höving et al., 2020b). A general difference between NCSC populations from different tissues and
442 niches was also reviewed by Shakhova and Sommer (Shakhova and Sommer, 2008). In general, trunk
443 NCSCs from dorsal root ganglia, sciatic nerve and gut seem to possess a higher capacity for ectodermal
444 differentiation, particularly into neurons and glia compared to their mesenchymal differentiation
445 potential into osteogenic or adipogenic cell types (reviewed in (Shakhova and Sommer, 2008)).
446 Recently, Groeneveldt and colleagues performed a direct comparison of human periosteum-derived
447 cells (hPDCs) from the tibia as a mesoderm-derived tissue with hPDCs from maxilla and mandible as
448 examples of cranial neural crest-derived cells (Groeneveldt et al., 2020). While all cell populations
449 exhibited similar differentiation capacities into chondrogenic, adipogenic and osteogenic derivates and
450 proliferation rates in vitro, global gene expression analysis showed a higher amount of differentially
451 expressed genes (DEG) between hPDCs from the tibia and each of the craniofacial hPDC populations

452 than between hPDCs from the maxilla and mandible. In addition, the expression of HOX family
453 members was upregulated in tibia-hPDCs compared to maxilla- or mandible-hPDCs. After
454 implantation in nude mice, tibia- and mandibular- but not maxilla-hPDCs participated to bone
455 formation. These different properties in differentiation potentials in vivo may be associated to the
456 differential expression of genes from the HOX and DLX family (Groeneveldt et al., 2020). Likewise,
457 Leucht and colleagues detected differences in the contribution to bone repair mechanisms between
458 murine neural crest-derived skeletal stem cells and mesoderm-derived cells, where the expression of
459 Hoxa11 plays a crucial role (Leucht et al., 2008). In this regard, transplantation experiments in quail-
460 chick chimeras showed that HOX-negative embryonic neural crest cells are able to adopt the HOX
461 status of a HOX-positive environment. Vice versa, transplanted HOX-positive NCCs did not loose
462 their HOX-status in a new HOX-negative environment (Grapin-Botton et al., 1995; Couly et al., 1998).
463 The here discussed findings emphasize the relevance of HOX-activation in neural crest development
464 and indicate its role in regulating adult NCSC-heterogeneity. Heterogeneous marker expression or
465 differentiation potentials between NCSC-populations derived from different embryological origins are
466 further discussed in chapter 10. On the contrary, NCSCs from bone marrow were reported to efficiently
467 give rise to neuronal and mesenchymal cell types. Notably, the embryonic counterparts of some of
468 these adult NCSCs populations were also reported to be heterogeneous in response to their
469 microenvironment *in vivo* and *in vitro* (Bixby et al., 2002; Wong et al., 2006)(see also (Shakhova and
470 Sommer, 2008) for review). For instance, E14 rat NCSCs from sciatic nerve were shown to be more
471 responsive to gliogenic factors, while NCSCs from the gut revealed a greater responsiveness to
472 neurogenic factors (Bixby et al., 2002). In addition, transplantation of either NCSC from the gut or
473 from the sciatic nerve into chick embryos showed population-specific differences. Here, gut NCSCs
474 efficiently migrated and formed enteric neurons in the developing gut, but NCSCs from the sciatic
475 nerve did not reveal this capacity (Mosher et al., 2007). Although these studies describe a high degree
476 of heterogeneity between different NCSC-populations, to the best of our knowledge, studies addressing
477 the issue of cellular heterogeneity within these adult NCSC-populations in the human organism still
478 remain elusive.

479 **9   Molecular regulators defining stemness and fate choices of NCSCs**

480 Heterogeneity within and between the NCSC-populations discussed above is directly related to the
481 activity of potential molecular regulators defining their stemness and differentiation behavior.
482 According to the role of EMT being a prerequisite for migration of embryonic neural crest cells out of
483 their niche, common EMT-drivers like SOX9, SOX10, TWIST, SLUG and SNAIL are still present in
484 adult NCSCs (see also chapter 3). Notably, activation of EMT is closely associated to stem cell
485 properties, with EMT transcription factors regulating stemness (Lamouille et al., 2014; Nieto et al.,
486 2016). EMT drivers were also described to regulate each other with SNAIL inducing upregulation of
487 TWIST(Casas et al., 2011) (Dave et al., 2011), which in turn both positively regulate SLUG (Boutet et
488 al., 2006; Casas et al., 2011). We suggest this regulatory network of EMT-drivers to be vital for
489 maintaining NCSC-stemness (Fig. 5). In this line, SOX10was demonstrated to be necessary for
490 maintaining multipotency and inhibiting neuronal differentiation of neural crest cells (Kim et al., 2003).
491 The EMT-transcription factor SLUG is also particularly noticed to regulate and determine stemness
492 states of adult stem cells (Tang et al., 2016). Interestingly, SLUG and SOX9 were also reported to
493 cooperatively determine the stemness state of human breast cancer stem cells (Guo et al., 2012). Our
494 very recent observations show a great heterogeneity in expression and protein amounts of SLUG
495 between individual ITSCs (Fig. 4), suggesting a direct association to the observed differences in
496 differentiation potentials between single ITSCs (see also chapter 4, Fig. 3C). Interestingly, canonical
497 Wnt-signaling, which is closely linked to EMT, was described as a major regulator promoting neuronal

498 fate choices of HBCs, thus driving the route of HBCs from quiescence to neuronal differentiation
499 (Fletcher et al., 2017). Accordingly, canonical Wnt-signaling is commonly noticed to maintain the
500 stemness of neural crest stem cells and ASCs and guide ASC-differentiation in dependence to the
501 environmental context (Fig. 5)(Kleber et al., 2005; Ring et al., 2014).
502 Next to EMT-drivers regulating each other, the transcription factor NF-κB was described to influence
503 their expression and activity. Here, the regulation of SOX9, SLUG and TWIST was reported to be
504 mediated by NF-κB in cancer stem cells and during early vertebrate development (Zhang et al., 2006;
505 Sun et al., 2013). In particular, binding of NF-κB to κB binding sites present in their promoters was
506 shown to lead to increased expression of SLUG, SOX9 and TWIST in breast and pancreatic cancer, in
507 turn enabling EMT (Li et al., 2012; Sun et al., 2013; Pires et al., 2017). With SLUG, SOX9 and TWIST
508 as well as NF-κB being commonly present in NCSCs (Toma et al., 2001; Fernandes et al., 2004; Hauser
509 et al., 2012; Müller et al., 2016; Ruiz-Perera et al., 2018)), we suggest a similar network being present
510 in adult NCSCs directly influencing fate decisions (Fig. 5). Accordingly, we recently demonstrated a
511 fate shift of ITSCs from the neuronal to oligodendroglial lineage by inhibition of NF-κB c-Rel (Ruiz-
512 Perera et al., 2020). Interestingly, we very recently identified p38-MAPK-signaling to be crucial for
513 protection of human cardiac NCSCs from senescence and promoting their proliferation (Höving et al.,
514 2020a), suggesting an additional regulatory role in NCSCs (Fig. 5). In addition to EMT-drivers and
515 NF-κB, the expression of the NCSC-marker Nestin is also directly associated with the differentiation
516 capacity of NCSCs. Young and coworkers demonstrated a highly heterogeneous expression of Nestin
517 between individual DPSCs clones, with only Nestin^{high} DPSCs being capable of neuronal and
518 oligodendrocyte differentiation (Young et al., 2016)(see also chapter 5). We likewise observed
519 differences in Nestin expression between single ITSCs, suggesting a linkage to differences in
520 differentiation potential (see also chapter 4, Fig. 3C, 4A). An additional potential marker for
521 multipotent self-renewing subpopulations could be the neurotrophin receptor p75. As discussed above
522 (see Chapter 8), p75$^+$ populations of rat sciatic nerve-derived NCSCs were able to differentiate into
523 neurons, Schwann cells and myofibroblasts while p75$^-$ cells were only able to differentiate into
524 myofibroblasts (Morrison et al., 1999). In our lab, p75$^+$ adult ITSCs exhibited increased proliferation
525 rates compared to their p75$^-$ counterparts (Hauser et al., 2012). In summary, an interplay between major
526 EMT-drivers like SOX9 or SLUG with NF-κB seems likely to orchestrate the stemness state of adult
527 NCSCs, although the exact regulatory mechanisms currently remain unknown (Fig. 5). Canonical Wnt-
528 and MAPK-signaling seem to play an additional role in mediating proliferation and fate decisions of
529 NCSCs (Fig. 5).

530 **10   Potential origins of NCSC-heterogeneity**

531 Cellular heterogeneity is known to be a general feature of multicellular organisms. Despite donor-to-
532 donor heterogeneity (Hauser et al., 2012; Belderbos et al., 2020)(Fig. 6), especially transcriptional
533 lineage segregation during human embryonic development as well as the requirement of tissue-specific
534 functionality in adulthood are reasons for distinct gene expression profiles (Xue et al., 2013; Yan et
535 al., 2013). This kind of lineage segregation also occurs in the development of different subpopulations
536 deriving from neural crest stem cells, which give rise to a broad variety of ectodermal and mesenchymal
537 cell types during embryogenesis (Dupin and Sommer, 2012; Kaltschmidt et al., 2012; Etchevers et al.,
538 2019). In accordance to their specific position on the anteroposterior axis, differentiation potential as
539 well as migration behavior is coordinated resulting in cranial, vagal (including cardiac), trunk and
540 sacral NC cells (Rothstein et al., 2018; Rocha et al., 2020) (see also chapter 3). Such developmental-
541 based heterogeneity results in tissue-specific gene expressions, which were recently investigated by
542 Han and colleagues using scRNA-seq to determine the cell-type composition of all major human
543 organs, leading to the construction of a scheme for the human cell landscape. Additionally, the authors

544 commented on discrepancies between differentiated cell types and stem cells concerning solidity of
545 gene expression, as stem and progenitor cells revealed more instable transcription profiles (Han et al.,
546 2020). These observations are in accordance with reported heterogeneity concerning differentiation
547 potentials as well as expression profiles of NCSCs deriving from different tissues (Höving et al.,
548 2020b)(Fig. 6). Such a niche-dependent heterogeneity is most likely driven by different extrinsic
549 stimuli based on variations within the microenvironments harboring stem cells (Trentin, 1971; Metcalf,
550 1998). An influence of extrinsic factors on heterogeneity may be also reflected by different culture
551 conditions of NCSCs, as serum-free culture was shown to favor neuronal fate decisions in comparison
552 to serum-containing culturing, which was shown to support proliferation (Ziller et al., 1983). This was
553 even reported for clonally grown NCSCs, where fate choices were influenced by the application of
554 specific growth factors (Sieber-Blum and Cohen, 1980). Calloni and colleagues isolated embryonic
555 cranial NCCs from the quail mesenchephalon and could show that treatment with the morphogen Sonic
556 Hedgehog (Shh) increased the number of multipotent subclones with the capacity to differentiate into
557 glia, neurons, melanocytes, myofibroblasts and chondrocytes (GNMFC-progenitors) while untreated
558 clones where more restricted to neural progenitors differentiating into neurons, glia and melanocytes
559 (GNM-progenitors) (Calloni et al., 2007; Calloni et al., 2009). Likewise, da Costa and colleagues
560 detected in clonally grown quail embryonic mesencephalic NCCs increased developmental potential
561 into glial cells, neurons, melanocytes, smooth muscle cells, chondrocytes, and adipocytes after the
562 simultaneous application of FGF8 and Shh (da Costa et al., 2018). Moreover, Dupin and colleagues
563 reviewed the differentiation capacities of embryonic NCCs from the cephalic and trunk regions of the
564 neural crest, discussing that trunk NCCs possess an in vivo differentiation potential into the neural,
565 glial and melanocytic lineage which can be extended in vitro to mesenchymal cell types like
566 connective, osteogenic, adipogenic and skeletogenic cells with Shh playing a central role (Dupin et al.,
567 2018). Nevertheless, stem cell heterogeneity within purified populations and even in clonally derived
568 cell lines may not only be regulated by extrinsic, but also intrinsic factors. As discussed above, clonal
569 cultures of oral cavity-derived NCSCs revealed specific variations in their differentiation potential
570 under uniform culture conditions (Jiang et al., 2019; Kobayashi et al., 2020). This was also reported
571 for ITSC clones, which gave rise to different ratios of ectodermal to mesodermal progeny upon
572 differentiation (see also chapter 4). Notably, ITSCs were precultivated using animal serum-free 3D
573 cultivation methods assuring genetic stability and stemness including mesenchymal and ectodermal
574 differentiation *in vitro* (Greiner et al., 2011; Hauser et al., 2012). Accordingly, Kerosuo and coworkers
575 postulated conserved multipotency of clonal NCSCs via long term culturing as so-called
576 'crestospheres', although the authors observed dynamic heterogeneity in the expression of neural crest
577 markers within clonally grown spheres. Nevertheless, this 3D culture method was shown to maintain
578 NCSCs self-renewal and multipotency for weeks avoiding spontaneous differentiation (Kerosuo et al.,
579 2015) and substantially reducing heterogeneity. However, the here discussed observations emphasize
580 the necessity to critically monitor cultivation conditions as a potential source of spontaneous
581 differentiation and artificial heterogeneity.

582 Further intrinsic factors driving heterogeneity of stem cells may include differences in gene expression
583 upon transcriptional regulation (see also chapter 9), cell cycle state (Kowalczyk et al., 2015; Tsang et
584 al., 2015), epigenetic heterogeneity based on differences in chromatin states (Yu et al., 2017)(reviewed
585 in (Carter and Zhao, 2020)) as well as stochastic fluctuations of the mechanisms underlying mRNA
586 and protein production (Raj et al., 2008)(see Fig. 6 for overview). Such stochastic fluctuations have
587 their origin in random segregation at the cell division stage (Huh and Paulsson, 2011) and are essential
588 for spontaneous generation of complex patterns and thus are crucial driver of evolution and selection
589 (Fraser et al., 2004). In this line, Wu and coworkers analyzed the heterogeneous expression of the
590 pluripotency marker Nanog in genetically identical human ESCs and linked the observed heterogeneity
591 to stochastic partitioning at division and transcriptional noise (Wu and Tzanakakis, 2012). Intrinsic

592 stochastic heterogeneity of transcription is emphasized to rely on a process named transcriptional
593 bursting, which describes the stochastic activation and inactivation of promoters (Raj et al., 2006;
594 Fukaya et al., 2016). Recently, Orchiai and colleagues used scRNA-seq to investigate the reasons for
595 this process in murine ESCs and reported kinetic properties of transcriptional bursting to be influenced
596 by multiple promoter-binding proteins, such as transcription elongation factors (Ochiai et al., 2020).
597 Although the influence of such stochastic events on NCSC heterogeneity cannot be completely
598 excluded, the here discussed observations emphasize the presence of distinct NCSC-stemness states
599 being based on differences in gene expression driven by molecular regulators like EMT-drivers as well
600 as NF-κB, canonical Wnt- and MAPK-signaling (see also chapter 9, Fig. 6). In this regard, the potential
601 further influence of cell cycle states and epigenetic regulation need to be assessed in future studies.
602 The findings summarized here further strongly suggest heterogeneity of NCSCs to be partly determined
603 by their niche of origin including the external and internal factors defined by the microenvironment as
604 discussed above.

11   Summary and Outlook: NCSC-identities between heterogeneous differentiation potential and common transcriptional signatures

607 In summary, the present review emphasizes the great heterogeneity of craniofacial and trunk NCSC-
608 populations. NCSC-heterogeneity was reported to be present on multiple levels particularly including
609 the donor, the sex of the donor, the cell population and the single stem cell. On donor level, variations
610 between donor-to-donor were described in the amount of NCSCs in their niche as well as sex-specific
611 differences in behavior during differentiation. Interpopulational differences further substantially
612 contribute to the heterogeneity between NCSCs observed in differentiation potential with particularly
613 regard to their niche of origin. On single cell level, differences in expression signatures of NCSCs were
614 further directly linked to individual fate decisions *in vitro* and *in vivo*. With regard to these diverse
615 levels of heterogeneity, even among clonally grown NCSCs, there is no overall ideal source of NCSCs
616 or culture condition to overcome single cell heterogeneity so far. Nevertheless, clonal 3D-culture
617 methods, including sphere cultures (Kerosuo et al., 2015) or matrices (Greiner et al., 2011; Hauser et
618 al., 2012) are increasingly noticed to reduce spontaneous differentiation, thus at least overcoming one
619 parameter of extrinsic heterogeneity. Despite the broad heterogeneity of NCSCs, we suggest that the
620 global presence of EMT-associated transcription factors like SLUG, SOX9 or SOX10 is not only
621 prerequisite for NCSC-identity but orchestrates their stemness state in co-regulation with NF-κB,
622 canonical Wnt- and MAPK-signaling. In addition, the neurotrophin receptor p75 may label
623 subpopulations of NCSCs with enhanced proliferation rates and differentiation capacities (Morrison et
624 al., 1999; Hauser et al., 2012). The observed heterogeneity in the expression of these NCSC markers
625 may thus directly contribute to heterogeneous stemness states but also further emphasizes the need for
626 a definite set of markers verifying NCSC-identity.
627 As a future perspective, comparisons between NCSC-populations of different niches may shed light
628 on the basis of heterogeneity observed in their differentiation potential. In this regard, we recently
629 demonstrated high similarities between the transcriptomes of craniofacial and cardiac human NCSCs,
630 despite the developmental differences between embryonic cranial and vagal NC cells. On the contrary,
631 the assessed global gene expression signatures likewise reflected differences between the adult NCSC-
632 populations with regard to their particular niche (Höving et al., 2020b). In this line, we also observed
633 differences in their differentiation potential likewise reflecting their origin in the craniofacial region or
634 the adult heart (Höving et al., 2020b). Next to comparing NCSC-populations, single cell analysis will
635 serve as a powerful tool to assess individual heterogeneities between NCSCs and broaden our
636 understanding of NCSC fate choices in tissue regeneration. However, single cell heterogeneity will be
637 an additional challenge for therapeutic applications of NCSCs, as one prerequisite of cell therapy is
638 consistency of cell populations as medical product to render unvarying clinical results. Overcoming

639 heterogeneity within an even clonally grown cell population will be nearly impossible, thus cellular
640 products for therapies have to be characterized regarding specific phenotype and molecular
641 mechanisms essential for the treatment of the respective disease. Consequently, heterogeneity of
642 NCSCs increases the complexity in developing cell-based therapeutics and single cell analysis may
643 provide new insights in the consequences of cellular heterogeneity in clinical applications. In this line,
644 the findings discussed here emphasize the assessment of heterogeneity of NCSCs between donors, cell
645 populations and single stem cells to be vital for understanding their roles in tissue homeostasis and
646 improving their applicability in regenerative medicine.

647 ## 11 Conflict of Interest

650 ## 12 Author Contributions

651 JG provided the conception and design of the manuscript, AH, BW and JG wrote the manuscript, BK,
652 CKa and CKn revised the manuscript critically for important intellectual content and provided funding.
653 All authors read and approved the submitted version of the manuscript.

654 ## 13 Funding

657 ## 14 Acknowledgments

660 ## 15 References

661 Alraies, A., Alaidaroos, N.Y., Waddington, R.J., Moseley, R., and Sloan, A.J. (2017). Variation in
662   human dental pulp stem cell ageing profiles reflect contrasting proliferative and regenerative
663   capabilities. *BMC Cell Biol* 18(1)**,** 12. doi: 10.1186/s12860-017-0128-x.
664 Alraies, A., Canetta, E., Waddington, R.J., Moseley, R., and Sloan, A.J. (2019). Discrimination of
665   Dental Pulp Stem Cell Regenerative Heterogeneity by Single-Cell Raman Spectroscopy. *Tissue
666   Eng Part C Methods* 25(8)**,** 489-499. doi: 10.1089/ten.TEC.2019.0129.
667 Amiel, J., Sproat-Emison, E., Garcia-Barcelo, M., Lantieri, F., Burzynski, G., Borrego, S., et al. (2008).
668   Hirschsprung disease, associated syndromes and genetics: a review. *J Med Genet* 45(1)**,** 1-14.
669   doi: 10.1136/jmg.2007.053959.

670 Annese, V., Navarro-Guerrero, E., Rodriguez-Prieto, I., and Pardal, R. (2017). Physiological Plasticity
671   of Neural-Crest-Derived Stem Cells in the Adult Mammalian Carotid Body. *Cell Rep* 19(3)**,**
672   471-478. doi: 10.1016/j.celrep.2017.03.065.
673 Arthur, A., Rychkov, G., Shi, S., Koblar, S.A., and Gronthos, S. (2008). Adult human dental pulp stem
674   cells differentiate toward functionally active neurons under appropriate environmental cues.
675   *Stem Cells* 26(7)**,** 1787-1795. doi: 10.1634/stemcells.2007-0979.
676 Baker, C.V., Bronner-Fraser, M., Le Douarin, N.M., and Teillet, M.A. (1997). Early- and late-
677   migrating cranial neural crest cell populations have equivalent developmental potential in vivo.
678   *Development* 124(16)**,** 3077-3087.
679 Barnett, S.C., Alexander, C.L., Iwashita, Y., Gilson, J.M., Crowther, J., Clark, L., et al. (2000).
680   Identification of a human olfactory ensheathing cell that can effect transplant-mediated
681   remyelination of demyelinated CNS axons. *Brain* 123 (Pt 8)**,** 1581-1588. doi:
682   10.1093/brain/123.8.1581.
683 Barraud, P., Seferiadis, A.A., Tyson, L.D., Zwart, M.F., Szabo-Rogers, H.L., Ruhrberg, C., et al.
684   (2010). Neural crest origin of olfactory ensheathing glia. *Proc Natl Acad Sci U S A* 107(49)**,**
685   21040-21045. doi: 10.1073/pnas.1012248107.
686 Belderbos, M.E., Jacobs, S., Koster, T.K., Ausema, A., Weersing, E., Zwart, E., et al. (2020). Donor-
687   to-Donor Heterogeneity in the Clonal Dynamics of Transplanted HumanCord Blood Stem
688   Cellsin Murine Xenografts. *Biol Blood Marrow Transplant* 26(1)**,** 16-25. doi:
689   10.1016/j.bbmt.2019.08.026.
690 Bixby, S., Kruger, G.M., Mosher, J.T., Joseph, N.M., and Morrison, S.J. (2002). Cell-intrinsic
691   differences between stem cells from different regions of the peripheral nervous system regulate
692   the generation of neural diversity. *Neuron* 35(4)**,** 643-656. doi: 10.1016/s0896-6273(02)00825-
693   5.
694 Blainey, P.C., and Quake, S.R. (2011). Digital MDA for enumeration of total nucleic acid
695   contamination. *Nucleic Acids Res* 39(4)**,** e19. doi: 10.1093/nar/gkq1074.
696 Boddupally, K., Wang, G., Chen, Y., and Kobielak, A. (2016). Lgr5 Marks Neural Crest Derived
697   Multipotent Oral Stromal Stem Cells. *Stem Cells* 34(3)**,** 720-731. doi: 10.1002/stem.2314.
698 Bolande, R.P. (1974). The neurocristopathies: A unifying concept of disease arising in neural crest
699   maldevelopment. *Human Pathology* 5(4)**,** 409-429. doi: https://doi.org/10.1016/S0046-
700   8177(74)80021-3.
701 Boutet, A., De Frutos, C.A., Maxwell, P.H., Mayol, M.J., Romero, J., and Nieto, M.A. (2006). Snail
702   activation disrupts tissue homeostasis and induces fibrosis in the adult kidney. *EMBO J* 25(23)**,**
703   5603-5613. doi: 10.1038/sj.emboj.7601421.
704 Brandl, C., Florian, C., Driemel, O., Weber, B.H., and Morsczeck, C. (2009). Identification of neural
705   crest-derived stem cell-like cells from the corneal limbus of juvenile mice. *Exp Eye Res* 89(2)**,**
706   209-217. doi: S0014-4835(09)00072-4 [pii]

707 10.1016/j.exer.2009.03.009 [doi].
708 Bryder, D., Rossi, D.J., and Weissman, I.L. (2006). Hematopoietic stem cells: the paradigmatic tissue-
709   specific   stem   cell.   *The   American   journal   of   pathology*   169(2).   doi:
710   10.2353/ajpath.2006.060312.
711 Buenrostro, J.D., Corces, M.R., Lareau, C.A., Wu, B., Schep, A.N., Aryee, M.J., et al. (2018).
712   Integrated Single-Cell Analysis Maps the Continuous Regulatory Landscape of Human
713   Hematopoietic Differentiation. *Cell* 173(6)**,** 1535-1548 e1516. doi: 10.1016/j.cell.2018.03.074.
714 Burns, A.J., and Douarin, N.M. (1998). The sacral neural crest contributes neurons and glia to the post-
715   umbilical gut: spatiotemporal analysis of the development of the enteric nervous system.
716   *Development* 125(21)**,** 4335-4347.

717 Calloni, G.W., Glavieux-Pardanaud, C., Le Douarin, N.M., and Dupin, E. (2007). Sonic Hedgehog
718   promotes the development of multipotent neural crest progenitors endowed with both
719   mesenchymal and neural potentials. *Proc Natl Acad Sci U S A* 104(50)**,** 19879-19884. doi:
720   10.1073/pnas.0708806104.
721 Calloni, G.W., Le Douarin, N.M., and Dupin, E. (2009). High frequency of cephalic neural crest cells
722   shows coexistence of neurogenic, melanogenic, and osteogenic differentiation capacities. *Proc*
723   *Natl Acad Sci U S A* 106(22)**,** 8947-8952. doi: 10.1073/pnas.0903780106.
724 Carter, B., and Zhao, K. (2020). The epigenetic basis of cellular heterogeneity. *Nat Rev Genet.* doi:
725   10.1038/s41576-020-00300-0.
726 Casas, E., Kim, J., Bendesky, A., Ohno-Machado, L., Wolfe, C.J., and Yang, J. (2011). Snail2 is an
727   essential mediator of Twist1-induced epithelial mesenchymal transition and metastasis. *Cancer*
728   *Res* 71(1)**,** 245-254. doi: 10.1158/0008-5472.CAN-10-2330.
729 Chai, Y., Jiang, X., Ito, Y., Bringas, P., Jr., Han, J., Rowitch, D.H., et al. (2000). Fate of the mammalian
730   cranial neural crest during tooth and mandibular morphogenesis. *Development* 127(8)**,** 1671-
731   1679.
732 Clewes, O., Narytnyk, A., Gillinder, K.R., Loughney, A.D., Murdoch, A.P., and Sieber-Blum, M.
733   (2011). Human epidermal neural crest stem cells (hEPI-NCSC)--characterization and directed
734   differentiation into osteocytes and melanocytes. *Stem Cell Rev* 7(4)**,** 799-814. doi:
735   10.1007/s12015-011-9255-5.
736 Coste, C., Neirinckx, V., Sharma, A., Agirman, G., Rogister, B., Foguenne, J., et al. (2017). Human
737   bone marrow harbors cells with neural crest-associated characteristics like human adipose and
738   dermis tissues. *PloS one* 12(7)**,** e0177962. doi: 10.1371/journal.pone.0177962.
739 Couly, G., Grapin-Botton, A., Coltey, P., Ruhin, B., and Le Douarin, N.M. (1998). Determination of
740   the identity of the derivatives of the cephalic neural crest: incompatibility between Hox gene
741   expression and lower jaw development. *Development* 125(17)**,** 3445-3459.
742 Creuzet, S.E. (2009). Regulation of pre-otic brain development by the cephalic neural crest. *Proc Natl*
743   *Acad Sci U S A* 106(37)**,** 15774-15779. doi: 10.1073/pnas.0906072106.
744 da Costa, M.C., Trentin, A.G., and Calloni, G.W. (2018). FGF8 and Shh promote the survival and
745   maintenance of multipotent neural crest progenitors. *Mech Dev* 154**,** 251-258. doi:
746   10.1016/j.mod.2018.07.012.
747 Dai, R., Hua, W., Xie, H., Chen, W., Xiong, L., and Li, L. (2018). The Human Skin-Derived Precursors
748   for Regenerative Medicine: Current State, Challenges, and Perspectives. *Stem Cells Int* 2018**,**
749   8637812. doi: 10.1155/2018/8637812.
750 Dave, N., Guaita-Esteruelas, S., Gutarra, S., Frias, A., Beltran, M., Peiro, S., et al. (2011). Functional
751   cooperation between Snail1 and twist in the regulation of ZEB1 expression during epithelial to
752   mesenchymal transition. *J Biol Chem* 286(14)**,** 12024-12032. doi: 10.1074/jbc.M110.168625.
753 Davies, L.C., Locke, M., Webb, R.D., Roberts, J.T., Langley, M., Thomas, D.W., et al. (2010). A
754   multipotent neural crest-derived progenitor cell population is resident within the oral mucosa
755   lamina propria. *Stem Cells Dev* 19(6)**,** 819-830. doi: 10.1089/scd.2009.0089.
756 del Barrio, M.G., and Nieto, M.A. (2002). Overexpression of Snail family members highlights their
757   ability to promote chick neural crest formation. *Development* 129(7)**,** 1583-1593.
758 Delorme, B., Nivet, E., Gaillard, J., Haupl, T., Ringe, J., Deveze, A., et al. (2010). The human nose
759   harbors a niche of olfactory ectomesenchymal stem cells displaying neurogenic and osteogenic
760   properties. *Stem Cells Dev* 19(6)**,** 853-866. doi: 10.1089/scd.2009.0267.
761 Dulken, B.W., Leeman, D.S., Boutet, S.C., Hebestreit, K., and Brunet, A. (2017). Single-Cell
762   Transcriptomic Analysis Defines Heterogeneity and Transcriptional Dynamics in the Adult
763   Neural Stem Cell Lineage. *Cell Rep* 18(3)**,** 777-790. doi: 10.1016/j.celrep.2016.12.060.

764 Dupin, E., Calloni, G.W., Coelho-Aguiar, J.M., and Le Douarin, N.M. (2018). The issue of the
765   multipotency of the neural crest cells. *Dev Biol* 444 Suppl 1**,** S47-S59. doi:
766   10.1016/j.ydbio.2018.03.024.
767 Dupin, E., and Sommer, L. (2012). Neural crest progenitors and stem cells: from early development to
768   adulthood. *Dev Biol* 366(1)**,** 83-95. doi: 10.1016/j.ydbio.2012.02.035.
769 Durante, M.A., Kurtenbach, S., Sargi, Z.B., Harbour, J.W., Choi, R., Kurtenbach, S., et al. (2020).
770   Single-cell analysis of olfactory neurogenesis and differentiation in adult humans. *Nat Neurosci*
771   23(3)**,** 323-326. doi: 10.1038/s41593-020-0587-9.
772 El-Helou, V., Beguin, P.C., Assimakopoulos, J., Clement, R., Gosselin, H., Brugada, R., et al. (2008).
773   The rat heart contains a neural stem cell population; role in sympathetic sprouting and
774   angiogenesis. *J Mol Cell Cardiol* 45(5)**,** 694-702. doi: 10.1016/j.yjmcc.2008.07.013.
775 Epstein, M.L., Mikawa, T., Brown, A.M., and McFarlin, D.R. (1994). Mapping the origin of the avian
776   enteric nervous system with a retroviral marker. *Dev Dyn* 201(3)**,** 236-244. doi:
777   10.1002/aja.1002010307.
778 Etchevers, H.C., Dupin, E., and Le Douarin, N.M. (2019). The diverse neural crest: from embryology
779   to human pathology. *Development* 146(5). doi: 10.1242/dev.169821.
780 Faure, S., McKey, J., Sagnol, S., and de Santa Barbara, P. (2015). Enteric neural crest cells regulate
781   vertebrate stomach patterning and differentiation. *Development* 142(2)**,** 331-342. doi:
782   10.1242/dev.118422.
783 Fernandes, K.J., McKenzie, I.A., Mill, P., Smith, K.M., Akhavan, M., Barnabe-Heider, F., et al. (2004).
784   A dermal niche for multipotent adult skin-derived precursor cells. *Nat Cell Biol* 6(11)**,** 1082-
785   1093. doi: 10.1038/ncb1181.
786 Fleming, W.H., Alpern, E.J., Uchida, N., Ikuta, K., Spangrude, G.J., and Weissman, I.L. (1993).
787   Functional heterogeneity is associated with the cell cycle status of murine hematopoietic stem
788   cells. *J Cell Biol* 122(4)**,** 897-902. doi: 10.1083/jcb.122.4.897.
789 Fletcher, R.B., Das, D., Gadye, L., Street, K.N., Baudhuin, A., Wagner, A., et al. (2017).
790   Deconstructing Olfactory Stem Cell Trajectories at Single-Cell Resolution. *Cell Stem Cell*
791   20(6)**,** 817-830 e818. doi: 10.1016/j.stem.2017.04.003.
792 Fraser, H.B., Hirsh, A.E., Giaever, G., Kumm, J., and Eisen, M.B. (2004). Noise minimization in
793   eukaryotic gene expression. *PLoS Biol* 2(6)**,** e137. doi: 10.1371/journal.pbio.0020137.
794 Freeman, B.T., Jung, J.P., and Ogle, B.M. (2015). Single-Cell RNA-Seq of Bone Marrow-Derived
795   Mesenchymal Stem Cells Reveals Unique Profiles of Lineage Priming. *PLoS One* 10(9)**,**
796   e0136199. doi: 10.1371/journal.pone.0136199.
797 Fukaya, T., Lim, B., and Levine, M. (2016). Enhancer Control of Transcriptional Bursting. *Cell* 166(2)**,**
798   358-368. doi: 10.1016/j.cell.2016.05.025.
799 Gadye, L., Das, D., Sanchez, M.A., Street, K., Baudhuin, A., Wagner, A., et al. (2017). Injury Activates
800   Transient Olfactory Stem Cell States with Diverse Lineage Capacities. *Cell Stem Cell* 21(6)**,**
801   775-790 e779. doi: 10.1016/j.stem.2017.10.014.
802 Gage, P.J., Rhoades, W., Prucka, S.K., and Hjalt, T. (2005). Fate maps of neural crest and mesoderm
803   in the mammalian eye. *Invest Ophthalmol Vis Sci* 46(11)**,** 4200-4208. doi: 10.1167/iovs.05-
804   0691.
805 Gonzalez, G., Sasamoto, Y., Ksander, B.R., Frank, M.H., and Frank, N.Y. (2018). Limbal stem cells:
806   identity, developmental origin, and therapeutic potential. *Wiley Interdiscip Rev Dev Biol* 7(2).
807   doi: 10.1002/wdev.303.
808 Graham, A., Begbie, J., and McGonnell, I. (2004). Significance of the cranial neural crest. *Dev Dyn*
809   229(1)**,** 5-13. doi: 10.1002/dvdy.10442.
810 Grapin-Botton, A., Bonnin, M.A., McNaughton, L.A., Krumlauf, R., and Le Douarin, N.M. (1995).
811   Plasticity of transposed rhombomeres: Hox gene induction is correlated with phenotypic
812   modifications. *Development* 121(9)**,** 2707-2721.

813　Greiner, J., Merten, M., Kaltschmidt, C., and Kaltschmidt, B. (2019a). Sexual dimorphisms in adult
814　　　　human neural, mesoderm-derived, and neural crest-derived stem cells. *FEBS Lett*. doi:
815　　　　10.1002/1873-3468.13606.
816　Greiner, J.F., Gottschalk, M., Fokin, N., Buker, B., Kaltschmidt, B.P., Dreyer, A., et al. (2019b).
817　　　　Natural and synthetic nanopores directing osteogenic differentiation of human stem cells.
818　　　　*Nanomedicine*. 17**,** 319-328. doi: 10.1016/j.nano.2019.01.018.
819　Greiner, J.F., Hauser, S., Widera, D., Muller, J., Qunneis, F., Zander, C., et al. (2011). Efficient animal-
820　　　　serum free 3D cultivation method for adult human neural crest-derived stem cell therapeutics.
821　　　　*Eur Cell Mater* 22**,** 403-419.
822　Griffiths, J.A., Scialdone, A., and Marioni, J.C. (2018). Using single-cell genomics to understand
823　　　　developmental processes and cell fate decisions. *Mol Syst Biol* 14(4)**,** e8046. doi:
824　　　　10.15252/msb.20178046.
825　Groeneveldt, L.C., Herpelinck, T., Marechal, M., Politis, C., van, I.W.F.J., Huylebroeck, D., et al.
826　　　　(2020). The Bone-Forming Properties of Periosteum-Derived Cells Differ Between Harvest
827　　　　Sites. *Front Cell Dev Biol* 8**,** 554984. doi: 10.3389/fcell.2020.554984.
828　Gronthos, S., Mankani, M., Brahim, J., Robey, P.G., and Shi, S. (2000). Postnatal human dental pulp
829　　　　stem cells (DPSCs) in vitro and in vivo. *Proc Natl Acad Sci U S A* 97(25)**,** 13625-13630. doi:
830　　　　10.1073/pnas.240309797.
831　Guo, W., Keckesova, Z., Donaher, J.L., Shibue, T., Tischler, V., Reinhardt, F., et al. (2012). Slug and
832　　　　Sox9 cooperatively determine the mammary stem cell state. *Cell* 148(5)**,** 1015-1028. doi:
833　　　　10.1016/j.cell.2012.02.008.
834　Han, X., Zhou, Z., Fei, L., Sun, H., Wang, R., Chen, Y., et al. (2020). Construction of a human cell
835　　　　landscape at single-cell level. *Nature* 581(7808)**,** 303-309. doi: 10.1038/s41586-020-2157-4.
836　Hatzistergos, K.E., Takeuchi, L.M., Saur, D., Seidler, B., Dymecki, S.M., Mai, J.J., et al. (2015). cKit+
837　　　　cardiac progenitors of neural crest origin. *Proc Natl Acad Sci U S A* 112(42)**,** 13051-13056.
838　　　　doi: 10.1073/pnas.1517201112.
839　Hauser, S., Widera, D., Qunneis, F., Muller, J., Zander, C., Greiner, J., et al. (2012). Isolation of novel
840　　　　multipotent neural crest-derived stem cells from adult human inferior turbinate. *Stem Cells Dev*
841　　　　21(5)**,** 742-756.
842　His, W. (1868). *Untersuchungen über die erste Anlage des Wirbeltierleibes. Die erste Entwicklung des*
843　　　　*Hühnchens im Ei.* Leipzig: Vogel.
844　Hofemeier, A.D., Hachmeister, H., Pilger, C., Schurmann, M., Greiner, J.F., Nolte, L., et al. (2016).
845　　　　Label-free nonlinear optical microscopy detects early markers for osteogenic differentiation of
846　　　　human stem cells. *Sci. Rep.* 6**,** 26716. doi: 10.1038/srep26716.
847　Höving, A.L., Schmidt, K.E., Merten, M., Hamidi, J., Rott, A.K., Faust, I., et al. (2020a). Blood Serum
848　　　　Stimulates p38-Mediated Proliferation and Changes in Global Gene Expression of Adult
849　　　　Human Cardiac Stem Cells. *Cells* 9(6). doi: 10.3390/cells9061472.
850　Höving, A.L., Sielemann, K., Greiner, J.F.W., Kaltschmidt, B., Knabbe, C., and Kaltschmidt, C.
851　　　　(2020b). Transcriptome Analysis Reveals High Similarities between Adult Human Cardiac
852　　　　Stem Cells and Neural Crest-Derived Stem Cells. *Biology (Basel)* 9(12). doi:
853　　　　10.3390/biology9120435.
854　Hu, Y.F., Gourab, K., Wells, C., Clewes, O., Schmit, B.D., and Sieber-Blum, M. (2010). Epidermal
855　　　　neural crest stem cell (EPI-NCSC)--mediated recovery of sensory function in a mouse model
856　　　　of spinal cord injury. *Stem Cell Rev Rep* 6(2)**,** 186-198. doi: 10.1007/s12015-010-9152-3.
857　Hu, Y.F., Zhang, Z.J., and Sieber-Blum, M. (2006). An epidermal neural crest stem cell (EPI-NCSC)
858　　　　molecular signature. *Stem Cells* 24(12)**,** 2692-2702. doi: 10.1634/stemcells.2006-0233.
859　Huang, C.Y., Pelaez, D., Dominguez-Bendala, J., Garcia-Godoy, F., and Cheung, H.S. (2009).
860　　　　Plasticity of stem cells derived from adult periodontal ligament. *Regen Med* 4(6)**,** 809-821. doi:
861　　　　10.2217/rme.09.55.

Huang, Z.H., Wang, Y., Cao, L., Su, Z.D., Zhu, Y.L., Chen, Y.Z., et al. (2008). Migratory properties of cultured olfactory ensheathing cells by single-cell migration assay. *Cell Res* 18(4), 479-490. doi: 10.1038/cr.2008.38.

Huh, D., and Paulsson, J. (2011). Non-genetic heterogeneity from stochastic partitioning at cell division. *Nat Genet* 43(2), 95-100. doi: 10.1038/ng.729.

Jiang, W., Wang, D., Alraies, A., Liu, Q., Zhu, B., Sloan, A.J., et al. (2019). Wnt-GSK3beta/beta-Catenin Regulates the Differentiation of Dental Pulp Stem Cells into Bladder Smooth Muscle Cells. *Stem Cells Int* 2019, 8907570. doi: 10.1155/2019/8907570.

Johansson, C.B., Momma, S., Clarke, D.L., Risling, M., Lendahl, U., and Frisén, J. (1999). Identification of a neural stem cell in the adult mammalian central nervous system. *Cell* 96(1), 25–34. doi: 10.1016/s0092-8674(00)80956-3.

Johnston, M.C. (1966). A radioautographic study of the migration and fate of cranial neural crest cells in the chick embryo. *Anat Rec* 156(2), 143-155. doi: 10.1002/ar.1091560204.

Joost, S., Jacob, T., Sun, X., Annusver, K., La Manno, G., Sur, I., et al. (2018). Single-Cell Transcriptomics of Traced Epidermal and Hair Follicle Stem Cells Reveals Rapid Adaptations during Wound Healing. *Cell Rep* 25(3), 585-597 e587. doi: 10.1016/j.celrep.2018.09.059.

Joost, S., Zeisel, A., Jacob, T., Sun, X., La Manno, G., Lonnerberg, P., et al. (2016). Single-Cell Transcriptomics Reveals that Differentiation and Spatial Signatures Shape Epidermal and Hair Follicle Heterogeneity. *Cell Syst* 3(3), 221-237 e229. doi: 10.1016/j.cels.2016.08.010.

Kaltschmidt, B., Kaltschmidt, C., and Widera, D. (2012). Adult craniofacial stem cells: sources and relation to the neural crest. *Stem Cell Rev* 8(3), 658-671. doi: 10.1007/s12015-011-9340-9.

Karimkhani, C., Green, A.C., Nijsten, T., Weinstock, M.A., Dellavalle, R.P., Naghavi, M., et al. (2017). The global burden of melanoma: results from the Global Burden of Disease Study 2015. *Br J Dermatol* 177(1), 134-140. doi: 10.1111/bjd.15510.

Katikireddy, K.R., Schmedt, T., Price, M.O., Price, F.W., and Jurkunas, U.V. (2016). Existence of Neural Crest-Derived Progenitor Cells in Normal and Fuchs Endothelial Dystrophy Corneal Endothelium. *Am J Pathol* 186(10), 2736-2750. doi: 10.1016/j.ajpath.2016.06.011.

Kawanabe, N., Murata, S., Murakami, K., Ishihara, Y., Hayano, S., Kurosaka, H., et al. (2010). Isolation of multipotent stem cells in human periodontal ligament using stage-specific embryonic antigen-4. *Differentiation* 79(2), 74-83. doi: 10.1016/j.diff.2009.10.005.

Kerosuo, L., Nie, S., Bajpai, R., and Bronner, M.E. (2015). Crestospheres: Long-Term Maintenance of Multipotent, Premigratory Neural Crest Stem Cells. *Stem Cell Reports* 5(4), 499-507. doi: 10.1016/j.stemcr.2015.08.017.

Kim, J., Lo, L., Dormand, E., and Anderson, D.J. (2003). SOX10 maintains multipotency and inhibits neuronal differentiation of neural crest stem cells. *Neuron* 38(1), 17-31. doi: 10.1016/s0896-6273(03)00163-6.

Kleber, M., Lee, H.Y., Wurdak, H., Buchstaller, J., Riccomagno, M.M., Ittner, L.M., et al. (2005). Neural crest stem cell maintenance by combinatorial Wnt and BMP signaling. *J Cell Biol* 169(2), 309-320. doi: 10.1083/jcb.200411095.

Klein, A.M., Mazutis, L., Akartuna, I., Tallapragada, N., Veres, A., Li, V., et al. (2015). Droplet barcoding for single-cell transcriptomics applied to embryonic stem cells. *Cell* 161(5), 1187-1201. doi: 10.1016/j.cell.2015.04.044.

Kobayashi, T., Torii, D., Iwata, T., Izumi, Y., Nasu, M., and Tsutsui, T.W. (2020). Characterization of proliferation, differentiation potential, and gene expression among clonal cultures of human dental pulp cells. *Hum Cell* 33(3), 490-501. doi: 10.1007/s13577-020-00327-9.

Korhonen, K., Salminen, T., Raitanen, J., Auvinen, A., Isola, J., and Haapasalo, H. (2006). Female predominance in meningiomas can not be explained by differences in progesterone, estrogen, or androgen receptor expression. *J Neurooncol* 80(1), 1-7. doi: 10.1007/s11060-006-9146-9.

Kowalczyk, M.S., Tirosh, I., Heckl, D., Rao, T.N., Dixit, A., Haas, B.J., et al. (2015). Single-cell RNA-seq reveals changes in cell cycle and differentiation programs upon aging of hematopoietic stem cells. *Genome Res* 25(12)**,** 1860-1872. doi: 10.1101/gr.192237.115.

Kruger, G.M., Mosher, J.T., Bixby, S., Joseph, N., Iwashita, T., and Morrison, S.J. (2002). Neural crest stem cells persist in the adult gut but undergo changes in self-renewal, neuronal subtype potential, and factor responsiveness. *Neuron* 35(4)**,** 657-669. doi: 10.1016/s0896-6273(02)00827-9.

Ksander, B.R., Kolovou, P.E., Wilson, B.J., Saab, K.R., Guo, Q., Ma, J., et al. (2014). ABCB5 is a limbal stem cell gene required for corneal development and repair. *Nature* 511(7509)**,** 353-357. doi: 10.1038/nature13426.

Kumar, P., Tan, Y., and Cahan, P. (2017). Understanding development and stem cells using single cell-based analyses of gene expression. *Development* 144(1)**,** 17-32. doi: 10.1242/dev.133058.

Lamouille, S., Xu, J., and Derynck, R. (2014). Molecular mechanisms of epithelial-mesenchymal transition. *Nat Rev Mol Cell Biol* 15(3)**,** 178-196. doi: 10.1038/nrm3758.

Le Douarin, N.M., and Teillet, M.A. (1973). The migration of neural crest cells to the wall of the digestive tract in avian embryo. *J Embryol Exp Morphol* 30(1)**,** 31-48.

Le Douarin, N.M., and Teillet, M.A. (1974). Experimental analysis of the migration and differentiation of neuroblasts of the autonomic nervous system and of neurectodermal mesenchymal derivatives, using a biological cell marking technique. *Dev Biol* 41(1)**,** 162-184. doi: 10.1016/0012-1606(74)90291-7.

Leinonen, J.V., Korkus-Emanuelov, A., Wolf, Y., Milgrom-Hoffman, M., Lichtstein, D., Hoss, S., et al. (2016). Macrophage precursor cells from the left atrial appendage of the heart spontaneously reprogram into a C-kit+/CD45- stem cell-like phenotype. *Int J Cardiol* 209**,** 296-306. doi: 10.1016/j.ijcard.2016.02.040.

Leucht, P., Kim, J.B., Amasha, R., James, A.W., Girod, S., and Helms, J.A. (2008). Embryonic origin and Hox status determine progenitor cell fate during adult bone regeneration. *Development* 135(17)**,** 2845-2854. doi: 10.1242/dev.023788.

Li, C.W., Xia, W., Huo, L., Lim, S.O., Wu, Y., Hsu, J.L., et al. (2012). Epithelial-mesenchymal transition induced by TNF-alpha requires NF-kappaB-mediated transcriptional upregulation of Twist1. *Cancer Res* 72(5)**,** 1290-1300. doi: 10.1158/0008-5472.CAN-11-3123.

Lignell, A., Kerosuo, L., Streichan, S.J., Cai, L., and Bronner, M.E. (2017). Identification of a neural crest stem cell niche by Spatial Genomic Analysis. *Nature communications* 8(1)**,** 1830. doi: 10.1038/s41467-017-01561-w.

Lopez-Barneo, J., Pardal, R., and Ortega-Saenz, P. (2001). Cellular mechanism of oxygen sensing. *Annu Rev Physiol* 63**,** 259-287. doi: 10.1146/annurev.physiol.63.1.259.

Lothian, C., and Lendahl, U. (1997). An evolutionarily conserved region in the second intron of the human nestin gene directs gene expression to CNS progenitor cells and to early neural crest cells. *Eur J Neurosci* 9(3)**,** 452-462. doi: 10.1111/j.1460-9568.1997.tb01622.x.

Lubeck, E., and Cai, L. (2012). Single-cell systems biology by super-resolution imaging and combinatorial labeling. *Nat Methods* 9(7)**,** 743-748. doi: 10.1038/nmeth.2069.

Lubeck, E., Coskun, A.F., Zhiyentayev, T., Ahmad, M., and Cai, L. (2014). Single-cell in situ RNA profiling by sequential hybridization. *Nat Methods* 11(4)**,** 360-361. doi: 10.1038/nmeth.2892.

Macosko, E.Z., Basu, A., Satija, R., Nemesh, J., Shekhar, K., Goldman, M., et al. (2015). Highly Parallel Genome-wide Expression Profiling of Individual Cells Using Nanoliter Droplets. *Cell* 161(5)**,** 1202-1214. doi: 10.1016/j.cell.2015.05.002.

Marynka-Kalmani, K., Treves, S., Yafee, M., Rachima, H., Gafni, Y., Cohen, M.A., et al. (2010). The lamina propria of adult human oral mucosa harbors a novel stem cell population. *Stem Cells* 28(5)**,** 984-995. doi: 10.1002/stem.425.

958 Matigian, N., Abrahamsen, G., Sutharsan, R., Cook, A.L., Vitale, A.M., Nouwens, A., et al. (2010).
959   Disease-specific, neurosphere-derived cells as models for brain disorders. *Dis Model Mech*
960   3(11-12)**,** 785-798. doi: 10.1242/dmm.005447.
961 McAdams, H.H., and Arkin, A. (1999). It's a noisy business! Genetic regulation at the nanomolar scale.
962   *Trends Genet* 15(2)**,** 65-69. doi: 10.1016/s0168-9525(98)01659-x.
963 McLeod, C.M., and Mauck, R.L. (2017). On the origin and impact of mesenchymal stem cell
964   heterogeneity: new insights and emerging tools for single cell analysis. *Eur Cell Mater* 34**,** 217-
965   231. doi: 10.22203/eCM.v034a14.
966 Messina, E., Angelis, L., Frati, G., Morrone, S., Chimenti, S., Fiordaliso, F., et al. (2004). Isolation and
967   expansion of adult cardiac stem cells from human and murine heart. *Circulation research* 95(9)**,**
968   911–921. doi: 10.1161/01.RES.0000147315.71699.51.
969 Metcalf, D. (1998). Lineage commitment and maturation in hematopoietic cells: the case for extrinsic
970   regulation. *Blood* 92(2)**,** 345-347; discussion 352.
971 Meus, M.A., Hertig, V., Villeneuve, L., Jasmin, J.F., and Calderone, A. (2017). Nestin Expressed by
972   Pre-Existing Cardiomyocytes Recapitulated in Part an Embryonic Phenotype; Suppressive Role
973   of p38 MAPK. *J Cell Physiol* 232(7)**,** 1717-1727. doi: 10.1002/jcp.25496.
974 Moffitt, J.R., Hao, J., Wang, G., Chen, K.H., Babcock, H.P., and Zhuang, X. (2016). High-throughput
975   single-cell gene-expression profiling with multiplexed error-robust fluorescence in situ
976   hybridization. *Proc Natl Acad Sci U S A* 113(39)**,** 11046-11051. doi:
977   10.1073/pnas.1612826113.
978 Moignard, V., and Gottgens, B. (2016). Dissecting stem cell differentiation using single cell expression
979   profiling. *Curr Opin Cell Biol* 43**,** 78-86. doi: 10.1016/j.ceb.2016.08.005.
980 Moignard, V., Macaulay, I.C., Swiers, G., Buettner, F., Schutte, J., Calero-Nieto, F.J., et al. (2013).
981   Characterization of transcriptional networks in blood stem and progenitor cells using high-
982   throughput single-cell gene expression analysis. *Nat Cell Biol* 15(4)**,** 363-372. doi:
983   10.1038/ncb2709.
984 Morrison, S.J., White, P.M., Zock, C., and Anderson, D.J. (1999). Prospective identification, isolation
985   by flow cytometry, and in vivo self-renewal of multipotent mammalian neural crest stem cells.
986   *Cell* 96(5). doi: 10.1016/s0092-8674(00)80583-8.
987 Mosher, J.T., Yeager, K.J., Kruger, G.M., Joseph, N.M., Hutchin, M.E., Dlugosz, A.A., et al. (2007).
988   Intrinsic differences among spatially distinct neural crest stem cells in terms of migratory
989   properties, fate determination, and ability to colonize the enteric nervous system. *Dev Biol*
990   303(1)**,** 1-15. doi: 10.1016/j.ydbio.2006.10.026.
991 Müller, J., Greiner, J.F., Zeuner, M., Brotzmann, V., Schafermann, J., Wieters, F., et al. (2016). 1,8-
992   Cineole potentiates IRF3-mediated antiviral response in human stem cells and in an ex vivo
993   model of rhinosinusitis. *Clin Sci (Lond)* 130(15)**,** 1339-1352. doi: 10.1042/CS20160218.
994 Müller, J., Ossig, C., Greiner, J.F., Hauser, S., Fauser, M., Widera, D., et al. (2015). Intrastriatal
995   transplantation of adult human neural crest-derived stem cells improves functional outcome in
996   parkinsonian rats. *Stem Cells Transl Med* 4(1)**,** 31-43. doi: sctm.2014-0078 [pii]
997 10.5966/sctm.2014-0078.
998 Murrell, W., Wetzig, A., Donnellan, M., Feron, F., Burne, T., Meedeniya, A., et al. (2008). Olfactory
999   mucosa is a potential source for autologous stem cell therapy for Parkinson's disease. *Stem Cells*
1000   26(8)**,** 2183-2192. doi: 10.1634/stemcells.2008-0074.
1001 Nagoshi, N., Shibata, S., Kubota, Y., Nakamura, M., Nagai, Y., Satoh, E., et al. (2008). Ontogeny and
1002   multipotency of neural crest-derived stem cells in mouse bone marrow, dorsal root ganglia, and
1003   whisker pad. *Cell stem cell* 2(4). doi: 10.1016/j.stem.2008.03.005.
1004 Nieto, M.A., Huang, R.Y., Jackson, R.A., and Thiery, J.P. (2016). Emt: 2016. *Cell* 166(1)**,** 21-45. doi:
1005   10.1016/j.cell.2016.06.028.

1006 Nieto, M.A., Sargent, M.G., Wilkinson, D.G., and Cooke, J. (1994). Control of cell behavior during
1007   vertebrate development by Slug, a zinc finger gene. *Science* 264(5160)**,** 835-839. doi:
1008   10.1126/science.7513443.

1009 Noden, D.M. (1975). An analysis of migratory behavior of avian cephalic neural crest cells. *Dev Biol*
1010   42(1)**,** 106-130. doi: 10.1016/0012-1606(75)90318-8.

1011 Noden, D.M. (1978a). The control of avian cephalic neural crest cytodifferentiation. I. Skeletal and
1012   connective tissues. *Dev Biol* 67(2)**,** 296-312. doi: 10.1016/0012-1606(78)90201-4.

1013 Noden, D.M. (1978b). The control of avian cephalic neural crest cytodifferentiation. II. Neural tissues.
1014   *Dev Biol* 67(2)**,** 313-329. doi: 10.1016/0012-1606(78)90202-6.

1015 Ochiai, H., Hayashi, T., Umeda, M., Yoshimura, M., Harada, A., Shimizu, Y., et al. (2020). Genome-
1016   wide kinetic properties of transcriptional bursting in mouse embryonic stem cells. *Sci Adv*
1017   6(25)**,** eaaz6699. doi: 10.1126/sciadv.aaz6699.

1018 Pardal, R., Ortega-Saenz, P., Duran, R., and Lopez-Barneo, J. (2007). Glia-like stem cells sustain
1019   physiologic neurogenesis in the adult mammalian carotid body. *Cell* 131(2)**,** 364-377. doi:
1020   10.1016/j.cell.2007.07.043.

1021 Pearse, A.G., Polak, J.M., Rost, F.W., Fontaine, J., Le Lievre, C., and Le Douarin, N. (1973).
1022   Demonstration of the neural crest origin of type I (APUD) cells in the avian carotid body, using
1023   a cytochemical marker system. *Histochemie* 34(3)**,** 191-203. doi: 10.1007/BF00303435.

1024 Phillips, M.T., Kirby, M.L., and Forbes, G. (1987). Analysis of cranial neural crest distribution in the
1025   developing heart using quail-chick chimeras. *Circ Res* 60(1)**,** 27-30. doi:
1026   10.1161/01.res.60.1.27.

1027 Picelli, S., Faridani, O.R., Bjorklund, A.K., Winberg, G., Sagasser, S., and Sandberg, R. (2014). Full-
1028   length RNA-seq from single cells using Smart-seq2. *Nat Protoc* 9(1)**,** 171-181. doi:
1029   10.1038/nprot.2014.006.

1030 Pires, B.R., Mencalha, A.L., Ferreira, G.M., de Souza, W.F., Morgado-Diaz, J.A., Maia, A.M., et al.
1031   (2017). NF-kappaB Is Involved in the Regulation of EMT Genes in Breast Cancer Cells. *PLoS*
1032   *One* 12(1)**,** e0169622. doi: 10.1371/journal.pone.0169622.

1033 Pittenger, M.F., Mackay, A.M., Beck, S.C., Jaiswal, R.K., Douglas, R., Mosca, J.D., et al. (1999).
1034   Multilineage potential of adult human mesenchymal stem cells. *Science (New York, N.Y.)*
1035   284(5411)**,** 143–147. doi: 10.1126/science.284.5411.143.

1036 Platero-Luengo, A., Gonzalez-Granero, S., Duran, R., Diaz-Castro, B., Piruat, J.I., Garcia-Verdugo,
1037   J.M., et al. (2014). An O2-sensitive glomus cell-stem cell synapse induces carotid body growth
1038   in chronic hypoxia. *Cell* 156(1-2)**,** 291-303. doi: 10.1016/j.cell.2013.12.013.

1039 Raj, A., Peskin, C.S., Tranchina, D., Vargas, D.Y., and Tyagi, S. (2006). Stochastic mRNA synthesis
1040   in mammalian cells. *PLoS Biol* 4(10)**,** e309. doi: 10.1371/journal.pbio.0040309.

1041 Raj, A., van den Bogaard, P., Rifkin, S.A., van Oudenaarden, A., and Tyagi, S. (2008). Imaging
1042   individual mRNA molecules using multiple singly labeled probes. *Nat Methods* 5(10)**,** 877-
1043   879. doi: 10.1038/nmeth.1253.

1044 Ramsköld, D., Luo, S., Wang, Y.-C., Li, R., Deng, Q., Faridani, O.R., et al. (2012). Full-Length
1045   mRNA-Seq from single cell levels of RNA and individual circulating tumor cells. *Nature*
1046   *biotechnology* 30(8)**,** 777–782. doi: 10.1038/nbt.2282.

1047 Ring, A., Kim, Y.M., and Kahn, M. (2014). Wnt/catenin signaling in adult stem cell physiology and
1048   disease. *Stem Cell Rev Rep* 10(4)**,** 512-525. doi: 10.1007/s12015-014-9515-2.

1049 Rios, A.C., Serralbo, O., Salgado, D., and Marcelle, C. (2011). Neural crest regulates myogenesis
1050   through the transient activation of NOTCH. *Nature* 473(7348)**,** 532-535. doi:
1051   10.1038/nature09970.

1052 Rocha, M., Beiriger, A., Kushkowski, E.E., Miyashita, T., Singh, N., Venkataraman, V., et al. (2020).
1053   From head to tail: regionalization of the neural crest. *Development* 147(20). doi:
1054   10.1242/dev.193888.

1055 Rochat, A., Kobayashi, K., and Barrandon, Y. (1994). Location of stem cells of human hair follicles
1056   by clonal analysis: Cell, 76(6), 1063-1073. doi: 10.1016/0092-8674(94)90383-2.
1057 Rodrigues, R.M., De Kock, J., Branson, S., Vinken, M., Meganathan, K., Chaudhari, U., et al. (2014).
1058   Human skin-derived stem cells as a novel cell source for in vitro hepatotoxicity screening of
1059   pharmaceuticals. *Stem Cells Dev* 23(1)**,** 44-55. doi: 10.1089/scd.2013.0157.
1060 Rodriguez-Fraticelli, A.E., Weinreb, C., Wang, S.W., Migueles, R.P., Jankovic, M., Usart, M., et al.
1061   (2020). Single-cell lineage tracing unveils a role for TCF15 in haematopoiesis. *Nature*
1062   583(7817)**,** 585-589. doi: 10.1038/s41586-020-2503-6.
1063 Rosenberg, A.B., Roco, C.M., Muscat, R.A., Kuchina, A., Sample, P., Yao, Z., et al. (2018). Single-
1064   cell profiling of the developing mouse brain and spinal cord with split-pool barcoding. *Science*
1065   360(6385)**,** 176-182. doi: 10.1126/science.aam8999.
1066 Rothstein, M., Bhattacharya, D., and Simoes-Costa, M. (2018). The molecular basis of neural crest
1067   axial identity. *Dev Biol* 444 Suppl 1**,** S170-S180. doi: 10.1016/j.ydbio.2018.07.026.
1068 Ruiz-Perera, L.M., Greiner, J.F.W., Kaltschmidt, C., and Kaltschmidt, B. (2020). A Matter of Choice:
1069   Inhibition of c-Rel Shifts Neuronal to Oligodendroglial Fate in Human Stem Cells. *Cells* 9(4).
1070   doi: 10.3390/cells9041037.
1071 Ruiz-Perera, L.M., Schneider, L., Windmoller, B.A., Muller, J., Greiner, J.F.W., Kaltschmidt, C., et al.
1072   (2018). NF-kappaB p65 directs sex-specific neuroprotection in human neurons. *Sci Rep* 8(1)**,**
1073   16012. doi: 10.1038/s41598-018-34394-8.
1074 Saliba, A.E., Westermann, A.J., Gorski, S.A., and Vogel, J. (2014). Single-cell RNA-seq: advances
1075   and future challenges. *Nucleic Acids Res* 42(14)**,** 8845-8860. doi: 10.1093/nar/gku555.
1076 Schurmann, M., Brotzmann, V., Butow, M., Greiner, J., Hoving, A., Kaltschmidt, C., et al. (2017).
1077   Identification of a Novel High Yielding Source of Multipotent Adult Human Neural Crest-
1078   Derived Stem Cells. *Stem Cell Rev*. doi: 10.1007/s12015-017-9797-2.
1079 Shakhova, O., and Sommer, L. (2008). "Neural crest-derived stem cells," in *StemBook*. (Cambridge
1080   (MA)).
1081 Sieber-Blum, M., and Cohen, A.M. (1980). Clonal analysis of quail neural crest cells: they are
1082   pluripotent and differentiate in vitro in the absence of noncrest cells. *Dev Biol* 80(1)**,** 96-106.
1083   doi: 10.1016/0012-1606(80)90501-1.
1084 Sieber-Blum, M., and Grim, M. (2004). The adult hair follicle: cradle for pluripotent neural crest stem
1085   cells. *Birth Defects Res C Embryo Today* 72(2)**,** 162-172. doi: 10.1002/bdrc.20008.
1086 Sieber-Blum, M., Grim, M., Hu, Y.F., and Szeder, V. (2004). Pluripotent neural crest stem cells in the
1087   adult hair follicle. *Dev Dyn* 231(2)**,** 258-269. doi: 10.1002/dvdy.20129.
1088 Singhatanadgit, W., Donos, N., and Olsen, I. (2009). Isolation and characterization of stem cell clones
1089   from adult human ligament. *Tissue Eng Part A* 15(9)**,** 2625-2636. doi:
1090   10.1089/ten.TEA.2008.0442.
1091 Sloan, A.J., and Waddington, R.J. (2009). Dental pulp stem cells: what, where, how? *Int J Paediatr*
1092   *Dent* 19(1)**,** 61-70. doi: 10.1111/j.1365-263X.2008.00964.x.
1093 Soldatov, R., Kaucka, M., Kastriti, M.E., Petersen, J., Chontorotzea, T., Englmaier, L., et al. (2019).
1094   Spatiotemporal structure of cell fate decisions in murine neural crest. *Science* 364(6444). doi:
1095   10.1126/science.aas9536.
1096 Southard-Smith, E.M., Kos, L., and Pavan, W.J. (1998). Sox10 mutation disrupts neural crest
1097   development in Dom Hirschsprung mouse model. *Nat Genet* 18(1)**,** 60-64. doi:
1098   10.1038/ng0198-60.
1099 Spokony, R.F., Aoki, Y., Saint-Germain, N., Magner-Fink, E., and Saint-Jeannet, J.P. (2002). The
1100   transcription factor Sox9 is required for cranial neural crest development in Xenopus.
1101   *Development* 129(2)**,** 421-432.

1102   Stevens, A., Zuliani, T., Olejnik, C., LeRoy, H., Obriot, H., Kerr-Conte, J., et al. (2008). Human dental
1103   pulp stem cells differentiate into neural crest-derived melanocytes and have label-retaining and
1104   sphere-forming abilities. *Stem Cells Dev* 17(6)**,** 1175-1184. doi: 10.1089/scd.2008.0012.
1105   Sun, L., Mathews, L.A., Cabarcas, S.M., Zhang, X., Yang, A., Zhang, Y., et al. (2013). Epigenetic
1106   regulation of SOX9 by the NF-kappaB signaling pathway in pancreatic cancer stem cells. *Stem*
1107   *Cells* 31(8)**,** 1454-1466. doi: 10.1002/stem.1394.
1108   Suslov, O.N., Kukekov, V.G., Ignatova, T.N., and Steindler, D.A. (2002). Neural stem cell
1109   heterogeneity demonstrated by molecular phenotyping of clonal neurospheres. *Proc Natl Acad*
1110   *Sci U S A* 99(22)**,** 14506-14511. doi: 10.1073/pnas.212525299.
1111   Suzuki, J., Yoshizaki, K., Kobayashi, T., and Osumi, N. (2013). Neural crest-derived horizontal basal
1112   cells as tissue stem cells in the adult olfactory epithelium. *Neurosci Res* 75(2)**,** 112-120. doi:
1113   10.1016/j.neures.2012.11.005.
1114   Tabakow, P., Raisman, G., Fortuna, W., Czyz, M., Huber, J., Li, D., et al. (2014). Functional
1115   regeneration of supraspinal connections in a patient with transected spinal cord following
1116   transplantation of bulbar olfactory ensheathing cells with peripheral nerve bridging. *Cell*
1117   *Transplant*. doi: 10.3727/096368914X685131.
1118   Tang, W., Martik, M.L., Li, Y., and Bronner, M.E. (2019). Cardiac neural crest contributes to
1119   cardiomyocytes in amniotes and heart regeneration in zebrafish. *Elife* 8. doi:
1120   10.7554/eLife.47929.
1121   Tang, Y., Feinberg, T., Keller, E.T., Li, X.Y., and Weiss, S.J. (2016). Snail/Slug binding interactions
1122   with YAP/TAZ control skeletal stem cell self-renewal and differentiation. *Nat Cell Biol* 18(9)**,**
1123   917-929. doi: 10.1038/ncb3394.
1124   Toma, J.G., Akhavan, M., Fernandes, K.J., Barnabe-Heider, F., Sadikot, A., Kaplan, D.R., et al. (2001).
1125   Isolation of multipotent adult stem cells from the dermis of mammalian skin. *Nat Cell Biol* 3(9)**,**
1126   778-784. doi: 10.1038/ncb0901-778 [doi]

1127   ncb0901-778 [pii].
1128   Tomita, Y., Matsumura, K., Wakamatsu, Y., Matsuzaki, Y., Shibuya, I., Kawaguchi, H., et al. (2005).
1129   Cardiac neural crest cells contribute to the dormant multipotent stem cell in the mammalian
1130   heart. *The Journal of cell biology* 170(7). doi: 10.1083/jcb.200504061.
1131   Trapnell, C., Cacchiarelli, D., Grimsby, J., Pokharel, P., Li, S., Morse, M., et al. (2014). The dynamics
1132   and regulators of cell fate decisions are revealed by pseudotemporal ordering of single cells.
1133   *Nat Biotechnol* 32(4)**,** 381-386. doi: 10.1038/nbt.2859.
1134   Trentin, J.J. (1971). Determination of bone marrow stem cell differentiation by stromal hemopoietic
1135   inductive microenvironments (HIM). *Am J Pathol* 65(3)**,** 621-628.
1136   Tsang, J.C., Yu, Y., Burke, S., Buettner, F., Wang, C., Kolodziejczyk, A.A., et al. (2015). Single-cell
1137   transcriptomic reconstruction reveals cell cycle and multi-lineage differentiation defects in
1138   Bcl11a-deficient hematopoietic stem cells. *Genome Biol* 16**,** 178. doi: 10.1186/s13059-015-
1139   0739-5.
1140   Vega-Lopez, G.A., Cerrizuela, S., Tribulo, C., and Aybar, M.J. (2018). Neurocristopathies: New
1141   insights 150 years after the neural crest discovery. *Dev Biol* 444 Suppl 1**,** S110-S143. doi:
1142   10.1016/j.ydbio.2018.05.013.
1143   Waddington, R.J., Youde, S.J., Lee, C.P., and Sloan, A.J. (2009). Isolation of distinct progenitor stem
1144   cell populations from dental pulp. *Cells, tissues, organs* 189(1-4). doi: 10.1159/000151447.
1145   Widera, D., Grimm, W.D., Moebius, J.M., Mikenberg, I., Piechaczek, C., Gassmann, G., et al. (2007).
1146   Highly efficient neural differentiation of human somatic stem cells, isolated by minimally
1147   invasive periodontal surgery. *Stem Cells Dev* 16(3)**,** 447-460. doi: 10.1089/scd.2006.0068 [doi].

1148 Widera, D., Zander, C., Heidbreder, M., Kasperek, Y., Noll, T., Seitz, O., et al. (2009). Adult palatum
1149   as a novel source of neural crest-related stem cells. *Stem Cells* 27(8)**,** 1899-1910. doi:
1150   10.1002/stem.104 [doi].
1151 Wilkie, A.O., and Morriss-Kay, G.M. (2001). Genetics of craniofacial development and malformation.
1152   *Nat Rev Genet* 2(6)**,** 458-468. doi: 10.1038/35076601.
1153 Wong, C.E., Paratore, C., Dours-Zimmermann, M.T., Rochat, A., Pietri, T., Suter, U., et al. (2006).
1154   Neural crest-derived cells with stem cell features can be traced back to multiple lineages in the
1155   adult skin. *J Cell Biol* 175(6)**,** 1005-1015. doi: 10.1083/jcb.200606062.
1156 Wu, A.R., Neff, N.F., Kalisky, T., Dalerba, P., Treutlein, B., Rothenberg, M.E., et al. (2014).
1157   Quantitative assessment of single-cell RNA-sequencing methods. *Nat Methods* 11(1)**,** 41-46.
1158   doi: 10.1038/nmeth.2694.
1159 Wu, J., and Tzanakakis, E.S. (2012). Contribution of stochastic partitioning at human embryonic stem
1160   cell division to NANOG heterogeneity. *PLoS One* 7(11)**,** e50715. doi:
1161   10.1371/journal.pone.0050715.
1162 Xue, Z., Huang, K., Cai, C., Cai, L., Jiang, C.Y., Feng, Y., et al. (2013). Genetic programs in human
1163   and mouse early embryos revealed by single-cell RNA sequencing. *Nature* 500(7464)**,** 593-
1164   597. doi: 10.1038/nature12364.
1165 Yan, L., Yang, M., Guo, H., Yang, L., Wu, J., Li, R., et al. (2013). Single-cell RNA-Seq profiling of
1166   human preimplantation embryos and embryonic stem cells. *Nat Struct Mol Biol* 20(9)**,** 1131-
1167   1139. doi: 10.1038/nsmb.2660.
1168 Yntema, C.L., and Hammond, W.S. (1954). The origin of intrinsic ganglia of trunk viscera from vagal
1169   neural crest in the chick embryo. *J Comp Neurol* 101(2)**,** 515-541. doi: 10.1002/cne.901010212.
1170 Yoshida, S., Shimmura, S., Nagoshi, N., Fukuda, K., Matsuzaki, Y., Okano, H., et al. (2006). Isolation
1171   of multipotent neural crest-derived stem cells from the adult mouse cornea. *Stem Cells* 24(12)**,**
1172   2714-2722. doi: 10.1634/stemcells.2006-0156.
1173 Young, F.I., Telezhkin, V., Youde, S.J., Langley, M.S., Stack, M., Kemp, P.J., et al. (2016). Clonal
1174   Heterogeneity in the Neuronal and Glial Differentiation of Dental Pulp Stem/Progenitor Cells.
1175   *Stem Cells Int* 2016**,** 1290561. doi: 10.1155/2016/1290561.
1176 Yu, V.W.C., Yusuf, R.Z., Oki, T., Wu, J., Saez, B., Wang, X., et al. (2016). Epigenetic Memory
1177   Underlies Cell-Autonomous Heterogeneous Behavior of Hematopoietic Stem Cells. *Cell*
1178   167(5)**,** 1310-1322.e1317. doi: 10.1016/j.cell.2016.10.045.
1179 Yu, V.W.C., Yusuf, R.Z., Oki, T., Wu, J., Saez, B., Wang, X., et al. (2017). Epigenetic Memory
1180   Underlies Cell-Autonomous Heterogeneous Behavior of Hematopoietic Stem Cells. *Cell*
1181   168(5)**,** 944-945. doi: 10.1016/j.cell.2017.02.010.
1182 Zhang, C., Carl, T.F., Trudeau, E.D., Simmet, T., and Klymkowsky, M.W. (2006). An NF-kappaB and
1183   slug regulatory loop active in early vertebrate mesoderm. *PLoS One* 1**,** e106. doi:
1184   10.1371/journal.pone.0000106.
1185 Zhang, X., Li, T., Liu, F., Chen, Y., Yao, J., Li, Z., et al. (2019). Comparative Analysis of Droplet-
1186   Based Ultra-High-Throughput Single-Cell RNA-Seq Systems. *Mol Cell* 73(1)**,** 130-142 e135.
1187   doi: 10.1016/j.molcel.2018.10.020.
1188 Zheng, G.X., Terry, J.M., Belgrader, P., Ryvkin, P., Bent, Z.W., Wilson, R., et al. (2017). Massively
1189   parallel digital transcriptional profiling of single cells. *Nat Commun* 8**,** 14049. doi:
1190   10.1038/ncomms14049.
1191 Zhou, F., Li, X., Wang, W., Zhu, P., Zhou, J., He, W., et al. (2016). Tracing haematopoietic stem cell
1192   formation at single-cell resolution. *Nature* 533(7604)**,** 487–492. doi: 10.1038/nature17997.
1193 Ziegenhain, C., Vieth, B., Parekh, S., Reinius, B., Guillaumet-Adkins, A., Smets, M., et al. (2017).
1194   Comparative Analysis of Single-Cell RNA Sequencing Methods. *Mol Cell* 65(4)**,** 631-643
1195   e634. doi: 10.1016/j.molcel.2017.01.023.

1196 Zilionis, R., Nainys, J., Veres, A., Savova, V., Zemmour, D., Klein, A.M., et al. (2016). Single-cell
1197   barcoding and sequencing using droplet microfluidics. *Nature Protocols* 12**,** 44. doi:
1198   10.1038/nprot.2016.154

1199 https://www.nature.com/articles/nprot.2016.154#supplementary-information.
1200 Ziller, C., Dupin, E., Brazeau, P., Paulin, D., and Le Douarin, N.M. (1983). Early segregation of a
1201   neuronal precursor cell line in the neural crest as revealed by culture in a chemically defined
1202   medium. *Cell* 32(2)**,** 627-638. doi: 10.1016/0092-8674(83)90482-8.

1203

1204

1205

1206

1207

1208

1209 **16 Figure legends**

1210 **Figure 1.** Determination of single stem cell identities gives insights into linage choices, regulatory
1211 networks, niches and model systems like cultured stem cell-derived spheroids as well as tissue
1212 regeneration.

1213 **Figure 2**. Schematic representation of diverse state-of-the-art tools for single cell analysis. Next to
1214 microfluidic based single cell sequencing methods, like Drop-seq, inDrop or 10X Genomic Chromium,
1215 for high throughput transcriptome analysis of single cells, fluorescence-based methods are used to
1216 investigate single cell transcriptomes. Further, Sequential barcoding methods like SPLIT-seq are
1217 applied for high throughput single cell sequencing. Less throughput, but higher precision was shown
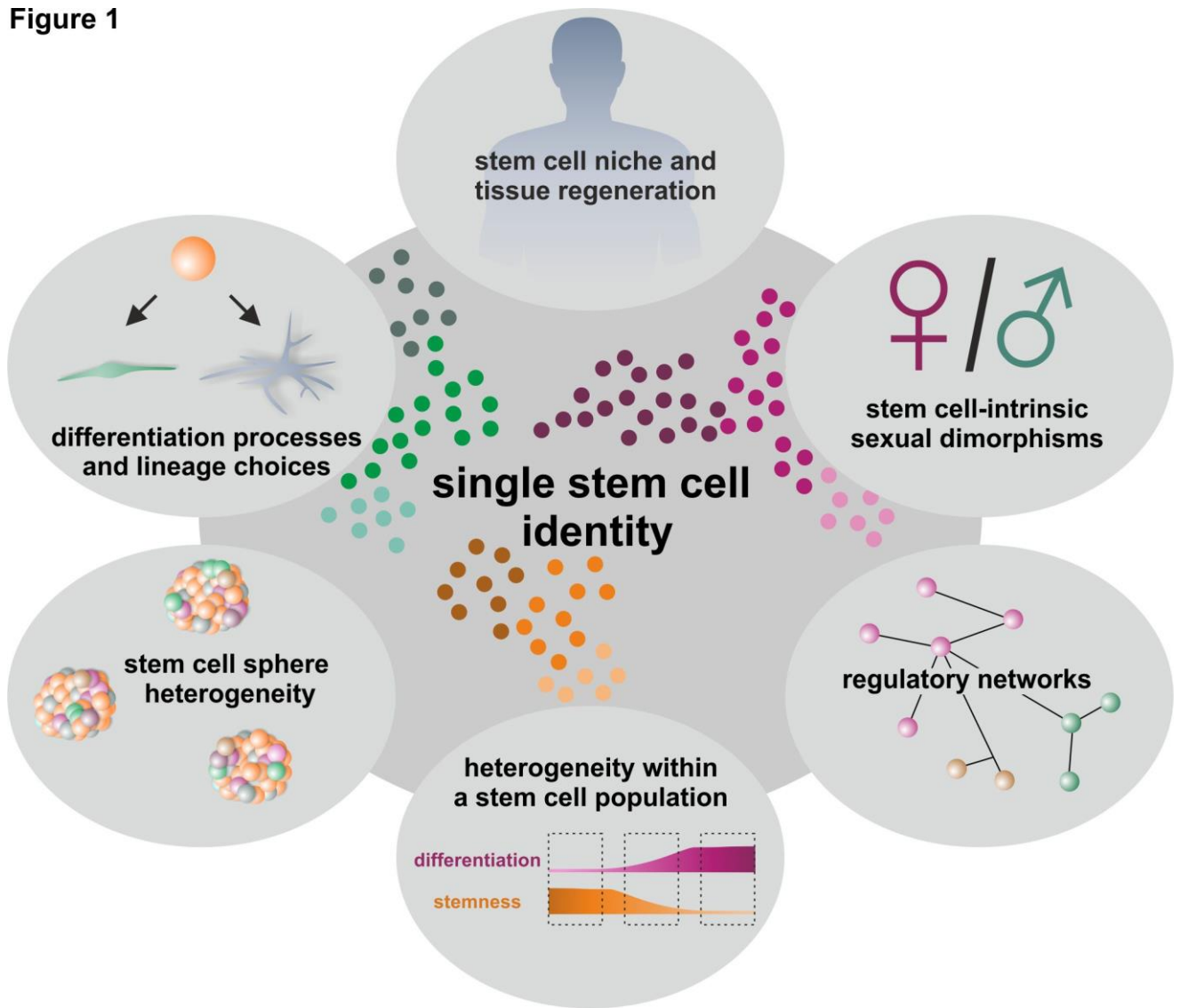1218 to be achieved using SMART-Seq methods with prior fluorescence activated cell sorting (FACS).

1219 **Figure 3.** Schematic view on the role of neural crest stem cells in embryogenesis (A) and adulthood
1220 (B) as well as suggested differences between favored fate choices of single NCSCs (C). (Panel A
1221 modified from (J. Greiner et al. 2019b) and (Srinivasan and Toh 2019)), NC: Neural crest, NCSCs:
1222 Neural crest-derived stem cells, PNS: Peripheral nervous system.

1223 **Figure 4.** Heterogeneity of single neural crest-derived inferior turbinate stem cells (ITSCs) isolated
1224 from the human nasal cavity. (A) qPCR following SMART-Seq2 of single ITSCs showed
1225 heterogeneity in expression levels of Slug, Snail and Nestin. (B-C) Heterogeneous nuclear fluorescence
1226 intensities of Slug protein in single ITSCs.

1227 **Figure 5.** Schematic view of potential molecular regulators defining self-renewal and fate choices of
1228 NCSCs.

1229 **Figure 6.** Schematic illustration of various extrinsic and intrinsic factors influencing NCSC
1230 heterogeneity. Single stem cell heterogeneity is influence by diverse variables including donor-to-
1231 donor variations, the stem cell niche, epigenetic modifications, stochasticity of mRNA and protein
1232 production and random segregation during cell division. All these aspects are involved in stem cell
1233 heterogeneity and are crucial for the development and the existence of multicellular organisms.
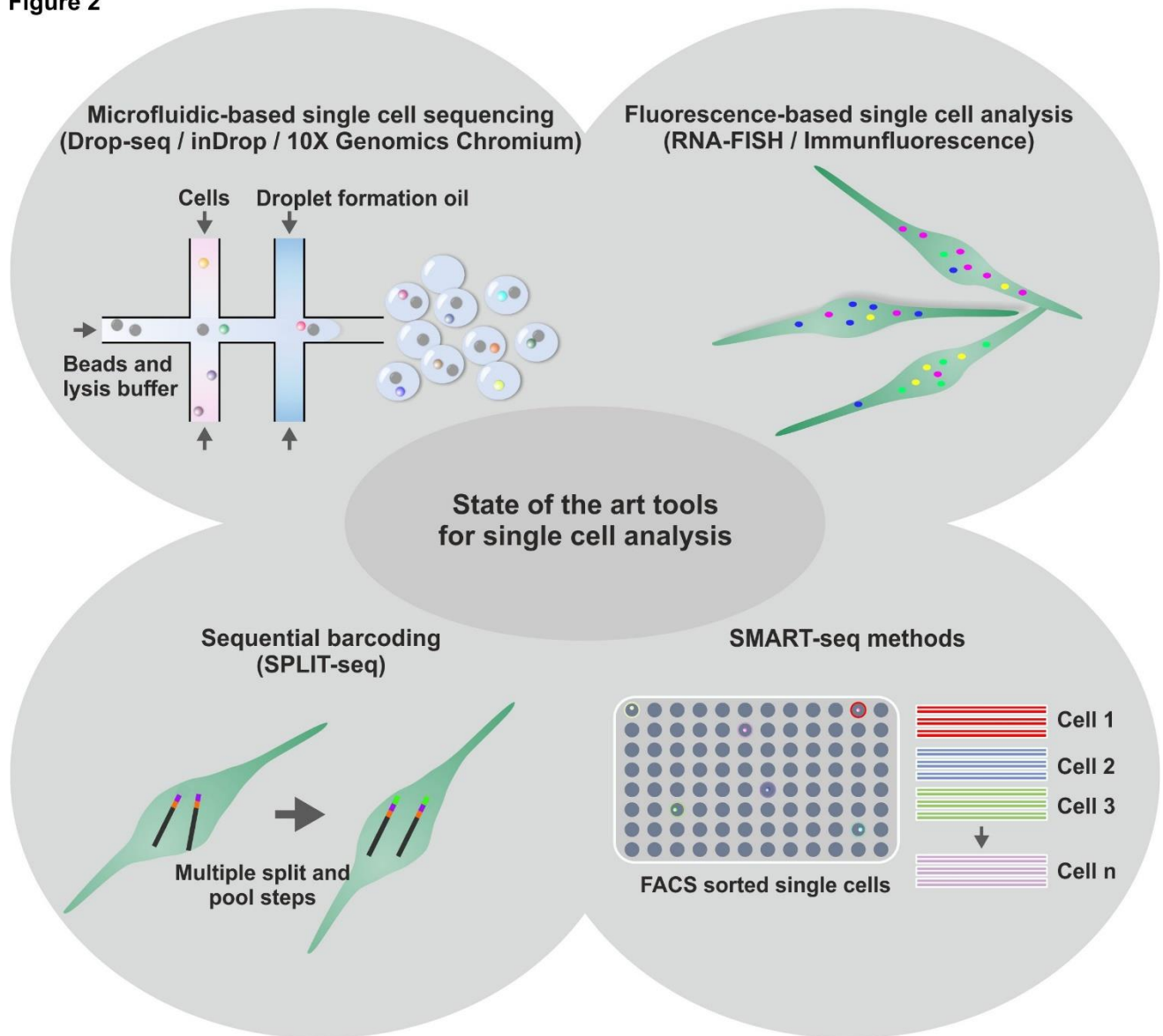
Figure 1

1234

1235

1236

1237

Figure 2

State of the art tools for single cell analysis

Microfluidic-based single cell sequencing (Drop-seq / inDrop / 10X Genomics Chromium)
- Cells
- Droplet formation oil
- Beads and lysis buffer

Fluorescence-based single cell analysis (RNA-FISH / Immunfluorescence)

Sequential barcoding (SPLIT-seq)
- Multiple split and pool steps

SMART-seq methods
- FACS sorted single cells
- Cell 1
- Cell 2
- Cell 3
- Cell n

1238

Figure 3

A Neural crest - origin and contribution to development

neural plate

neural plate border

Epidermis

migrating neural crest cells

neural tube

cranial NC

vagal NC

trunk NC

B Differentiation potential of NCSCs during adulthood

adult neural crest-derived stem cells

ectodermal derivates

Schwann cells

neurons (PNS)

mesodermal derivates

osteoblasts

adipocytes

C Suggested differences in fate choices between individual NCSCs

view on bulk NCSC samples

view on individual NCSCs

ectodermal derivates

mesodermal derivates

1239

Figure 4

A

Slug

Snail

Nestin

fold change of relative expression levels

100 ITSCs

single inferior turbinate stem cells

B

Slug

Slug/DNA

ITSCs (female donor)

Slug

Slug/DNA

ITSCs (male donor)

50 µm

C

Slug

Single nuclear fluorescence intensity of Slug

ITSCs from female donors

ITSCs from male donors

1240

Figure 5

NF-κB

Slug

Sox9

MAPK

Wnt

self-renewal

fate choice
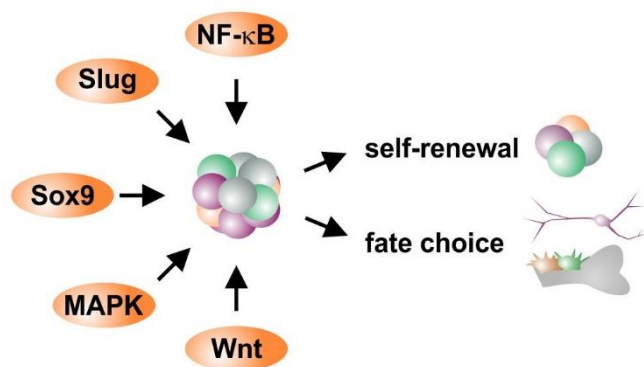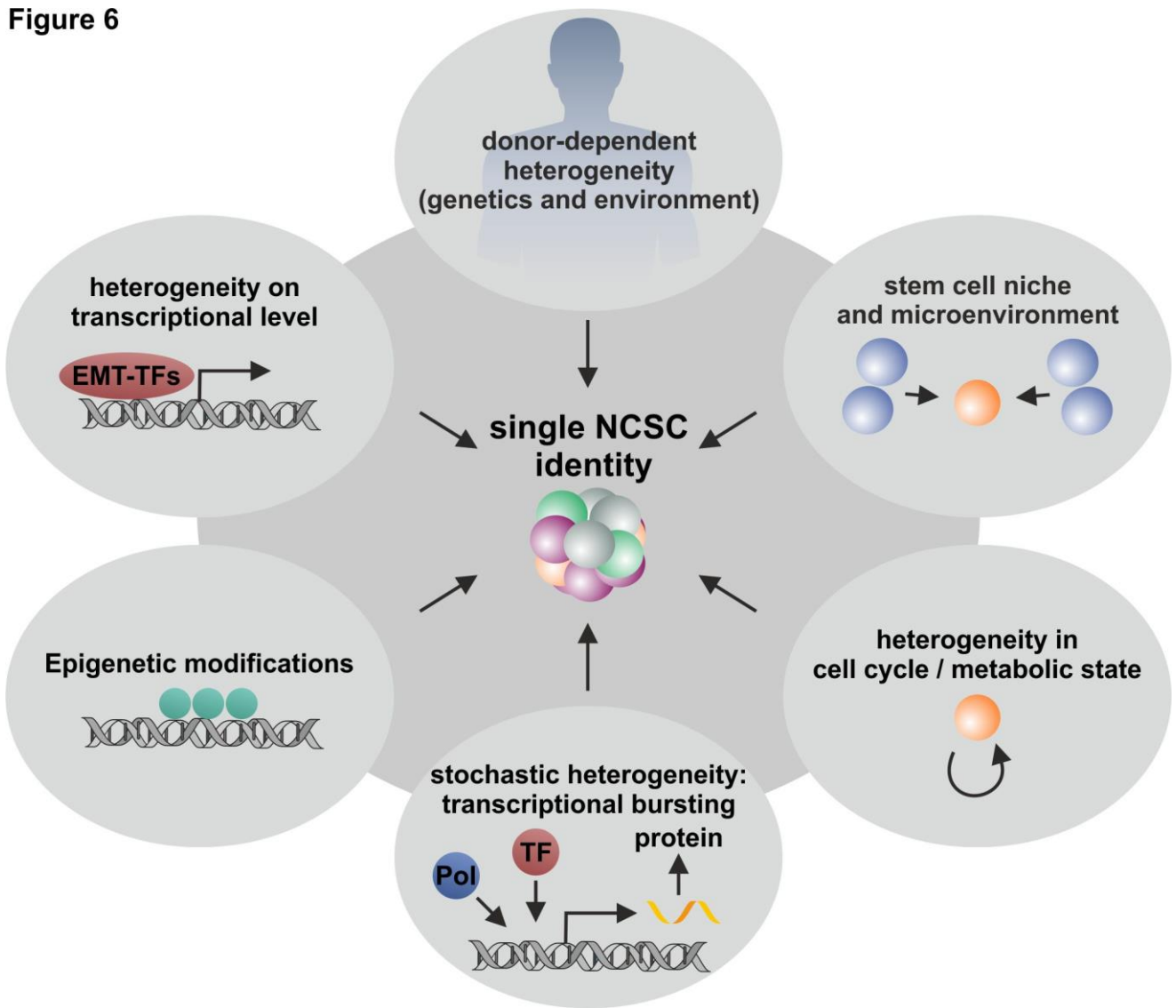
1241

Figure 6

1242

1243   **Table 1**. Overview of single cell experiments in NCSC populations

NCSC population	Single cell Method	Key findings	Reference
Murine horizontal basal cells (HBCs)	scRNA-seq using FACS and SMART-Seq technology / *in vivo* lineage tracing	• direct fate conversion of quiescent HBCs into either sustentacular cells or globose basal cells prior to cell division • olfactory neurogenesis via differentiation of globose basal cells • Canonical Wnt signaling regulates differentiation into the neuronal lineage	(Fletcher et al., 2017)
Murine HBCs	scRNA-seq using FACS and SMART-Seq technology / *in vivo* lineage tracing	• Injury activates a highly heterogenous transient state in HBCs • differentiation into sustentacular cells involved proliferation of HBCs	(Gadye et al., 2017)
Human HBCs from olfactory neuroepithelium	scRNA-seq using 10X Genomics Chromium	• Stemness state of HBCs under non injury conditions suggested to be similar to injury conditions in rodents	(Durante et al., 2020)
Rodent olfactory ensheathing cells (OEC)	Single cell migration assays	• distinct OEC subpopulations display different migratory properties	(Huang et al., 2008)
Human inferior turbinate stem cells (ITSCs)	Immunocytochemistry	• ITSC-derived neurons from female donors revealed elevated oxidative stress-induced cell death in comparison to male neurons	(Ruiz-Perera et al., 2018)
Human ITSCs	Immunocytochemistry	• ITSC clones revealed different ratios of ectodermal to mesodermal progeny upon differentiation	(Greiner et al., 2011) (Hauser et al., 2012)
Murine Dental Pulp Stem/Progenitor Cells (DPSCs)	Immunocytochemistry	• DPSC clones reveal heterogeneity in neuronal differentiation capacity	(Young et al., 2016)
Human DPSCs	Immunocytochemistry and DNA microarray	• Human dental pulp stem cell clones reveal differences in	(Kobayashi et al., 2020)

		proliferation, differentiation potential and gene expression, with characteristic DPSC-markers being mainly conserved	
Human DPSCs	FACS / Immunocytochemistry	• Canonical Wnt-GSK3β/β-catenin pathway contributes to DPSC differentiation into mature SMCs. However, different clones reveal heterogeneity in differentiation potential	(Jiang et al., 2019)
Human DPSCs	Single-cell Raman spectroscopy	• Subpopulations of highly proliferative/multipotent DPSCs and low proliferative/unipotent were identified in human third molars	(Alraies et al., 2019)
Murine hair follicle bulge stem cells	scRNa-seq using microfluidic based Fluidigm C1 Autoprep System	• Lack of common stemness expression signature but segregation of cell populations in relation to their location during tissue homeostasis	(Joost et al., 2016)
Murine hair follicle bulge stem cells	scRNa-seq using microfluidic based Fluidigm C1 Autoprep System / *in vivo* lineage tracing	• Stem cells activate interfollicular epidermis stem cell-like gene expression signature during wound healing even before migration to the lesion • great cellular plasticity of single stem cells allowing rapid transcriptional adaptations during wound healing	(Joost et al., 2018)
Embryonic quail mesencephalic neural crest cells	Analysis of single cell-derived clones	• treatment with the morphogen Sonic Hedgehog (Shh) increased the number of multipotent subclones with the capacity to differentiate into glia, neurons, melanocytes, myofibroblasts and chondrocytes	(Calloni et al., 2007; Calloni et al., 2009)

Embryonic quail mesencephalic neural crest cells	Analysis of single cell-derived clones	• increased developmental potential into glial cells, neurons, melanocytes, smooth muscle cells, chondrocytes and adipocytes after the simultaneous application of FGF8 and Shh	(da Costa et al., 2018)
Fetal rat sciatic nerve-derived NCSCs	FACS	• p75+ subpopulations were able to differentiate into neurons, Schwann cells and myofibroblasts while p75- cells were only able to differentiate into myofibroblasts	(Morrison et al., 1999)

1244

1245